BEHAVIOR OF TRADITIONAL TIMBER FRAME STRUCTURES SUBJECTED TO LATERAL LOAD

Robert G. Erikson

Richard J. Schmidt

Department of Civil and Architectural Engineering
University of Wyoming
Laramie, WY 82071

A report on research co-sponsored by:

USDA NRI/CGP
Washington, DC

Timber Frame Business Council
Hamilton, MT

Timber Framers Guild
Becket, MA

August 2003

UNIVERSITY OF WYOMING

50272–101

REPORT DOCUMENTATION PAGE	1. REPORT NO.	2.	3. Recipient's Accession No.

4. Title and Subtitle
Behavior of Traditional Timber Frame Structures Subjected to Lateral Load

5. Report Date
August 2003

6.

7. Author(s)
Robert G. Erikson & Richard J. Schmidt

8. Performing Organization Report No.

9. Performing Organization Name and Address
Department of Civil and Architectural Engineering
University of Wyoming
Laramie, Wyoming 82071

10. Project/Task/Work Unit No.

11. Contract(C) or Grant(G) No.
(C)
(G)

12. Sponsoring Organization Name and Address
USDA NRI/CGP
CSREES
Wash., DC 20250

Timber Frame Business Council
217 Main Street
Hamilton, MT 59840

Timber Framers Guild
PO Box 60
Becket, MA 01223

13. Type of Report & Period Covered
final

14.

15. Supplementary Notes
USDA NRI/CGP Contract No. 97–35103–5053

16. Abstract (Limit: 200 words)

Timber framing is a method of construction in which heavy timber members are connected with carpenter-style joinery and wood pegs. Timber frames are commonly enclosed with structural insulated panels (SIPs). Current building codes do not provide guidelines for wood structures with wood pegged connections. The intent of this research was to provide a basis for implementing provisions for this type of structure in building codes.

Specifically, this project investigated the effects of lateral load on the stiffness of full-scale timber frames. The frames were tested in both the unsheathed and sheathed condition and were modeled with a structural analysis program. Load-slip characteristics for single-fastener SIP-to-timber connections were developed.

Excessive displacements of the frames indicated unacceptable flexibility when subjected to reversible lateral loads. This lack of stiffness was due to the inefficiency of knee braces for resisting lateral load. However, the knee brace system provided exceptional strength characteristics due to the substantial available compressive action of the joints. The addition of SIP sheathing significantly improved frame stiffness.

In order to accurately model the displacement characteristics of a frame, the characteristics of the pegged connections must be included in the model. For sheathed frame models, the implementation of nonlinear SIP-to-timber connection elements produced accurate predictions of sheathed frame stiffness.

17. Document Analysis
a. Descriptors

traditional timber framing, heavy timber construction, structural analysis, wood peg fasteners, mortise and tenon connections, dowel connections, lateral load response

b. Identifiers/Open–Ended Terms

c. COSATI Field/Group

18. Availability Statement	19. Security Class (This Report)	21. No. of Pages
Release Unlimited	unclassified	221
	20. Security Class (This Page)	22. Price
	unclassified	

(See ANSI–Z39.18)

OPTIONAL FORM 272 (4–77)
Department of Commerce

Acknowledgments

Primary funding for this research project was provided by the USDA–NRI/CGP. Additional support was provided by the Timber Frame Business Council and the Timber Framers Guild. Timber frames were donated by The Cascade Joinery, Benson Woodworking, Riverbend Timber Framing, and Earthwood Homes. Structural insulated panels were donated by Great Lakes Insulspan and Premier Building Systems.

1. Introduction

1.1. Background

1.1.1. Definition of Traditional Timber Frame

Timber framing is a method of construction in which a system of relatively large wood columns and beams is connected with wood pegs. The most common joint in this type of structure is a mortise and tenon pinned with a wood dowel or "peg." Timber framing should not be confused with "post and beam" construction, which also utilizes large wood members but has joints connected with metal plates and fasteners.

Timber frames are constructed as residences, public facilities, commercial and retail shops, and agricultural buildings. Historic covered timber frame bridges are common in the eastern United States. An example of the finished interior of a timber frame structure is shown in Figure 1-1. The photograph shows the large columns, beams, and knee braces typical of timber frame buildings along with traditional wood pegged, mortise and tenon joints.

Figure 1-1 Typical Timber Frame (courtesy of Riverbend Timber Framing)

Timber frames may be enclosed in a variety of manners, but the most common enclosure system is the structural insulated panel (SIP). SIPs are constructed of oriented strand board (OSB) outer skins laminated to a foam core, thus creating a structural panel with excellent thermal properties.

The North American craft of traditional timber frame construction declined in the latter part of the 19th century and was replaced by the modern light-frame system. However, beginning in the 1970's, a renewed interest led to a revival of traditional timber framing methods.

1.1.2. Engineering Design Difficulties

Currently the engineered design of timber structures in the United States is based on the National Design Specification for Wood Construction (NDS) (AFPA 2001). The major building codes utilized by most jurisdictions in the United States are based on provisions specified in the NDS, which provides guidelines for design of structural

members as well as connections created with metal fasteners such as bolts, lag screws and nails. However, no such provisions exist for connections fastened with wood dowels.

At this juncture in the evolution of building design, timber frame structures are often designed based on the study of historic buildings. However, such a design method is not acceptable to either professional engineers or local building code officials. Also, no procedures exist to determine the load sharing between a timber frame and its enclosure system. To facilitate acceptance of wood-pegged structural connections and the use of SIPs on traditional timber frames, it is imperative that appropriate guidelines be developed and incorporated into the NDS. The research described herein is an important step towards acceptance of traditional timber frame structures.

1.2. Objectives

The goal of this study is to develop or identify behavior models that represent the full-scale response of two-dimensional timber frames subjected to lateral load. Frame performance will be modeled for both unsheathed and sheathed frames.

The objectives of this research are to:

1. Investigate the behavior of unsheathed two-dimensional timber frames subjected to lateral load.
2. Investigate the behavior of two-dimensional timber frames sheathed with structural insulated panels (SIPs) and subjected to lateral load.
3. Develop viable stiffness based methods of modeling the service-level behavior of stand-alone timber frames subjected to lateral load.

1.3. Scope of Work

1.3.1. Full-scale Testing

Two distinct frame types were examined. The first type consisted of one-story, one-bay (1S1B) frames, 12 feet wide by 8 feet high as shown in Figure 1-2. The second consisted of two-story, two-bay (2S2B) frames, 24 feet wide and 16 feet high frame as shown in Figure 1-3. Frame dimensions are measured from centerline to centerline of columns and from the base of the columns to the top of the beams. The frames were supplied by several manufacturers, and consequently, are of varying species and construction details. Structural insulated panels (SIPs) were attached to selected frames with screws.

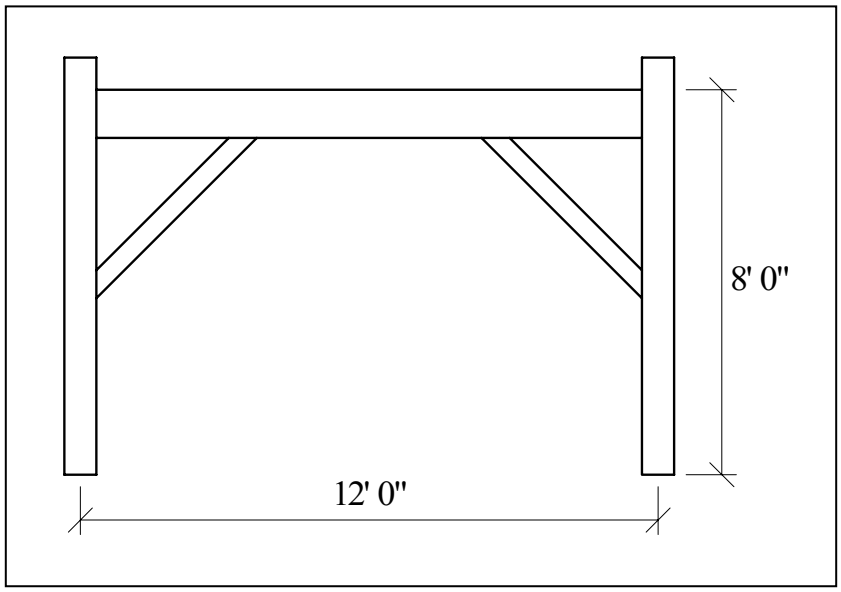

Figure 1-2 One-Story, One Bay Frame

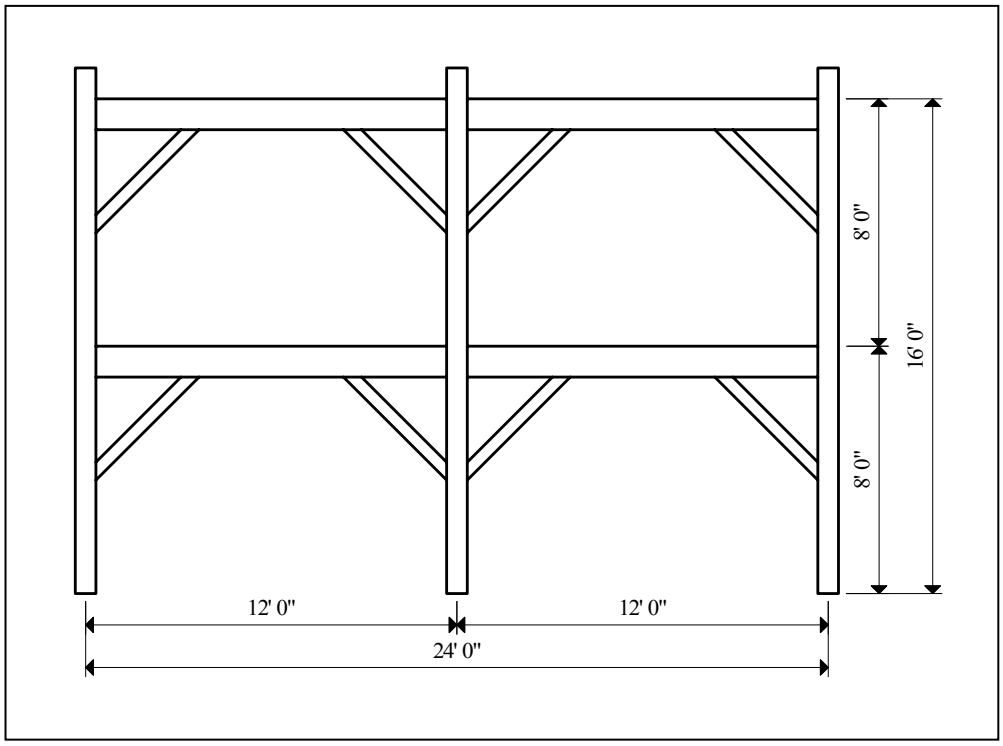

Figure 1-3 Two-Story, Two-Bay Frame

The frames were tested by applying horizontal load to one side of the frame at the beam elevation(s). A single actuator was used for both frame types. Two equal point loads were applied to the 2S2B frame via a load splitting apparatus. The applied load was reversible, thus each frame was examined for performance in both directions. Each frame was typically displaced 3 inches in each horizontal direction, although additional lateral displacement was applied to selected frames. At a lateral displacement of 3 inches, a frame was assumed to be well beyond an acceptable level of serviceability.

Eight 1S1B frames and four 2S2B frames were tested. Dimensions and descriptions of the individual structures are provided in Chapter 2 (1S1B) and Chapter 3 (2S2B).

1.3.2. SIP Connection Testing

The individual SIP to frame connection was also considered in order to characterize the performance of the sheathed frames. This was accomplished with the test setup schematically shown in Figure 1-4.

The connection tests examined several variables including timber species, grain orientation, fastener type, countersinking of the fastener, and the use of a shim between the panel and timber. Timber species included Douglas fir, eastern white pine and white oak. The panel was attached with either a 3/16-inch diameter screw or a 3/16-inch diameter ring shank nail. Load was applied with a universal testing machine.

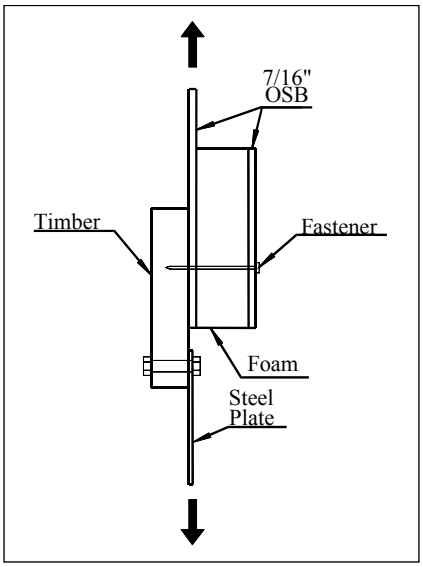

Figure 1-4 SIP to Timber Connection Test

1.3.3. Modeling

Unsheathed frames were modeled with SAP 2000 version 8.16 (SAP 2003). All models were plane-frame structures with three degrees of freedom (DOF) per node. The structures were modeled in a relatively simple fashion with all knee braces pinned at each end, thus limiting their actions to axial force only. Beam-to-column connections were also modeled as pin connections.

Classical methods were also used to analyze the unsheathed 1S1B frames. Basic statics was used to predict frame actions, and frame stiffness was modeled using a work-energy method. For the classical models, the frame was assumed to have infinite material stiffness for frame elements such that all deformation occurred at the joints.

Behavior of single fastener SIP to timber connections was modeled from experimental load-slip relationships. Such relationships are of the form shown in Equation 1.1 (Foschi, 1974) where P is the applied load, δ is the joint displacement, C is the initial slope of the curve, B is the final slope of the curve, and A is the point at which a line drawn tangent to the final slope intercepts the vertical axis.

$$P=(A+B\delta)[1-e^{(-C\delta/A)}] \quad \textbf{(1.1)}$$

1.4. Literature Review

1.4.1. Unsheathed Frames

There had been no published research on timber frames prior to the publication of a dissertation by Brungraber (1985). This extensive document describes exploratory research that included individual joint testing, full-scale frame testing, finite element analysis of joint behavior and a computer model that incorporated connection behavior. Brungraber's computer simulation used finite element analysis to create a two-dimensional frame model. A three-spring joint model was utilized to simulate connection behavior. The research by Brungraber raised many questions that have led to additional timber frame research at several institutions.

A limited amount of timber frame research has been completed in Germany by Kessel and Augustin. Kessel and Augustin first examined 12 wood-pegged connections and concluded that oak pegs have sufficient strength for use in modern wood construction (Kessel and Augustin 1995). Reconstruction of an eight-story timber frame in Germany (Kessel *et al* 1988) provided the impetus for Kessel and Augustin's next investigation into wood-pegged connections (Kessel and Augustin 1996). Approximately 110 joint tests were conducted on oak and spruce samples joined with oak pegs.

Recommendations were proposed for short-duration allowable design loads based on peg diameter, minimum spacing of pegs, end and edge distance of pegs, and timber dimensions. The results of these tests are specific to the species and timber sizes used in the experiments, and extrapolation to other configurations was not recommended.

Several studies of timber frame behavior have been performed at Michigan Technological University. The first published work included the examination of 60 frame subassemblies including four different types of traditional joints (Sandberg *et al* 1996). The tests were conducted on partial frame assemblies including a column and beam section connected with or without knee braces. The results of these tests indicated a significant strength capacity of the joints but a weakness in the tensile capacity of knee brace connections. It is important to note, however, that the tests simulated gravity load, or uplift in the case of the tensile test, and the conclusions may not be representative of lateral load situations.

Researchers at Michigan Technological University published additional results in which individual joint tests were compared to the modified connection yield model (Sandburg *et al* 2000). These results provide strength predictions for joint configurations with white oak pegs and various geometric configurations. The load-displacement plots of this work are of particular interest. All of the plots exhibit low stiffness at initial loading of the specimen followed by increased stiffness as load increased. Although it was not discussed in their paper, the low initial stiffness may be a factor in full-scale frame behavior.

The characterization of dowel bearing strength in pegged connections was studied at the University of Idaho (Church and Tew 1997). The results of this research indicated that the effects of peg orientation and over-sizing of the peg hole by 1/8" or less had minimal effect on dowel bearing strength.

A significant number of timber frame research projects have been conducted at the University of Wyoming (UW). MacKay first conducted extensive tests on pegs and

base materials (Schmidt and MacKay 1997). These tests examined the bending and shear strength of pegs and the dowel bearing strength of wood pegs on base materials. Testing was also performed on a limited number of full-size mortise and tenon joints with two oak pegs. This study discovered additional dowel failure modes not described by the existing yield models for connection design.

Daniels continued the work at UW with additional material tests and full-scale joint tests (Schmidt and Daniels 1999). Daniels presented two main types of failure – ductile peg bearing and/or bending failures and brittle joint failures. As shown in Figure 1-5, Daniels presented two existing joint failure modes and proposed three new joint failure modes. Existing mode I_m is a bearing failure of the tenon (main) member and existing mode I_s is a bearing failure of the mortise (side) member. Peg bearing failure was proposed as mode I_d. Peg bending failure with a single flexural hinge was proposed as mode III_m. The proposed mode V_d, is a shear failure with fractures due to bending near ultimate loads.

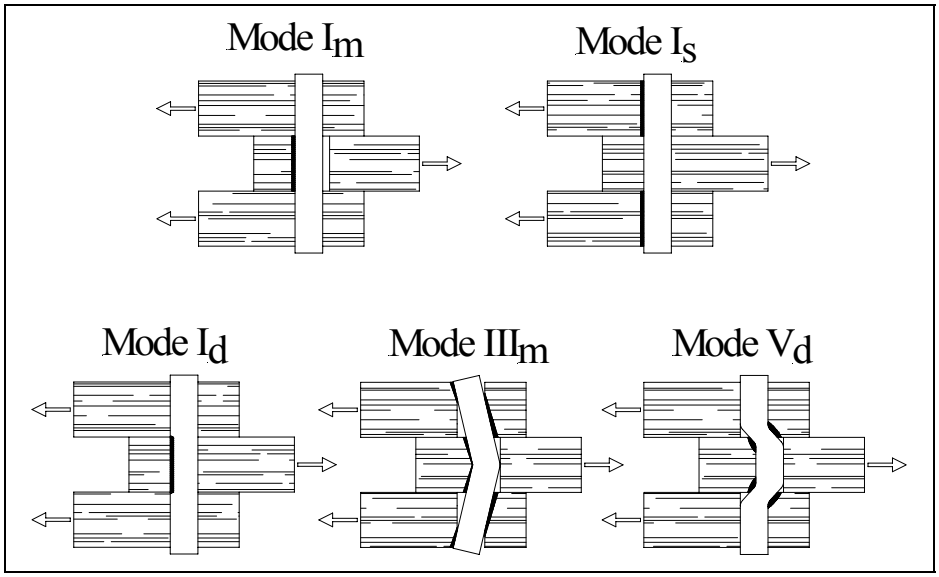

Figure 1-5 Proposed Joint Failure Modes (Schmidt and Daniels 1999)

Typical failure of the tenon is shown in Figure 1-6. This type of failure is commonly called a relish failure and is characterized by a single split or a block shear failure behind the peg hole. Providing adequate end distance on the tenon can control this failure mode.

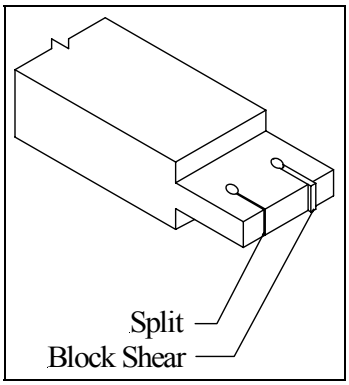

Figure 1-6 Tenon Relish Failure (Schmidt and Daniels 1999)

As shown in Figure 1-7, failure of the mortise member is characterized by splitting due to tension perpendicular to grain. This failure is a result of inadequate edge distance from the peg hole to the loaded edge of the mortise member.

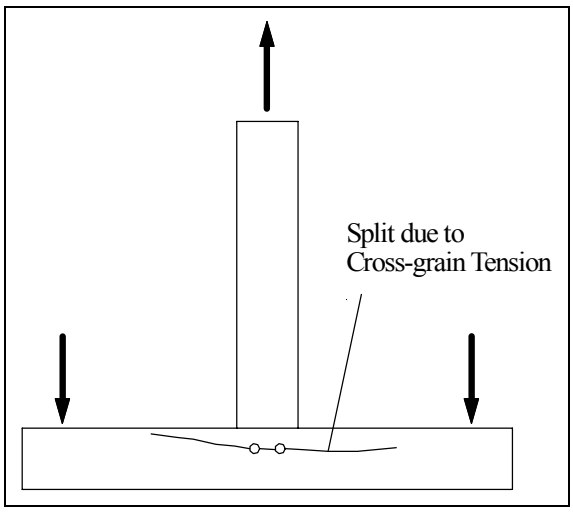

Figure 1-7 Mortise Member Failure Due to Tension Perpendicular to Grain (Schmidt and Daniels 1999)

Daniels proposed minimum detailing requirements for end distance, edge distance, and spacing such that joint failure will occur only after significant deformation of the peg.

In many of the load versus displacement curves of the work by Daniels, there is the aforementioned low stiffness at low load. That is to say, stiffness increases significantly after the joint displaces a finite distance.

Scholl completed testing of individual joints at the UW by studying load-duration and seasoning effects (Schmidt and Scholl 2000). Scholl revised Daniel's minimum detailing requirements and proposed that one peg diameter be added to the end distances when drawboring is used.

Scholl conducted long-term seasoning and load duration tests. He concluded that the yield values for the long-term tests were not significantly different from short-term tests. Scholl also concluded that seasoning effects were a concern in white oak joints, where differential shrinkage created tenon splitting.

The load-deflection plots of the work performed by Scholl also demonstrate the low stiffness near zero displacement with an increase in stiffness corresponding to increased joint displacement.

There are several books that discuss the history, architecture, and construction of timber frame structures (Benson and Gruber 1980, Sobon and Schroeder 1984, Sobon 1994, and Benson 1997). Unfortunately, they do not provide information about the strength and stiffness of wood pegged joints relative to the specifics of joint design. However, one author provides a brief statement that proved to be an apt insight to the results of the work to be described henceforth. Benson (1997) states that knee brace

joints in compression are likely to provide much more resistance to racking loads than are tension joints. The results of the experiments described herein have shown this statement to be quite sage.

1.4.2. SIP Sheathed Frames

Published work discussing the lateral load resistance of SIP enclosed timber frame is limited to a paper by Carradine (2002). The work by Carradine investigated the parallels between metal clad and SIP clad timber frames.

There is a significant quantity of published research on testing and analysis of individual laterally loaded nailed joints and on testing and analysis of full-scale light-frame walls subjected to lateral load. It is commonly accepted that the load-deflection behavior of shear walls is primarily a function of the individual connection characteristics. Several researchers have investigated load-slip behavior of fasteners in light-frame construction. A small sample of the available literature is reviewed here. Based on work by Kuenzi (1955), Wilkinson (1971, 1972) developed a theoretical solution for the lateral stiffness of nailed joints. Foschi (1974) developed a finite element solution for the lateral behavior and the finite element solution was expanded by many including Malhotra and Thomas (1982) and Hunt and Bryant (1990).

The connection research described above has focused on nailed or bolted joints. There are guidelines for nailed or screwed connections in the NDS (AFPA 2001) and the Wood Handbook (1999). However, there is no published research relating to the lateral load resistance of long screws with large thread pitch typical of SIP on timber applications.

Schmidt and Moody (1989) developed a model called Rack3D for predicting deformations and load distribution of laterally loaded light-frame buildings. This model incorporates nonlinear load/slip curves for fasteners to predict nonlinear behavior of full-scale frames.

1.5. Results

The results of this study have led to several recommendations that are intended for use by those who design, engineer and build timber frames. These recommendations will also be of assistance to those who write code rules specific to the timber frame industry and to those who implement such codes. The following paragraphs provide a brief summary of these recommendations, and a complete discussion is provided in Chapter 8.

The most important result of this study is the demonstrated lack of stiffness of an unsheathed frame subjected to lateral load. Based on this finding, it is recommended that structural loads on timber frames be limited to gravity loads with lateral loads carried by SIP sheathing, conventional shear walls or a similar structural system. If a timber frame is designed such that it must carry lateral load, knee braces should be as long as possible, and the frame should be constructed of a relatively dense material such as white oak. Also, all joints should have at least two pegs, and detailing should follow recommendations of previous research (Schmidt and Daniels 1999), (Schmidt and Scholl 2000).

The stiffness of a wood-pegged timber frame is highly dependent on the stiffness of the individual pegged connections. Therefore, structural timber frame models should include the stiffness characteristics of all connections. Inclusion of joint stiffness will

facilitate correct modeling of overall frame stiffness and internal actions. Accuracy of frame stiffness models can be improved through the use of nonlinear joint elements.

SIPs should be designed and installed within the following guidelines. Panels should be installed with fasteners located around the full perimeter of the panel. The use of shims between SIPs and frame members should be avoided. Panel joints should be located at frame members. SIPs should be fastened with screws rather than nails. Since the results of this study demonstrate reduced connection properties for 6-inch SIPs as compared to 4-inch SIPs, lateral load resisting frames should be designed with the thinnest possible panel. Computer models of sheathed frames should use nonlinear load-slip properties to simulate the behavior of laterally loaded SIP-to-timber connections.

2. 1S1B Unsheathed Frame Testing

2.1. Overview

The primary objective of this part of the research project was to characterize the full-scale response of two-dimensional one-story, one-bay (1S1B) timber frames subjected to lateral load. In addition, these full-scale tests have presented the opportunity to closely observe the nuances of overall frame performance and individual joint behavior. These timber frame characteristics have been noted and summarized as potential strengths or weaknesses of this type of construction.

The objective was accomplished by subjecting several frames to a single lateral point load. The applied load and global displacement were measured and recorded with a computerized data acquisition system.

2.2. Test Assemblies

2.2.1. Frame Dimensions

All frames had an 8-foot story height and 12-foot nominal bay width. Story height was measured to the top of the beam, and bay width was measured from center to center of the columns. A typical frame is shown in Figure 2-1.

Figure 2-1 1S1B Frame

A general schematic of typical frame geometry is shown in Figure 2-2. Knee brace dimension labeled *kb* was either 30 inches or 36 inches, depending on frame manufacturer.

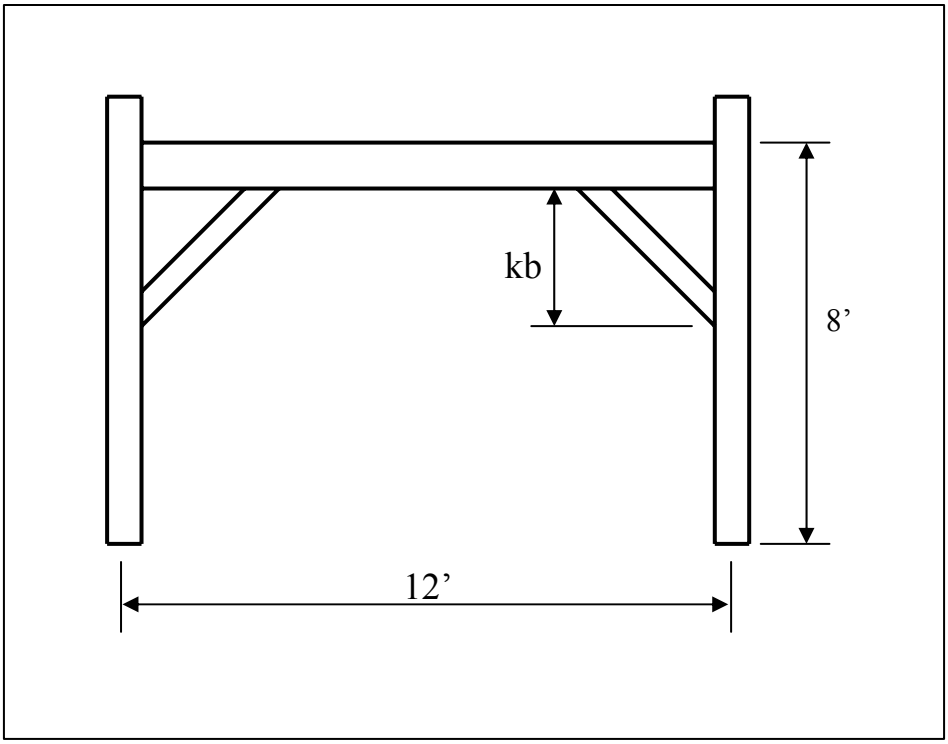

Figure 2-2 Typical 1S1B Frame Geometry

Five frames were tested. Dimensions and descriptions of the individual structures follow.

2.2.2. Frame Manufacturer and Species

Frames were provided by various manufacturers and were milled from several species of wood. The timbers for the first structure to be tested were milled from locally grown ponderosa pine by 2 Dog Construction of Laramie, Wyoming. University of Wyoming civil engineering faculty and students constructed the frame.

Four companies each donated one unassembled frame. The Cascade Joinery, Everson, Washington provided a frame manufactured from Douglas fir; Benson Woodworking, Walpole, New Hampshire furnished an eastern white pine structure; and

Riverbend Timber Framing, Blissfield, Michigan supplied a white oak frame. Earthwood Homes, Sisters, Oregon donated a Port Orford cedar frame that was milled by non-professionals at a timber-framing workshop.

2.2.3. Mortise and Tenon Joinery

All frames were constructed with traditional mortise and tenon connections fastened with wood pegs. Figure 2-3 depicts a portion of an unassembled frame showing typical parts. The unassembled frame of Figure 2-4 has a beam-to-column spline rather than a mortise and tenon joint. A photograph of a typical column mortise with beam housing is shown in Figure 2-5. The housing as shown is offset such that the outer face of the beam is flush with the column to facilitate sheathing installation. Use of a housing is a detail that was not utilized on all frames.

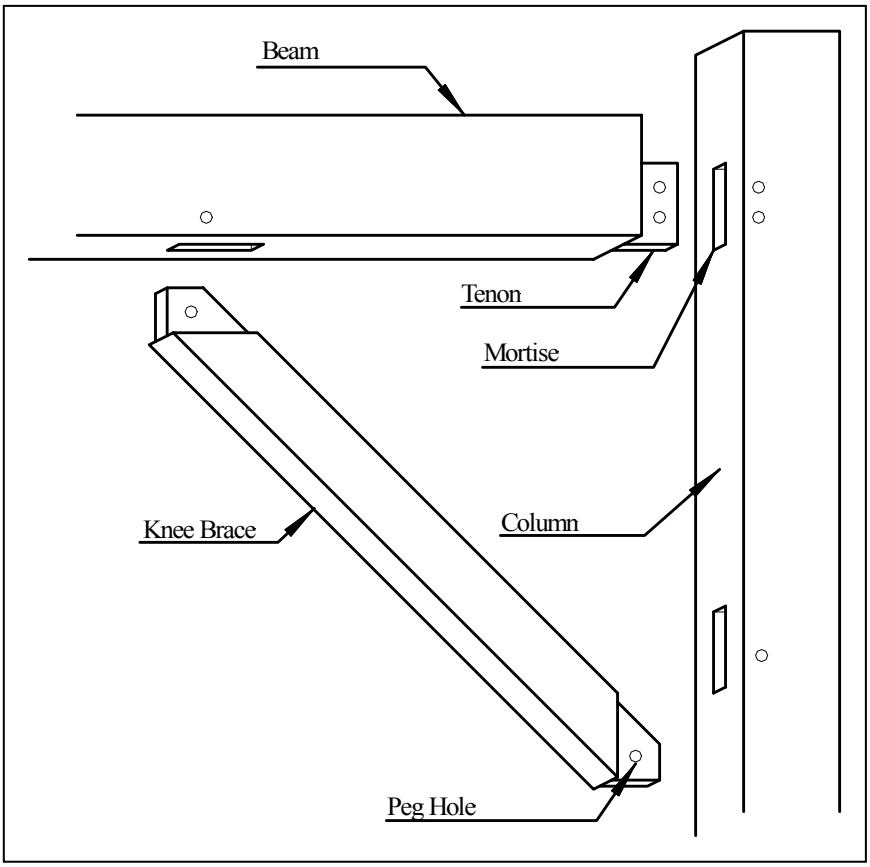

Figure 2-3 Typical Mortise and Tenon Joinery

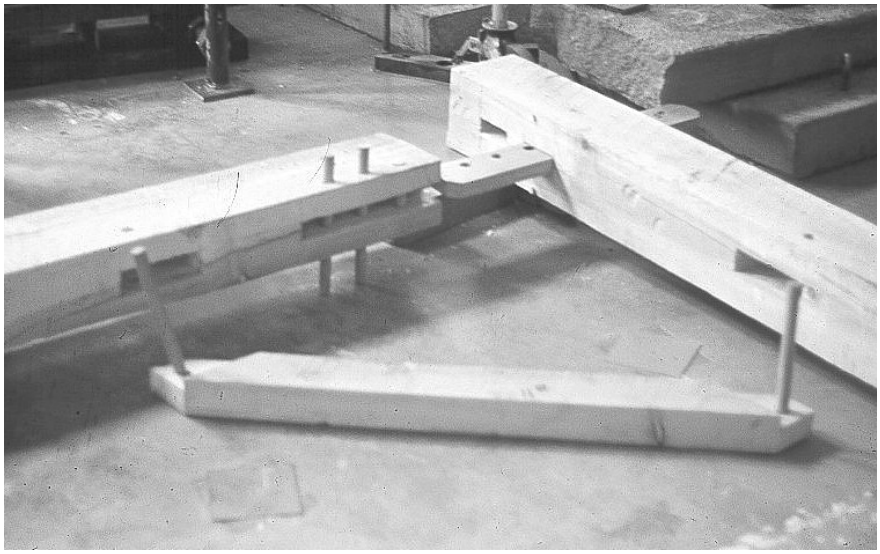

Figure 2-4 Disassembled Ponderosa Pine Frame

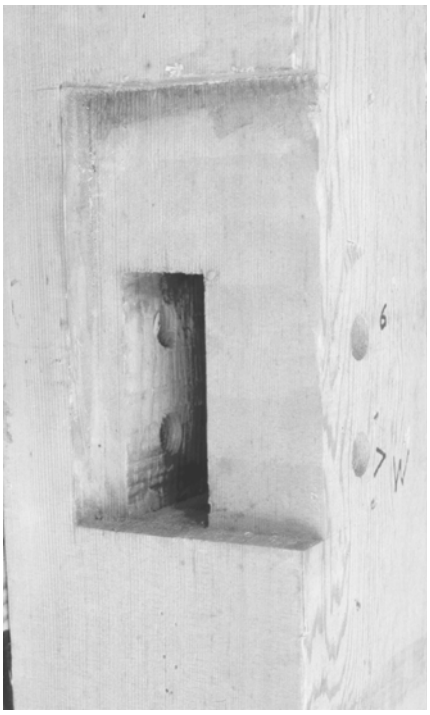

Figure 2-5 Mortise and Housing, Douglas Fir Frame

2.2.4. Peg species and size

All frames utilized one-inch pegs at all joints with one exception. The eastern white pine frames had ¾-inch pegs at the knee brace joints. The ponderosa pine and white oak frames had white oak pegs, while the Douglas fir and Port Orford cedar frames incorporated red oak pegs.

2.2.5. Member Dimensions

As shown in Table 2-1 the timber cross-section dimensions and knee brace distances varied with each manufacturer.

Table 2-1 1S1B Frame Member Dimensions

	Beam		Column		Knee Brace		Knee Brace
	Width (in)	Depth (in)	Width (in)	Depth (in)	Width (in)	Depth (in)	Distance, *kb* (in)
Douglas Fir	5.25	9.25	7.25	7.25	3.25	5.25	30
Eastern White Pine	5.75	9.75	7.75	7.75	2.75	5.75	36
Ponderosa Pine	6.25	9	7	7	3	4.75	30
Port Orford Cedar	5.25	9.25	7.5	7.5	3.5	5.5	30
White Oak	6.75	8.75	6.75	10.75	4	6	36

The frames were typically shipped in the green moisture condition and all timbers were planed with the exception of the ponderosa pine frame. However, due to the extended period of the testing schedule, significant drying and consequential shrinkage occurred in the timbers. Therefore, the dimensions listed are approximate and may vary as much as 0.25 inches for a given frame part.

2.2.6. Knee Brace Joint Details

Details of knee brace joint dimensions are listed in Table 2-2. As shown in Figure 2-6, there are two possible values of end distance for a single-peg knee brace joint: end distance *a* or end distance *b*. The recorded distance is the lesser of the two values. All frames, with the exception of the white oak assemblies, used a single peg at each knee brace joint. As shown in Figure 2-7, the white oak frame knee brace joint had two pegs spaced transversely at 2.75 inches. The recorded knee brace joint end distance for a given joint within the white oak frame is the minimum of the four possible values. The reported end distance is the average recorded value for a given frame.

Table 2-2 1S1B Knee Brace Joint Details

	End Distance (in)	Edge Distance (in)	Tenon Width (in)	Housing Depth (in)	Number of Pegs	Peg Diameter (in)
Douglas Fir	2.25	2.5	2	.5	1	1
Eastern White Pine	1.5	1.75	1.5	0	1	.75
Ponderosa Pine	1.5	2	1.5	0	1	1
Port Orford Cedar	2.5	2	2	.5	1	1
White Oak	1.5	1.5	2	0	2	1

The knee brace peg holes in the beams and columns were typically drilled prior to shipment to the laboratory, but the tenon holes were drilled during frame assembly. Shrinkage and warping of the timbers prior to assembly caused difficulty with frame assembly. Consequently, tenon end distances within a given frame varied significantly.

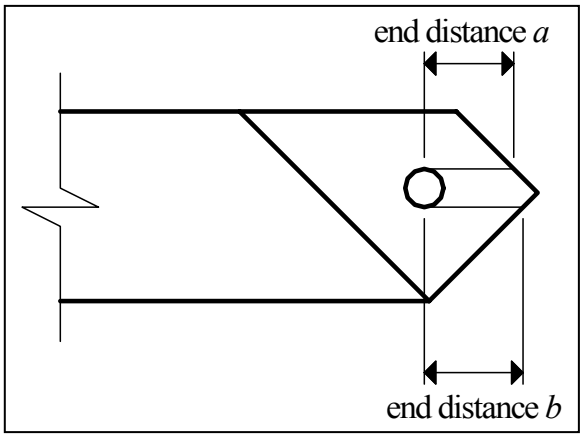

Figure 2-6 Single Peg Knee Brace End Distance

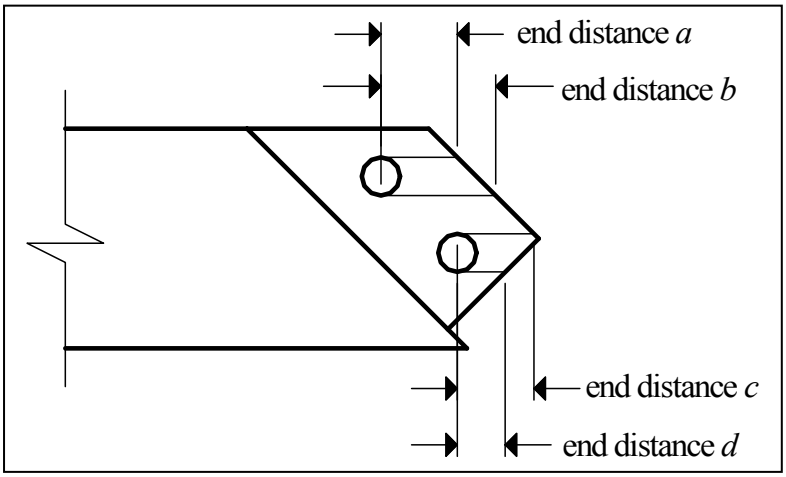

Figure 2-7 Double Peg Knee Brace End Distance

2.2.7. Beam-to-Column Connection

Details of the beam-to-column connection for three of the frames are listed in Table 2-3. Figure 2-8 illustrates typical mortise and tenon construction of the beam-to-column joint used on these three frames.

Table 2-3 1S1B Beam-to-Column Joint Details

	End Dist. (in)	Edge Dist. (in)	Tenon Width (in)	Tenon Height (in)	Housing Depth (in)	Number of Pegs	Spacing (in)
Douglas Fir	3	3	2	5.25	1	2	2.5
Port Orford Cedar	2.5	3	2	5.0	1	1	-
White Oak	2.5	1.5	2	8.25	0	2	2.75

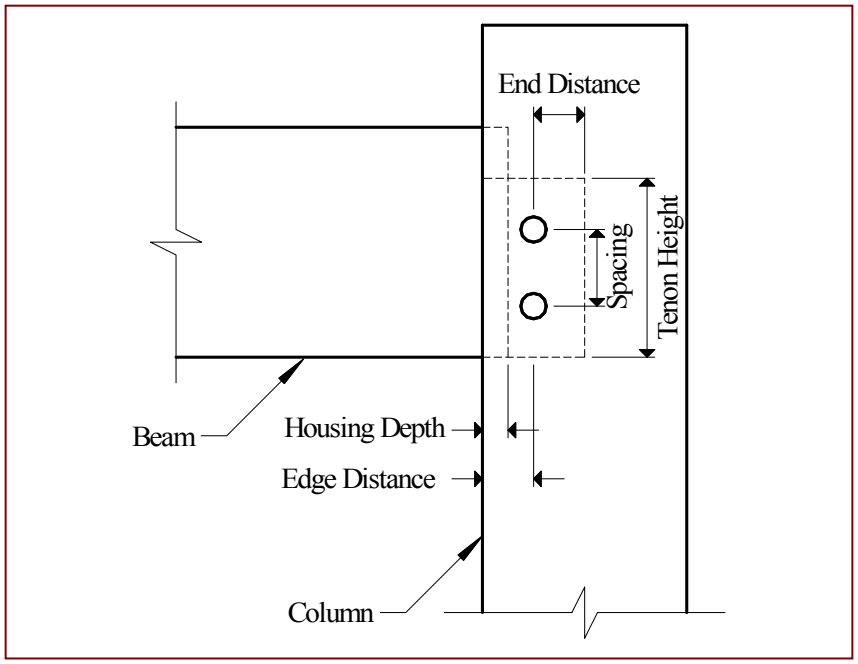

Figure 2-8 Typical Beam-to-Column Joint Detail

As shown in Figure 2-9, the ponderosa pine frame beam-to-column connection was formed with a 1.5-inch thick red oak through-spline pegged to the column and wedged to the outside column face. The eastern white pine frame also had splined beam-to-column connections, but as shown in Figure 2-10, the spline was pegged to both the beam and column.

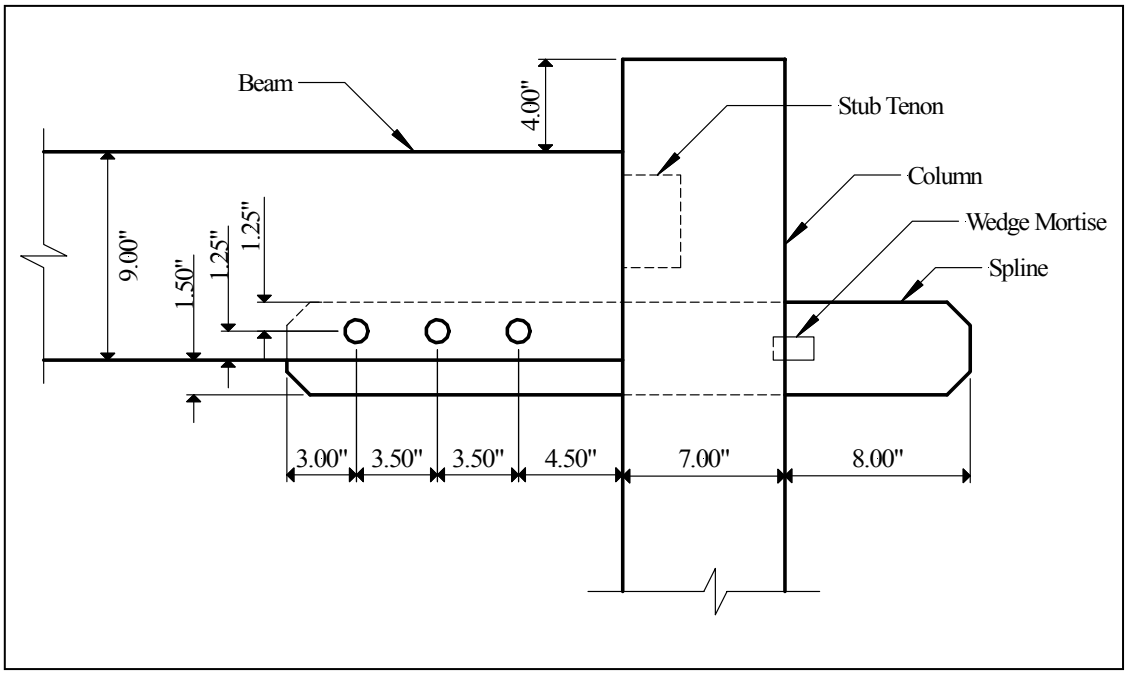

Figure 2-9 Ponderosa Pine Beam-to-Column Joint Detail

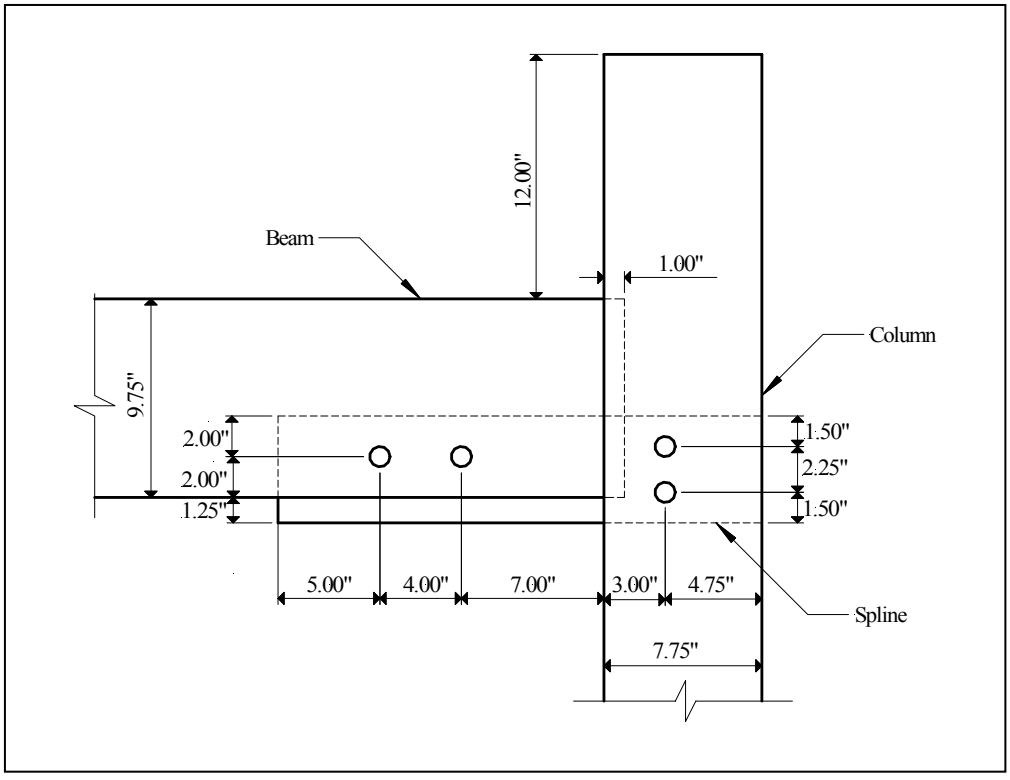

Figure 2-10 Eastern White Pine Beam-to-Column Joint Detail

2.3. Experimental Program

2.3.1. Test Setup

A schematic of frame loadings, reactions and global displacement is shown in Figure 2-11. The lateral load, P was applied by an MTS hydraulic actuator system with a load capacity of 55 kips and available displacement of 3 inches in each direction (6 inches total). Lateral load was applied to the beam of each assembly via steel plates lag screwed to each side of the beam. Application of the load to the beam most closely represented uniform lateral load transfer via diaphragm action. Applied force was measured with a load cell at the actuator. Global frame displacement, Δ_{top} was measured with a linear potentiometer located at the top of the frame.

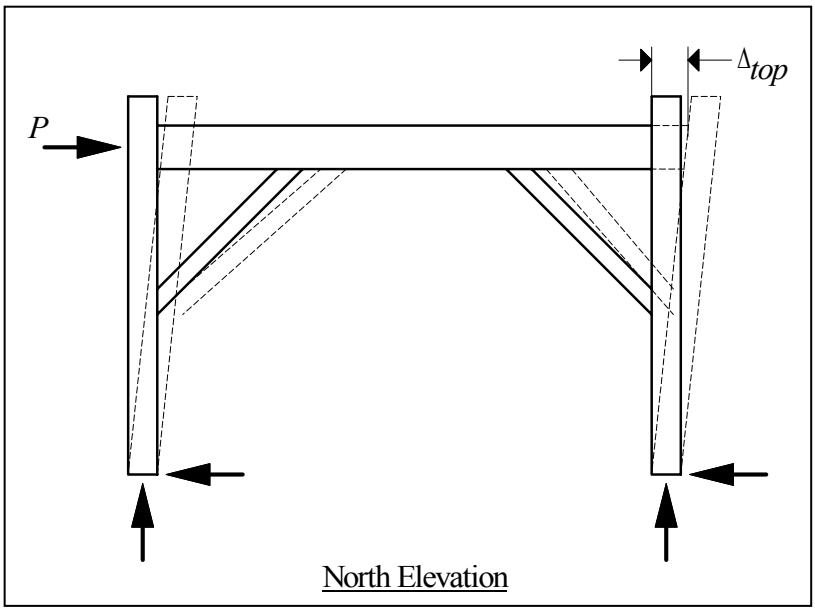

Figure 2-11 Load and Displacement Measurements

Displacement was imposed in both directions. As viewed from the north, load applied to the right is referred to as the "push" stroke and is plotted as a positive load on

all charts. Load applied to the left is referred to as the "pull" stroke and is plotted as a negative load on all charts.

2.3.2. Load Magnitude

The approximate magnitudes of the lateral load applied to the experimental frames were determined based on assumed structure location and dimensions. The following calculations for design lateral wind load are based on ASCE 7-02, Minimum Design Loads for Buildings and Other Structures (ASCE 2002). Equation (2.1) provides the velocity pressure, q_z in psf at any height. K_z is the velocity pressure exposure coefficient; K_{zt} is the topographic factor; K_d is the wind directionality factor; V is the basic wind speed in miles per hour; and I is the importance factor.

$$q_z = 0.00256 K_z K_{zt} K_d V^2 I \qquad \textbf{(2.1)}$$

For heights less than 15 feet, Equation (2.2) provides the expression for velocity pressure coefficient, K_z where z_g is the gradient height and α is the power law coefficient. These two coefficients are empirical values provided in Table 6-5 of ASCE 7-02.

$$K_z = 2.01(15/z_g)^{2/\alpha} \qquad \textbf{(2.2)}$$

For calculating a design load, the structure was assumed to be located in exposure category C; therefore z_g= 900, α = 9.5 and subsequently, K_z = 0.849. The structure was assumed to be in category II occupancy, therefore the importance factor is 1.0. Assuming a basic wind speed of 90 mph, a topographic factor of 1.0 and a wind directionality factor of 1.0, Equation 2.2 provides a velocity pressure q_z = 17.6 pounds per square foot (psf). This value is constant for any height up to 15 feet.

Design wind pressure, p_z is a function of building geometry and is calculated as shown in Equation (2.3), where q_z is the velocity pressure in psf; G is the gust effect factor; and C_p is the external pressure coefficient.

$$p_z = q_z G C_p \quad \textbf{(2.3)}$$

The structure was assumed flat-roofed and square in plan dimensions. Given these assumptions, the windward wall pressure coefficient is 0.8 and the leeward wall coefficient is –0.5. The gust factor is 0.85. Therefore, the windward wall design pressure is 12.0 psf and the leeward wall pressure is –7.5 psf. Statical division of the load dictates half of the load will be transferred to the top of the frame and half will be transferred to the bottom of the frame at the foundation. Assuming even lateral force distribution through a horizontal diaphragm and a bent spacing of 12 feet, the design wind load on one frame is 930 pounds.

In practice, the design wind load would vary depending on the aforementioned variables. Within this paper, the design wind load is provided only as a means to compare an applied test load to an anticipated design load. The maximum lateral load applied during the first cycle of frame loading was approximately equal to the design wind load of 930 pounds.

2.3.3. Gravity Load

Selected frames were tested with additional gravity load applied. The load was created by hanging several 300-pound concrete cylinders from each side of the beam. The load was typically applied as three point loads on the top of the beam to give a total load of 1800 pounds. As with the wind load, assuming bents spaced 12 feet on center, a total load of 1800 pounds would be equivalent to a uniformly distributed load of 12.5 psf. A distributed load of 12.5 psf is a reasonable estimate of expected dead load along with some sustained live load.

2.4. Moisture Content and Joint Numbering

A Delmhorst J2000 meter with a probe length of 1.5 inches was used to measure moisture content at the joint locations of all frame members. Averages of moisture content for the 1S1B frames are listed in Table 2-4. Complete moisture content data are shown in Appendix A with the joints numbered as shown in Figure 2-12. Moisture content was not measured on the ponderosa pine frame.

Table 2-4 1S1B Frame Moisture Content (%)

	Columns	Beams	Knee Braces
Eastern White Pine	15.7	9.7	8.8
White Oak	18.6	18.4	16.8
Douglas Fir	16.8	15.2	15.6
Port Orford Cedar	9.4	9.8	8.9

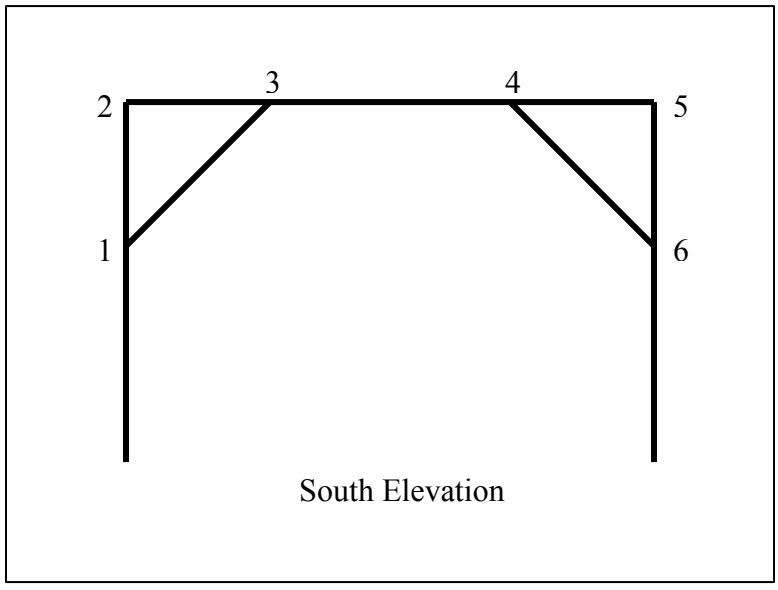

Figure 2-12 Joint Numbering for 1S1B Frames.

2.5. Overview of Test Results

The following sections provide a brief description of the load cycles for each of the five frames. Due to the need to investigate nuances of each frame, the number of load cycles applied to four of the five frames frame ranged from 3 cycles to 19 cycles. The Port Orford cedar frame was selected for the study of fatigue loading and therefore, was subjected to 912 reversible load cycles. Summary tables for the load cycles are provided in Appendix B.

Brief descriptions of observed joint damage and failure are also included in the following sections. In no instance was any frame loaded beyond its ultimate load. In other words, at the point of maximum load, the all frames were able to resist additional load.

Joint failure or damage was observed in many forms. The pegs commonly failed in two manners: a single hinged flexural failure labeled mode III as shown in Figure 2-13, and a double hinged shear and flexural failure labeled mode V as shown in Figure 2-14. Mode III and mode V failures are discussed in Chapter 1. Minor crushing of the peg material was also common in many of the joints.

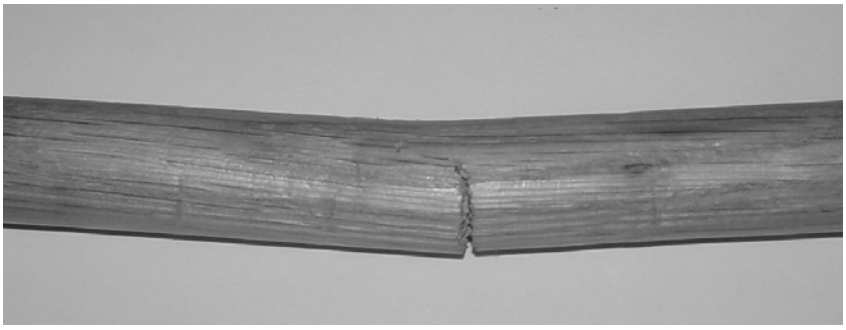

Figure 2-13 Mode III Flexural Peg Failure

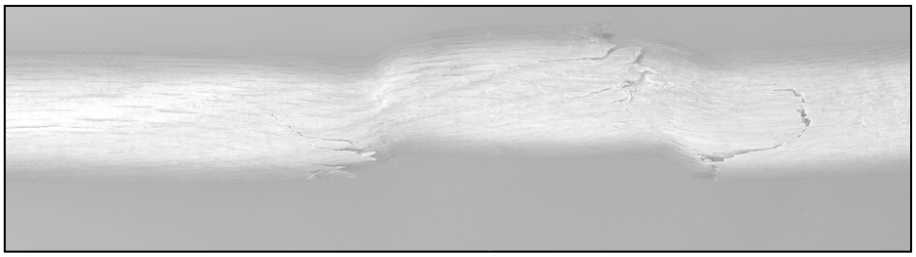

Figure 2-14 Mode V Shear-Flexural Peg Failure

Failure of the tenon relish was common in many frames. An example of relish failure is shown in Figure 2-15. There were also some instances of a single tenon split from the peg hole to the tenon end. Crushing of the tenon material at the edges of the peg hole was evident in many joints, particulary those of relatively low material specific gravity, such as eastern white pine. Similar damage occurred at the edges of the mortise peg holes.

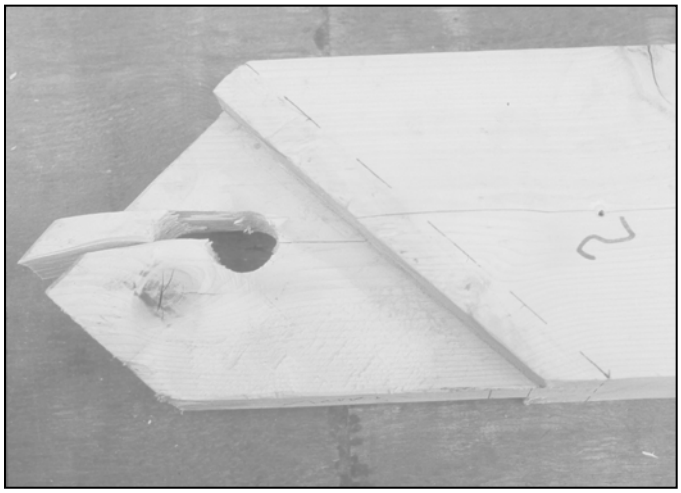

Figure 2-15 Tenon Relish Failure

Other forms of damage or failure occurred in isolated instances and are described individually in the appropriate section.

2.5.1. Douglas Fir

The Douglas fir frame was load cycled three times. The first cycle included no gravity load other than the frame's self weight, but the second and third cycles included 1800 pounds of additional gravity load. Maximum lateral loads of 2640 pounds on the push stroke and 2560 pounds on the pull stroke were applied on the final cycle.

Disassembly after testing revealed that the pegs located at the beam-to-column joints had minimal damage. However, three of the four knee brace pegs failed in flexure mode III. The knee brace peg at joint 1 had some bearing damage but otherwise did not fail. There was minimal damage to the members.

2.5.2. Eastern White Pine

The eastern white pine frame was subject to a total of 10 load cycles. The frame was initially cycled with no additional gravity load. Prior to the second cycle 1800 pounds of additional gravity load was applied and remained in place for the duration of testing. On the third cycle the wood knee brace pegs were replaced with steel dowels. All knee brace pegs were removed entirely for the fourth cycle and new woods pegs were reinstalled prior to the fifth cycle.

Cycles 5 through 7 included increasing load for each cycle with the applied load reduced to service level for the eighth cycle. Spline pegs were removed for the ninth cycle. New spline pegs were reinstalled for the tenth and final cycle, while all knee brace and column to beam joint pegs were removed.

No indication of failure was exhibited during testing. Disassembly of the frame revealed crushing of the peg located at knee brace joint 1. All of the knee brace tenons (joints 1, 2, 4, and 5) had slight damage near the peg hole. The holes were slightly

elongated and a minimal amount of spalling was present at the surface of the tenon. No damage was visible at the column to beam joints.

2.5.3. Ponderosa Pine

The ponderosa pine frame was initially cycled 7 times on the push stroke and once on the pull stroke, but several of those cycles were at loads less than 500 pounds. Multidirectional loading began on the ninth cycle. Additional gravity load of 3000 pounds was added for cycle 11 and reduced to 1200 pounds for cycle 12. The additional gravity load of 1200 pounds remained for the duration of testing.

The frame was tested with knee brace pegs removed for cycle 16, and the new pegs were reinstalled for subsequent tests.

Initial failure, during cycle 17, was exhibited by a loud "pop" sound from joint 4 as the frame reached an applied load of 2200 pounds in the push direction. Joint 4 was in tension during the push stroke. Although there was a tensile failure in the knee brace joint, the frame was able to resist additional load due to the compressive capacity of the opposing knee brace.

Cycle 18 produced a maximum displacement of 2.46 inches at a load of 2660 pounds on the push stroke, and 2.25 inches at 2190 pounds on the pull stroke.

Disassembly of the frame revealed no significant damage to the pegs, but there were tenon relish failures in knee brace joints 1 and 4.

2.5.4. Port Orford Cedar

The Port Orford cedar frame was subjected to a total of 912 load cycles. Of these, data was collected for only 11 cycles. The remaining cycles were conducted at a relatively rapid frequency of 12 cycles per minute with an imposed deflection of one inch in each direction.

Repair of joint 1, column to knee brace, was performed after 376 cycles. The knee brace mortise was originally mislocated and a patch or "Dutchman" had been installed with polyurethane glue. Although there is evidence to suggest that polyurethane glue is an acceptable structural adhesive (Vick 1998), it may not be appropriate for repairing timber frame joints. The original patch suffered significant delamination and was repaired prior to cycle 377 with a resorcinol adhesive. Testing immediately after repair indicated the patch had minimal effect on overall frame performance. The joint then performed as expected and no further repair was required.

Also, after 376 cycles, all pegs and both knee braces were replaced. Inspection of the original pegs revealed mode III failures in knee brace joints 1 and 4. A tenon relish failure also occurred at knee brace joint 4. The remaining pegs and tenons had minimal damage.

Replacement of the east knee brace included a load cell in-line with the member. As shown in Figure 2-16, this setup facilitated direct measurement of knee brace force.

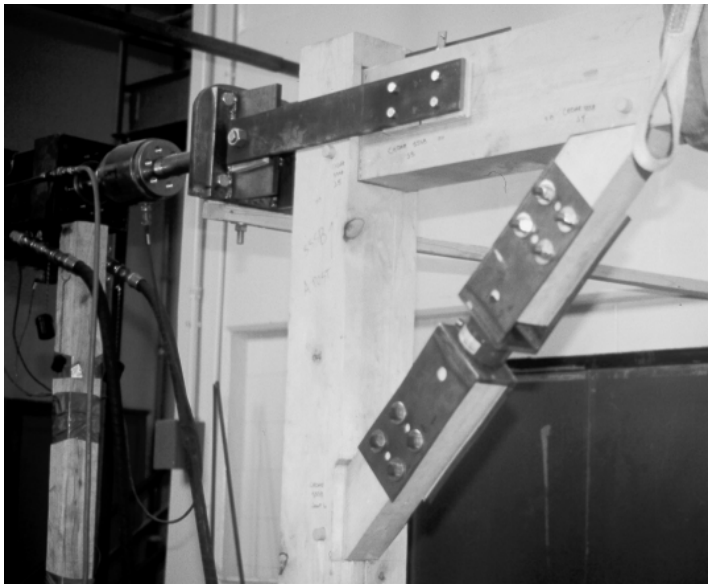

Figure 2-16 Port Orford Cedar 1S1B Knee Brace Load Cell

Prior to the final test, after cycle 1312, all pegs were again replaced. The pegs that were installed during cycles 377 through 1312 had significant failures. All of the pegs with the exception of knee brace joint 3 had mode III failures. The peg from joint 3 had only minor bearing damage.

The final test cycle subjected the frame to a maximum load of 2512 pounds on the push stroke and 2687 pounds on the pull stroke. Upon frame disassembly the following damage was observed: all of the pegs incurred mode III failures, and there was no damage to any frame tenons.

2.5.5. White Oak

The white oak frame was cycled eight times; however, five of the cycles were with SIP sheathing installed. The frame was initially cycled without gravity load and then 1800 pounds of dead weight was added for the second cycle. SIPs were then installed and the frame was cycled five times. Performance of sheathed frames is reported in Chapter 5. The panels were removed for the final cycle, but the data collected on the last cycle is of minimal value, because the frame appeared to be damaged during cycling with panels installed.

This frame had one of the few member failures observed throughout all of the testing. As the load approached the maximum of 2600 pounds on the push stroke, the west column began to split at the top. This was due to cross grain tension applied by the beam as it tended to withdraw from the column.

All of the pegs installed on this frame exhibited some bearing damage and several of the knee brace joint pegs failed. At the west knee brace, both pegs from joint 1 appeared to have the initial stage of mode V failure, as did one of the pegs at joint 3, and the other peg from joint 3 failed in a combination of mode III and mode V. Two of the pegs at the east knee brace failed in mode V, one of the pegs at joint 6 exhibited a combination of mode III and mode V failure, and one of the pegs at joint 4 showed only bearing damage. The white oak frame had significantly more peg damage compared to the other frames.

Relish failures were limited to the east knee brace. Joints 4 and 6 each had one relish failure.

2.6. Results

2.6.1. Service Level Load Results

Table 2-5 provides global stiffness results for the first load cycle that subjected each frame to the design lateral force of 930 pounds. The frames were subjected to lateral load and self weight only (no additional gravity load was applied). With an average stiffness of 3000 pounds per inch, the white oak frame had more than twice the stiffness of the other frames. The higher stiffness of the white oak frame is primarily due to the higher stiffness of oak joints and the additional peg at all knee brace connections.

Table 2-5 Service Level Performance With No Added Gravity Load

Frame	Push Stroke			Pull Stroke			Average Stiffness at Max Load (lb/in)	Total Free Disp. (in)
	Max Load (lb)	Max Disp. (in)	Stiffness at Max Load (lb/in)	Max Load (lb)	Max Disp. (in)	Stiffness at Max Load (lb/in)		
Douglas Fir	1010	1.13	1030	1010	1.14	990	1010	0.23
Eastern White Pine	1000	0.94	1340	1000	1.10	1130	1240	0.40
Ponderosa Pine	1200	1.05	1260	1200	1.28	1110	1190	0.30
Port Orford Cedar	990	0.85	1180	1000	0.83	1640	1410	0.25
White Oak	1520	0.50	3170	1530	0.56	2820	3000	0.05

As discussed in Chapter 1, previous joint testing by others has shown a reduced stiffness at low load. Such reduced low-load stiffness causes an interval of relatively low stiffness in the load-displacement curve of the full-scale frames. This deflection, termed *free displacement* $\Delta_{free,}$ is shown in the typical chart of Figure 2-17. The chart demonstrates the method of determining maximum global stiffness k_G and free displacement. Free displacement for all frames is shown in Table 2-5. The value ranges from a high of 0.40 inches for the eastern white pine frame to a low of 0.05 inches for the white oak frame. Again, the favorable value for the white oak frame is primarily a function of material properties and the added knee brace peg.

Service level load-displacement curves for all frames are shown in Appendix C.

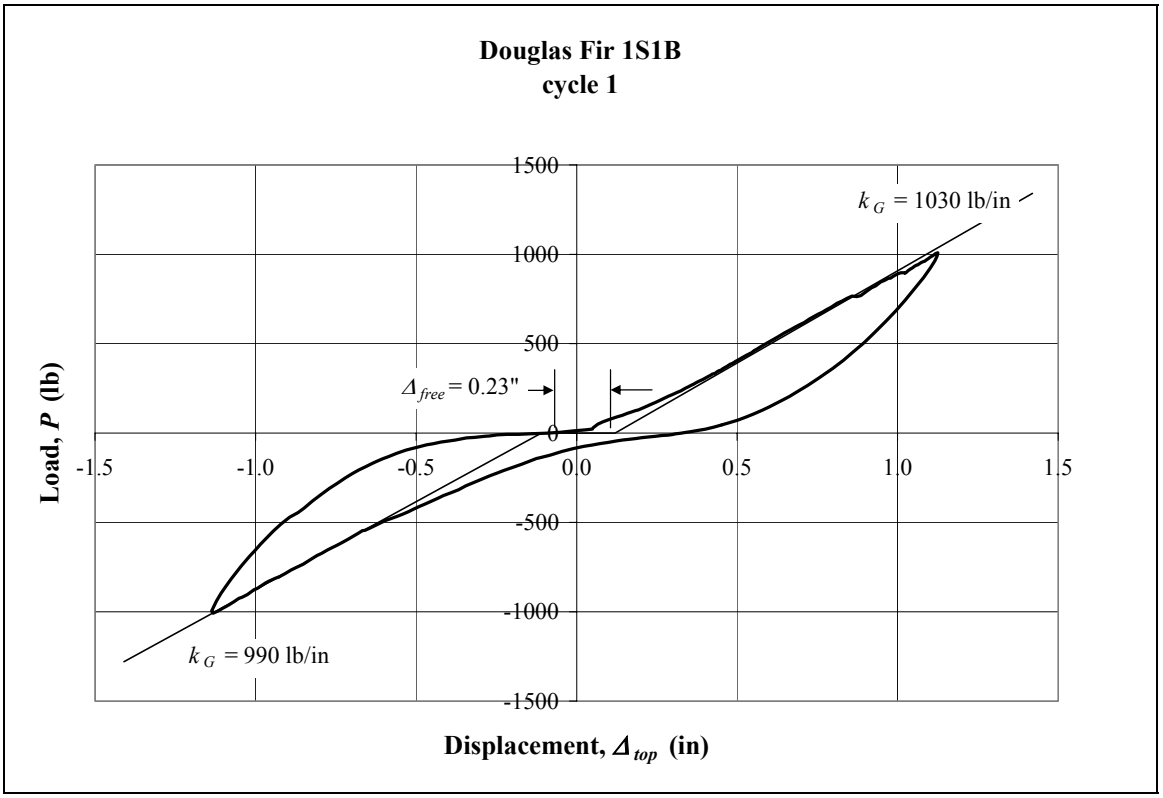

Figure 2-17 Typical Service Level Load vs. Displacement Curve

2.6.2. Effect of Gravity Load

Four of the frames were tested with additional gravity load applied to the beam and the results are shown in Table 2-6. Three of the frames were tested with 1800 pounds of additional gravity load, while the ponderosa pine frame was tested with both 1200 pounds and 3000 pounds of additional gravity load. Three of the four frames exhibited zero free displacement with the additional gravity load (the ponderosa pine frame required the full 3000 pounds before free displacement was eliminated). Figure 2-18 shows a load versus displacement curves for a frame with gravity load overlaying the curve for the same frame with no gravity load, thus indicating the reduction in free displacement. Curves for all frames with added gravity load are shown in Appendix D.

Table 2-6 Service Level Performance with Added Gravity Load

Frame	Gravity Load (lb)	Push Stroke			Pull Stroke			Average Stiffness at Max Load (lb/in)	Total Free Disp. (in)
		Max Load (lb)	Max Disp. (in)	Stiffness at Max Load (lb/in)	Max Load (lb)	Max Disp. (in)	Stiffness at Max Load (lb/in)		
Douglas Fir	1800	1000	1.07	1080	1030	1.10	1100	1090	0.30
Eastern White Pine	1800	1010	0.68	1490	1010	0.71	1430	1460	0
Ponderosa Pine	1200	1200	1.08	1440	1200	1.08	1120	1280	0.25
Ponderosa Pine	3000	1200	0.95	1200	1200	0.95	1060	1130	0
White Oak	1800	1500	0.35	3750	1580	0.42	3770	3760	0

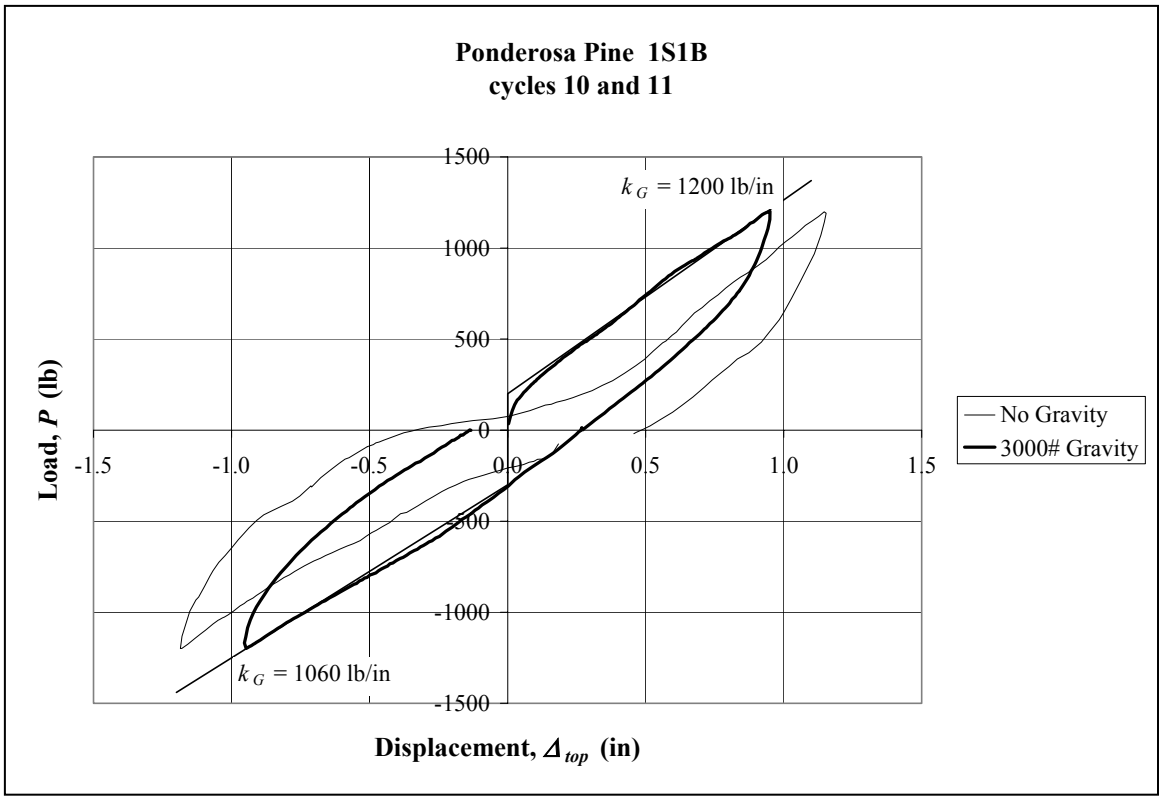

Figure 2-18 Reduction in Free Displacement Due to Gravity Load

The results for the Douglas fir frame are somewhat anomalous in that the frame exhibited **increased** free displacement when gravity load was added. As shown in Table 2-7 the addition of gravity load typically increased global frame stiffness and reduced total free displacement.

Table 2-7 Effect of Added Gravity Load

Frame	Gravity Load (lb)	Percent Increase in Stiffness	Percent Decrease in Free Displacement
Douglas Fir	1800	8%	-30%
Eastern White Pine	1800	18%	100%
Ponderosa Pine	1200	8%	17%
Ponderosa Pine	3000	-5%	100%
White Oak	1800	25%	100%

2.6.3. Removal of Knee Brace Pegs

An investigation of the effectiveness of knee brace pegs was performed by removing such pegs from the eastern white pine frame and comparing results to a previous test. A gravity load of 1800 pounds was in place for both tests.

As shown in Figure 2-19, removal of the knee brace pegs resulted in increased free displacement; however, the frame stiffness of 1270 pounds per inch is not significantly less than the fully pegged frame stiffness of 1460 pounds per inch. This indicates that a compressive knee brace attains increased stiffness as the knee brace shoulder bears on the column or beam surfaces. In this case, the stiffness of the single compressive knee brace was nearly as large as the combined stiffness of both a compressive and tensile knee brace.

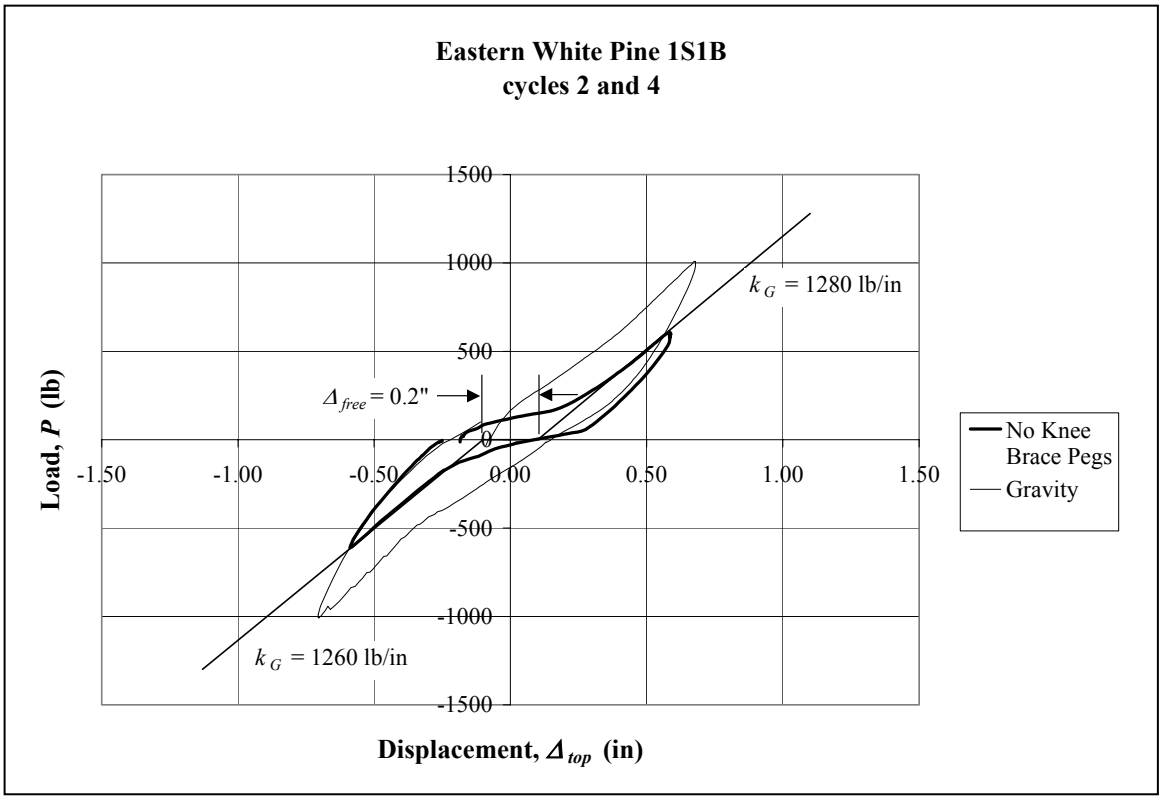

Figure 2-19 Effect of Removing Knee Brace Pegs

2.6.4. Direct Measurement of Knee Brace Force

As shown in Figure 2-16, a load cell was installed in one of the knee braces of the Port Orford cedar frame. Figure 2-20 shows both applied load and knee brace force plotted versus global frame displacement. This chart demonstrates the relatively higher proportion of lateral resistance provided by the knee brace when in compression compared to when it was subjected to tensile loading. The knee brace carried a compressive force that was 75 percent greater than the tensile force, 2419 pounds compression versus 1386 pounds tension.

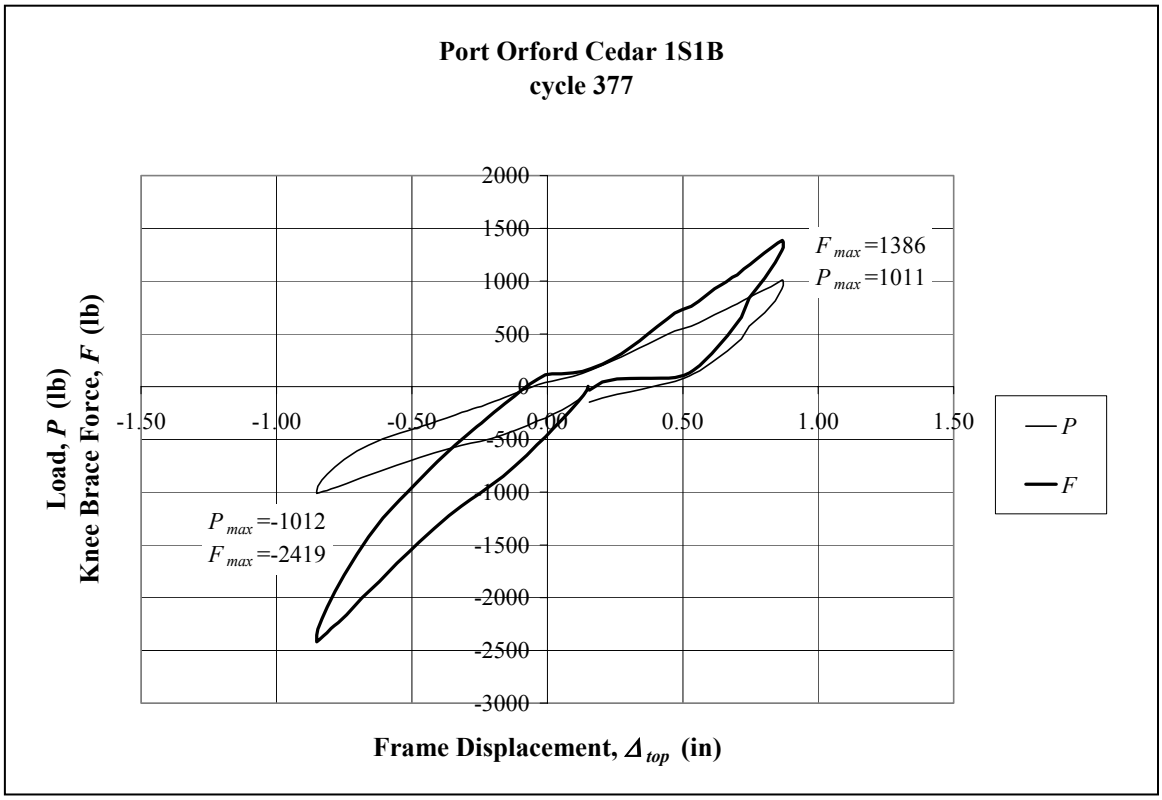

Figure 2-20 Knee Brace Force vs. Applied Load

In Figure 2-21, knee brace force is plotted against the sum of the corresponding knee brace displacements. The results can be interpreted two different ways for characterizing knee brace behavior.

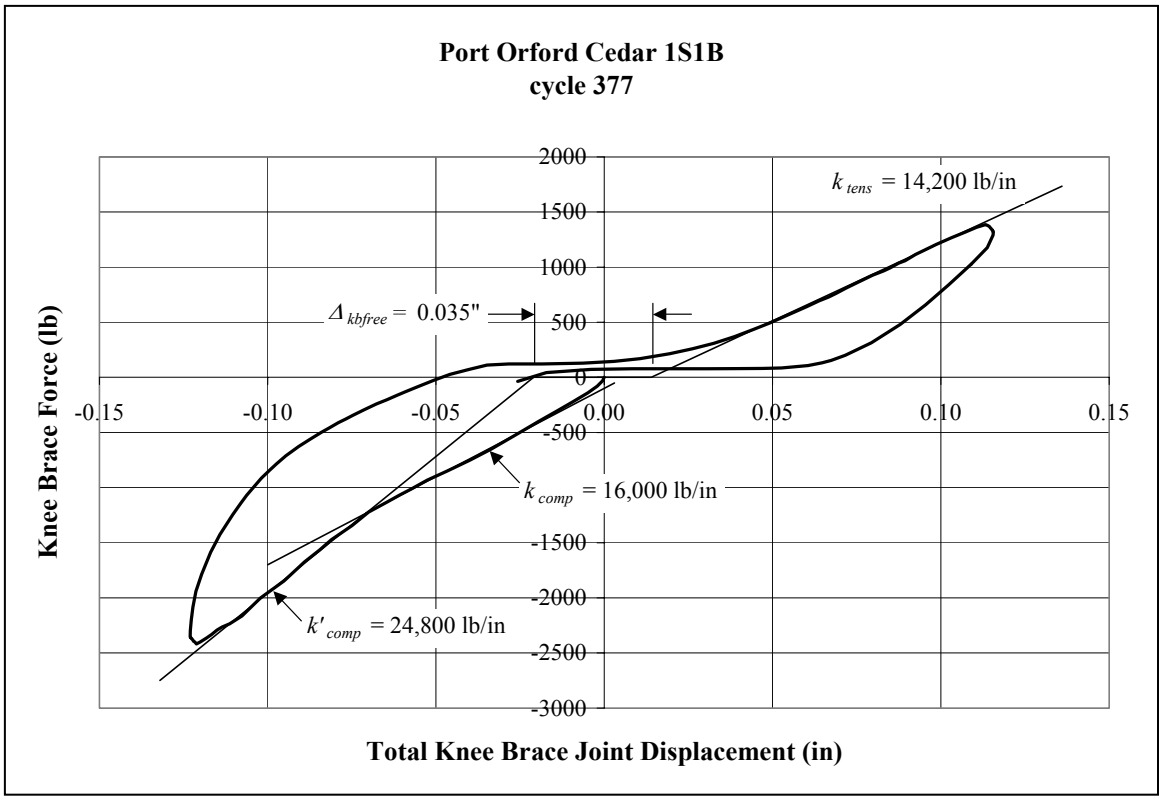

Figure 2-21 Knee Brace Stiffness

One method of interpretation assumes constant stiffness across the full range of displacement, although allowing a distinction between compressive and tensile actions. Tensile knee brace stiffness, k_{tens} = 14,200 pounds per inch, and compressive knee brace stiffness, k_{comp} = 24,800 pounds per inch with a free joint displacement Δ_{kbfree} = 0.035 inches.

However, Figure 2-21 obviously indicates two distinct parts of compressive behavior: an initial stiffness k_{comp} and a secondary stiffness k'_{comp}. The initial compressive stiffness k_{comp} = 16,000 pounds per inch is comparable to the tensile stiffness, and this behavior is assumed to be load transfer exclusively through the pegs. The significantly higher secondary stiffness k'_{comp} is assumed to be due primarily to bearing action of the knee brace shoulder onto the beam and column surfaces.

2.6.5. Unbraced Stiffness

In most modeling situations a wood-pegged mortise and tenon joint is assumed to act as a pinned connection. That is, the joint is expected to act as a hinge, thereby allowing no moment transfer between adjoining members. If the beam-to-column joint actually has some moment capacity, an unbraced frame would retain some minimal global stiffness. In order to evaluate this assumption, the eastern white pine frame was examined with the knee braces removed.

Figure 2-22 compares the frame with knee braces removed to the initial load displacement cycle. Gravity load of 1800 pounds was applied in both cases. Removal of the knee braces reduced the stiffness from the original average of 1460 pounds per inch to 300 pounds per inch. Although the frame retains some residual stiffness due to friction and the rotational restraint of the beam-to-column joint, the magnitude of this stiffness is minimal compared to the stiffness of the braced frame. Also of importance is the increase in free displacement to 0.5 inches, whereas the braced frame with gravity load had no free displacement.

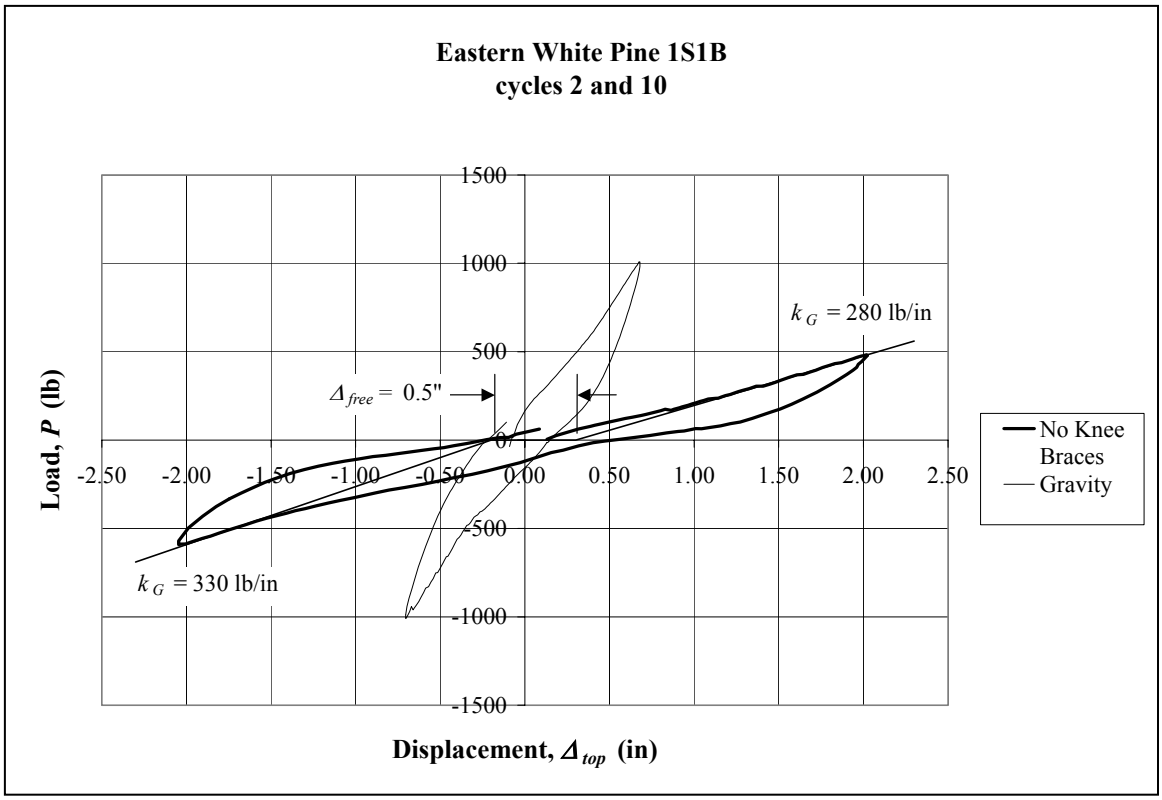

Figure 2-22 Effect of Removing Knee Braces

2.6.6. Cyclic Effects

The Port Orford cedar frame was cycled 350 times. The effects of cyclic loading are compared in Figure 2-23. The average global stiffness increased slightly from an average stiffness of 1410 pounds per inch prior to 1640 pounds per inch after 350 cycles. The increase in frame stiffness is not readily explainable but may be due to densification of the pegs, causing increased dowel bearing stiffness. While frame stiffness increased slightly, the free displacement increased dramatically from 0.25 inches to 0.75 inches.

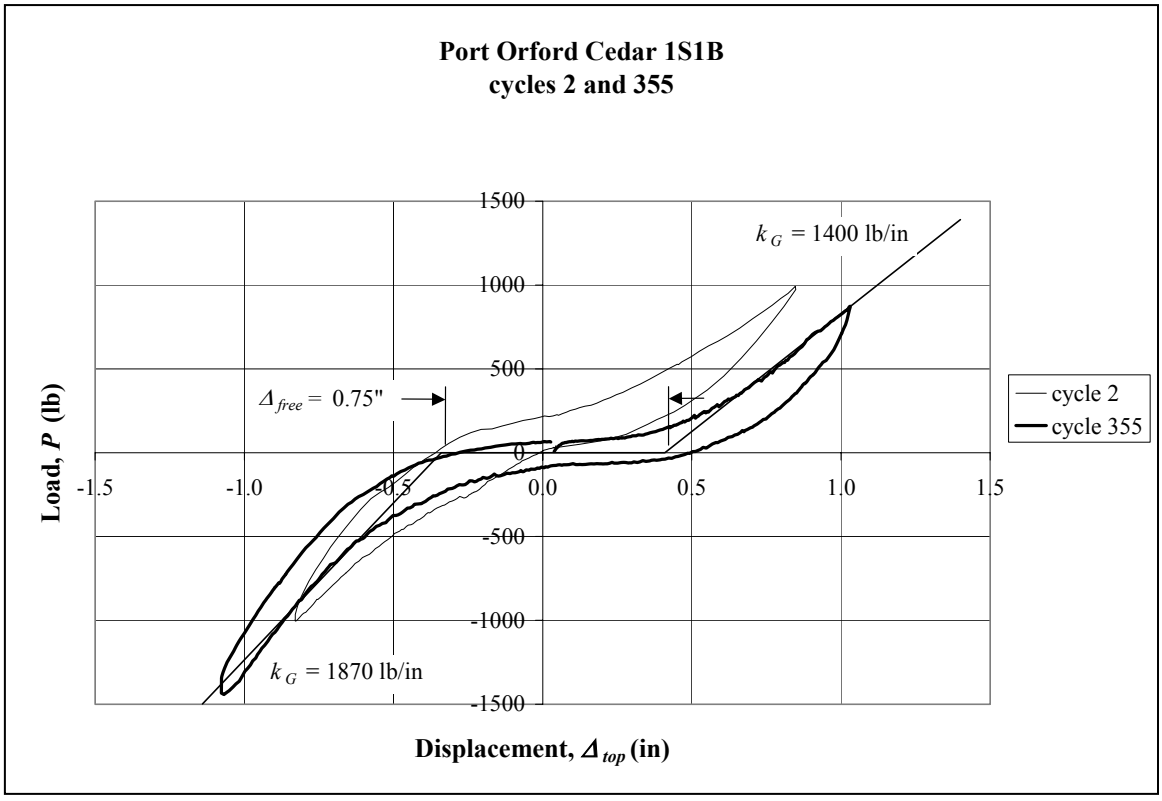

Figure 2-23 Cyclic Effects

Upon completion of the cyclic loading, both knee braces and all pegs were replaced. Additional testing then revealed that frame performance returned to the original level and free displacement was greatly diminished. Although the loads applied during cyclic loading were relatively low, the frame experienced displacements of 1 inch

in each direction. The high displacement was assumed to have caused peg and tenon damage resulting in consequential large free displacement.

2.6.7. Peg Effects

The significance of peg properties on frame performance was investigated by replacing the oak pegs with steel dowels in the knee brace joints of the eastern white pine frame. The global frame stiffness increased only slightly from 1460 pound per inch to 1510 pounds per inch and there was no free displacement. Gravity load was applied for both cases. As shown in Figure 2-24, there is little difference between the two curves.

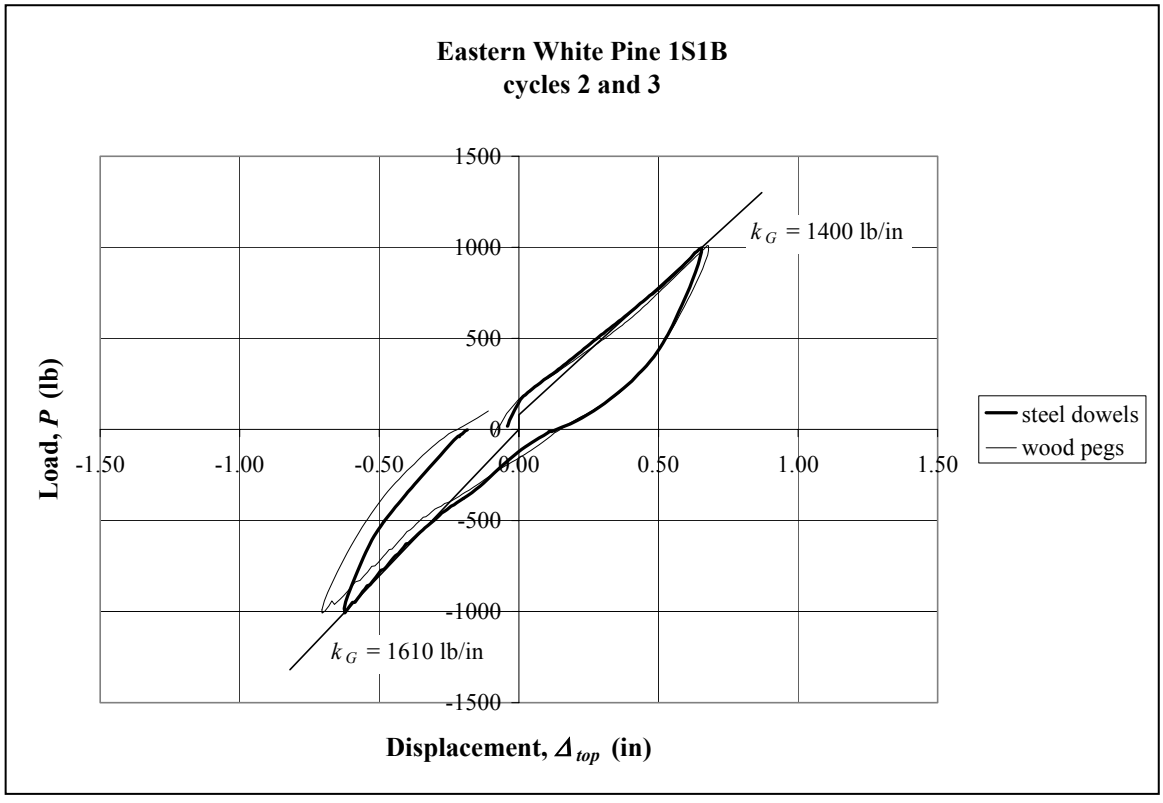

Figure 2-24 Effect of Peg Material

2.6.8. Maximum Load

A typical chart of the maximum displacement cycle is shown in Figure 2-25. Although there are spikes in the curve due to local failures, the frame continued to carry increasing load up to the maximum available displacement of approximately 3 inches. At such a high level of displacement, the frame is assumed to be well beyond any serviceability limit. Therefore, since this curve is typical of all frames examined, it can be concluded that stiffness, not strength, is likely to be the controlling design factor for unsheathed frames under lateral load.

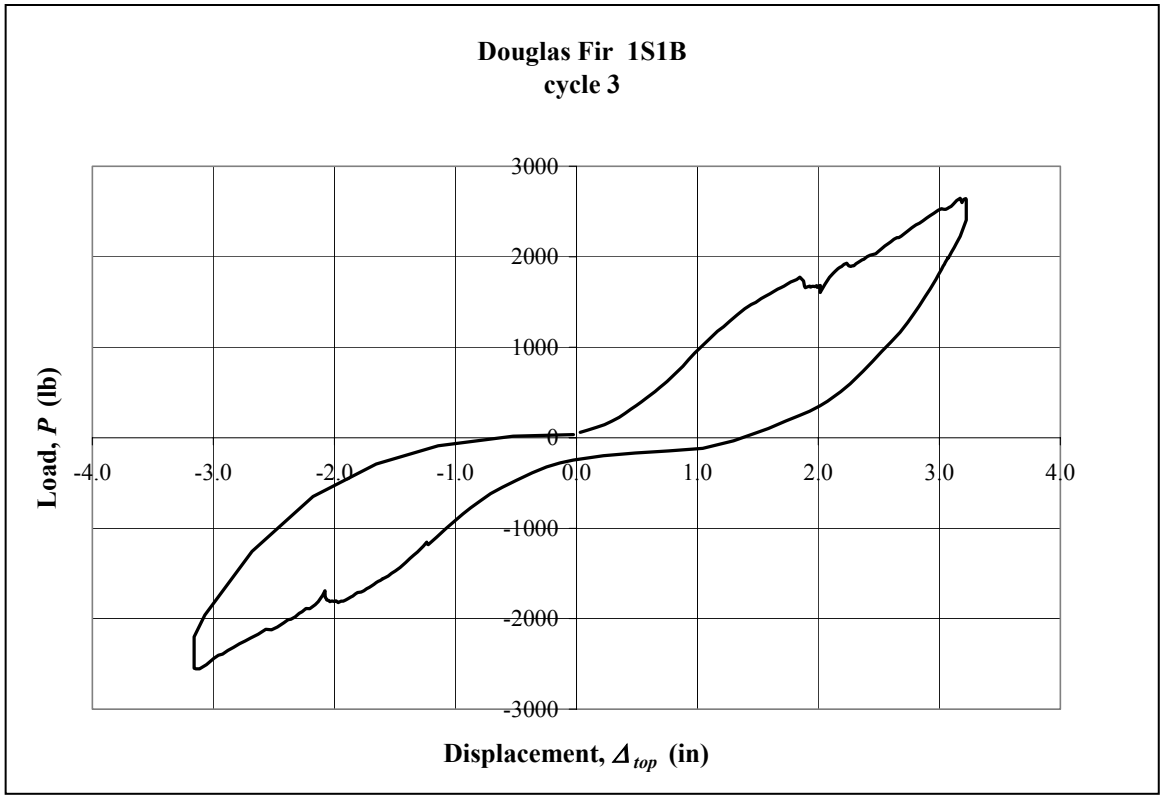

Figure 2-25 Typical 1S1B Maximum Load Cycle

Maximum load cycles for all frames are shown in Appendix E.

2.7. Summary

Using an allowable deflection of height/400, the allowable drift due to wind load on an eight-foot high frame would be approximately 0.25 inches. Given the design wind load of 930 pounds for a 1S1B frame, the minimum required frame stiffness would be 3720 pounds per inch. The stiffness of all frames was lower than this value. This indicates that traditional timber frames with knee braces as the primary lateral load support do not have adequate stiffness to resist typical wind loads. However, at displacements far beyond serviceable limits, all frames continued to carry increasing load. Therefore, these frames have sufficient strength to resist lateral load.

All frames exhibited free-displacement at low load levels. While this free-displacement may be an important design consideration, in all but one instance it was significantly reduced or eliminated with the application of additional gravity load. It is expected that most frames would be constructed and utilized such that additional gravity load due to floors, partition walls, finish materials and furnishings is always present.

Direct measurement of the knee brace force on the Port Orford cedar frame indicates that the knee brace in compression carries significantly more force than the tension brace. This is also supported by the test in which the knee brace pegs were removed from the eastern white pine frame. In this situation, the compression knee brace resisted all lateral load. Although the frame exhibited increased free-displacement, the magnitude of frame stiffness was nearly as large as the fully pegged frame.

Analysis of knee brace joint displacement versus force in the Port Orford cedar frame indicates that the compression component consists of two parts. The joint stiffness is initially relatively low at small displacement but increases as displacement increases.

A step increase in compression side stiffness is assumed to be due to the additional joint stiffness realized as the joint surfaces bear against one another.

The low stiffness of the unbraced eastern white pine frame indicates that the knee braces provide a majority of the frame stiffness. Thus, the assumption of a perfect hinge at the beam-to-column joint is acceptable.

Cyclic loading of the Port Orford cedar frame indicates that although there is minimal change in frame stiffness, the free-displacement increased significantly.

Substitution of the steel dowels in place of oak pegs in the eastern white pine frame revealed minimal change in frame behavior. Peg properties are therefore expected to have minimal effect on the behavior of frames constructed of low-density wood such as pine.

3. 2S2B Unsheathed Frame Testing

3.1. Overview

The primary objective of this part of the research project was to characterize the response of full-scale, two-dimensional, two-story two-bay (2S2B) timber frames subjected to lateral load. In addition, these full-scale tests presented the opportunity to closely observe the nuances of frame behavior and individual joint failure mechanisms.

The objective was accomplished by subjecting several frames to lateral load. The applied load and global displacement were measured and recorded with a computerized data acquisition system.

3.2. Test Assemblies

3.2.1. Frame Dimensions

The frames had an 8-foot story height and 12-foot nominal bay width; thus these frames had a total height of 16 feet measured to the top of the upper beam and nominal width of 24 feet measured from center to center of the outer columns. A photograph of a typical 2S2B frame is shown in Figure 3-1.

Figure 3-1 2S2B Frame

A general schematic of typical frame geometry is shown in Figure 3-2. Knee brace dimension, *kb* was either 30 inches or 36 inches, depending on frame manufacturer. Four frames were tested. Dimensions and descriptions of the individual structures follow.

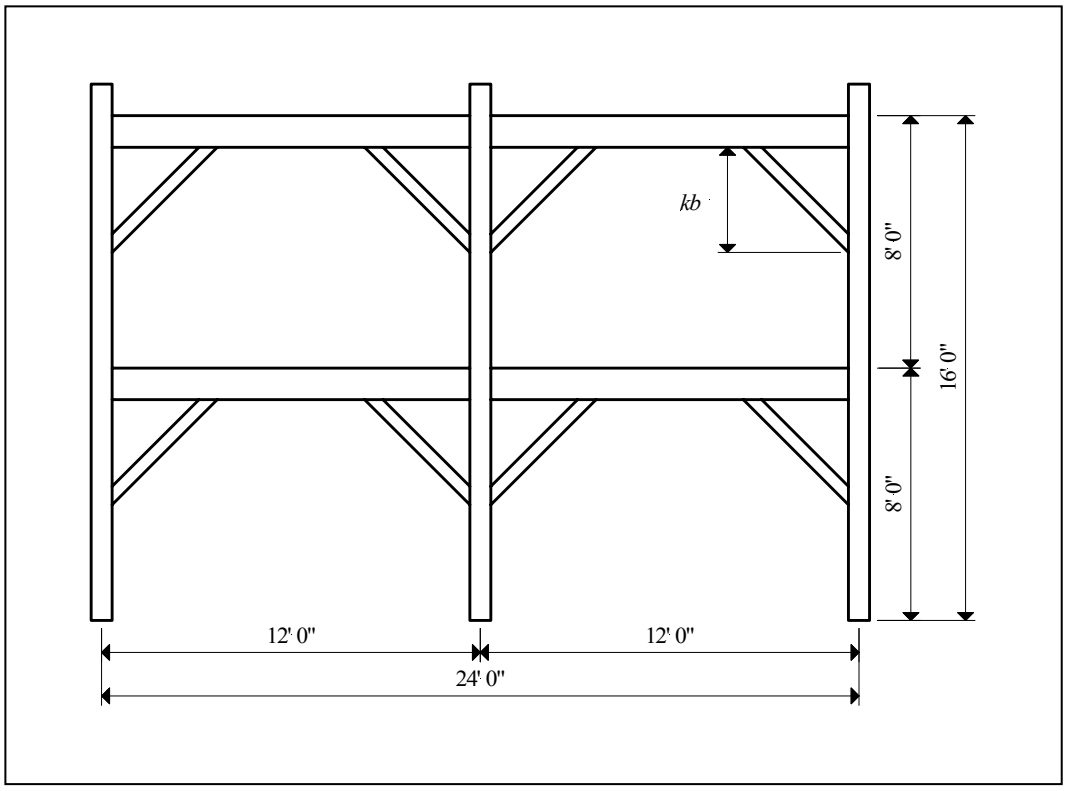

Figure 3-2 Typical 2S2B Frame Geometry

3.2.2. Frame Manufacturer and Species

Frames were provided by various manufacturers and were milled from several species of wood. Four companies each donated one frame: Riverbend Timber Framing, Blissfield, Michigan supplied a northern white oak frame; Benson Woodworking, Walpole, New Hampshire furnished an eastern white pine structure; Earthwood Homes, Sisters, Oregon donated a Port Orford cedar frame that was cut by non-professionals at a timber-framing workshop; and The Cascade Joinery, Everson, Washington provided a frame manufactured from Douglas fir.

3.2.3. Mortise and Tenon Joinery

The frames were constructed with traditional mortise and tenon connections fastened with wood pegs as described in Chapter 2.

3.2.4. Peg species and size

All joints utilized one-inch pegs with two exceptions. The white pine frames had ¾-inch pegs at the knee brace joints, and the white oak frame had 1¼-inch pegs at the beam-to-column splines.

The Port Orford cedar and eastern white pine frames had white oak pegs. The white oak frame also had white oak pegs with the exception of the spline pegs, which were red oak. The Douglas fir frame utilized red oak pegs.

3.2.5. Member Dimensions

As shown in Table 3-1 the timber cross-section dimensions and knee brace distance varied with each manufacturer.

Table 3-1 2S2B Frame Dimensions

	Beam		Column		Knee Brace		Knee Brace
	Width (in)	Depth (in)	Width (in)	Depth (in)	Width (in)	Depth (in)	Distance, *kb* (in)
Douglas Fir	5.25	9.25	7.25	7.25	3.25	5.25	30
Eastern White Pine	5.75	9.75	7.75	7.75	2.75	5.75	36
Port Orford Cedar	5.25	9.25	7.5	7.5	3.5	5.5	30
White Oak	6.75	8.75	6.75	10.75	4	6	36

The frames were typically shipped in the green moisture condition and all timbers were planed. However, due to the extended period of the testing schedule, significant drying and consequential shrinkage occurred in the timbers. Therefore, the dimensions listed are approximate and may vary as much as 0.25 inches for a given frame member.

3.2.6. Knee Brace Joint Details

Details of knee brace joint dimensions are listed in Table 3-2. The criteria for measuring and recording joint details are described in Chapter 2. Two values for end distance are listed for the 2S2B frames. The first is the end distance for knee braces located at the exterior (ext) columns. The second set of end distance refers to the interior (int) columns where interference from opposing braces may have required the knee brace tenons to be clipped, thus resulting in reduced end distance.

Table 3-2 2S2B Knee Brace Joint Details

	End Distance (in)		Edge Distance (in)	Tenon Width (in)	Housing Depth (in)	Number of Pegs	Peg Diameter (in)
	ext	int					
Douglas Fir	3.25	2.25	2.5	2	0.5	1	1
Eastern White Pine	1.5	1.5	1.75	1.5	0	1	0.75
Port Orford Cedar	2.5	2	2	2	0.5	1	1
White Oak	1.5	1.5	1.5	2	0	2	1

3.2.7. Beam to Exterior Column Connection

With one exception, the beam to exterior column connection was a typical mortise and tenon, pegged joint. Such a joint detail is shown in Chapter 2, Figure 2-8. The dimensions of the beam-to-column connections are listed in Table 3-3.

Table 3-3 2S2B Beam to Exterior Column Joint Details

	End Dist. (in)	Edge Dist. (in)	Tenon Width (in)	Tenon Height (in)	Housing Depth (in)	Number of Pegs	Spacing (in)
Douglas Fir	3	3	2	5	1	2	2.5
Eastern White Pine (lower beam)	4.75	1.75	2	9.5	0	2	2.5
Port Orford Cedar	2.75, 3.75	3, 2	2	5	1	2	3
White Oak	2.25	1.5	1.75	8.25	1	2	2.5

As noted in the table, the dimensions are valid for only the lower beam of the eastern white pine frame. The upper beam of the eastern white pine frame was connected to the exterior column with a fork and tongue joint as shown in Figure 3-3. Tenon thickness was 2 inches.

In the Port Orford cedar frame the peg holes of the beam to exterior column joints were offset; therefore, two values of end distance are provided. The columns of the Douglas fir frame extended approximately 12 inches above the level of the upper beam.

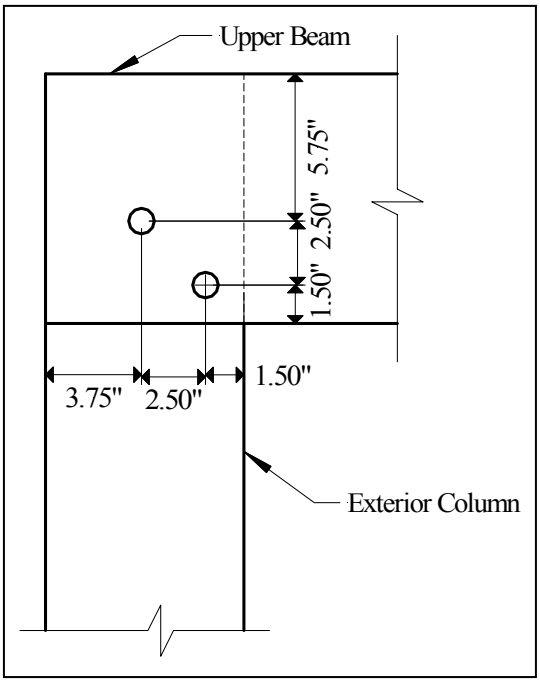

Figure 3-3 Eastern White Pine Exterior Column to Upper Beam Fork and Tongue Joint

3.2.8. Beam to Interior Column Connection

All frames had continuous columns with the lower beams connected across the interior column via a spline. Figure 3-4 shows typical details of the lower beam to interior column spline connection, and dimensions are shown in Table 3-4. For the eastern white pine frame, the spline was mortised into the top surface of the beam rather than the bottom.

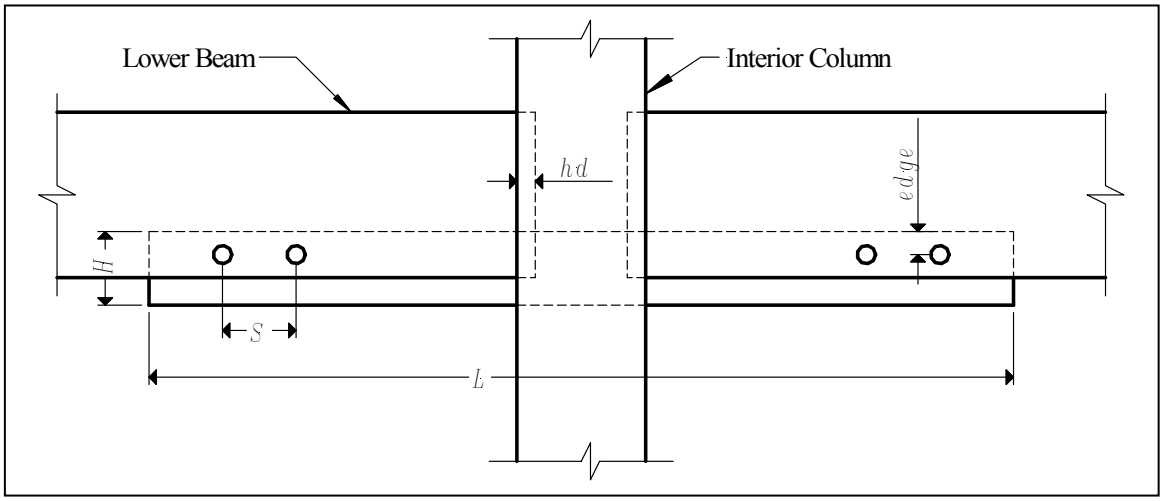

Figure 3-4 Beam to Interior Column Spline Connection

Table 3-4 2S2B Beam to Interior Column Spline Joint Details

	Spline Dimensions			Spline Material	No. of Pegs (total)	Peg Diam. (in)	Peg Space, *S* (in)	Edge Dist, *edge* (in)	House. Depth, *hd* (in)
	L (in)	*H* (in)	Thick (in)						
Douglas Fir	48	4.5	1	LVL	8	1	4	1.5	1
Eastern White Pine	40	4	1.5	Oak	4	1	4	2.5	0
Port Orford Cedar	48	3.5	1.5	Lodge-pole Pine	4	1	4	2	0
White Oak	48	4.75	2	Red Oak	4	1.25	6	1.5	1

The details in Table 3-4 apply to both the middle and upper beams of the Douglas fir and white oak frames. However, the upper beam of the eastern white pine and Port Orford cedar frames were continuous across the center column; therefore, typical mortise and tenon construction was utilized. Details of the Port Orford cedar and eastern white pine interior column to upper beam connection are shown in Figure 3-5 and Figure 3-6 respectively. The column tenon of the eastern white pine frame extended through the beam. The tenon thickness was 2 inches for the eastern white pine frame and 1.5 inches for the Port Orford cedar frame.

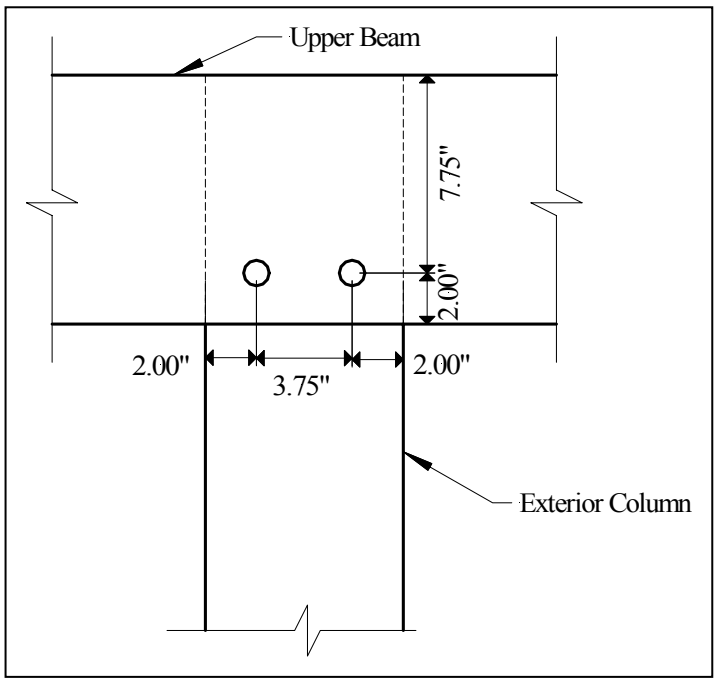

Figure 3-5 Eastern White Pine Upper Beam to Interior Column Connection

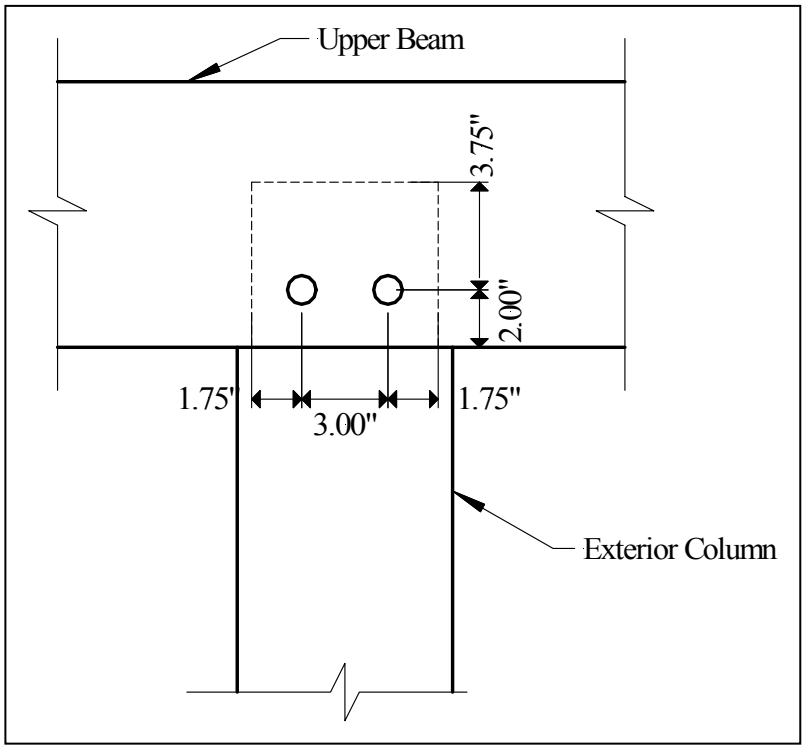

Figure 3-6 Port Orford Cedar Upper Beam to Interior Column Connection

3.3. Experimental Program

3.3.1. Test Setup

A schematic of frame loadings, reactions and global displacements is shown in Figure 3-7. Lateral load *P* was applied by an MTS hydraulic actuator system with a load capacity of 55 kips and available displacement of 3 inches in each direction (6 inches total). The applied force was measured with a load cell at the actuator. The actuator load was transferred equally to the upper and lower beams via a load splitting mechanism. Half of the actuator force *P*/2 was applied to each beam level via steel plates lag screwed to each side of the beam. Application of the load to the beams most closely represented uniform lateral load transfer via diaphragm action. Global displacements, Δtop and Δmid were measured with two 15-inch string potentiometers, one each at the upper and lower beam levels.

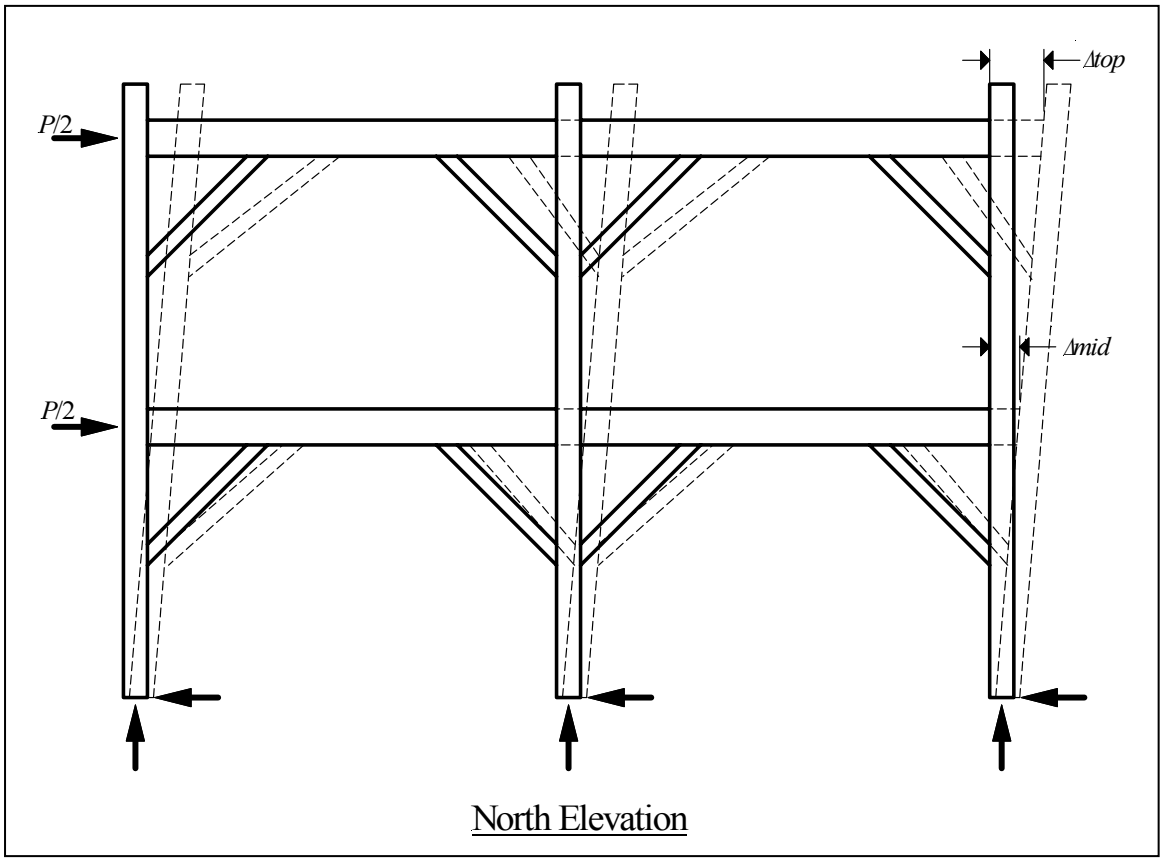

Figure 3-7 2S2B Load, Reactions and Global Displacements

Displacement was imposed in both directions. As viewed from the north, load applied to the right is referred to as the "push" stroke and is plotted as a positive load on all charts. Load applied to the left is referred to as the "pull" stroke and is plotted as a negative load on all charts.

3.3.2. Load Magnitude

Although the magnitudes of the lateral load applied to the experimental frames were selected somewhat arbitrarily, a comparative value of design lateral load has been determined based on assumed structure location and dimensions. Based on these assumptions, a total design wind pressure of 19.5 psf was calculated in Chapter 2. Assuming the structure was flat roofed and square in plan with 12-foot bent spacing and

also assuming half of the load applied at the lower level will be transferred directly to the foundation, the total design wind load for the 2S2B frame is 2800 pounds. This value would vary depending on the aforementioned variables and is only provided as a means to compare an applied test load to an anticipated design load.

3.3.3. Gravity Load

No additional gravity load was applied to the 2S2B frames.

3.4. Moisture Contents and Joint Numbering

A Delmhorst J2000 meter with 1.5-inch probes was used to measure moisture content at the joint locations of all frame members. Averages of moisture content for the 2S2B frames are listed in Table 3-5. Complete moisture content data are shown in Appendix F.

Table 3-5 2S2B Frame Moisture Content (%)

	Columns	Beams	Knee Braces
Douglas Fir	9.6	8.4	8.0
Port Orford Cedar	7.8	7.7	7.7
Eastern White Pine	7.0	7.0	6.8
White Oak	6.5	6.6	6.2

Figure 3-8 shows the joint numbering scheme that is referred to in the following discussion of joint failures.

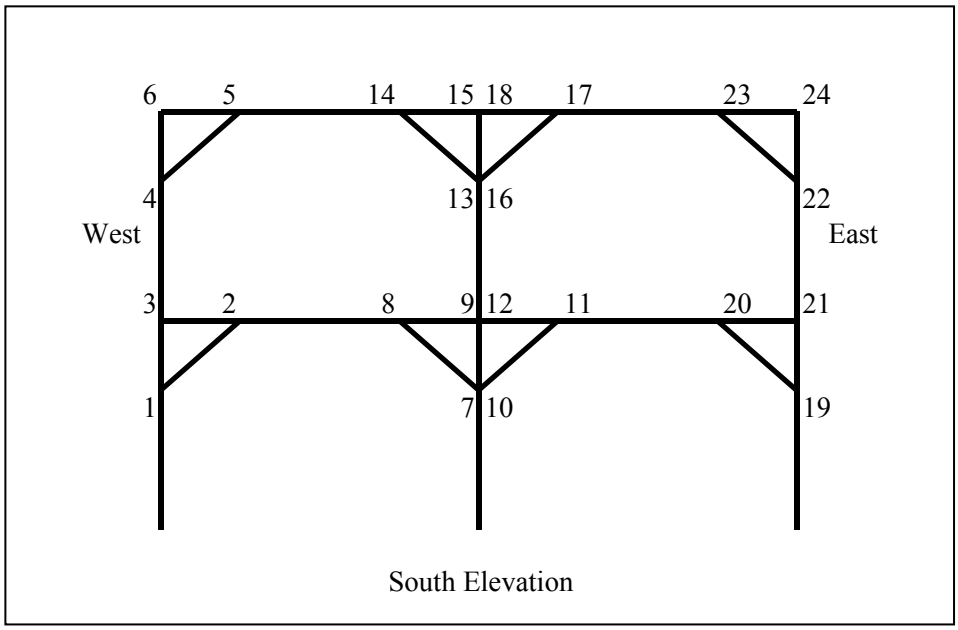

Figure 3-8 2S2B Joint Numbering

3.5. Overview of Test Results

The following sections provide a brief description of the load cycles for each of the five frames. Summary tables for the load cycles are provided in Appendix G. Brief descriptions of observed joint damage and failure are also included in the following sections.

Failure of individual frame joints was observed in many forms as described in Chapter 2. The failure types include flexural type mode III, combined flexural and shear mode V, and tenon relish. Tenon splitting and crushing of peg, tenon, and mortise base material was also observed. Other, isolated instances of failure or damage are described in the appropriate section.

3.5.1. Douglas Fir

The Douglas fir frame was cycled 115 times, however, 109 of the cycles were performed with SIP sheathing installed. The frame was cycled three times prior to panel installation and then three times after panels were removed. The frame was displaced a maximum of two inches of ram stroke in each direction with the panels installed.

Disassembly of the frame revealed a single relish failure at knee brace joint 20. Peg failures occurred at knee brace joints 1, 4, and 22. All of these failures occurred at knee braces located at the outer columns. Mode III peg failures were present at knee brace joints 1, 4, and 22. These failures occurred at both the upper and lower beam levels.

3.5.2. Eastern White Pine

The white pine frame was cycled 19 times, but 13 of the cycles were performed with SIPs installed. The frame was initially cycled four times without panels, 13 times with SIPs installed, and two final times with the panels removed.

Failure of this frame was achieved by subjecting the frame to a high magnitude of displacement. Additional displacement was created by pushing the frame to maximum available ram stroke, relieving load, and resetting the load fixture. By repeating this process two times, a total of 8 inches of displacement at the ram was effected. The load reached a maximum of 6150 pounds at a top beam lateral displacement of 6.90 inches. Although several joints had failed, the frame was continuing to carry load, but a cross grain tensile failure occurred at the west column reaction connection. This failure rendered the frame unable to carry additional load.

Inspection of the joints upon disassembly revealed relish failures at joints 2, 8, 13, 16, 19, and 23. In addition to the relish failures, there was a cross grain tension failure of the tenon in the top beam at joint 6 and there was also significant spalling due to wedging of the beam at joint 16.

Mode III peg failures occurred at knee brace joints 2, 4, 10, and 20 and at beam-to-column joint 21. The failure of the peg located at joint 21 occurred in the vicinity of a small knot in the peg.

3.5.3. Port Orford Cedar

The cedar frame was cycled 609 times; however, data was recorded for only 13 of the cycles. The frame was initially cycled five times and then oscillated 600 times at a period of one second and a ram displacement of one inch in each direction. The frame was then cycled six more times

No failures were present in the frame joints. The knee brace peg at joint 10 had a mode III failure but the peg had sloped grain and a small knot near the failure These defects likely contributed to failure of the peg.

3.5.4. White Oak

The white oak frame was cycled 9 times. As with the eastern white pine frame, additional ram stroke was obtained by successive loading and resetting of the load fixture. In this manner, the frame was subjected to a maximum top displacement of 8.51 inches in the push direction at total load of 15,700 pounds.

Ultimate frame failure occurred at joint 6, the location of upper beam to west column connection. Tenon relish failures occurred at several joints. A single relish failure occurred at knee brace joints 13, 14, and 19. Relish failure was present at both peg holes in knee brace joints 8 and 22. Splitting of the tenon occurred at knee brace joints 1 and 4, and joint 2 had a relish failure at one peg hole and a split in the tenon behind the other peg. The tenon at knee brace joint 20 was destroyed with the tenon severed across both peg holes.

The oak splines also failed. Both splines had relish failure through both peg holes at one end. The peg in the spline at joint 12 also incurred a mode III failure.

Mode III failures were present in a single peg at knee brace joints 1, 4, 11, 13, and 22 and at beam-to-column joint 3. Both pegs at knee brace joint 5 incurred mode III failures. Mode V failures were present in a single peg at knee brace joint 4 and at both pegs in knee brace joint 2. Mode V failure was also exhibited in a single peg at beam-to-column joint 3 and in both pegs at beam-to-column joint 6. Note that most of the failures are near the west side of the frame, which appeared to resist a larger portion of the load when subjecting the frame to the maximum displacement to the west.

3.6. Results

3.6.1. Service Level Load Results

Table 3-6 provides global stiffness k_G results for the first viable load cycle of significant lateral load. A typical load-displacement plot is shown in Figure 3-9.

With an average stiffness of 3060 pounds, the white oak frame had more than twice the stiffness of the other frames. The increased stiffness of the white oak frame is primarily due to the higher stiffness of oak joints and the additional peg at all knee brace connections.

Table 3-6 Summary of Service Level Testing

Frame	Cycle	Push Stroke			Pull Stroke			Average Stiffness at Max. Load (lb/in)
		Max. Load (lb)	Max. Disp. (in)	Stiffness at Max. Load (lb/in)	Max. Load (lb)	Max. Disp. (in)	Stiffness at Max. Load (lb/in)	
Douglas Fir	2	983	1.01	790	1147	1.02	1010	900
Eastern White Pine	3	1990	1.54	1450	2050	1.53	1130	1290
Port Orford Cedar	4	1515	1.13	1240	1524	1.2	1160	1200
White Oak	1	3050	1.02	3270	3360	1.02	2860	3060

Contrary to indications of the 1S1B frames, the 2S2B results revealed no free displacement at low loads.

Load-displacement plots of service level load for all frames are shown in Appendix H.

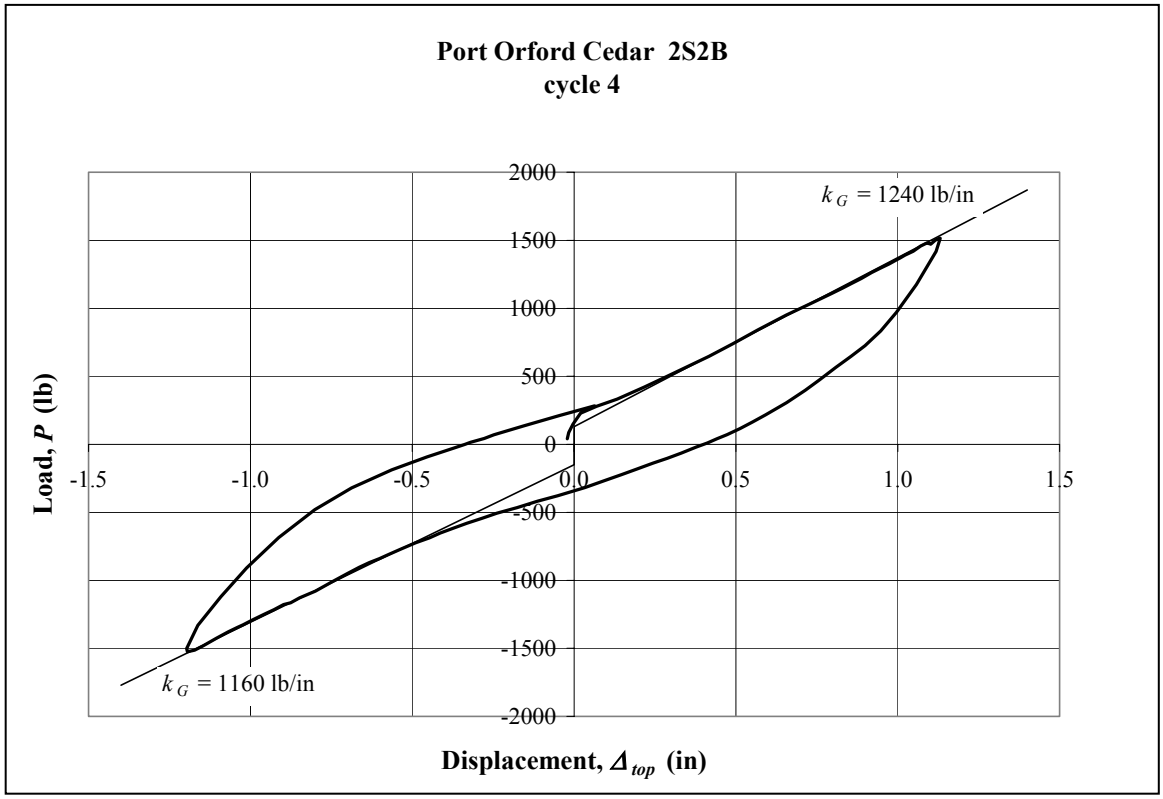

Figure 3-9 Typical Service Level Load vs. Displacement Curve

3.6.2. Effect of Removing Knee Brace Pegs

The effects of removing knee brace pegs were explored on the white oak frame. In this frame, each knee brace joint had two pegs. One of the pegs was removed for cycle 5 and both were removed for cycle 6. As shown in Table 3-7, the removal of one peg reduced frame stiffness by only 16% while removing both pegs reduced stiffness by 79%. The results of peg removal are graphically demonstrated in Figure 3-10.

Table 3-7 Removal of Knee Brace Pegs

Cycle	Condition	Push Stroke		Pull Stroke		Average Stiffness at Max. Load (lb/in)	Difference
		Max. Load (lb)	Stiffness at Max. Load (lb/in)	Max. Load (lb)	Stiffness at Max. Load (lb/in)		
1	Fully pegged	3050	3270	3360	2860	3060	0%
5	One peg removed	2190	2450	2470	2700	2570	16%
6	Both pegs removed	698	760	623	530	640	79%

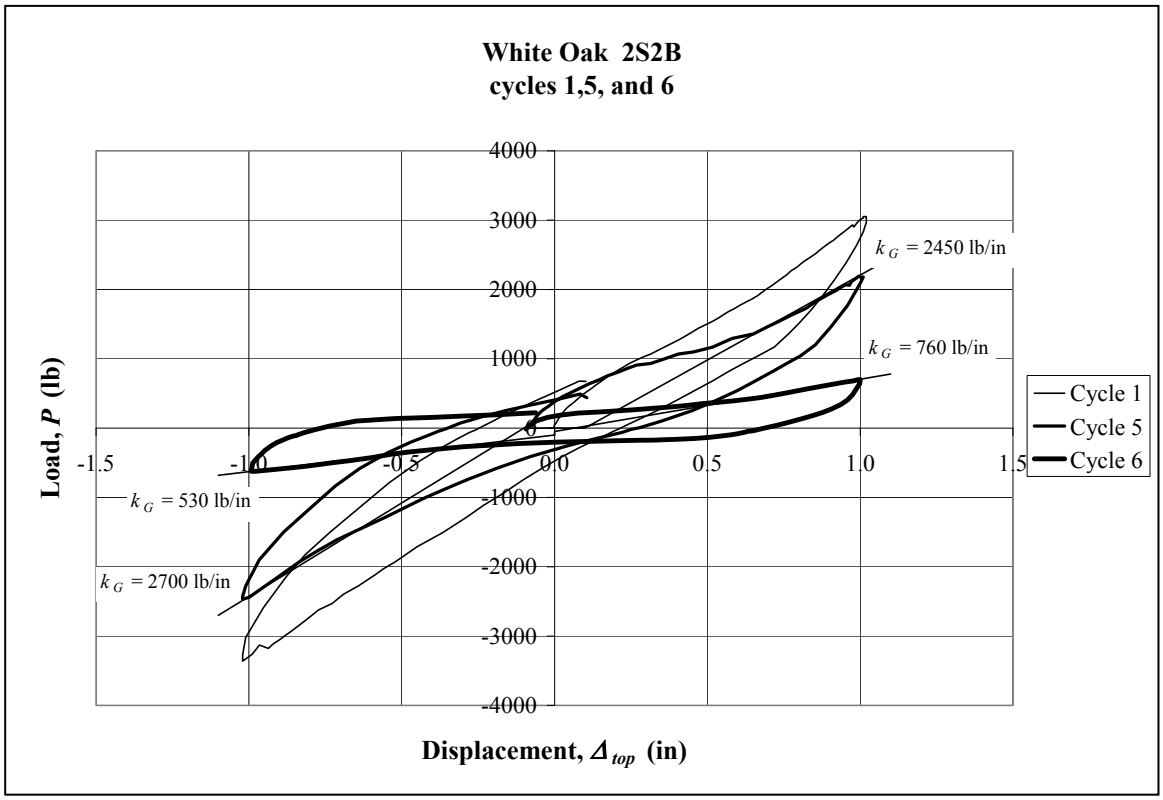

Figure 3-10 Effect of Removing Knee Brace Pegs

3.6.3. Cyclic Effects

Two frames were examined for the effects of multiple load cycles. The Douglas fir frame was subjected to approximately 100 cycles with SIPs installed. Figure 3-11 compares the load-displacement response of cycle 114 to cycle 2. The average frame stiffness was reduced from 900 pounds per inch to 670 pounds per inch, but there was no evidence of free displacement.

As shown in Figure 3-12, subjecting the Port Orford cedar frame to 600 cycles did not significantly affect global stiffness, but the effects of cycling created a free displacement of 0.3 inches. This was the only incidence of free displacement in a 2S2B frame subjected to service level lateral loading.

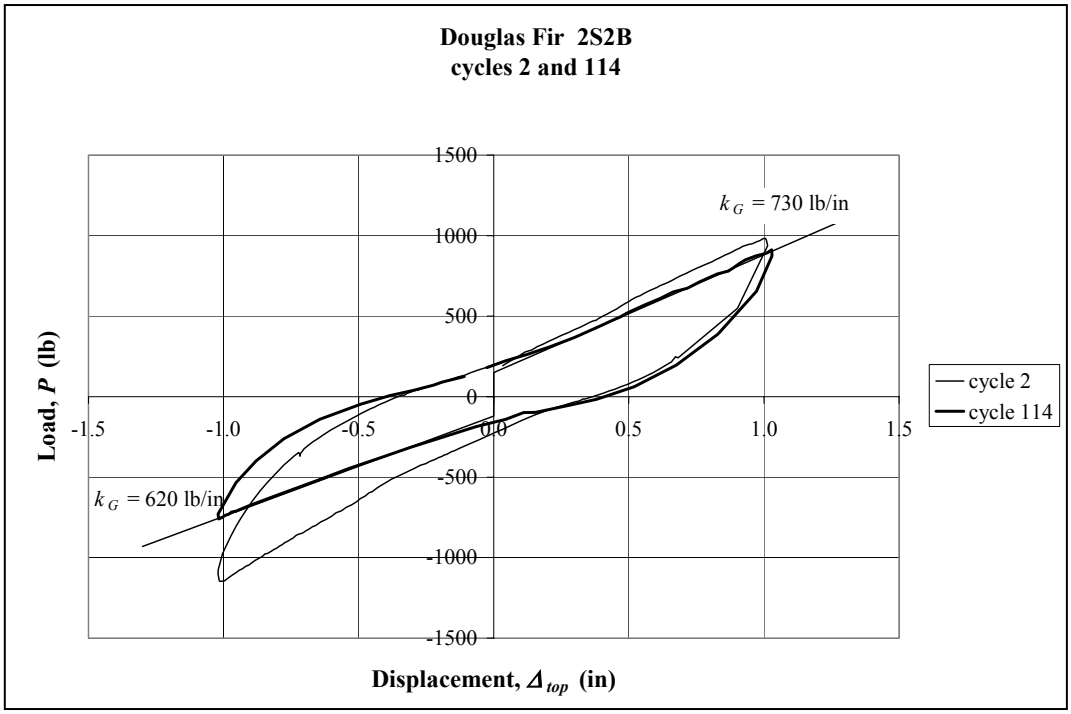

Figure 3-11 Cyclic Effects on Douglas Fir Frame

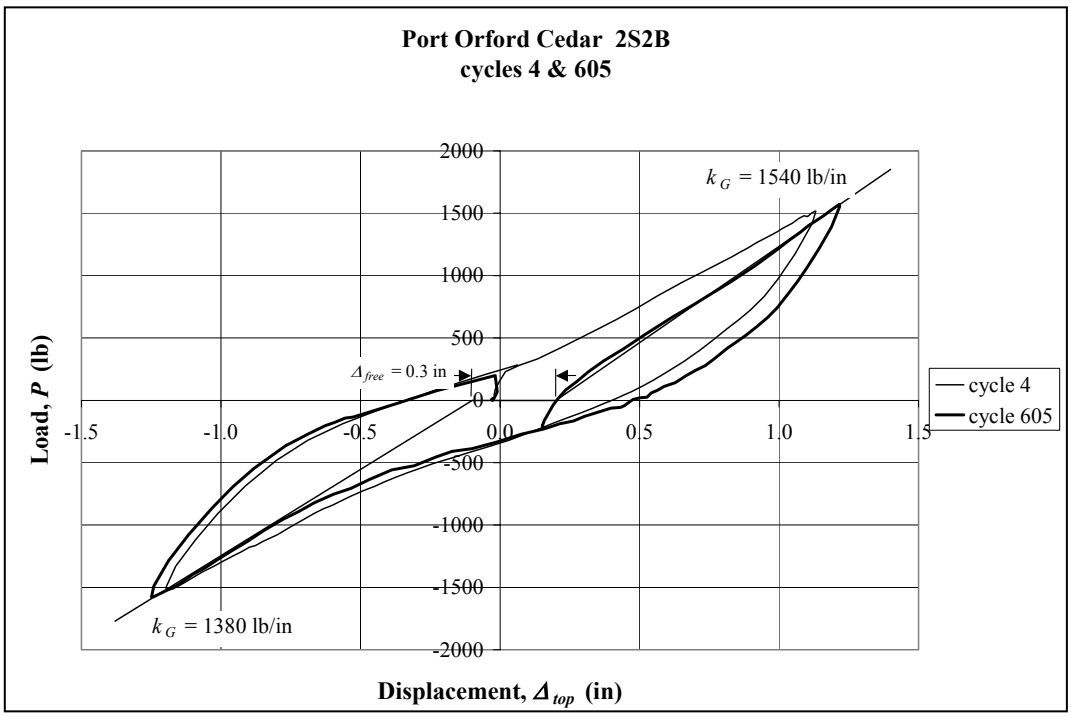

Figure 3-12 Cyclic Effects on Port Orford Cedar Frame

3.6.4. Maximum Load

The Douglas fir and Port Orford cedar frames were each subjected to the maximum available actuator displacement. Both frames were able to carry additional load at this point. Pinching of the load-displacement curve for these frames indicates the presence of free displacement, but this is likely due to joint damage or cycling effects as previously described.

In order to cause failure of a frame, additional displacement in the push direction was applied to the eastern white pine and white oak frames. This was accomplished by applying maximum displacement, holding the frame and then resetting the actuator for three successive applications. As shown in Figure 3-13, the eastern white pine frame incurred a failure due to its attachment to the test fixture at an imposed top displacement of 7.9 inches.

Figure 3-13 Eastern White Pine 2S2B Column Failure at Reaction

The white oak frame was the only 2S2B frame displaced sufficiently to reach an ultimate load within the frame itself rather than at the support fixture. At an imposed displacement of 6 inches, several joints had failed but the frame continued to carry additional load. The failure of knee brace to column connection at joint 20 is shown in Figure 3-14and Figure 3-15. The ultimate load was reached at an imposed displacement of 9.23 inches corresponding to an applied load of 15.7 kips. Ultimate load failure was characterized by mortise member (column) splitting at the upper beam to west column (joint 6).

Figure 3-14 White Oak 2S2B Knee Brace Tenon Failure

Figure 3-15 White Oak 2S2B Column Mortise Tear-out at Knee Brace Connection

The maximum load cycle of the white oak frame is presented in Figure 3-16. Maximum load and displacement for all frames are listed in Table 3-8. Load-displacement curves for the maximum load cycles are shown in Appendix I.

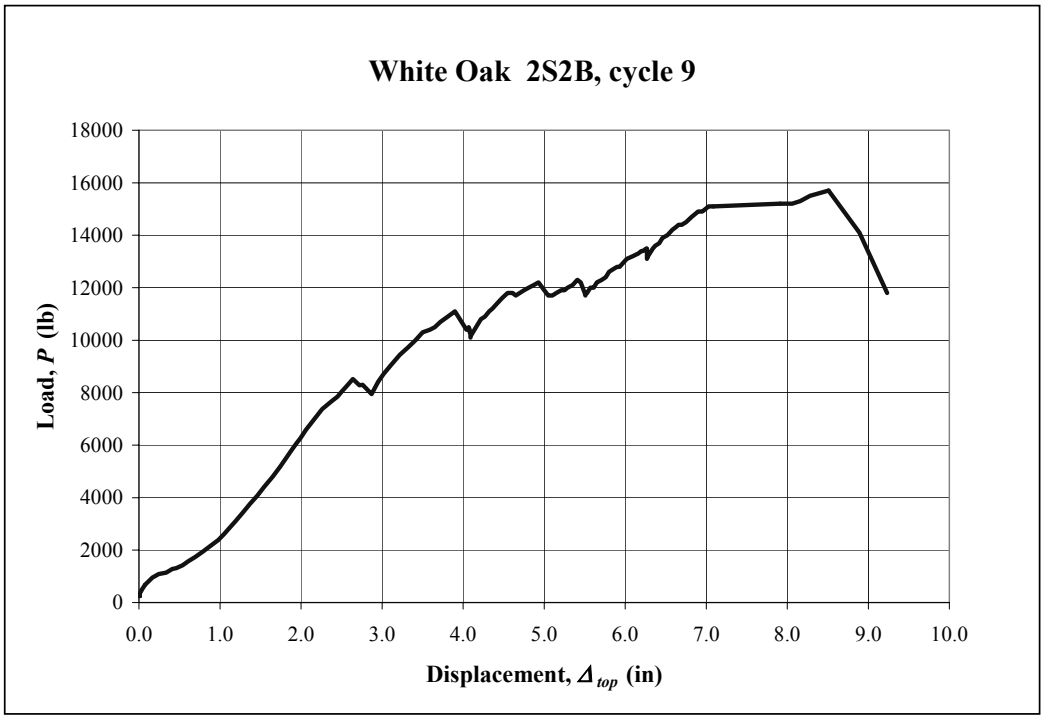

Figure 3-16 Maximum Load Cycle for White Oak Frame

Table 3-8 Summary of Maximum Load Cycles

Frame	Cycle	Push Stroke Maximum Load (lb)	Push Stroke Maximum Disp. (in)	Pull Stroke Maximum Load (lb)	Pull Stroke Maximum Disp. (in)	Failure Mode
Douglas Fir	115	3608	4.23	3176	2.88	None
Eastern White Pine	19	6150	7.92	-	-	Reaction
Port Orford Cedar	609	3881	3.48	4150	3.31	None
White Oak	9	15,700	8.51	-	-	Beam-column

3.7. Summary

Average frame stiffness values are summarized in Table 3-9.

Table 3-9 2S2B Maximum Frame Stiffness

	Average Frame Stiffness (lb/in)	Maximum Load (lb)
Douglas Fir	900	3608
Eastern White Pine	1290	6150
Port Orford Cedar	1200	3881
White Oak	3060	15,700

Using an allowable deflection of height/400, the allowable drift due to wind load on an 16-foot high frame would be approximately 0.50 inches. Given the design wind load of 2800 pounds for a 2S2B frame, the minimum required frame stiffness would be 5600 pounds per inch. The stiffness of all frames was significantly lower than this value. This indicates that traditional timber frames that rely on knee braces for lateral load resistance do not have adequate stiffness to resist typical wind loads without the addition of a supplemental lateral load-carrying system.

However, the experimental results indicate that all frames were able to resist loads significantly greater than the assumed design load. Therefore, these frames are expected to have sufficient strength to resist lateral load.

The free displacement typical of the 1S1B frames was not evident with the 2S2B frames. This may indicate that free displacement is not a design concern with typical traditional timber frames.

A majority of the joint failures in 2S2B frames occurred at knee braces located at exterior columns. This indicates that the outer columns are resisting more load than the interior column.

Ultimate failure of the white oak frame was caused by subjecting the frame to displacement and load far beyond expected service conditions. Although local failures (in the form of peg fracture or tenon failure) were common and the eastern white pine frame failed at the reaction location, no frame other than the white oak frame was loaded beyond maximum capacity. Even at displacements far beyond serviceable limits, all frames continued to carry an increasing load.

4. Unsheathed Frame Structural Analysis

4.1. Overview

Unsheathed 1S1B and 2S2B frames were modeled with SAP 2000 Nonlinear version 7.42 (Computers and Structures, Inc. 2001). All models were plane-frame structures with three degrees of freedom (DOF) per node. The structures were modeled in a relatively simple fashion with all knee braces pinned at each end, thus limiting their actions to axial force only. Beam-to-column connections were also modeled as pin connections. The models of this study represented three species: Douglas fir, eastern white pine, and white oak. The frames were manufactured by different companies, and although the frames may hereafter be distinguished by species, it must be recognized that species is not the only distinction. Geometry and joint detailing were considerably different among frame manufacturers and significantly affected performance.

In order to demonstrate the ease by which frames with a minimal amount of redundancy can be analyzed, the 1S1B frames were also modeled using classical techniques. The classical method was based on the assumption of statical determinacy for determination of frame actions. The method of work/energy was used to determine frame stiffness.

4.2. Model Details

Wood-pegged joints were modeled as axial springs, and a standard frame element was used to represent the joint spring. The stiffness k_j of a joint spring is determined by Equation 4-1. In order to simplify the model, the area A and length L of the joint element were both assigned unit values. Therefore, joint stiffness was equal to modulus of

elasticity *MOE*, which was adjusted accordingly for each frame element representing a joint spring.

$$k_j = (A)(MOE)/(L) \quad \textbf{(4.1)}$$

Model joint stiffness as shown in Table 4-1 was based on experimental work by Scholl (Schmidt and Scholl, 2000). These average values are derived from static tests of wood-pegged mortise and tenon joint specimens. The experimental joints were pinned with two white oak pegs, thus the results of the aforementioned study have been halved to provide a value for a mortise and tenon joint connected with one peg. Also, the values have been rounded to two significant digits.

Table 4-1 Experimental Wood-Pegged Joint Stiffness (one peg per joint)

Base Material	Peg Diameter (in)	Joint Stiffness (lb/in)
Douglas Fr	1	25,000
Eastern White Pine	3/4	18,000
Eastern White Pine	1	22,000
White Oak	1	50,000

In order to demonstrate the capability to model a frame in a nonlinear fashion, the white oak 1S1B frame was also modeled with nonlinear joints. In order to insure accurate nonlinear representation of a typical pegged joint, a calibration model was created for a single connection and then applied to the frame model. Nonlinearity was added to either the tensile joints alone or both tensile and compressive joints. The nonlinear models were compared to models with rigid or linear spring connections.

The timbers in each experimental frame were not graded, but for modeling purposes, all timbers are assumed to be No. 1 grade. Appropriate MOE values as shown

in Table 4-2 were obtained from the NDS (1997). The NDS values for MOE are expected averages for a group of timber.

Table 4-2 Frame Material Modulus of Elasticity

Base Material	Modulus of Elasticity (lb/in^2)
Douglas Fr	1,600,000
Eastern White Pine	1,100,000
White oak	1,000,000

Load on all models was applied as a point load at the left side of the frame. The load was applied to the node(s) corresponding to the intersection of the beam and column.

4.3. 1S1B Linear Frame Analysis

4.3.1. Linear SAP Model

The geometry for the 1S1B SAP model is shown in Figure 4-1. The model includes 12 nodes and 15 frame elements. The knee brace dimension labeled *kb* is either 30 inches or 36 inches. The dimensions of the experimental frame members, joint end distances, and joint offsets vary slightly among the frame manufacturers. These small differences are assumed to have minimal relative effect on global frame performance. Therefore, node locations are approximate compared to actual frame dimensions but are generally accurate to within one inch.

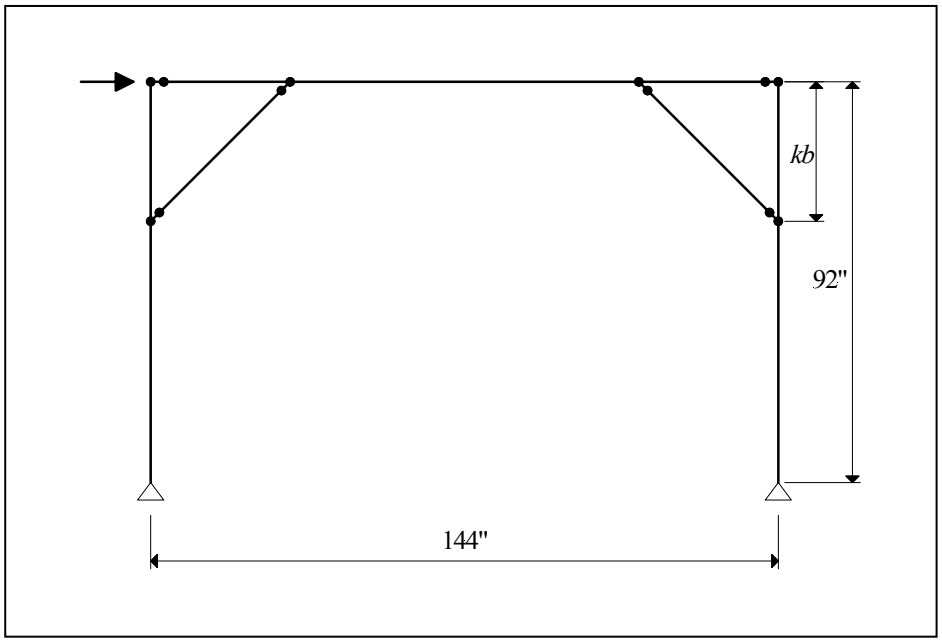

Figure 4-1 1S1B Model

Three different frames were modeled: Douglas fir, eastern white pine, and white oak. The Douglas fir frames had a knee brace dimension *kb* = 30 inches while the eastern white pine and white oak frames had a knee brace dimension *kb* = 36 inches. All other dimensions and node locations were identical for all frames. Frame elements were modeled with rectangular cross-section dimensions as listed in Chapter 2. As shown in Figure 4-2, elements with length and area of unity were used for the beam-to-column joints and the knee brace joints. The joint elements had large bending and shear stiffness and were released for moment at the intersecting end.

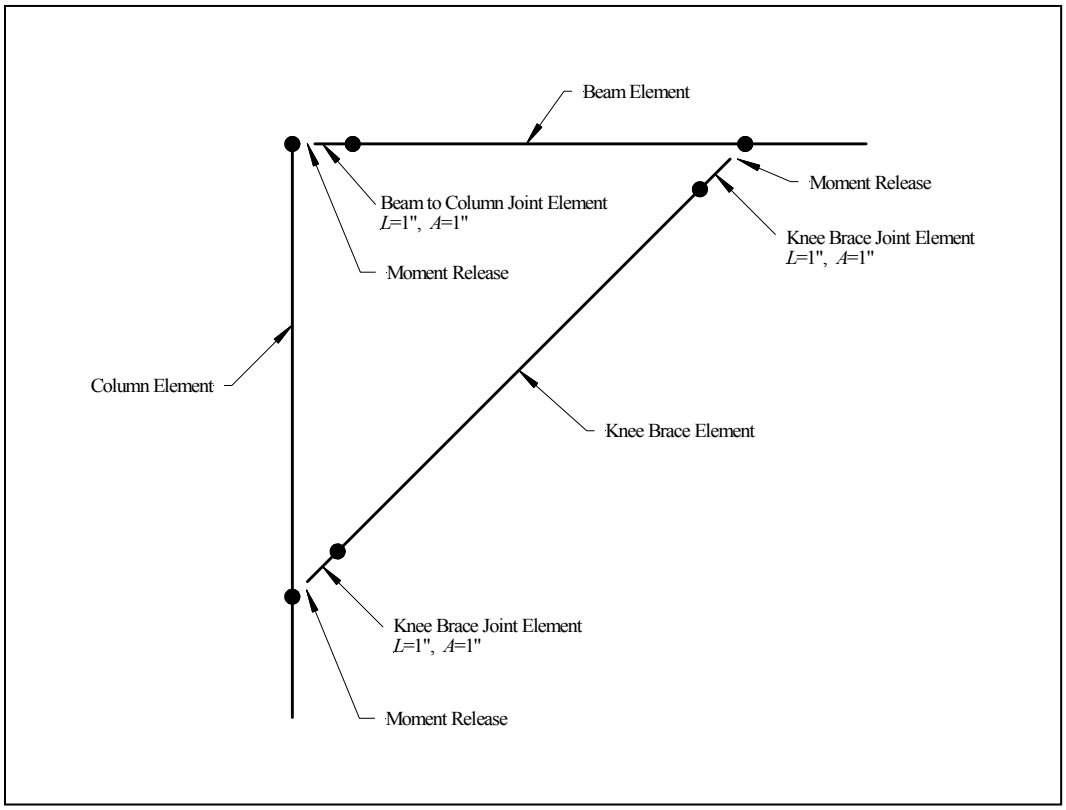

Figure 4-2 SAP Model Joint Details

4.3.2. Classical Model

The frames were analyzed with equilibrium techniques to determine member actions. In this model, the frame was assumed symmetrical with all joints having equal characteristics in tension and compression. Given this assumption, the frame was statically determinate with the lateral load split equally between the two horizontal (shear) reactions at the column bases.

Frame stiffness was modeled using the work-energy method. The frame was assumed to have infinite frame element material stiffness such that all deformation occurred at the joints. Frame stiffness k_f was calculated by Equation 4-2 where k_{kb} is the knee brace joint stiffness, k_{bc} is the beam-to-column joint stiffness, h is the frame height and kb is the knee brace dimension.

$$k_f = \frac{1}{\frac{2}{k_{kb}}\left[\left(\frac{h}{kb}\right)^2\right] + \frac{1}{2k_{bc}}\left[\left(\frac{h}{kb}\right)^2 + 1\right]} \qquad \textbf{(4-2)}$$

Derivation of this equation is shown in Appendix P.

4.3.3. 1S1B White Oak Nonlinear SAP Models

The 1S1B white oak frame was modeled with nonlinear springs replacing the linear joint elements. Nonlinear spring properties were based on joint test results from experimental work by Scholl (Schmidt and Scholl 2000) and a SAP calibration model was created to verify correct model inputs. The experimental joint tests consisted of a two-peg joint subject to direct tension. Therefore, the nonlinear model represents tensile behavior, and as such, does not likely represent actual behavior for joints carrying

compressive loads. The calibration model consisted of two timbers connected by a non-linear link based on hysteretic behavior proposed by Wen (Wen, 1976). Inputs for the Wen link are shown in Table 4-3.

Table 4-3 Nonlinear Link Inputs

Wen Link Inputs	
Initial Stiffness	74,000 lb/in
Post Yield Stiffness / Initial Stiffness	0.02
Yield Strength	6000 psi
Yielding Exponent	2

In the Wen model, yield strength is defined as the point at which linear curves defined by initial stiffness and post yield stiffness intersect. Initial stiffness, post yield stiffness and yield strength were based on average experimental values of two-peg white oak joint tests. A joint test that most closely represented the average of all tests was selected for comparison to the joint model, and the yielding exponent was visually adjusted to fit the model to the selected experimental curve. Comparison of the model to Scholl test specimen WO37 is shown in Figure 4-3.

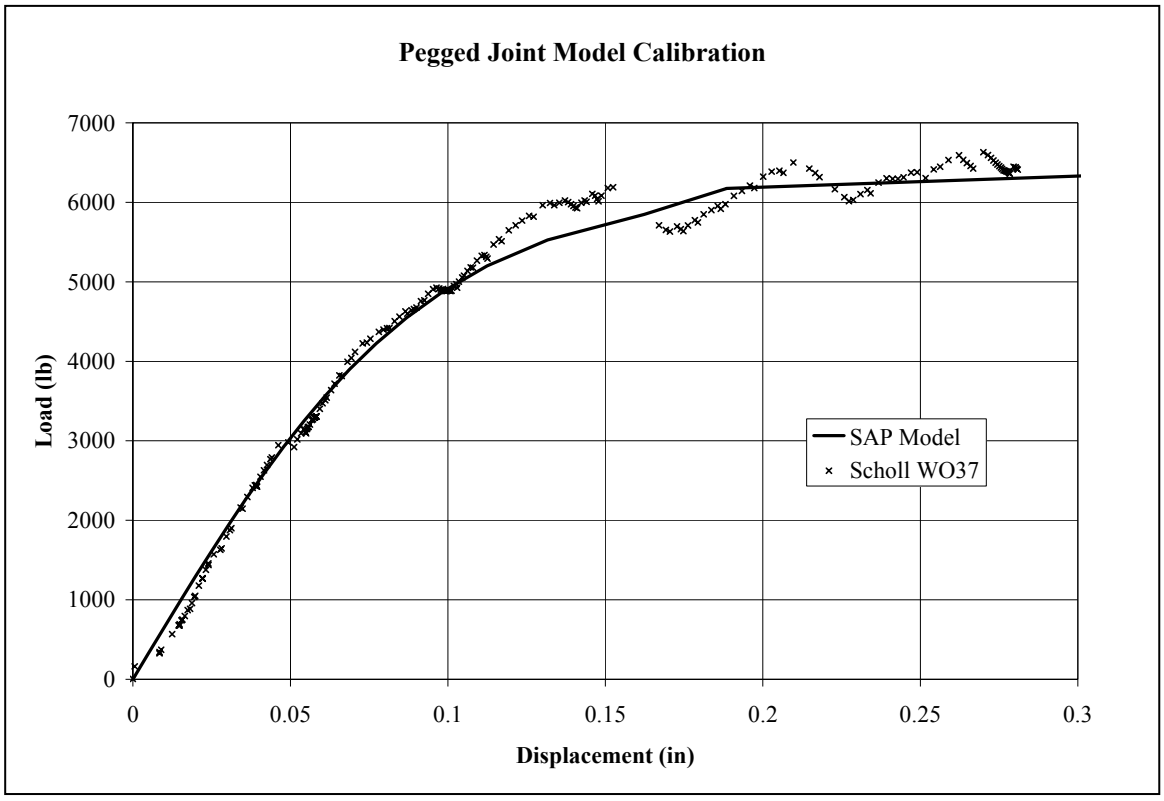

Figure 4-3 Model Verification for Two Peg White Oak Joint

The fully nonlinear model was compared to experimental cycle 13 and five other SAP models. The models consisted of a variety of combinations of rigid, linear, and nonlinear connections as listed in Table 4-4 . All linear connections had a stiffness of 74,000 lb/in and rigid connections had a stiffness of $1x10^{12}$ lb/in.

Table 4-4 1S1B White Oak Comparison Models

Model number	Model Name	Compressive Joint Properties	Tensile Joint Properties
1	C & T Rigid	rigid	rigid
2	C Rigid and T Linear	rigid	linear
3	C & T Linear	linear	linear
4	C Rigid & T Nonlinear	rigid	nonlinear
5	C Linear & T Nonlinear	linear	nonlinear
6	C & T Nonlinear	nonlinear	nonlinear

4.4. 1S1B Results

4.4.1. Linear Frame Stiffness

Table 4-5 shows the results of the SAP model analysis of three frames with linear joint elements. Comparisons of model results to actual frame tests are also included. Frame stiffness is based on the load applied at the top of the frame divided by global horizontal deflection at the top of the frame. Experimental frame stiffness is based on maximum stiffness determined by the first experimental test that subjected the frame to a lateral load of 1000 pounds. As shown in the results, model predictions are close to actual frame stiffness.

Table 4-5 1S1B Linear Frame Stiffness

	Douglas Fir	Eastern White Pine	White Oak
Knee brace distance (in)	30	36	36
Knee brace joint stiffness (lb/in)	25,000	18,000	100,000 (2 pegs)
Beam/column joint stiffness (lb/in)	50,000 (2 pegs)	31,000 (spline)	100,000 (2 pegs)
Model frame stiffness (lb/in)	907	933	2683
Experimental frame stiffness (lb/in)	980	1240	3000
Percent difference	7%	25%	11%

Joint stiffness was taken directly from Table 4-1 with adjustments for the number of pegs in the joint. The beam/column joint of the eastern white pine frame consisted of a red oak spline connected to each member with two 1-inch pegs. The spline is assumed to have relatively large stiffness. Therefore, the total joint stiffness is derived from two pegs in eastern white pine in series with two pegs in oak. The resulting stiffness is shown in Equation 4-3 where k_{bcEWP} is the total joint stiffness for the beam-to-column spline in the eastern white pine frame.

$$k_{bcEWP} = \frac{1}{\frac{1}{2\left(22{,}000\frac{\text{lb}}{\text{in}}\right)} + \frac{1}{2\left(50{,}000\frac{\text{lb}}{\text{in}}\right)}} = 31{,}000\frac{\text{lb}}{\text{in}} \tag{4.3}$$

4.4.2. Alternative Linear Model Comparisons

The global frame stiffness and member forces predicted by alternative models with linear joint elements are shown in Table 4-6, Table 4-7, and Table 4-8. Each table includes the results of three models. The model titled "As tested SAP" was the SAP model that most closely resembled the experimental frames as described in Chapter 2.

The as-tested SAP model included the effects of both joint and member flexibility. The second model titled "Simplified SAP" included only the stiffness contribution of the members. This was accomplished by removing the frame element used to represent the joint spring. The third, "Classical", model included stiffness due to joints only by increasing member stiffness approximately five orders of magnitude. All comparisons are made relative to the As-tested SAP model because it was assumed to be most accurate compared to the experimental frames.

As seen from the tabulated results, frame actions (moment, axial force, and shear) are relatively insensitive to the model assumptions. Differences in frame actions were typically around 3% with a high value of 8% occurring in the classical model of the white oak frame. As expected the differences in frame actions was low since the frames are nearly statically determinate. However, the predicted frame stiffness increased significantly as joint stiffness increased. Modeling the frame with rigid frame material also produced a stiffer frame in all cases.

Table 4-6 Douglas Fir 1S1B Model Results

	As-Tested SAP Model	Simplified SAP Model		Classical Model	
	Value	Value	*Difference*	Value	*Difference*
Knee brace joint stiffness (lb/in)	25,000	rigid		25,000	
Beam/column joint stiffness (lb/in)	50,000	rigid		50,000	
Frame material MOE (lb/in^2)	1,600,000	1,600,000		rigid	
Model frame stiffness (lb/in)	907	4,044	*346%*	1,168	*29%*
<u>Moment (lb·in)</u>					
left column at knee brace	-30,069	-30,993	*3%*	-31,000	*3%*
right column at knee brace	-31,931	-31,007	*-3%*	-31,000	*-3%*
beam at left knee brace	27,319	26,823	*-2%*	26,833	*-2%*
beam at right knee brace	-26,347	-26,843	*2%*	-26,833	*2%*
<u>Axial force (lb)</u>					
left knee brace	2,108	2,168	*3%*	2,168	*3%*
right knee brace	-2,238	-2,169	*-3%*	-2,168	*-3%*
beam at left column	-2,002	-2,033	*2%*	-2,033	*2%*
beam at right column	1,064	1,034	*-3%*	1,033	*-3%*
<u>Shear (lb)</u>					
beam at left column	-924	-894	*-3%*	-894	*-3%*
beam at right column	-865	-895	*3%*	-894	*3%*

Table 4-7 Eastern White Pine 1S1B Model Results

	As-Tested SAP Model	Simplified SAP Model		Classical Model	
	Value	Value	*Difference*	Value	*Difference*
Knee brace joint stiffness (lb/in)	18,000	rigid		18,000	
Beam/column joint stiffness (lb/in)	31,000	rigid		31,000	
Frame material MOE (lb/in^2)	1,100,000	1,100,000		rigid	
Model frame stiffness (lb/in)	933	4,417	*373%*	1,180	*38%*
Moment (lb·in)					
left column at knee brace	-27,125	-27,182	*0%*	-28000	*3%*
right column at knee brace	-28,875	-28,818	*0%*	-28000	*-3%*
beam at left knee brace	23,160	23,254	*0%*	23000	*-1%*
beam at right knee brace	-22,840	-22,746	*0%*	-23000	*1%*
Axial force (lb)					
left knee brace	1,754	1,758	*0%*	1,807	*3%*
right knee brace	-1,867	-1,863	*0%*	-1,807	*-3%*
beam at left column	-1,753	-1,755	*0%*	-1,778	*1%*
beam at right column	802	801	*0%*	778	*-3%*
Shear (lb)					
beam at left column	-656	-658	*0%*	-639	*-3%*
beam at right column	-622	-619	*0%*	-639	*3%*

Table 4-8 White Oak 1S1B Model Results

	As-Tested SAP Model	Simplified SAP Model		Classical Model	
	Value	Value	*Difference*	Value	*Difference*
Knee brace joint stiffness (lb/in)	100,000	rigid		100,000	
Beam/column joint stiffness (lb/in)	100,000	rigid		100,000	
Frame material MOE (lb/in^2)	1,000,000	1,000,000		rigid	
Model frame stiffness (lb/in)	2,683	4,873	*82%*	4165	*55%*
Moment (lb·in)					
left column at knee brace	-25,967	-25,894	*0%*	-28000	*8%*
right column at knee brace	-30,034	-30,106	*0%*	-28000	*-7%*
beam at left knee brace	22,922	22,803	*-1%*	23000	*0%*
beam at right knee brace	-23,078	-23,197	*1%*	-23000	*0%*
Axial force (lb)					
left knee brace	1,686	1,681	*0%*	1,807	*7%*
right knee brace	-1,948	-1,953	*0%*	-1,807	*-7%*
beam at left column	-1,721	-1,719	*0%*	-1,778	*3%*
beam at right column	834	836	*0%*	778	*-7%*
Shear (lb)					
beam at left column	-661	-658	*0%*	-639	*-3%*
beam at right column	-617	-620	*1%*	-639	*4%*

4.4.3. Joint Stiffness Effects

Table 4-9 demonstrates the effect of varying joint stiffness for the analysis model. Global frame stiffness and frame element actions for three Douglas fir models with varied joint stiffness are compared to the Douglas fir as-tested model. As shown, changes in beam-to-column and/or knee brace joint stiffness had minimal effect on frame actions. Also changing the beam-to-column joint stiffness had little effect on global frame stiffness. However, a doubling of the knee brace joint stiffness resulted in a 52% increase in frame stiffness.

Table 4-9 Effects of Varying Joint Stiffness

	Base model	**Double knee brace joint stiffness**	***Diff.***	**Double beam/column joint stiffness**	***Diff.***	**Double all joint stiffness**	***Diff.***
Knee brace distance (in)	30	30		30		30	
Knee brace joint stiff. (k/in)	25	50		25		50	
Beam/col. joint stiff. (k/in)	50	50		100		100	
Global Frame Stiffness (lb/in)	907	1378	*52%*	952	*5%*	1483	*63%*
Moment (kip·in)							
left column at knee brace	-30.1	-29.7	*-1%*	-30.3	*1%*	-30.0	*0%*
right column at knee brace	-31.9	-32.3	*1%*	-31.7	*-1%*	-32.0	*0%*
beam at left knee brace	27.3	26.8	*-2%*	27.6	*1%*	27.2	*0%*
beam at right knee brace	-26.3	-26.9	*2%*	-26.0	*-1%*	-26.4	*0%*
Axial Force (lb)							
left knee brace	2108	2084	*-1%*	2124	*1%*	2105	*0%*
right knee brace	-2238	-2263	*1%*	-2223	*-1%*	-2242	*0%*
beam at left column	-2002	-1991	*-1%*	-2010	*0%*	-2001	*0%*
beam at right column	1064	1076	*1%*	1057	*-1%*	1066	*0%*
Shear (lb)							
beam at left column	-924	-907	*-2%*	-935	*1%*	-922	*0%*
beam at right column	-865	-882	*2%*	-854	*-1%*	-867	*0%*

4.4.4. 1S1B White Oak Model Comparisons for Models with Rigid, Linear, or Nonlinear Joints

Comparison of several 1S1B white oak models to experimental frame results is shown in Figure 4-4. Based on a visual analysis of the plots, implementation of nonlinear joints at all locations is not advisable since the model with all joints modeled as nonlinear springs greatly overestimated frame displacement. Since the compressive joints can be assumed to be more linear than tensile joints due to bearing, the compressive links were successively replaced with linear and rigid elements. Replacing all compressive joints with linear springs reduced frame displacement, but it was still overestimated. The model with nonlinear tensile joint springs and rigid compressive joints most closely simulated actual frame behavior. The models with rigid or linear spring connections at all joints provide reasonable models of low load behavior but do not predict nonlinear behavior at higher loads. The model with rigid compressive joints and linear tensile joints provided the best model for linear frame response.

As with many of the frame test cycles, the experimental data implies the presence of low load free displacement in the frame joints resulting in reduced stiffness at low loads. Although no attempt was made to model this free displacement xxxx provides some insight into simulating free displacement. The chart chows that the initial slope of the experimental data at low loads is similar to the model with linear compressive and tensile joint springs. As the load increases from 2500 pounds to 5000 pounds, the slope of the experimental data more closely equals the slope of the model with rigid compressive joint springs and linear tensile joint springs. Above 5000 pounds, the slope

of the experimental data is the same as the slope of the model with rigid compressive joint springs and nonlinear tensile joint springs.

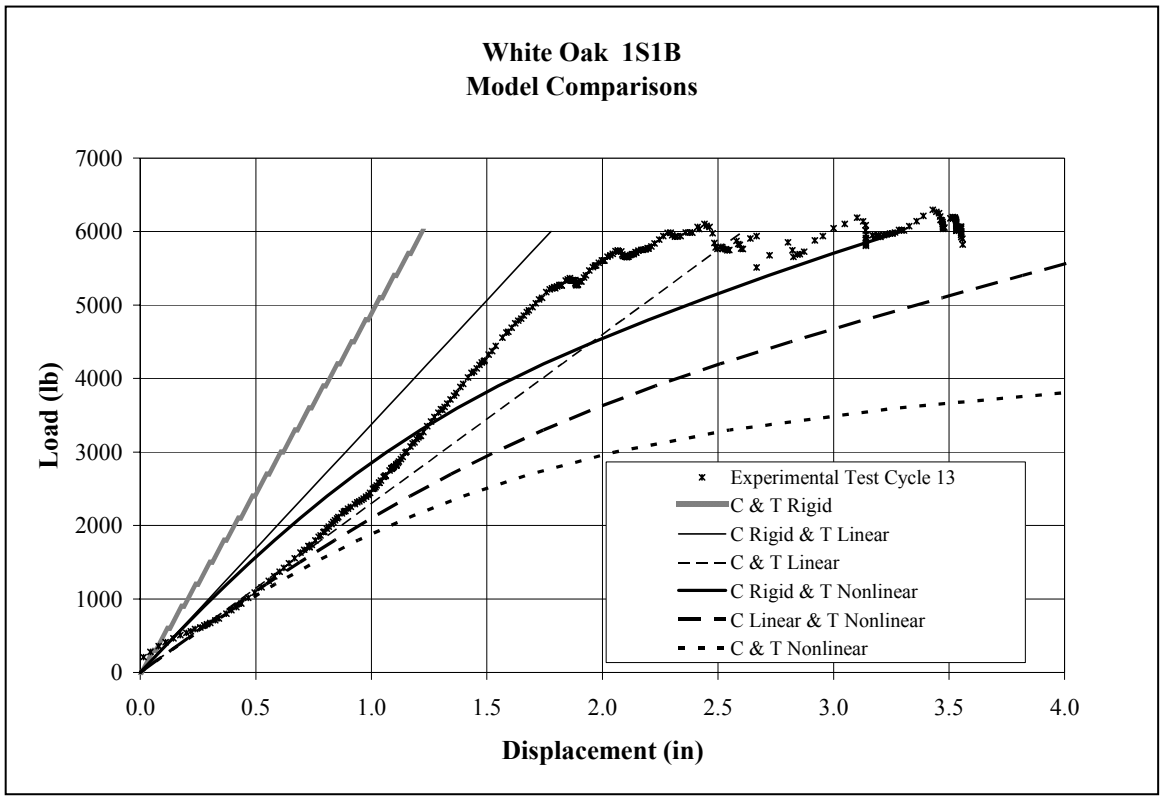

Figure 4-4 SAP Model Comparisons

4.4.5. Effects of Joint Stiffness and Knee Brace Distance on Frame Stiffness

As shown in Table 4-5, the modeled stiffness of both the as-tested Douglas fir frame and the as-tested white oak frame were relatively close to the experimental stiffness for each respective frame. Therefore these two models were chosen for a comparative parametric study to determine the potential benefits by varying individual frame parameters. The 1S1B white oak model was re-created with geometry and joint stiffness identical to that of the 1S1B Douglas fir frame and with all joints modeled in a linear fashion. As shown in Table 4-10, the stiffness of this model was 891 pounds per

inch which is only two percent lower than the linear Douglas fir frame model stiffness of 901 pounds per inch. This difference is due to differing cross section dimensions of the frame members and material modulus of elasticity. Joint stiffness and knee brace distance (vertical dimension from the bottom of the knee brace to the bottom of the beam) were individually incremented relative to the "White oak with Douglas fir geometry and joint stiffness" model to investigate the effects of these parameters on frame stiffness.

Model	Knee Brace Distance (in)	Knee Brace Joint Stiffness (lb/in)	Beam-Column Joint Stiffness (lb/in)	Frame Stiffness (lb/in)	Difference
White Oak Frame with Douglas Fir Geometry and Joint Stiffness	30	25,000	50,000	891	
Double Knee Brace Joint Stiffness	30	50,000	50,000	1416	59%
4 x Knee Brace Joint Stiffness	30	100,000	50,000	1794	101%
Double Beam-to-Column Joint Stiffness	30	25,000	100,000	934	5%
36 inch Knee Brace Distance	36	25,000	50,000	1247	40%

Table 4-10 Effects of Frame Parameters on Frame Stiffness

Previous research has demonstrated that a two-peg white oak joint is approximately twice as stiff as a two-peg Douglas fir joint (Schmidt and Daniels 1999). It is assumed that a two-peg joint is twice as stiff as a one-peg joint. As shown in Table 4-10, a doubling of the knee brace stiffness (representing the addition of a second peg or a doubling of joint stiffness due to the use of white oak) resulted in a 59% increase in frame stiffness. A four-fold increase in knee brace stiffness (representing the addition of a second peg and a doubling of joint stiffness due to the use of white oak) resulted in a 101% increase in frame stiffness. Based on these results, it can be concluded that significant increases in the lateral stiffness of traditional timber frame can be realized

through the use of additional pegs in the knee brace joints or the use of a stiffer timber species such as white oak. A doubling of the stiffness of the beam-to-column joint had minimal effect on frame stiffness.

A relatively small increase in knee brace distance resulted in a large increase in frame stiffness. When the modeled knee brace distance was increased 20% (from 30 inches to 36 inches) the frame stiffness increased 40%. This indicates that knee brace distance should be set at as large a magnitude as possible in order to maximize timber frame lateral stiffness.

The stiffness of the experimental white oak 1S1B frame was approximately three times the stiffness of the experimental Douglas fir 1S1B frame. Comparison of the stiffnesses of the respective frame models indicates a similar ratio. The results of this parametric study demonstrate that frame geometry and joint stiffness are the driving influences on frame behavior while member size and stiffness is incidental. This parametric study also demonstrates that conventional analysis models with spring elements representing joint behavior are effective in modeling frame behavior.

4.5. 2S2B Frame Analysis

4.5.1. SAP Model

The SAP model geometry for a typical 2S2B frame is shown in Figure 4-5. Member element numbering is included as a reference for actions listed in a subsequent section. Model dimensions are approximate relative to actual frame dimensions but are generally accurate to within 1 inch. Three different frames were modeled: Douglas fir, eastern white pine, and white oak. The Douglas fir frame had a knee brace dimension *kb* equal to 30 inches while the eastern white pine and white oak frames had a knee brace dimension *kb* equal to 36 inches. All joints in the 2S2B models were linear in all analyses.

The Douglas fir and white oak models included 48 nodes and 56 member elements. Due to a continuous upper beam, the eastern white pine model had 47 nodes and 55 member elements. Details of the knee brace and outer column to beam joints are identical to the 1S1B details as shown in Figure 4-2 of a previous section.

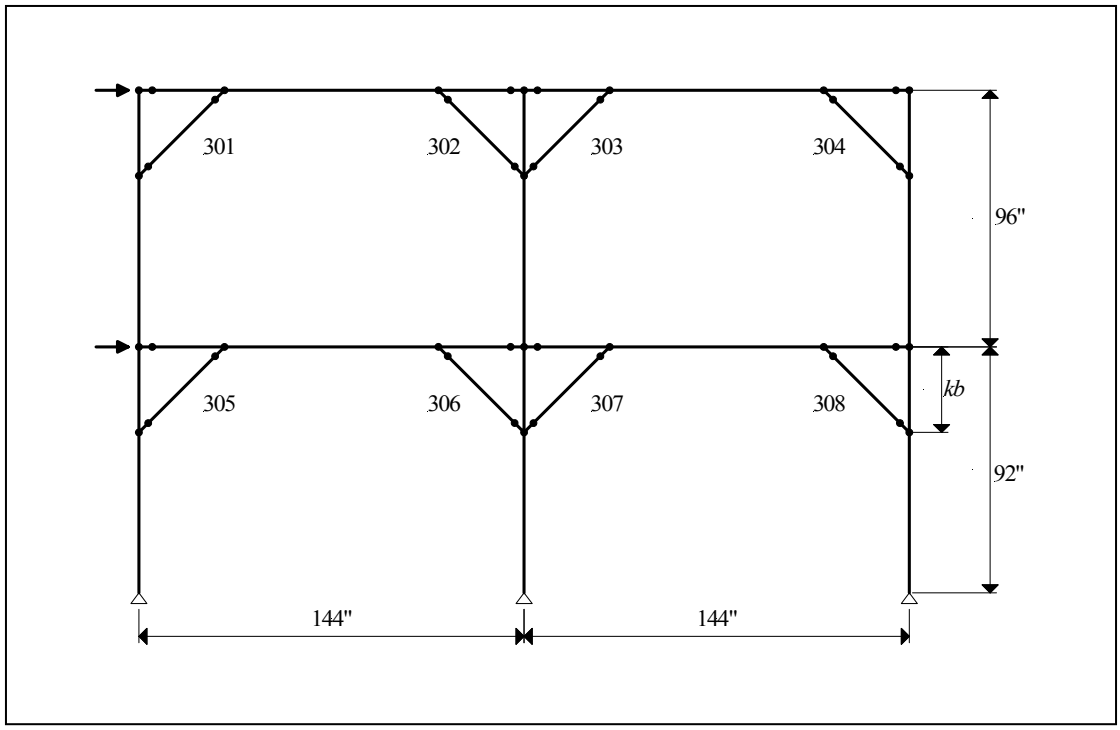

Figure 4-5 2S2B Model

The experimental eastern white pine frame had a continuous upper beam, while the Douglas fir and white oak frames had upper beams joined at the center column. Details for the model of a continuous upper beam are shown in Figure 4-6. The upper beam is modeled with moment continuity across the column joint, but the column is hinged at the joint. Beam-to-column joint stiffness is modeled as described for the 1S1B frame.

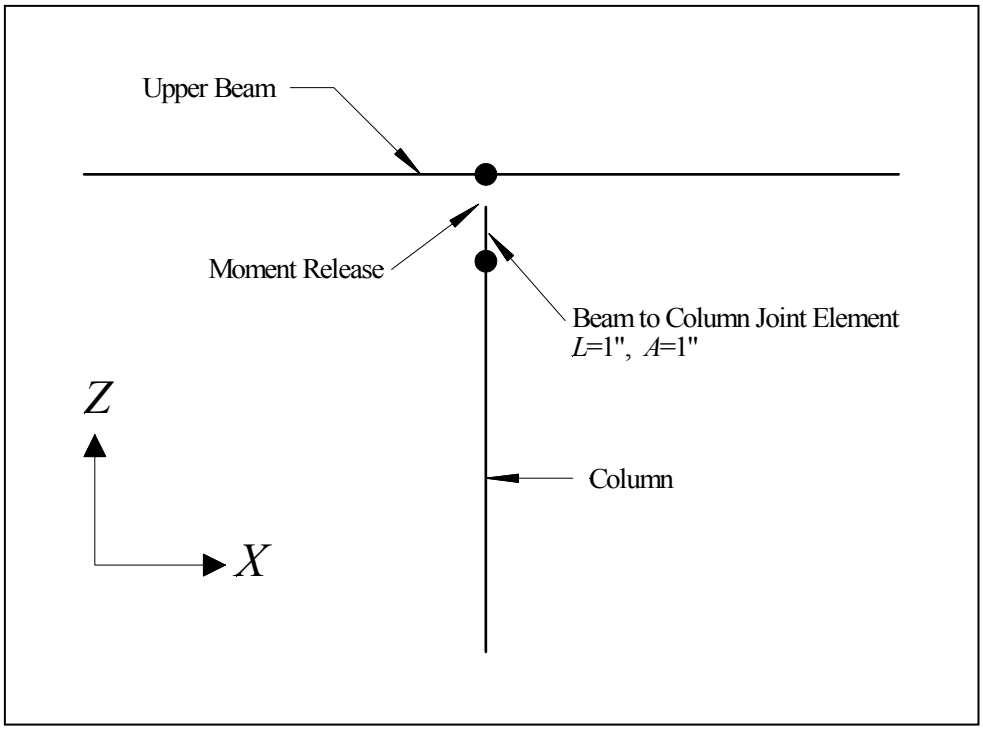

Figure 4-6 Continuous Upper Beam

For the case of a discontinuous upper beam, a spline was used to connect the opposing beams. The model for a discontinuous top beam with a spline is shown in Figure 4-7. As with the knee brace joints, the beam to spline joint was designed with unit values for the area *A* and length *L,* and element stiffness was thereby determined by *MOE*. The spline was perceived to have limited moment capacity, and the model results were reviewed to ensure no excessive moment occurred at the spline. In practice, a similar review of internal spline action is warranted.

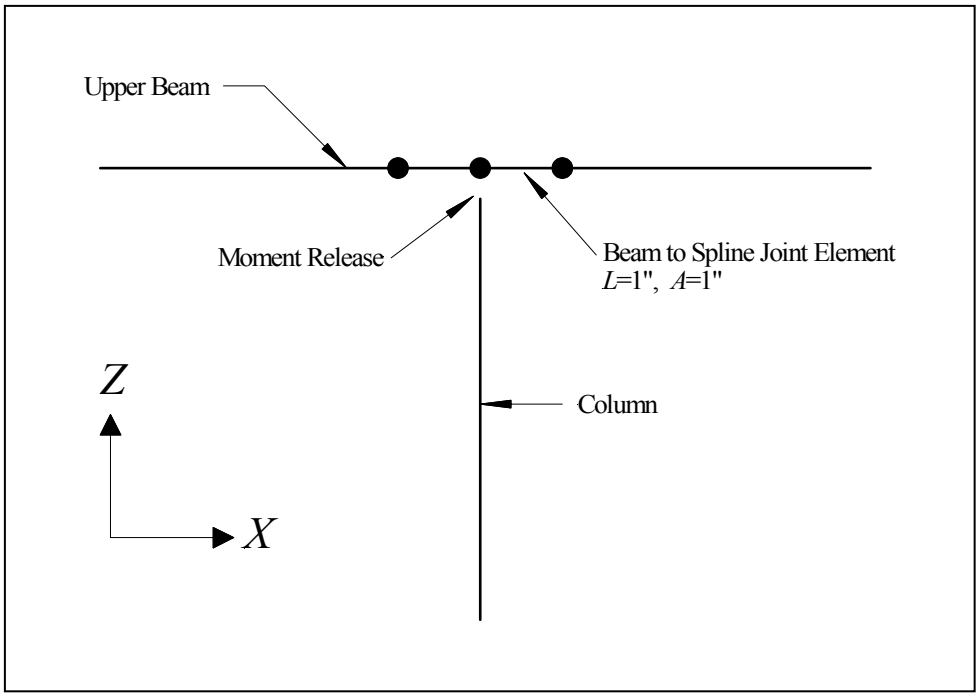

Figure 4-7 Splined Upper Beam

In all experimental frames, the lower beam to center column connection was formed by a through-spline connecting opposing beams. Neither the beams nor spline was pegged to the column. As shown in Figure 4-8, all models had double coincident nodes at the intersection of the center column and lower beam. These coincident nodes were constrained for horizontal and vertical displacements but were released for rotation. Therefore, the beam and column are constrained to translate together at the coincident nodes. In addition, there was no moment release at the spline, such that there is moment continuity from beam to beam but the beams were allowed to rotate relative to the column. Again the joint element has $L = 1$ and $A = 1$ such that stiffness = MOE. The spline was perceived to have limited moment capacity and all model results were reviewed to ensure no excessive moment occurred at this location. In practice, a similar review of internal spline action is warranted.

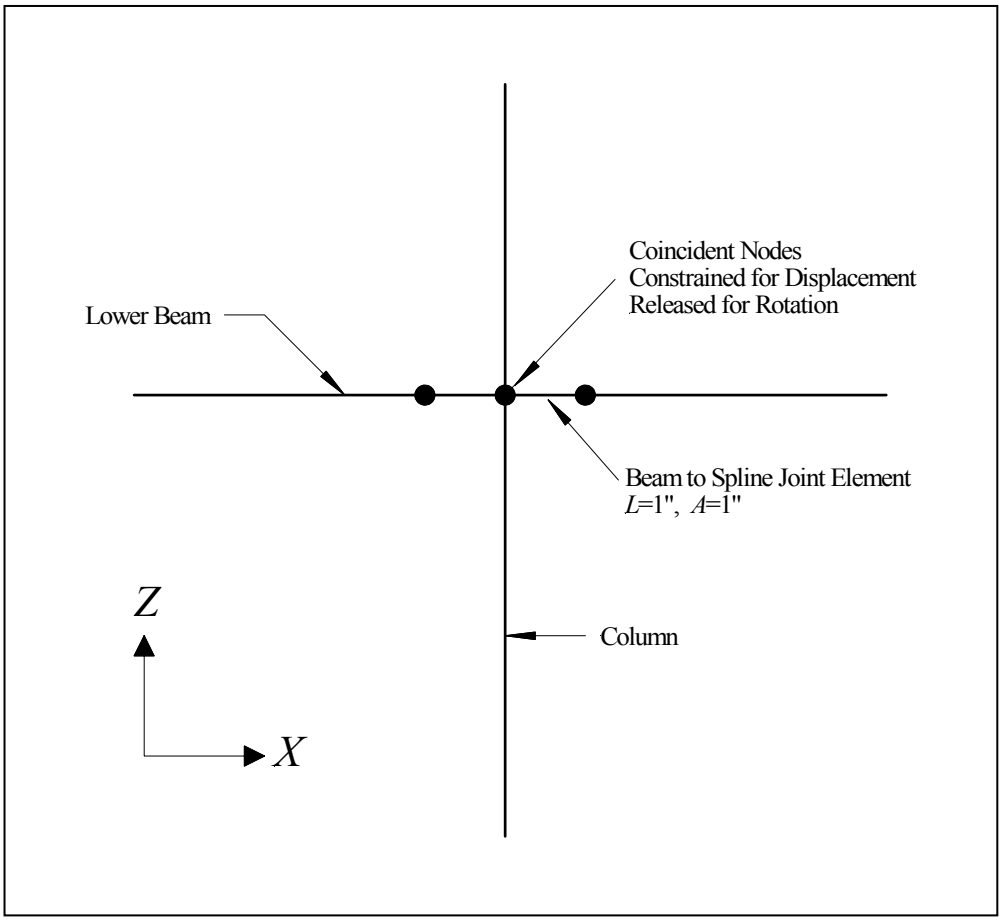

Figure 4-8 Center Beam to Center Column Detail

4.6. 2S2B Results

4.6.1. Frame Stiffness

Table 4-11 shows the results of model analysis of three 2S2B frames all of which had linear joint springs. Comparisons of model results to actual frame tests are also included. Frame stiffness is based on the load applied at the top of the frame divided by the global deflection at the top of the frame. Actual frame stiffness is based on maximum stiffness determined by the first experimental test that subjected the frame to a total load of 1000 pounds.

The model predictions for global frame stiffness are again satisfactory.

Table 4-11 2S2B Frame Stiffness

	Douglas Fir	Eastern White Pine	White Oak
Knee brace dimension (in)	30	36	36
Knee brace joint stiffness (lb/in)	25,000	18,000	100,000
Beam/column joint stiffness (lb/in)	50,000	36,000	100,000
Model frame stiffness (lb/in)	1,078	1,141	3,161
Experimental frame stiffness (lb/in)	900	1,290	3,060
Difference	*20%*	*12%*	*3%*

4.6.2. Alternative Model Comparisons

The global frame stiffness and member forces predicted by alternative models are shown in Table 4-12, Table 4-13, and Table 4-14. Each table includes the axial force results of two models: the as-tested SAP model and a conventional SAP model in which all joints were rigid. The location label refers to the knee brace numbering shown in Figure 4-5. Beam-to-column locations relate to the associated knee brace location.

Percent difference values should be reviewed with caution. Small changes in relatively insignificant values may yield large percent differences.

The elimination of joint springs significantly increased the global frame stiffness of all models. The eastern white pine frame had the greatest increase with a nearly fourfold increase in stiffness.

As shown in the tables, axial force is somewhat sensitive to joint stiffness. The most significant difference in axial force occurred at knee brace location 303 on the Douglas fir frame. Elimination of the joint spring resulted in an axial force reduction of 574 pounds to 268 pounds (a 53% reduction).

Table 4-12 Douglas Fir 2S2B Model Results

	As-tested SAP Model	Conventional SAP Model	*Difference*
Knee brace joint stiffness (lb/in)	25,000	rigid	
Beam/column joint stiffness (lb/in)	50,000	rigid	
Frame material MOE (lb·in)	1,600,000	1,600,000	
Model frame stiffness (lb/in)	1,078	4,902	*355%*
<u>Knee brace joint axial force (lb)</u>			
Location			
301	578	341	*-41%*
302	-672	-517	*-23%*
303	574	268	*-53%*
304	-679	-478	*-30%*
305	1,015	1,288	*27%*
306	-1,070	-1,278	*19%*
307	944	1,036	*10%*
308	-1,106	-1,434	*30%*
<u>Beam/column joint axial force (lb)</u>			
Location			
301	-834	-647	*-22%*
302	44	-47	*-207%*
303	-515	-323	*-37%*
304	364	197	*-46%*
305	-995	-1,219	*23%*
306	472	588	*25%*
307	-843	-887	*5%*
308	600	852	*42%*

Table 4-13 Eastern White Pine 2S2B Model Results

	As-tested SAP Model	Conventional SAP Model	*Difference*
Knee brace joint stiffness (lb/in)	18,000	rigid	
Beam/column joint stiffness (lb/in)	36,000	rigid	
Frame material MOE (lb·in)	1,100,000	1,100,000	
Model frame stiffness (lb/in)	1,141	5417	*375%*
<u>Knee brace joint axial force (lb)</u>			
Location	449	295	*-34%*
301	-542	-412	*-24%*
302	503	250	*-50%*
303	-573	-388	*-32%*
304	859	1,077	*25%*
305	-883	-1,054	*19%*
306	804	881	*10%*
307	-914	-1,170	*28%*
308			
<u>Beam/column joint axial force (lb)</u>			
Location			
301	-752	-609	*-19%*
302	-55	-114	*107%*
303	-478	-308	*-36%*
304	278	138	*-50%*
305	-875	-1,080	*23%*
306	352	422	*20%*
307	-722	-776	*7%*
308	488	669	*37%*

Table 4-14 White Oak 2S2B Model Results

	As-tested SAP Model	Conventional SAP Model	*Difference*
Knee brace joint stiffness (lb/in)	100,000	rigid	
Beam/column joint stiffness (lb/in)	100,000	rigid	
Frame material MOE (lb·in)	1,000,000	1,000,000	
Model frame stiffness (lb/in)	3,161	5733	*81%*
<u>Knee brace joint axial force (lb)</u>			
Location			
301	368	291	*-21%*
302	-606	-569	*-6%*
303	366	257	*-30%*
304	-604	-546	*-10%*
305	813	870	*7%*
306	-1,009	-1,119	*11%*
307	781	798	*2%*
308	-1,033	-1,128	*9%*
<u>Beam/column joint axial force (lb)</u>			
Location			
301	-703	-644	*-8%*
302	-28	-50	*79%*
303	-396	-329	*-17%*
304	276	225	*-18%*
305	-850	-906	*7%*
306	424	487	*15%*
307	-698	-700	*0%*
308	571	648	*13%*

4.7. Summary

The global stiffness of a two-dimensional timber frame under lateral load is highly dependent on individual joint stiffness. In a case where story drift is of interest, it is imperative that a structural model include the flexibility of wood-pegged mortise and tenon joints. There are many methods of modeling such a spring connection, including the two discussed in this chapter: the stiffness based computer model and the classic work-energy method.

The method of analyzing internal member actions requires a more subjective decision based on the level of frame redundancy. A relatively determinate frame, such as the 1S1B frame of this study, can be accurately modeled without regard for joint stiffness. However, as the frame and corresponding model become more indeterminate, joint flexibility becomes increasingly important for accurate determination of frame actions. Knee brace joint flexibility appears to have more effect on global stiffness than does beam/column joint flexibility.

Implementation of nonlinear springs at tensile joints may improve model accuracy. However, the use of nonlinear springs at compressive joints is not recommended based on anticipated higher stiffness and linearity due to bearing resistance.

5. Sheathed Frame Testing

5.1. Overview

Traditional timber frames provide gravity and lateral load resistance, but the term "timber frame" does not imply any particular form of building envelope. There are many methods of enclosing timber frames, but the most common technique is to apply structural insulated panels (SIPs) to the exterior of the structure. As demonstrated in Chapters 2 and 3, unsheathed timber frames may not have adequate stiffness to resist lateral loads. The addition of SIPs is expected to significantly increase the resistance to lateral loads.

SIPs can be attached to a frame with either screws or nails. The nails will typically have a ring shank that provides additional withdrawal resistance compared to a smooth shank fastener. The primary advantage of using nails to attach a panel is the speed at which a nail can be hammer driven versus the additional time required to install screws. Screws, however, provide superior withdrawal resistance compared to ring-shank nails.

The objective of this part of the research project was to characterize the response of sheathed full-scale timber frames subjected to lateral load. Two 1S1B and two 2S2B frames were sheathed with SIPs, nominally 4 or 6 inches thick.

The intent was to investigate the response with the assumption that all lateral load is initially applied to the frame, then transferred into the SIPs via the interfacing connection, and transferred back to the frame reactions points. Although it may be possible in some cases for lateral load to be resisted directly by the sheathing without

traveling through the timber frame, it was assumed for the purpose of this research that all lateral load must be transferred from the timber frame to the reaction via the SIPs.

5.2.Test Assemblies

5.2.1. Frame and Panel Dimensions

Two 1S1B and two 2S2B sheathed frames were tested. Dimensions of the 1S1B and 2S2B frames are described in Chapters 2 and 3, respectively.

The SIPs were of two nominal thicknesses: 4-inch and 6-inch. The 4-inch panel consisted of a 3.5 inch extruded polystyrene (EPS) core enclosed by 7/16 inch oriented strand board (OSB) skins to create a panel thickness of approximately 4.5 inches. The 6-inch panel had 5.5 inches of EPS core with 7/16" OSB skins to provide a total thickness of approximately 6.5 inches. The 4-inch panels were supplied by Great Lakes Insulspan of Blissfield, Michigan and the 6-inch panels were provided by Premier Building Systems of Fife, Washington. All panels were installed with screws that had a shank diameter of 0.190 inches. Screw length was 6 inches for the 4-inch panels and 8 inches for the 6-inch panels unless noted otherwise.

Two six-inch panels were attached to a 1S1B Douglas fir frame. The panels were oriented as shown in Figure 5-1. The panels were joined by a continuous 7/16" x 4" OSB spline attached to each OSB skin of the SIP with 8d nails 6 inches apart (nails had clipped heads and were driven with a pneumatic nail gun). This frame is distinct from the frame described in Chapter 2 and will hereafter be labeled the "Sheathed 1S1B Douglas Fir Frame."

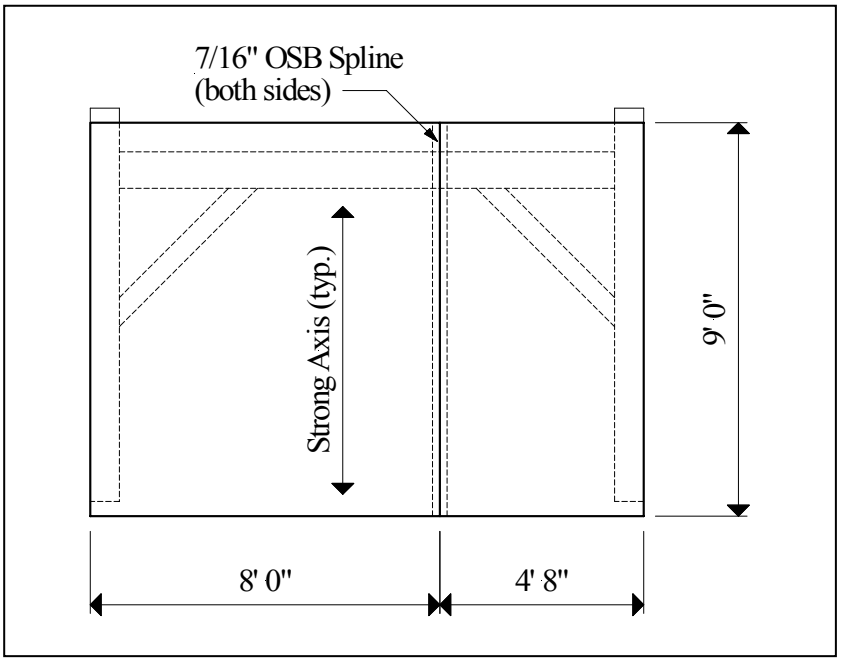

Figure 5-1 Douglas Fir 1S1B Sheathed Frame

A continuous four-inch panel, 12’ wide by 8’ high, was applied to the 1S1B white oak frame, which was also tested in the unsheathed condition as described in Chapter 2.

The 2S2B Douglas fir frame was sheathed with four six-inch panels of size and orientation as shown in Figure 5-2. The panels were joined by a continuous 7/16” x 4” OSB spline attached to each OSB skin of the SIP with 8d nails 4 inches apart.

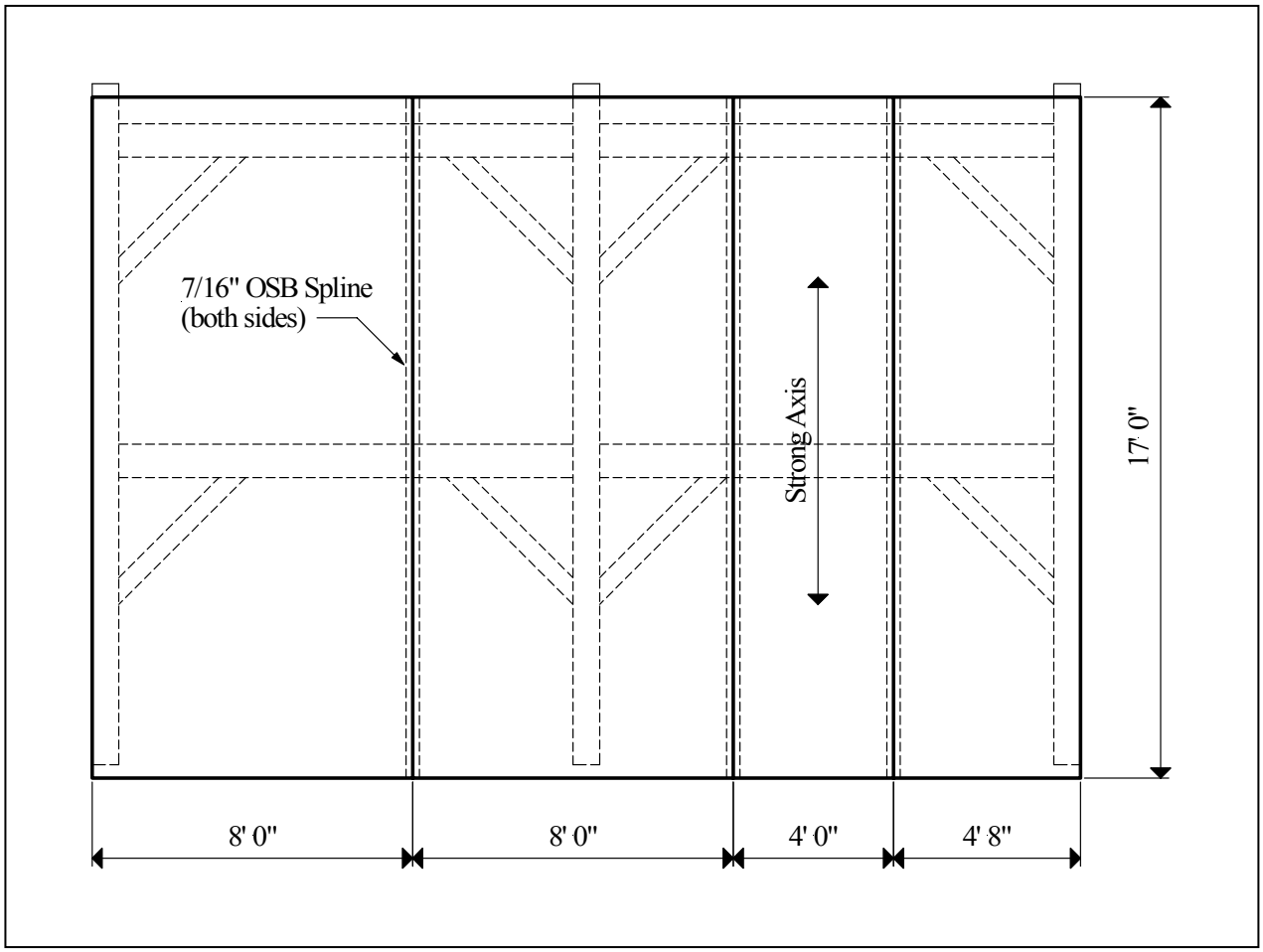

Figure 5-2 Douglas Fir 2S2B with SIPs

The 2S2B eastern white pine frame was sheathed with four, four-inch panels each of which was 12’ wide by 8’ high as shown in Figure 5-3. All panel joints were coincident with frame members, and no splines were used. Both 2S2B frames were also loaded in the unsheathed condition as described in Chapter 3.

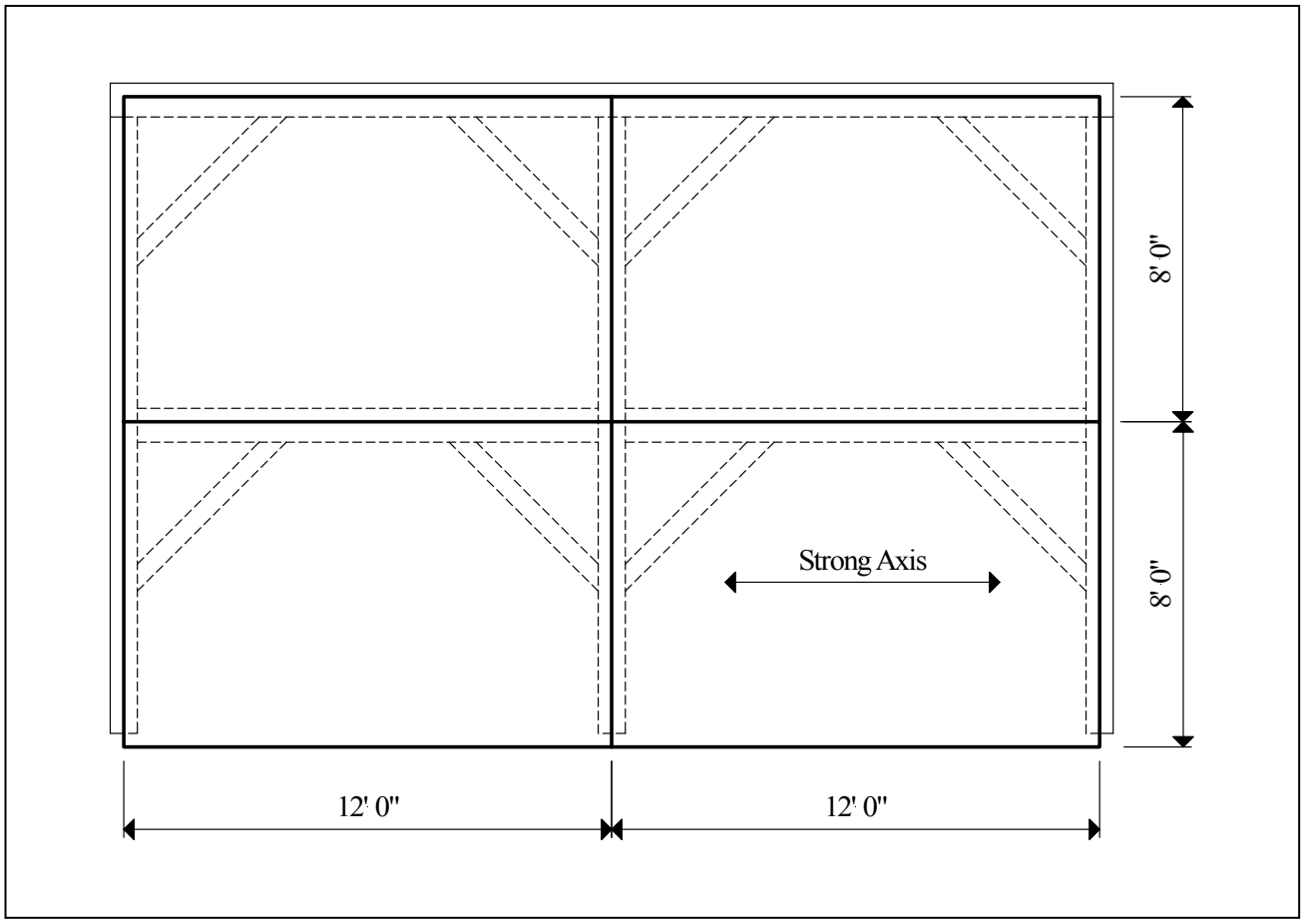

Figure 5-3 Eastern White Pine 2S2B with SIPs

5.3.Experimental Program

The methods of loading and data collection are described in Chapters 2 and 3 for the 1S1B and 2S2B frames, respectively.

5.4.Overview of Test Results

A description of the load cycles for all frames is provided in Appendix B for the 1S1B frame and Appendix G for the 2S2B frames. A brief summary of the load cycles and attachment methods for each of the sheathed frames is given in the following sections.

5.4.1. 1S1B Sheathed Douglas Fir

The sheathed 1S1B Douglas fir frame is distinct from the unsheathed 1S1B Douglas fir frame as described in Chapter 2. The sheathed 1S1B Douglas fir frame was load cycled four times with SIPs installed followed by two cycles without sheathing. The first two load cycles were conducted with screws 12 inches apart and the final two were conducted with screws 8 inches apart.

Inspection of the frame upon disassembly along with analysis of the results indicated significant joint damage occurred during the cycles with SIPs installed. Therefore, this frame is not included in the discussion of unsheathed frames nor will its results be compared to any results for the unsheathed condition.

5.4.2. 1S1B White Oak

The unsheathed 1S1B white oak frame was initially cycled 3 times prior to installation of SIPs. SIPs were installed for cycles 4 through 10. As mentioned previously, the intent was for the load path to be from timber frame into the sheathing and back out via the timber frame reaction points. Unfortunately, due to interference caused by the reaction fixtures, the load path was disrupted for cycles 4 through 8; therefore, discussion of results will be limited to cycles 9 and 10.

The panel was attached with 6-inch screws located at 16 inches on center. Screw holes (1/8 inch diameter) were predrilled through the panel and into the timber to facilitate screw penetration into the frame. Washers were installed under the heads of all

screws, and a 0.5-inch plywood shim was installed between the frame and panel resulting in a screw penetration of 1 inch into the frame timbers.

5.4.3. 2S2B Douglas Fir

The 2S2B Douglas fir frame was subjected to 115 load cycles. The first three and the last three load cycles were conducted in the unsheathed condition. The intermediate 99 load cycles were conducted with 6-inch SIPs installed. Load cycles 4 through 58 were conducted with screws installed 12 inches apart and cycles 59 through 112 were conducted with screws 24 inches apart. Cycles 8 through 57 and 61 through 110 subjected the frame to 0.5 inches of displacement in each direction at a rate of 1 cycle per second.

The cross-sectional width of the beams was less than that of the columns. In order to provide a flush surface for installation of SIPs, shims were installed along the entire length of all beams. A double layer of 7/16-inch OSB shims provided a total shim depth of 0.875 inches. Given the screw length of 8 inches, panel thickness of 6.5 inches and a shim thickness of 0.875 inches, the screws penetration into the beams was only 0.625 inches.

5.4.4. 2S2B Eastern White Pine

The 2S2B eastern white pine frame was subjected to 118 load cycles. The first three and the last two load cycles were conducted in the unsheathed condition. Load cycles 1 through 5 were conducted without a sill timber and then a sill was installed for the remaining cycle. The sill facilitated full perimeter attachment of the SIPs. All tests were conducted with 6-inch screws located 12 inches apart.

Openings were cut in the panels for load cycles 11 through 116. The openings simulated window or door openings and these tests were conducted as a preliminary investigation for future research.

Load cycles 15 through 114 subjected the frame to 0.5 inches of displacement in each direction at a rate of 1 cycle per second, and no data was recorded for these cycles.

5.5.Results

5.5.1. Comparison of Unsheathed and Sheathed Frame Stiffness

In order to simplify comparison of frame stiffness, the stiffness of all frame cycles discussed in this chapter was determined by the slope of a line connecting the points of maximum load and displacement (pull stroke to push stroke). As shown in Figure 5-4, addition of the SIP resulted in a 71 percent stiffness increase for the 1S1B white oak frame.

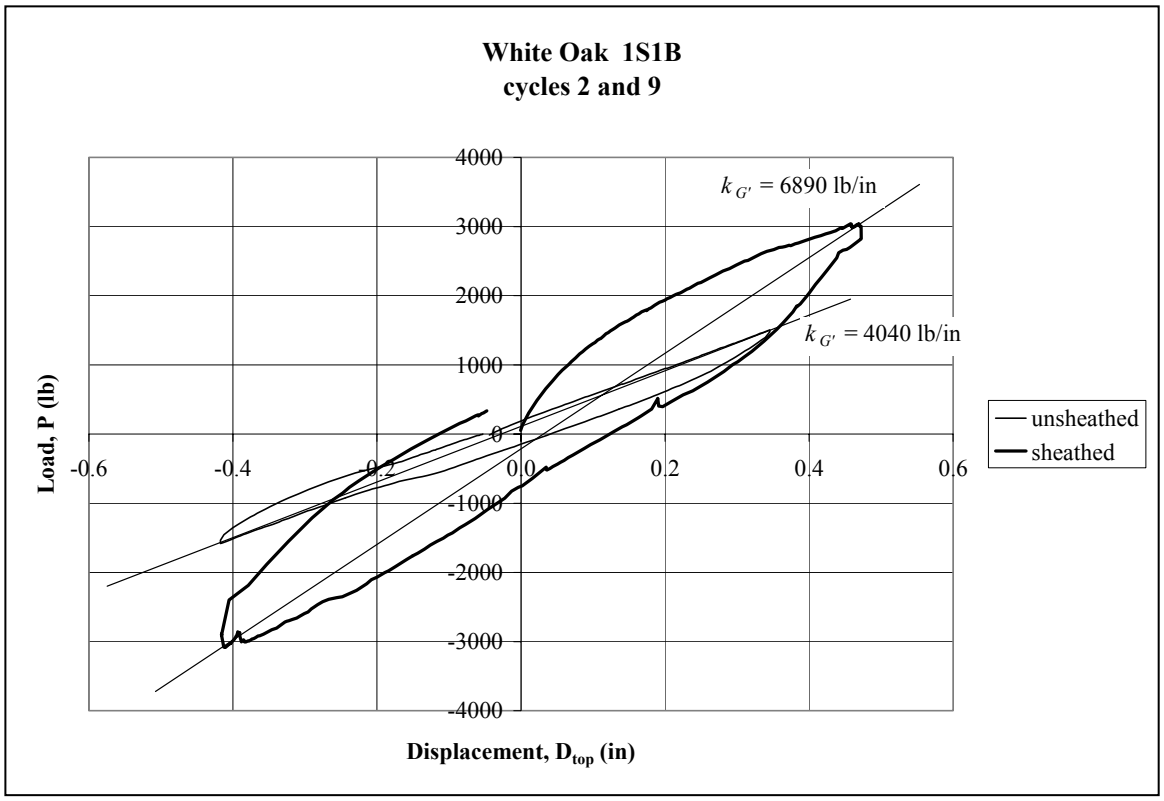

Figure 5-4 Unsheathed versus Sheathed Stiffness (1S1B White Oak)

The stiffness increase for the 2S2B Douglas fir frame was much more dramatic as shown in Figure 5-5. The stiffness increased over 900 percent from 1050 lb/in to 10,710 lb/in.

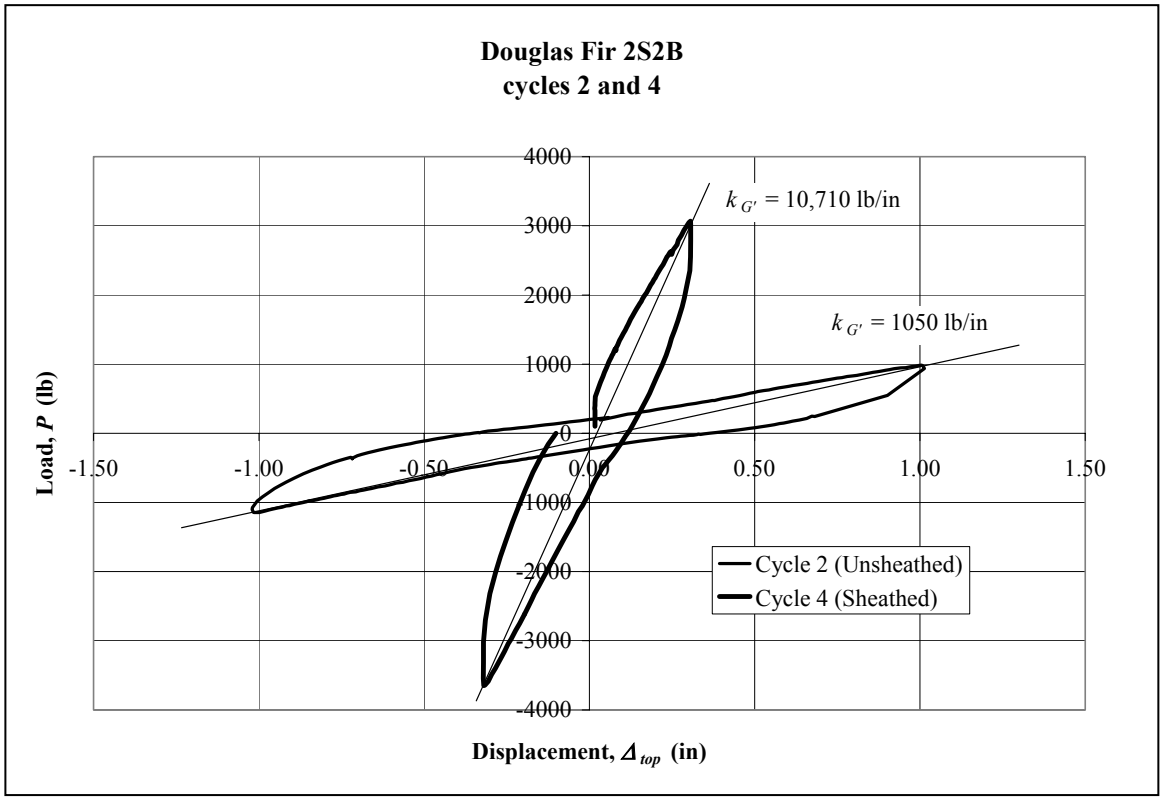

Figure 5-5 Unsheathed versus Sheathed Stiffness (2S2B Douglas Fir)

5.5.2. Effect of Adding a Sill Timber

All but one of the frames was tested without the benefit of full perimeter attachment of the SIPs. A sill timber was added to the 2S2B eastern white pine frame. The results are shown in Figure 5-6. This frame had the highest sheathed stiffness at 16,540 lb/in and the stiffness doubled to 37,560 lb/in with the attachment of the SIPs to the sill timber. Figure 5-6 also demonstrates the 748 percent increase in stiffness from the unsheathed to sheathed condition.

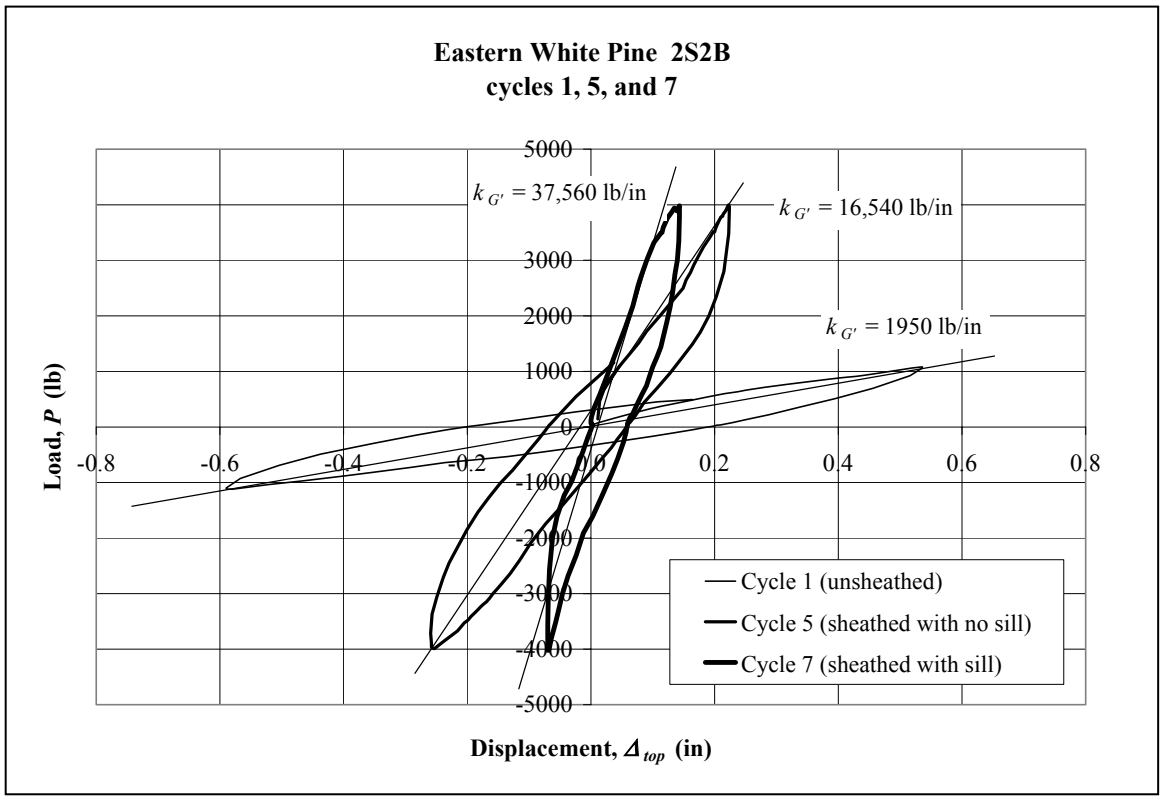

Figure 5-6 Effect of Full Perimeter Sheathing Attachment

5.5.3. Effects of Multiple Load Cycles

The 2S2B Douglas fir frame was subjected to 54 load cycles of approximately equal displacement. The data as recorded for the first three cycles and last cycle is shown in Figure 5-7. The frame exhibited a 20 percent reduction in stiffness at the final load cycle. This degradation in stiffness indicates that frame response based on a single load cycle may be unconservative.

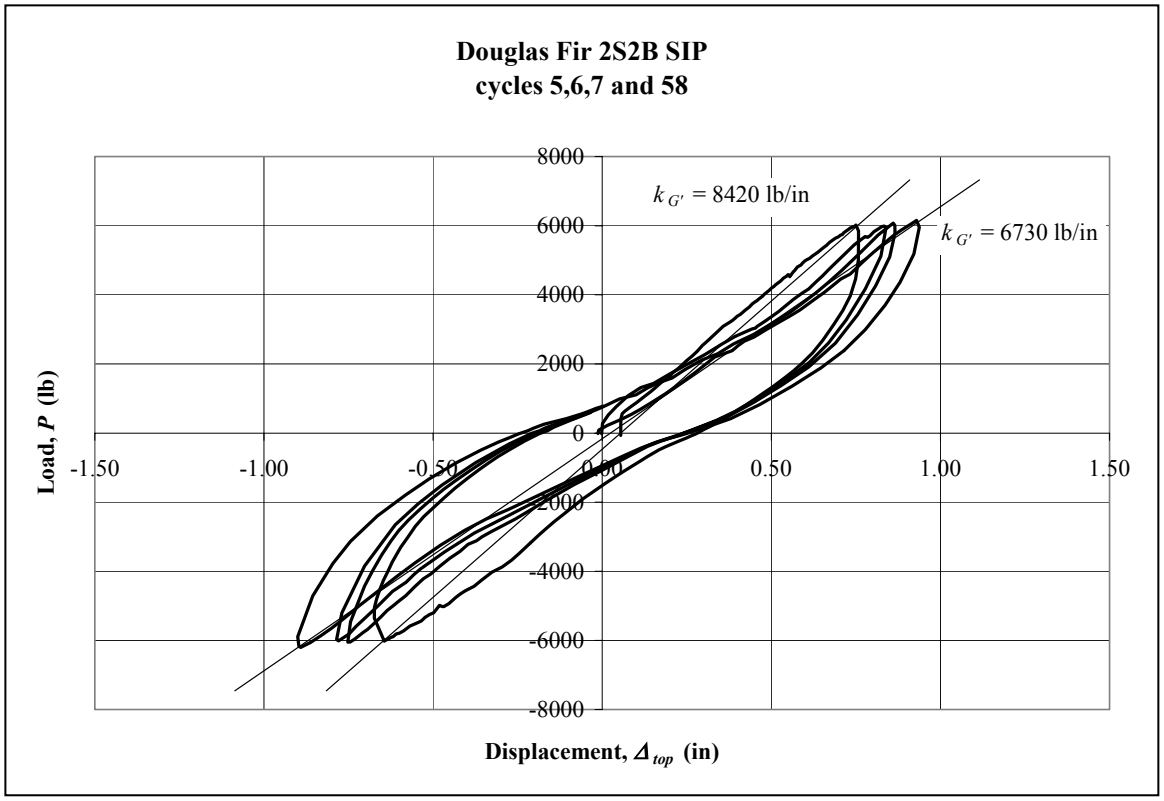

Figure 5-7 Effects of Multiple Load Cycles

5.5.4. Effects of Screw Spacing

The effects of varied screw spacing were investigated on two frames. The sheathed 1S1B frame Douglas fir was the first frame to be examined relative to screw spacing. As shown in Figure 5-8, reinstalling the screws 8 inches apart resulted in a 41 percent increase in frame stiffness compared to the condition with screws 12 inches apart.

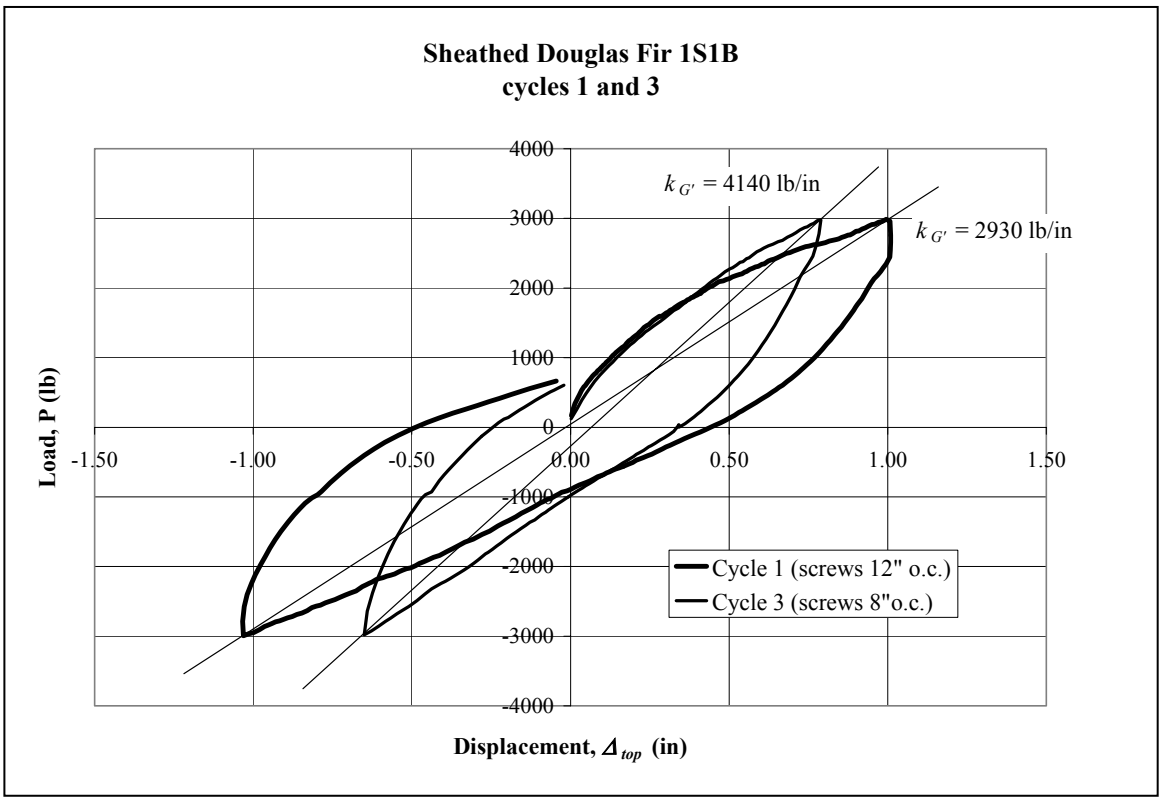

Figure 5-8 Effects of Screw Spacing (Douglas Fir 1S1B)

As shown in Figure 5-9, increasing the screw spacing on the 2S2B Douglas fir frame from 12 inches to 24 inches resulted in a 36 percent decrease in frame stiffness.

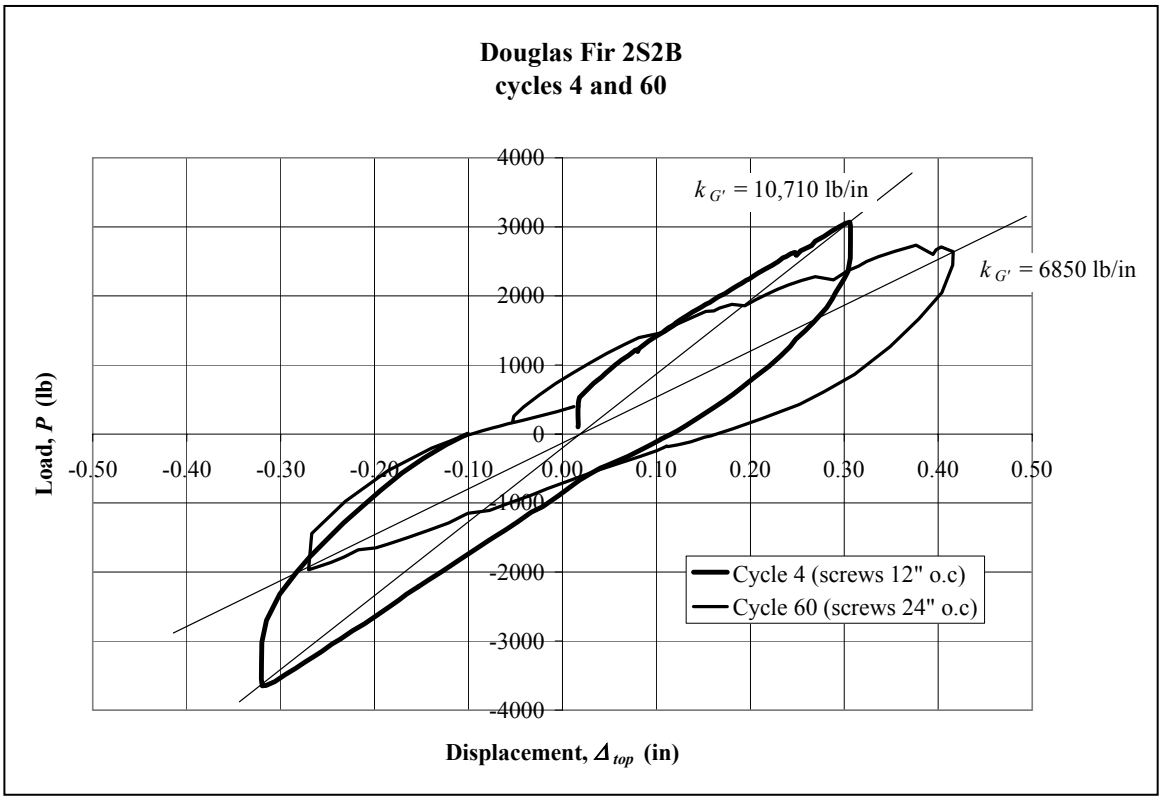

Figure 5-9 Effects of Screw Spacing (Douglas Fir 2S2B)

5.5.5. Maximum Load Cycles

The results of applying the maximum available displacement to the sheathed 1S1B Douglas fir frame are demonstrated in Figure 5-10. With screws installed 12 inches apart, screw failure resulted in an ultimate applied load of 4370 pounds on the push stroke, therefore the frame was not cycled in the pull direction. Screw failure occurred at the base of the columns with two shear failures at the west column and one failure at the east column. Significant screw deformation occurred in several screws located in the lower region of each column.

With screws installed 8 inches apart, the frame was able to carry increasing load throughout the full available displacement in the push direction. However, screw failure occurred in the pull cycle at an ultimate applied load of 7210 pounds. Screw failure occurred at the base of the columns with two shear failures in each column, and significant screw deformation occurred in several screws located in the lower region of each column.

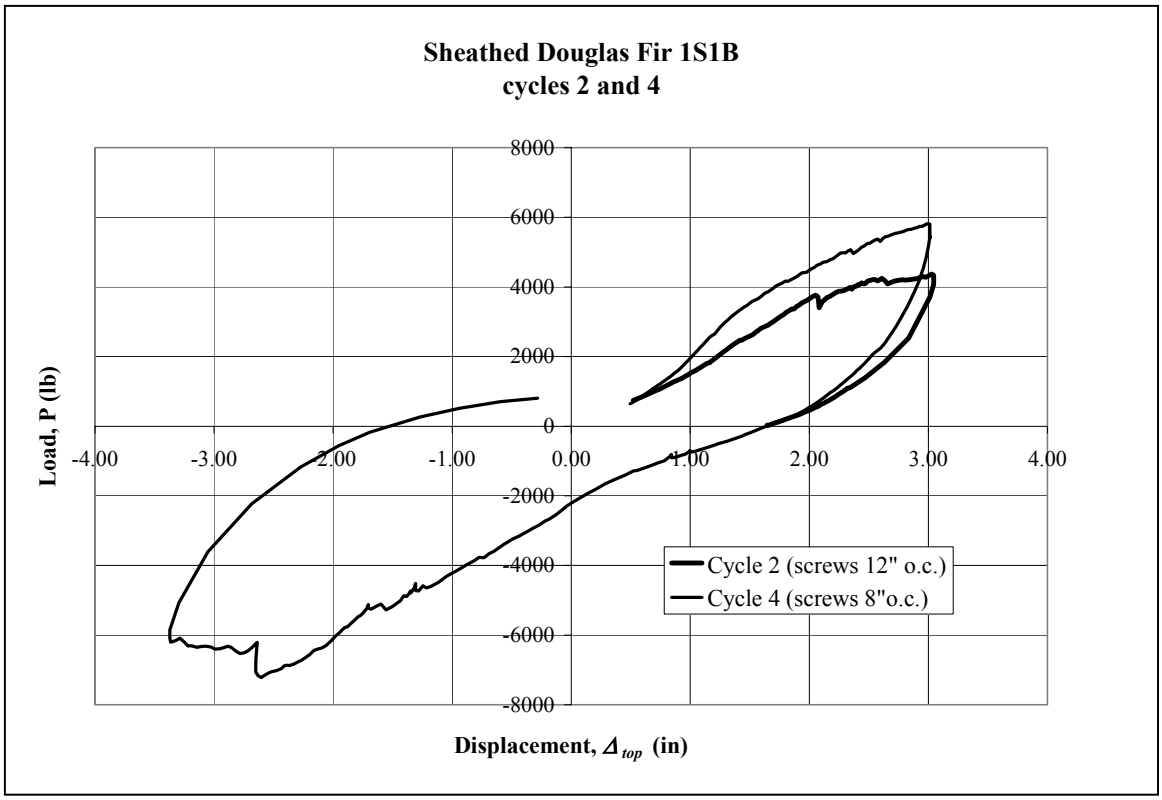

Figure 5-10 Maximum Load Cycles (Sheathed 1S1B Douglas Fir)

The maximum load cycle for the sheathed white oak 1S1B frame is shown in Figure 5-11. Removal of the SIPs revealed three screws had failed in shear. Two of the failures were at the base of the west column and one was at the base of the east column. These screw failures are evident in the maximum load plot. As the load approached the ultimate load of 5000 pounds, the screws began to fail resulting in increased displacement without increased load.

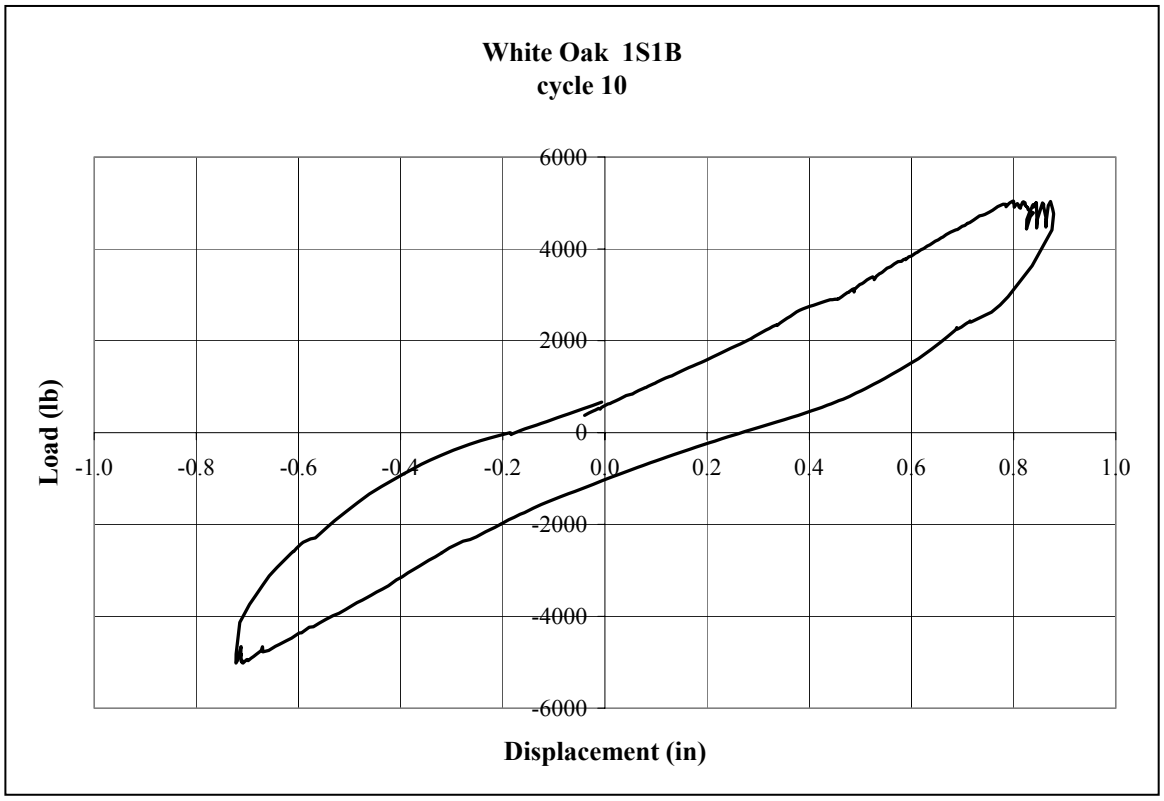

Figure 5-11 Maximum Load Cycle (White Oak 1S1B)

The maximum load cycles for the 2S2B Douglas fir frame are shown in Figure 5-12. The stiffness $k_{G'}$ based on deflection at maximum load was reduced by 14 percent when screw spacing was increased from 12 inches to 24 inches. In both conditions, several screw failures occurred at the base of all columns.

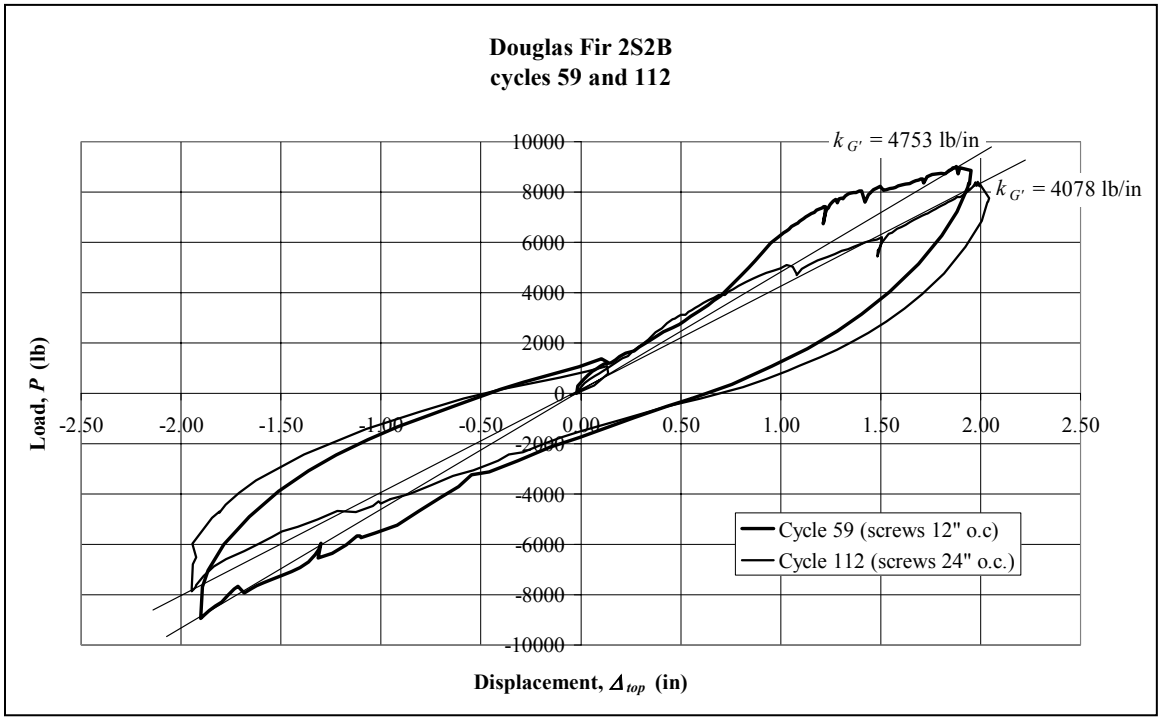

Figure 5-12 Maximum Load Cycle (2S2B Douglas Fir)

The maximum load cycle for the 2S2B eastern white pine frame is shown in Figure 5-13. The chart represents a load cycle for which the sill was installed and the panels were attached at all edges. The frame was not subjected to large load without the sill installed. The frame withstood a load of 10,000 pounds on the push stroke without incurring any apparent damage. The maximum load of 10,000 pounds was also obtained on the pull stroke but at a larger displacement of 0.62 inches. Again there is no evidence of screw failure in the chart and removal of the screws revealed only minor damage to any of the fasteners.

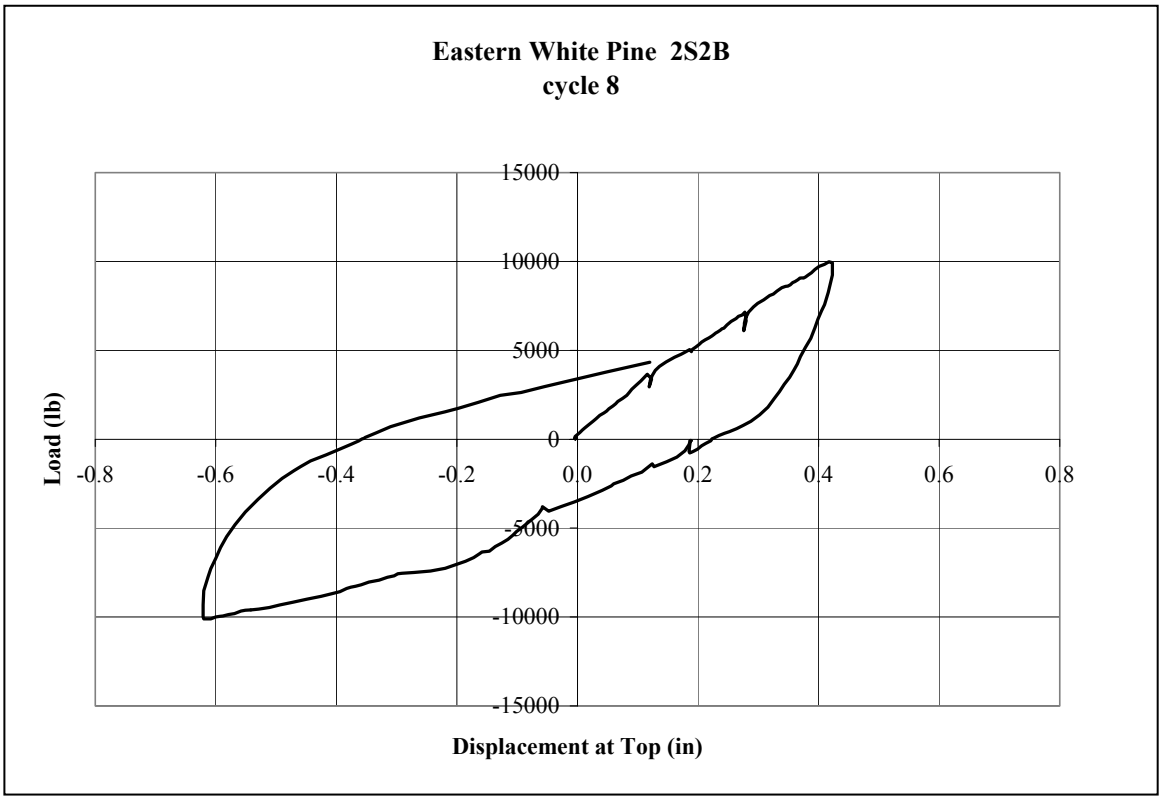

Figure 5-13 Maximum Load Cycle (2S2B Eastern White Pine)

5.5.6. Effect of Openings

Openings of progressively larger area were cut in the center of each of the four panels installed on the 2S2B eastern white pine frame. As shown in Figure 5-14, cycle 10 represents the response of the frame with no openings, cycle 11 represents frame response with 6 foot by 4 foot openings at each bay, cycle 12 represents a 6 foot by 6 foot opening at each bay, and cycle 13 represents the openings on the lower story enlarged to 6 feet by 7 feet. The stiffness of cycle 11 is 17 percent less than the sheathed frame stiffness of 16,970 lb/in, and as expected, the stiffness decreased further as the opening was enlarged.

Even with a relatively large opening, the frame stiffness of 8930 lb/in was still greater than the expected required design stiffness of 6040 lb/in (see Chapter 3).

Damage to the OSB skins did not occur until the frame was subjected to a load of 10,000 pounds on a subsequent cycle. Failure was exhibited by cracking at the upper corners of the lower openings. The cracks propagated diagonally upward and outward from the opening to the edge of the panel. Removal of the fasteners revealed significant screw deformation at several locations around the perimeter of the lower panels.

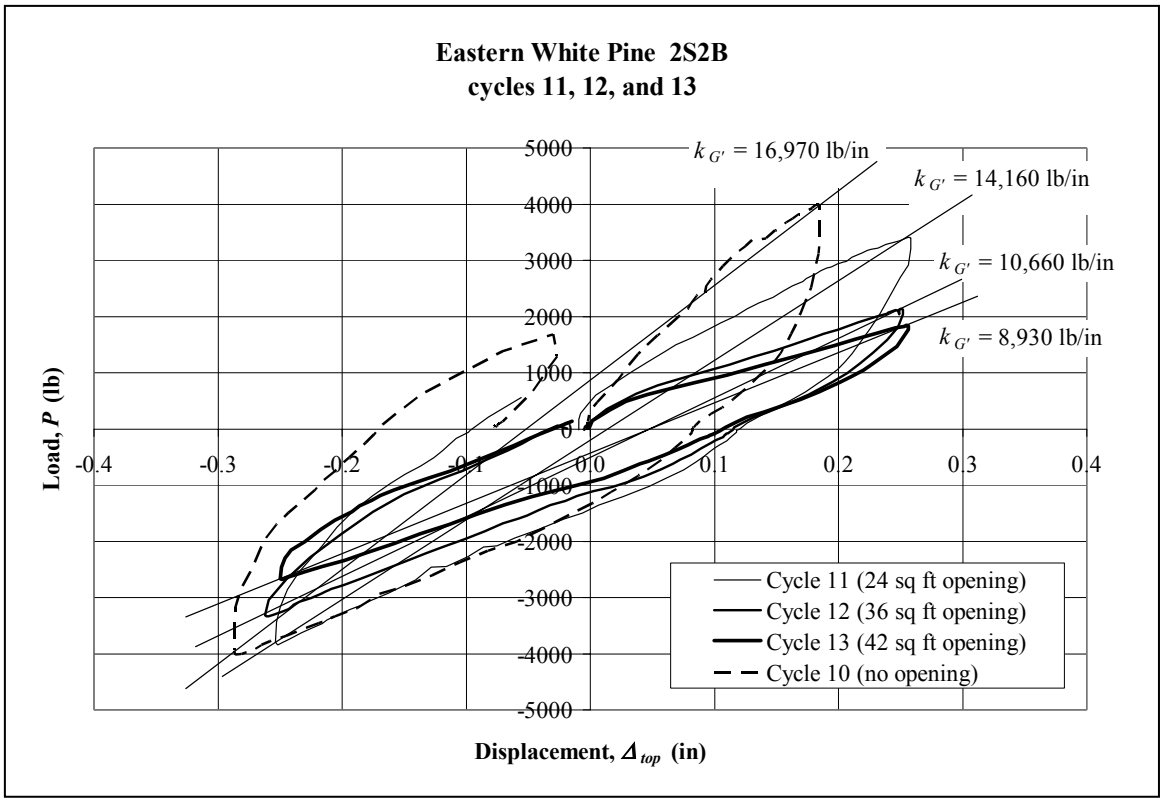

Figure 5-14 Effects of Panel Openings

5.6.Summary

As expected, the addition of SIP sheathing increased frame stiffness to levels required for serviceability. Attachment of the panels around the full perimeter resulted in a significant increase in frame stiffness; therefore, attachment of the SIP to a sill is recommended to obtain maximum performance. Without the use of a sill, significant screw damage was confined to the lower portions of the columns, indicating that the load was not equally distributed to all fasteners.

Cycling of the sheathed frame at service level loads caused a decrease in frame stiffness. However, cyclic loading was only conducted on a frame without a sill timber, and in this case, the reduction in stiffness may be due to localized connection damage at the base of the columns.

When a sill timber was installed and large openings were cut in the panels, the eastern white pine frame exhibited acceptable performance levels. This indicates the potential benefits of SIP panels on walls with many openings. It is important to note that these tests were conducted with contiguous panels. In many instances, window walls are sheathed with smaller pieces of SIP resulting in many joints that are not coincident with a frame timber. In this case the SIPs may not provide the required contribution to frame stiffness unless special shearwall detailing is provided.

6. SIP Connection Tests

6.1. Overview

The lateral stiffness and strength of a sheathed timber frame structure is dependent on the characteristics of the panel to frame mechanical connection. The characteristics of this interface must be determined in order to produce an accurate model of SIP-enclosed traditional timber frames.

One objective of this portion of the study was to develop load-slip models that represent various types of SIP to timber interfaces. A second objective was to statistically compare the effects of variation in connection details.

6.2. Test Specimens

Four-inch wide SIP specimens were cut from panels of either 4-inch or 6-inch nominal thickness. SIP specimen length varied, but the distance from fastener to end of panel was a minimum of 2 inches or ten times the fastener diameter (10D) for all tests. The timber specimens were of three species: Douglas fir, white oak, and eastern white pine. All timber sections were 3.5 inches wide but of varying length and thickness. All specimens had sufficient thickness such that no fastener fully penetrated through the timber, and in all instances, the fastener was at least 2 inches from the end of the timber for a minimum end distance of 10D.

The connection was made with either a 0.190 inch diameter screw or a 0.180 inch diameter ring shank nail. The nail size was chosen to be as close as possible to screw diameter. All fasteners were imbedded 1.5 inches into the timber or 8D. The NDS specifications recommend a screw penetration of 12D; however, it is common timber framing practice to use screws 1.5 inches longer than SIP thickness. All screws had 2 inches of threaded length; therefore, threads were included in the shear plane at the inner skin of the SIP panel. The nail shank had annular rings along three inches of length, thus the shear plane at the inner skin of the nail-connected panel included the rings. The panel was installed tight against the timber such that there were no gaps between the mating surfaces.

As shown in Figure 6-1, load was applied in-line with the panel to timber interface. Application of the load in this manner eliminated any moment due to eccentric loading and thus lateral restraint of the specimen was not provided. This method of load application is based on the assumption that the inner skin of a SIP carries all of the shear

actions. This is a conservative assumption in that a small amount of load may be transferred to the outer skin via the cantilever action of the fastener.

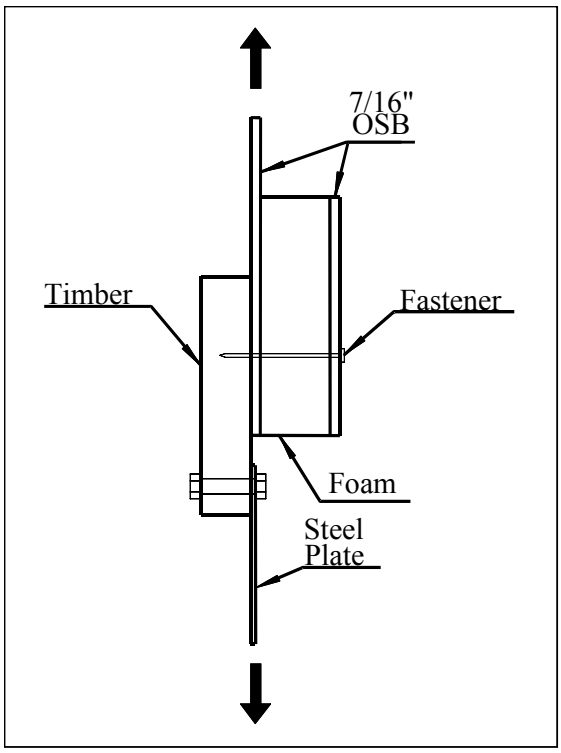

Figure 6-1 Schematic of Typical Test Set-up

6.3. Experimental Program

The testing was conducted in three phases. The procedures of each phase are slightly different as described in the following sections.

6.3.1. Phase 1

The first phase of testing was conducted on a Tinius Olsen hydraulic test system. Ram pressure was measured with a pressure transducer and converted to load within the data acquisition software. Slip between the SIP specimen and the timber was measured with a 0.5-inch linear potentiometer. Actuator displacement was controlled manually with the fluid flow-control valves. Although a target load rate was established with a chart of displacement versus time provided by the data acquisition system, the actual rate of displacement was slightly variable due to manual operation of the test system. The target rate for displacement was approximately 0.0005 inches per second.

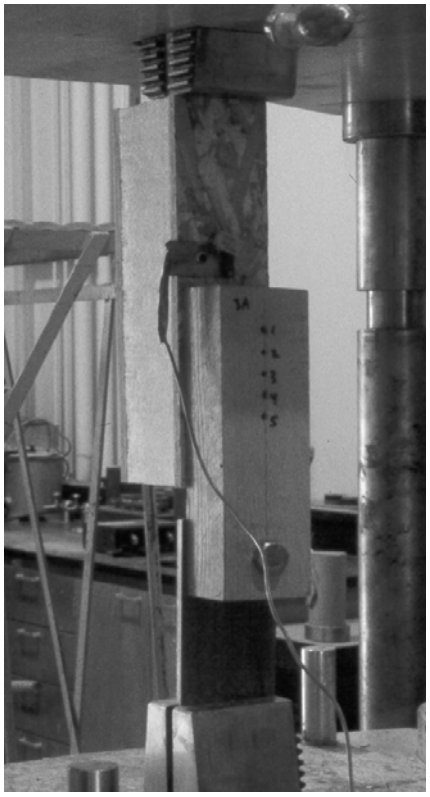

Figure 6-2 Phase 1 Test Set-up

6.3.2. Phase 2

The second phase of testing was performed on an Instron servo hydraulic universal testing machine. A photograph of an example of phase 2 testing is shown in Figure 6-3. Load was measured with a 5-kip load cell and transmitted to the data acquisition system via a 10-volt signal. Displacement was measured with a 0.5-inch linear potentiometer. Actuator displacement was controlled with an MTS Test Star computer system. The rate of displacement was set to 0.0005 inches per second.

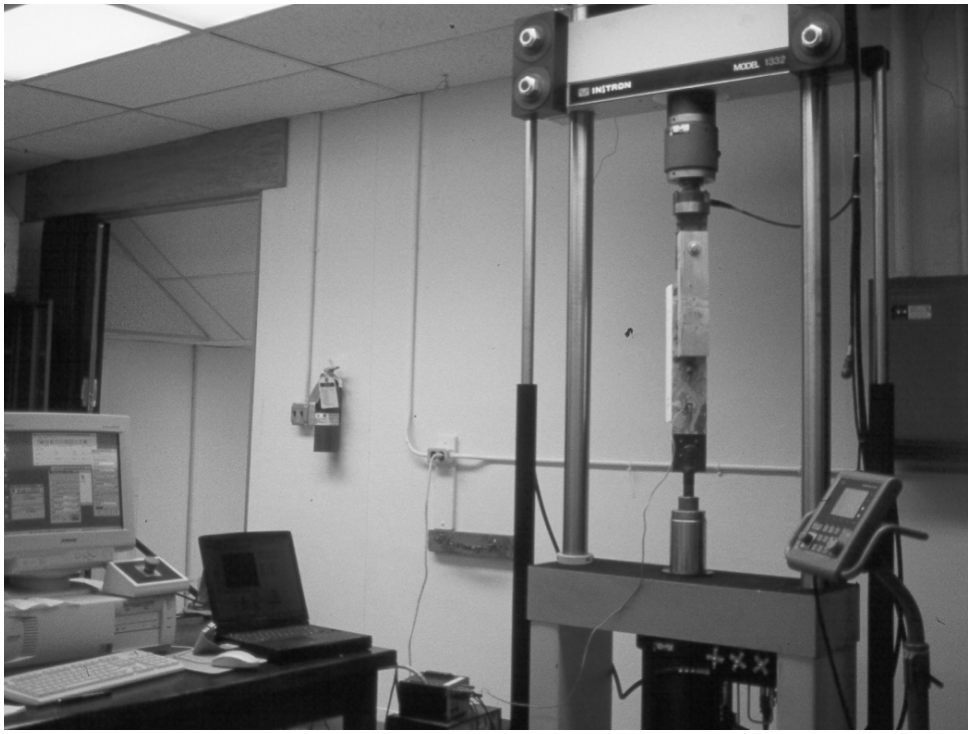

Figure 6-3 Phase 2 Test Setup

6.3.3. Phase 3

The testing procedure of phase 3 was identical to phase 2 with the exception that measured displacement was provided by the MTS system directly from load head translation.

6.4. Experimental Groups

Experimental testing was performed on 14 named groups of specimens.

6.4.1. Phase 1

The first phase of testing was performed on four distinct sample groups, and each group had ten connection specimens. All phase 1 test specimens consisted of a 4-inch thick SIP screw-connected to a white oak timber. A 5/32" pilot hole was drilled in all of the timber specimens. Load was applied parallel to the grain of the timber.

A summary of the variables of phase 1 is shown in Table 6-1. Group "screwwo" was considered as the base test group and had no washer or shim installed, and the panel was predrilled with a 5/32" drill bit. Group "washer" was identical to group "screwwo" except a two-inch diameter washer was installed at the screw head. Group "shim" included a 5/8" thick OSB shim installed between the panel and the timber. The shim was not mechanically affixed to either the panel or the timber. Group "nopredrill" was also identical to the base test, but the SIP panel was not predrilled.

Table 6-1 Phase 1 Summary of Tests

Test Name	SIP predrill	Washer	Shim
screwwo	yes	No	No
washer	yes	Yes	No
shim	yes	No	Yes
nopredrill	no	No	No

6.4.2. Phase 2

The second phase of testing was performed on six distinct sample groups, and each group had ten connection specimens. As shown in Table 6-2 several variables were examined in phase 2. The combination of tests provides for comparison between a timber species of moderate specific gravity (Douglas fir) and one of low specific gravity (eastern white pine). Both screws and nails were tested in each species but no shins or washers were used in phase 2. Load was applied both parallel and perpendicular to timber grain for the Douglas fir screw connected specimens. For the group "osbdf", the outer OSB skin and the inner foam core were removed from the panel in order to examine the contribution of these elements. Testing a single sheet of OSB was conducted to investigate the assumption that the inner skin carries a majority of the shear load thereby possibly simplifying future SIP fastener testing by using only a conventional test configuration.

Table 6-2 Phase 2 Summary of Tests

Test Name	Fastener	Timber species	SIP thickness	Timber Grain Orientation
screwdf	Screw	DF	4 ½"	Parallel
naildf	Nail	DF	4 ½"	Parallel
screwwp	Screw	EWP	4 ½"	Parallel
nailwp	Nail	EWP	4 ½"	Parallel
perpdf	Screw	DF	4 ½"	Perpendicular
osbdf	Screw	DF	½"	Parallel

6.4.3. Phase 3

The third phase of testing was performed on four distinct sample groups of varying size. All specimens consisted of panels screw-connected to a Douglas fir timber. The group titled "long" was identical to group "screwdf" in phase 2. Group "short" consisted of a countersunk 2" screw bearing directly on the inner skin of the panel. The "wax" group had three sheets of wax paper applied between the panel and timber in order to reduce any contribution of friction on connection stiffness. The "thick" group was again identical to both the "long" group of phase 2 and the "screwdf" group of phase 3, except the panel was 2 inches thicker with a correspondingly longer fastener. Neither washers nor shims were used in phase 3.

Table 6-3 Phase 3 Summary of Tests

Test Name	Number of Tests	Screw length	SIP thickness	Timber Grain Orientation
long	10	6"	4 ½"	Parallel
short	10	2"	4 ½"	Parallel
wax	12	6"	4 ½"	Parallel
thick	11	8"	6 ½"	Parallel

6.5. Results

6.5.1. Method of Analysis

In order to quantify and compare the results, a regression analysis was performed on the experimental data set for each specimen. The regression was performed on the natural log of deflection versus load. The equation has the form $P = a\ln\delta + b$ where P is the applied load, δ is the fastener slip, a is the slope of the curve and b is the intercept. At a displacement of zero, the slope of this curve is undefined, therefore all data for a load less than approximately 50 pounds was disregarded in the analysis.

The results of the regression were then used to define each dataset with an equation of the form $P=(A+B\delta)[1\text{-}e^{(-C\delta/A)}]$ (Foschi, 1974). P is the applied load, δ is the fastener slip, C is the initial slope of the curve, B is the final slope of the curve, and A is the point at which a line drawn tangent to the final slope intercepts the load axis. This equation form is graphically demonstrated in Figure 6-4.

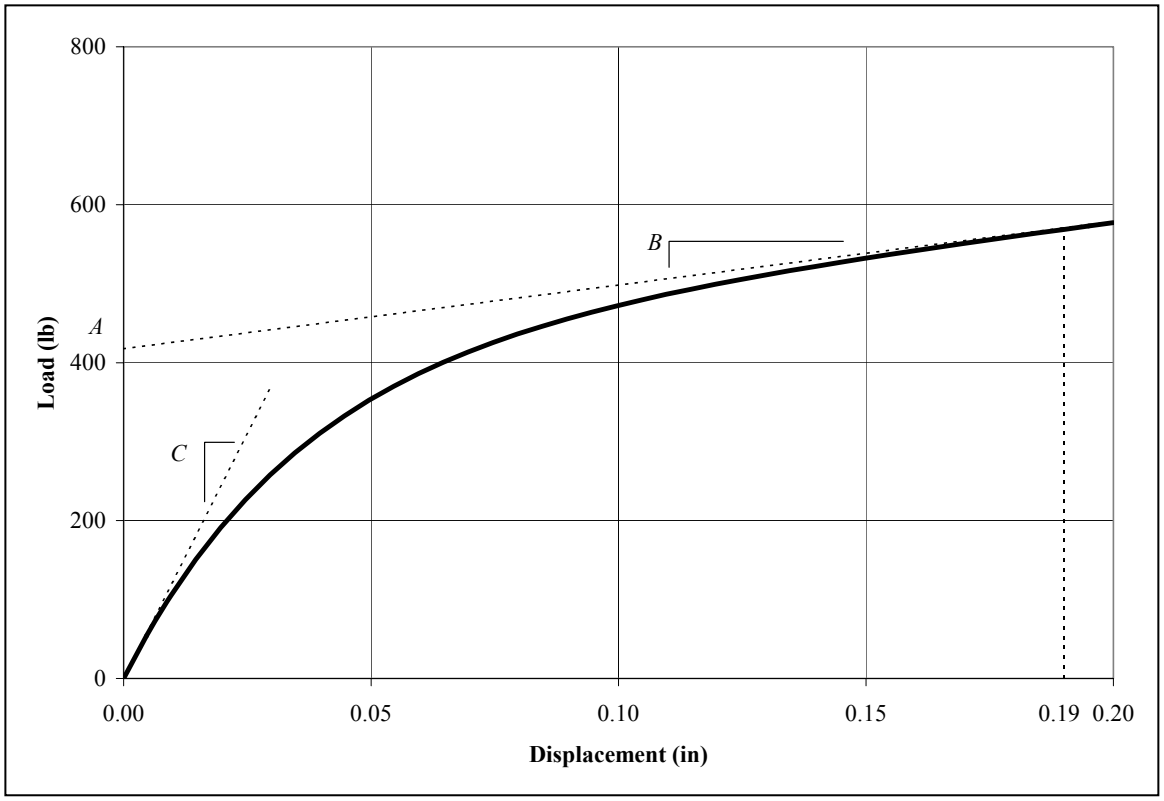

Figure 6-4 Graphical Definition of Coefficients for $P=(A+B\delta)[1-e^{(-C\delta A)}]$

Initial slope coefficient C was determined based on a linear regression of δ versus P over the range of P greater than 25 percent and less than 50 percent of design lateral load for a given connection. Design lateral load Z' was determined based on NDS (AFPA 2001) equations and was increased with a load duration factor of 1.6. The design load and the resulting boundaries are listed in Table 6-4.

Table 6-4 Boundary Values for Determination of Coefficient *C*

Timber Species	Fastener	*Z'* (lb)	0.25*Z'* (lb)	0.50*Z'* (lb)
Douglas Fir	Screw	260	65	130
Eastern White Pine	Screw	213	53	106
White Oak	Screw	289	72	145
Douglas Fir	Nail	205	51	102
Eastern White Pine	Nail	170	42	85

Slope coefficient B was determined based on the slope of the natural logarithm regression, $P = a\ln\delta + b$ at a displacement of 0.19 inches (approximate fastener diameter). The intercept A was then derived by extrapolating the tangent line determined by B to the vertical axis. Graphical results of a typical group are shown in Figure 6-5.

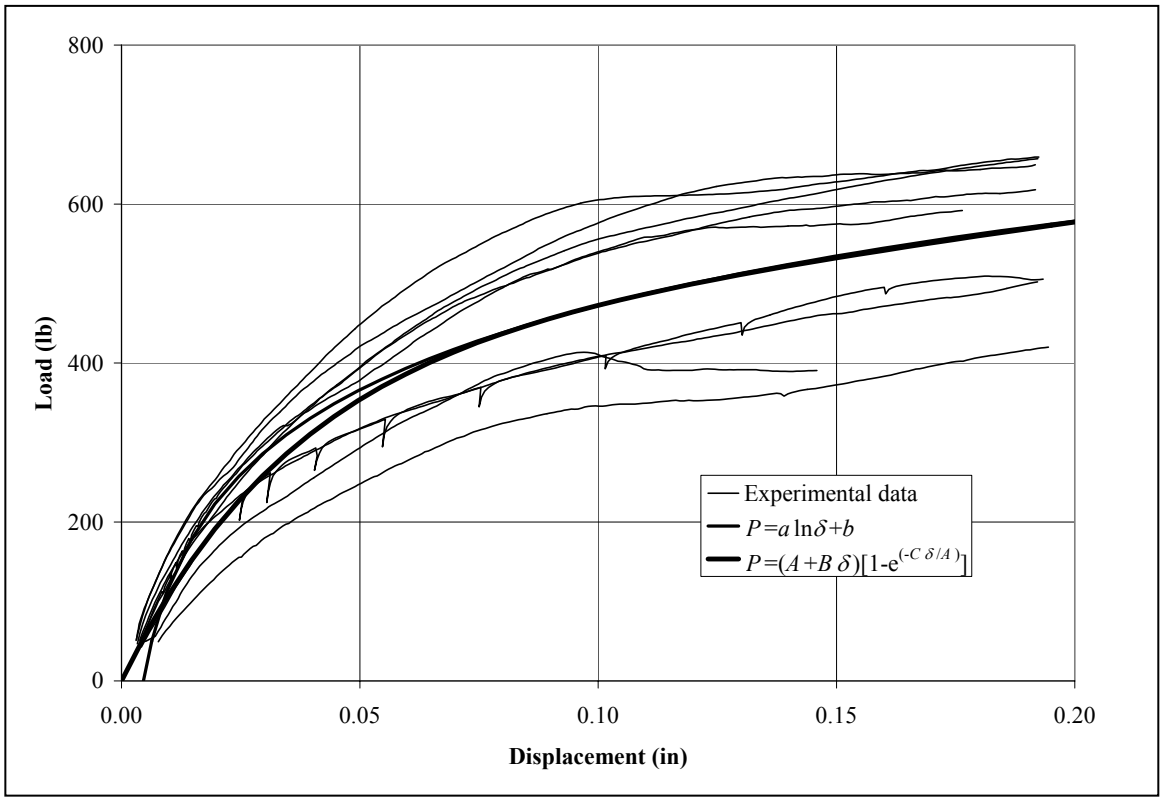

Figure 6-5 Typical Experimental Data and Fitted Curves

Determination of a yield value is subjective. The 5-percent offset method is often used, but this approach results in a yield load that is dependent on the initial stiffness. In order to establish an independent analysis of the yield value for statistical comparison among specimen groups, yield load was determined simply by finding the load at a deflection of 0.95 inches (one half of the screw diameter). Since the results of this experiment are used for comparative purposes rather than for determination of an absolute yield value, the yield load of nail-connected specimens is also based on 0.95 inches (rather than half of the nail diameter or 0.90 inches).

6.6. Regression Coefficients and Yield Load

The regression coefficients and yield value of each test were averaged to provide a single regression equation for each group. The mean values for phases 1, 2, and 3 are shown in Table 6-5,Table 6-6, and Table 6-7 respectively.

Table 6-5 Phase 1 Regression Coefficients and Yield Load

	$P=a\ln(\delta)+b$			$P=(A+B\delta)[1-e^{(-C\delta/A)}]$			$F_{D/2}$
	a	b	R^2	A	B	C	
screwwo	150	905	0.98	507	787	19822	564
washer	162	956	0.99	525	852	17993	583
shim	155	706	0.99	301	796	6686	341
nopredrill	132	783	0.99	431	696	15796	472

Table 6-6 Phase 2 Regression Coefficients and Yield Load

	$P=a\ln(\delta)+b$			$P=(A+B\delta)[1-e^{(-C\delta/A)}]$			$F_{D/2}$
	a	b	R^2	A	B	C	
screwdf	153	825	0.98	418	807	12381	480
naildf	187	871	0.97	373	984	7582	430
screwwp	146	783	0.98	395	767	12204	452
nailwp	173	844	0.98	384	909	9161	440
perpdf	137	737	0.99	372	723	10373	419
osbdf	117	608	0.99	296	618	7040	341

Table 6-7 Phase 3 Regression Coefficients and Yield Load

	$P=a\ln(\delta)+b$			$P=(A+B\delta)[1-e^{(-C\delta/A)}]$			$F_{D/2}$
	a	b	R^2	A	B	C	
long	149	824	0.97	429	782	16363	470
short	167	902	0.94	458	878	21739	501
wax	180	828	0.94	467	686	9174	398
thick	153	713	0.95	306	806	7585	346

The regression coefficients and yield values for each specimen are provided in Appendices J, K, and L. Plots of the data are provided in Appendices M, N, and O.

6.7. Statistical Comparisons

The statistical comparisons have been limited to two critical variables: the initial connection stiffness C and the yield load $F_{D/2}$ defined as the resisting force at a displacement of one-half of the fastener diameter (0.095 inches).

The statistical analysis was limited to comparisons within each phase. One of the groups within each phase was identified as the base specimen set and the remaining groups were compared to the base group. Since each comparison was intended to investigate a predicted result, all comparisons were one tailed t-tests with an alpha of 0.05.

6.7.1. Phase 1 t-test

The three comparative variables examined included the addition of a washer at the screw head, the use of a shim between the SIP and the timber, and the lack of pre-drilling the SIP panel.

Based on differences in both initial slope and yield load as shown in Table 6-8, the use of a shim significantly reduced both connection stiffness and yield strength, and lack of SIP pre-drilling also significantly reduced connection properties. The predrilling issue is not of great importance since it is unlikely that a field installer would predrill; therefore, subsequent tests should be done without predrilling. The specimens were predrilled in order to facilitate accurate screw placement in the specimen and reduce the possibility of timber splitting.

The addition of a washer did not significantly affect connection performance.

Table 6-8 Phase 1 t-test Results

Comparison	Initial Slope C		Yield Load $F_{D/2}$	
	P-value	Difference?	P-value	Difference?
screwwo vs. washer	0.198	No	0.304	No
base vs. shim	0.000	Yes	0.000	Yes
base vs. nopredrill	0.022	Yes	0.017	Yes

6.7.2. Phase 2 t-test

The test group "screwdf" was considered as the base group. Several variables were examined including comparison between the timber species Douglas fir and eastern white pine, nail versus screw fastener, removal of the outer portion of the SIP, and loading perpendicular to the timber grain.

As shown Table 6-9, removal of the outer sheet of OSB and the foam core significantly reduced both connection stiffness and yield strength. This result suggests that future SIP fastener tests should not be simplified to a singe panel conventional test.

Although there was not a statistical difference in yield load for fastener type, both species had a statistically significant reduction in stiffness for a nailed connection. This result indicates a preference for the use of screws in SIP to timber connections.

Timber species did not have a significant effect on connection stiffness or yield strength. This indicates that the controlling factor in behavior is the properties of the OSB inner skin.

There was no significant difference between the base sample with load applied parallel to timber grain as compared to the sample with load applied perpendicular to grain. This indicates that there is no need to model the orientation of frame members.

Table 6-9 Phase 2 t-test Results

Comparison	Initial Stiffness C		Yield Load $F_{D/2}$	
	P-value	Difference?	P-value	Difference?
screwdf vs. naildf	0.001	Yes	0.086	No
screwdf vs. screwwp	0.450	No	0.223	No
screwdf vs. nailwp	0.033	yes	0.149	No
screwdf vs. perpdf	0.090	No	0.053	No
screwdf vs. osbdf	0.001	Yes	0.001	Yes

6.7.3. Phase 3 t-test

The test group "long" was considered as the base group. The parameters of this group were identical to those of phase 2, group "screwdf". The intermediate designation "long" merely indicates that the primary objective of this phase was to investigate the potential advantage of using a short screw countersunk such that the head bears on the interior OSB sheet.

In addition to investigating the short screw, this phase also included sample group "wax" with several sheets of waxed paper between the panel and timber, and a sample group "thick" using 6-inch nominal SIP specimens rather than 4-inch SIPs as all other groups used.

As shown inTable 6-10, the addition of a low frictional waxed paper interface significantly reduced connection properties. This demonstrates the importance of full contact between SIP and frame to include the additional stiffness due to friction.

The group with 6-inch SIPs also had significantly reduced properties as compared to the thinner 4-inch SIPs. This shows that increased lateral stiffness can be gained through the use of relatively thinner panels.

Although the use of a countersunk screw resulted in a 33 percent increase in stiffness this was not statistically significant based on an alpha level of 0.05. However, since there was such a large change in stiffness and the p-value was 0.054, the results lead the suggestion of future investigation on the use of short, countersunk screws.

Table 6-10 Phase 3 t-test Results

Comparison	Initial Slope C		Yield Load $F_{D/2}$	
	P-value	Difference?	P-value	Difference?
long vs. short	0.054	No	0.149	No
long vs. wax	0.003	Yes	0.008	Yes
long vs. thick	0.001	Yes	0.002	Yes

6.8. Summary

The regression equations for load-slip can be directly imported into a two-dimensional modeling program to predict nonlinear lateral load behavior of a sheathed timber frame. Although the connection properties due to timber species and fastener type may not be statistically different, the model should include average values of these parameters. Timber orientation had no effect on connection properties, and can be ignored. Friction between the panel and timber increases both strength and stiffness, but due to frame irregularities high friction is not expected to be present in a typical application utilizing full size panels.

Comparison of the various connection parameters indicates that the addition of a shim between the SIP and timber will significantly reduce connection strength and stiffness. When compared to the base test the shimmed connection had 66 percent lower initial stiffness and 40 percent lower yield load. If a shim is used in construction, it should be mechanically fastened to the timbers at regular intervals determined according to appropriate code requirements.

Connection properties are also dependent on the core thickness of the SIP. The results indicate that the outer skin contributes to both stiffness and strength, and a connection with a thicker panel has reduced properties.

The connection that used a 2-inch screw countersunk through the outer skin and core of the SIP did not have statistically significant improved strength or stiffness. However, although it was not statistically significant based on an alpha of 0.05, there was a large increase in connection stiffness, and additional study may show that a countersunk screw can improve connection stiffness.

7. Sheathed Frame Structural Analysis

7.1. Overview

Nonlinear computer models were created with the SAP2000 version 8.1.6 structural analysis program for the sheathed frames described in Chapter 5. Full-scale frame models were created for the 1S1B white oak frame, the 1S1B Douglas fir frame and the 2S2B eastern white pine frame.

The load-slip relationship of the SIP to frame connection was modeled based on the nonlinear equation $P=(A+B\delta)[1-e^{(-C\delta/A)}]$ (Foschi, 1974) where P is the applied load, δ is the fastener slip, C is the initial slope of the curve, B is the final slope of the curve, and A is the point at which a line drawn tangent to the final slope intercepts the load axis. This equation form is graphically demonstrated in Figure 6-4.

7.2. Model Details

All models consisted of frame timbers connected to a 7/16 inch thick OSB membrane through nonlinear links. In all models the membrane was arbitrarily offset 1 inch from the timber in order to facilitate model construction, but the offset had no effect on model performance. The omission of the SIP outer skin and foam core were based on the assumptions that the outer skin improves connection stiffness through restraint of the fastener but the outer skin does not significantly contribute to panel stiffness. The OSB panels were modeled with a thickness of 0.43 inches and a modulus of elasticity of 950,000 psi. Fastener performance is accounted for in the connection model by basing all load-slip interaction equations on data from full thickness, two-skin, SIP to timber

experimental specimens. All pegged joints in the frame were modeled with linear elements.

7.2.1. Fastener Model Verification

A single-fastener SAP model was created for a SIP to Douglas fir timber connection and a SIP to white oak timber connection to ensure accurate implementation of SIP to frame connection behavior within the full-scale frame models. The connection model was based the Foschi equation but implemented into SAP according to hysteretic behavior proposed by Wen (Wen, 1976). The connection model consisted of a single frame element connected to a mesh of membrane elements via a discrete nonlinear link element with material properties representative of actual construction. A typical plot comparing the theoretical Foschi model to the SAP model is shown in Figure 7-1.

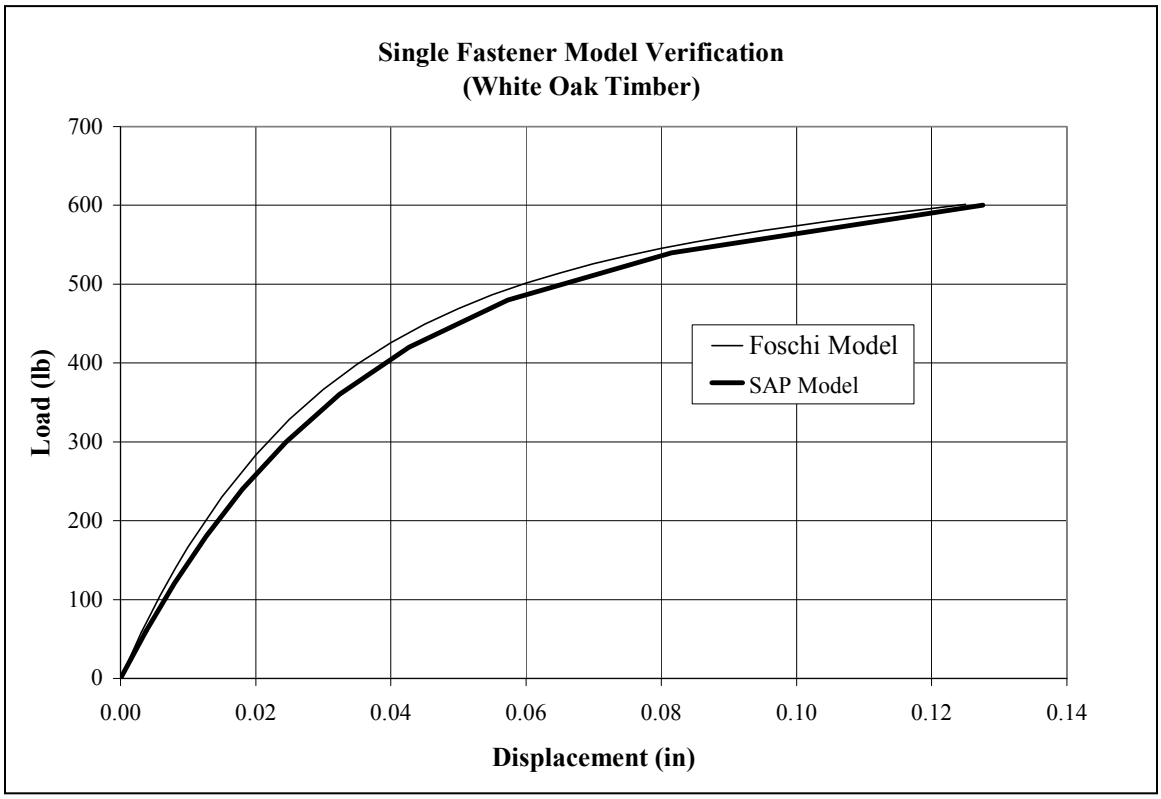

Figure 7-1 Single Fastener Model Verification

7.2.2. 1S1B White Oak Model

The 1S1B white oak model shown in Figure 7-2 was based on the sheathed frame as described in Chapter 5. The input data for the screw connection link element is provided in Table 7-1.

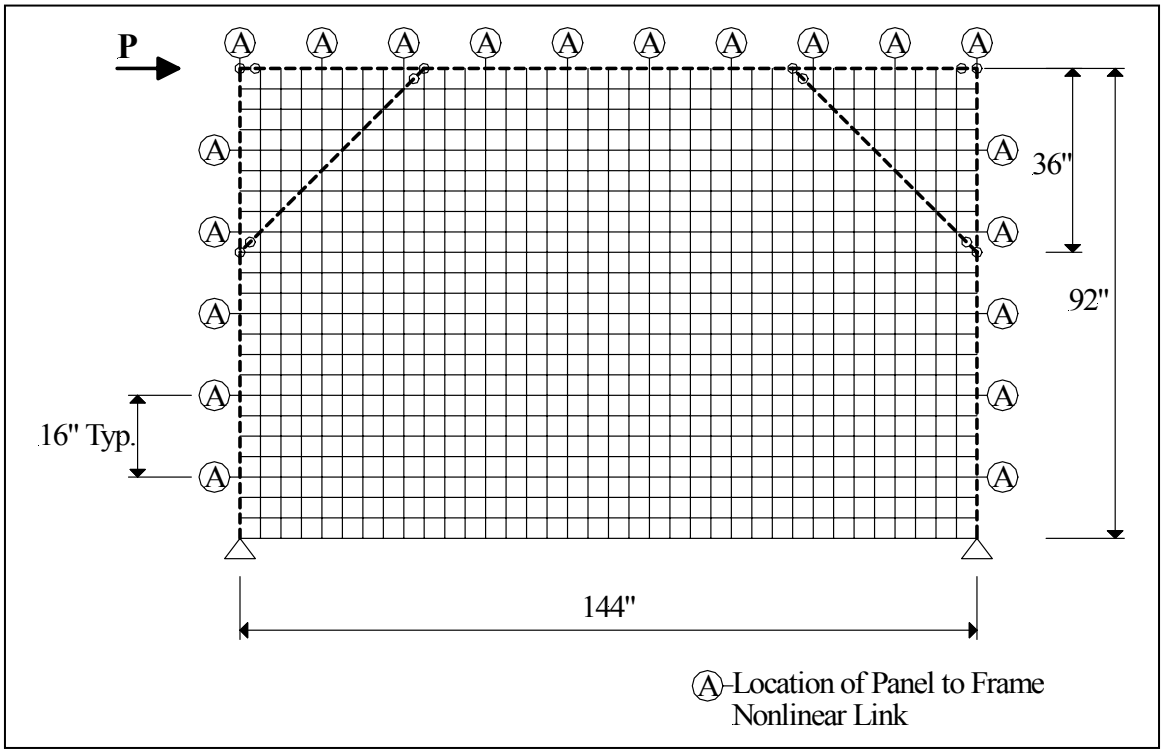

Figure 7-2 1S1B White Oak Sheathed Frame Model

Table 7-1 SIP to Timber Connection Inputs for 1S1B White Oak Frame

Wen Nonlinear Link			
Initial Stiffness (lb/in)	Post Yield Stiffness / Initial Stiffness	Yield Strength (lb)	Yielding Exponent
19,800	0.040	530	1

7.2.3. 1S1B Douglas Fir Model

The 1S1B Douglas fir model was based on the sheathed frame as described in Chapter 5. The SIP of the experimental frame consisted of two sections joined by a 5/8-

inch OSB spline, and this joint was modeled with nonlinear link elements as shown in Figure 7-3. The beam of the experimental 1S1B Douglas fir frame was laterally offset from the columns thereby requiring a shim between the beam and the SIP. This shim was accounted for in the SAP model.

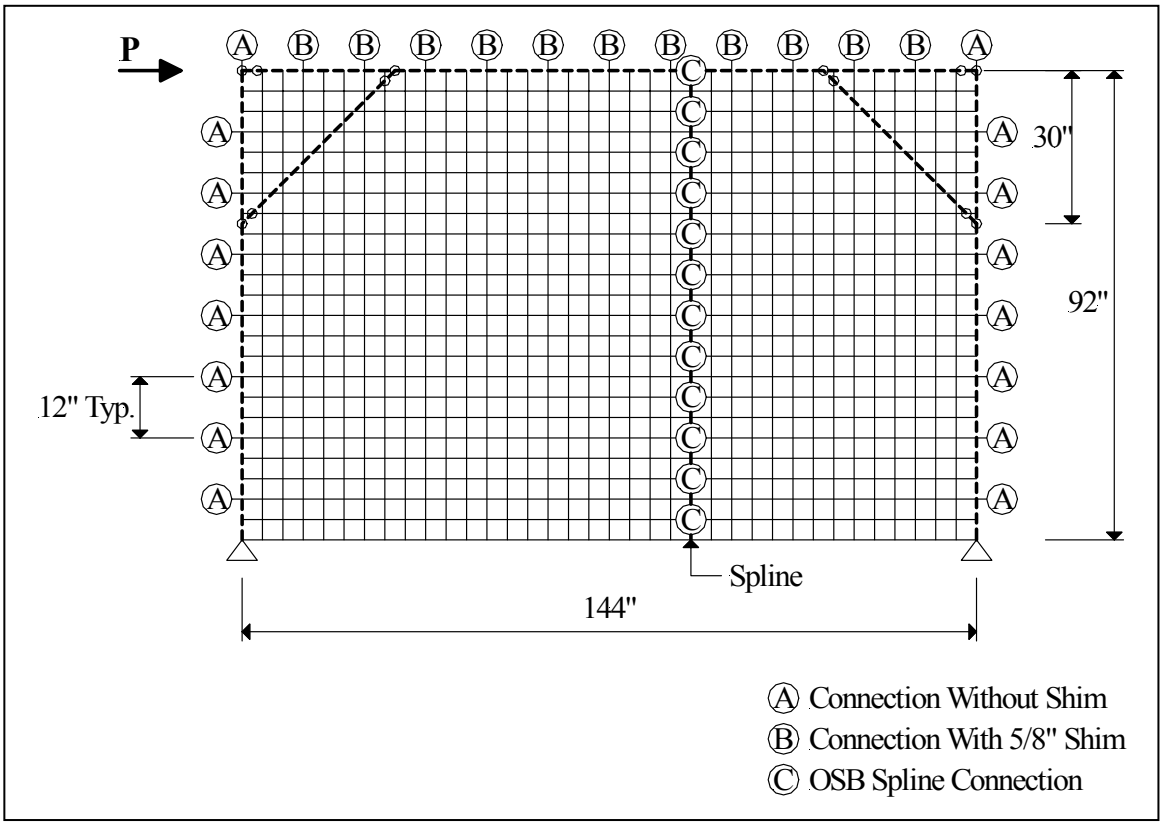

Figure 7-3 1S1B Douglas Fir Sheathed Frame Model

The sheathed Douglas fir frame had a 6-inch SIP installed rather than a 4-inch SIP as was modeled in the single fastener verification model. Results of individual connection tests reveal that there is approximately a 25 percent reduction in connection properties of a 6-inch panel as compared to a 4-inch SIP and the model input data were adjusted accordingly. The input data for the un-shimmed screw connection link element

representing a 6-inch SIP is given in Table 7-2. As shown in Table 7-2, the properties for a shimmed connection are slightly lower than the un-shimmed connection. The model input data for the nonlinear nailed spline connecting the two panels is also shown in Table 7-2.

Table 7-2 SIP to Timber Connection Inputs for 1S1B Douglas Fir Frame

Connection Type	Wen Nonlinear Link			
	Initial Stiffness (lb/in)	Post Yield Stiffness / Initial Stiffness	Yield Strength (lb)	Yielding Exponent
Un-shimmed 6-inch SIP to Douglas Fir	9,300	0.065	340	1
Shimmed 6-inch SIP to Douglas Fir	4,650	0.130	220	1
5/8-inch OSB Spline	1000	0.100	100	1

7.2.4. 2S2B Eastern White Pine Model

The 2S2B eastern white pine model was based on the sheathed frame as described in Chapter 5. The input data for the screw connection link element is provided in Table 7-3.

Table 7-3 Model Inputs for 1S1B Eastern White Pine Frame

Wen Nonlinear Link			
Initial Stiffness (lb/in)	Post Yield Stiffness / Initial Stiffness	Yield Strength (lb)	Yielding Exponent
12200	0.063	420	1

The 2S2B eastern white pine experimental frame had four discrete SIP's applied with all panel joints occurring over frame timbers, therefore there were no panel splines. Panel joints were created in the SAP model by forming a gap between the membrane meshes at the center column and mid-height beam. Discrete nonlinear links connecting

the membrane to frame were spaced 12 inches apart to represent 12 inch o.c screw spacing. Two models were created to represent two as-tested experimental frames. The first model did not have a sill member at the bottom of the frame while the second model had a sill.

7.3. Results

7.3.1. 1S1B White Oak Model

The 1S1B white oak model was subjected to a load ranging from zero to 3000 pounds in increments of 300 pounds. The maximum membrane-to-frame connection shear force occurred at the lower right-side connection. At the design wind load of 930 pounds the connection shear force in the model was 325 pounds, which is 42 percent lower than the connection yield load of 564 pounds from Table 6-5.

Comparison of the SAP model to experimental results is shown in Figure 7-4. The SAP model is stiffer than the as-tested experimental frame with a 34 percent difference in displacement at the maximum load of 3000 pounds; however, initial stiffness of the model is nearly identical to the stiffness of the experimental frame.

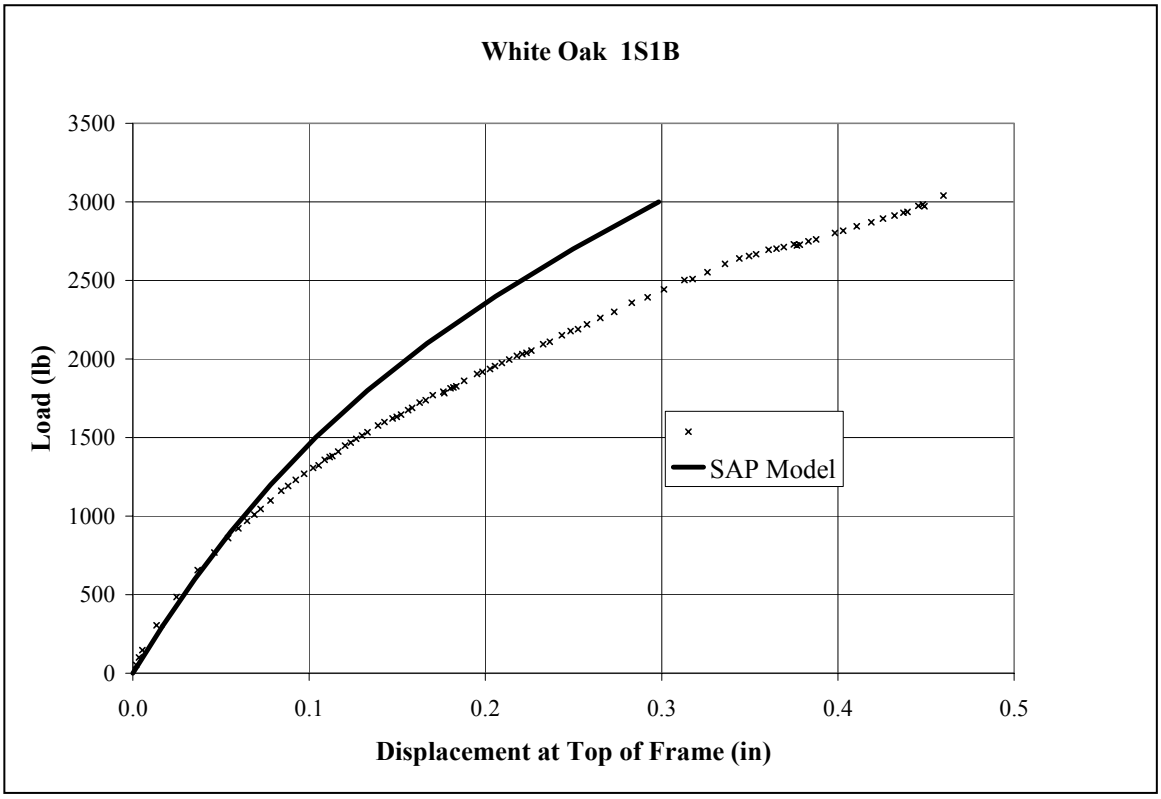

Figure 7-4 1S1B White Oak Model Verification

The effect of varied screw spacing was investigated by creating two additional models. The initial screw spacing of 16 inches was reduced by half to 8 inches and increased 50 percent to 24 inches. As shown in Table 7-4 and Figure 7-5, frame displacement increases with increase in screw spacing.

Table 7-4 Change in Model Displacement as a Function of Screw Spacing

SIP Connection Screw Spacing (in)	Model Frame Displacement at 930 LB Applied Load (in)	Change in Displacement	Model Frame Displacement at 3000 LB Applied Load (in)	Change in Displacement
16	0.058		0.298	
8	0.044	-24%	0.188	-37%
24	0.069	19%	0.427	43%

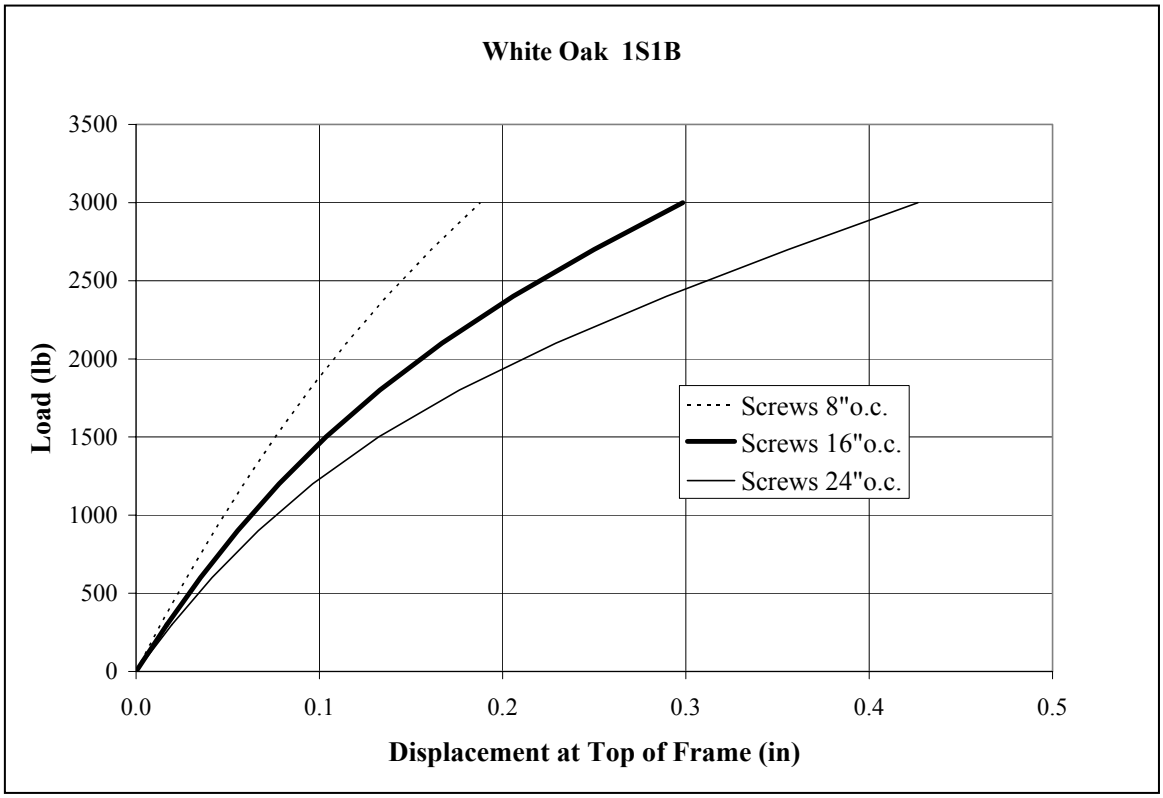

Figure 7-5 Effects of SIP Connection Screw Spacing

7.3.2. 1S1B Douglas Fir Model

The 1S1B Douglas fir model was loaded from zero to 3000 pounds in increments of 300 pounds. The maximum SIP to timber connection shear force in an un-shimmed location occurred at the lower left-side connection. At the design wind load of 930 pounds, the maximum connection shear force of 250 pounds was 48 percent lower than the connection yield load of 480 pounds from Table 6-6. The maximum model connection shear force in a shimmed location occurred at the upper left-side beam connection and was relatively low at 51 pounds.

Model results for three different Douglas fir models are shown in Figure 7-6. All models produced frame stiffnesses greater than the experimental frame at maximum load. Compared to the experimental data, the as-tested model had approximately 68 percent of experimental frame displacement at maximum load of 3000 pounds. However, up to the design lateral load of 930 pounds the as-tested SAP model produced displacements nearly identical to the experimental frame displacements. In the model analyzed with the links representing the shimmed beam to panel connections replaced by un-shimmed links, frame stiffness was slightly greater than the as-tested model. Given the relatively low connection forces at the shimmed locations, a significant difference in overall model stiffness was not expected. In the model analyzed with the panel spline links removed such that the SIP acted as a continuous panel, frame stiffness was only slightly greater than the as-tested model indicating the spline caused modest reduction in overall frame displacement.

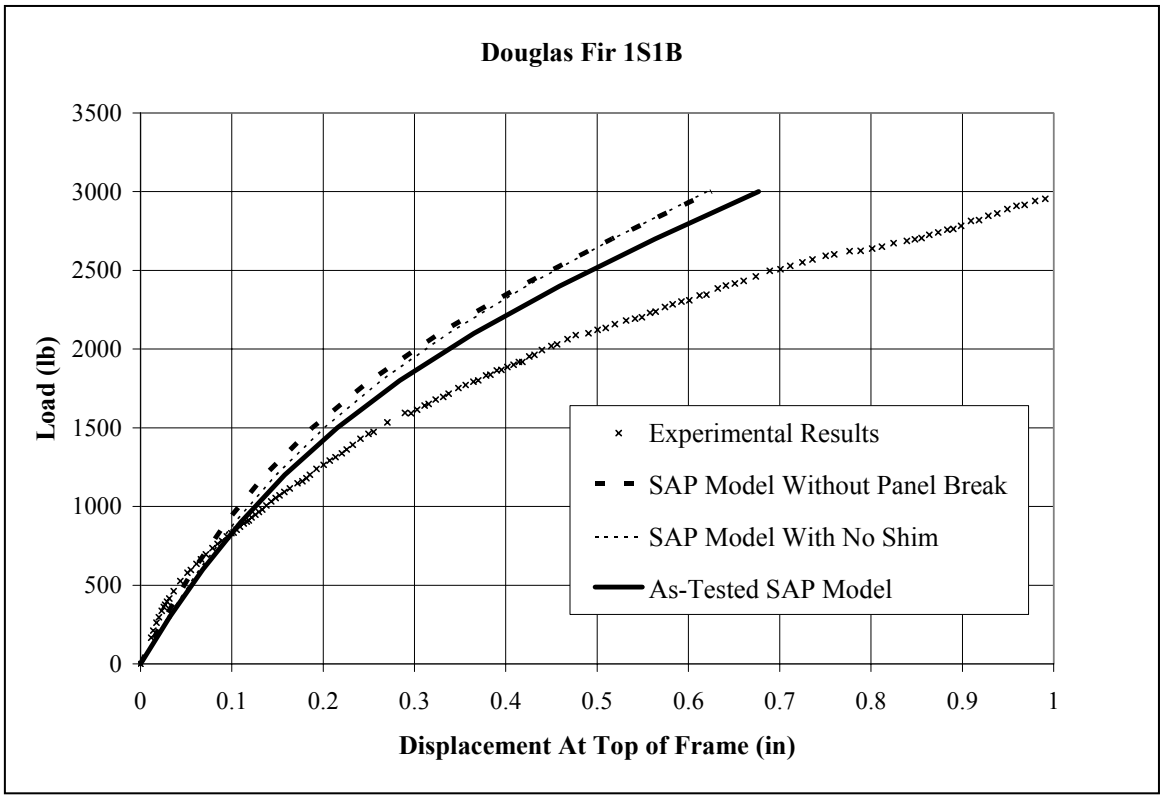

Figure 7-6 1S1B Douglas Fir Model Verification

7.3.3. 2S2B Eastern White Pine Model

The 2S2B eastern white pine model was subjected to a load from zero to 4000 pounds in increments of 400 pounds. The load was applied to the left-side column and equally divided between the mid-height and top beam locations. As shown in Figure 7-7 the SAP model accurately predicted frame displacement. Both the frame-with-sill and frame-without-sill models produce nonlinear curves that overlay the experimental data with an exception at high loads in the frame with no sill where the experimental data shows stiffening behavior.

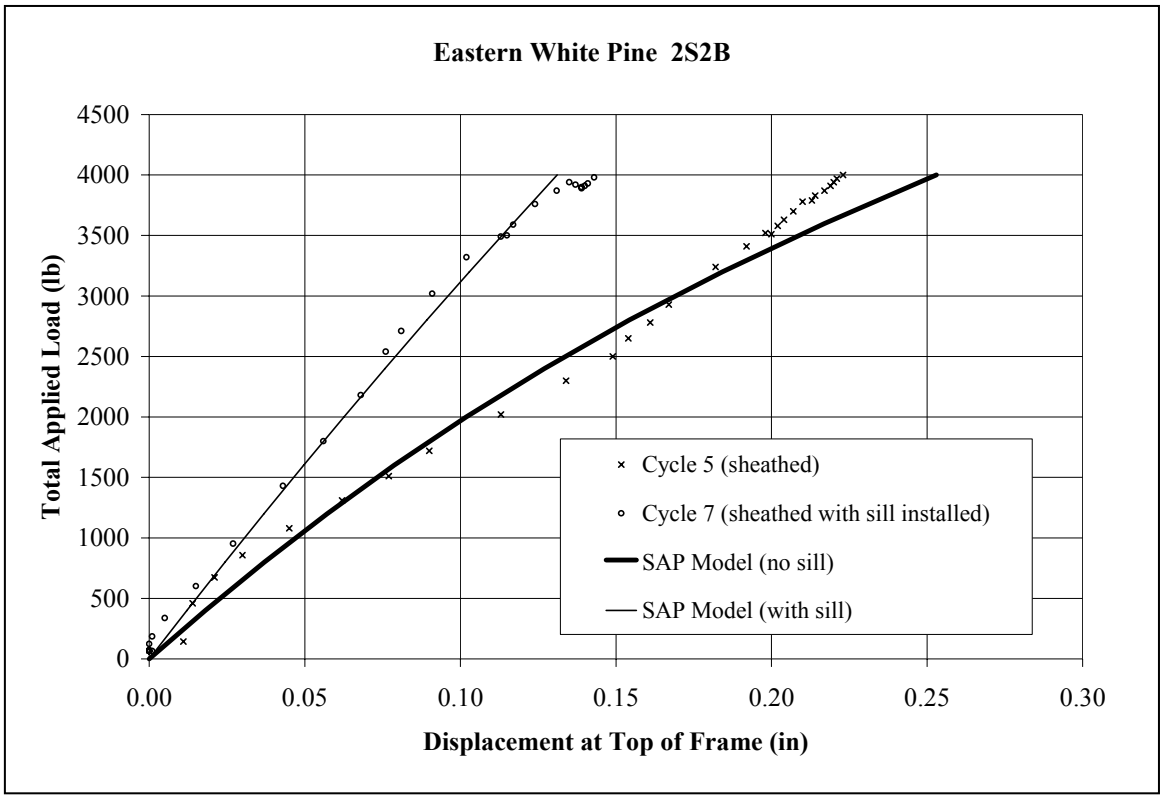

Figure 7-7 2S2B SAP Model Verification

7.4. Summary

SIP to timber connections can be adequately modeled by utilizing a Wen nonlinear link in SAP 2000 with inputs based on the Foschi equation. Analysis of full-scale two-dimensional sheathed timber frames can be adequately modeled by utilizing nonlinear links representing panel-to-frame connections.

Analysis of the full-scale models revealed that maximum connection forces at the design load were significantly lower than the yield load for a given connection.

Increased model flexibility in the Douglas fir frame was present due to both the shim and spline connections. This indicates splines and shims should be included in analysis models to correctly evaluate structure stiffness. Splines can be eliminated by locating all panel joints at frame timbers.

Inclusion of a sill plate significantly stiffens a sheathed frame as shown in the results of the 2S2B frame. Full-perimeter attachment of SIP's is imperative to achieve maximum performance.

8. Conclusions and Recommendations

8.1. Summary Statement

The most important result of this study is the demonstrated lack of stiffness of an unsheathed frame subjected to lateral load. While traditional timber frames have stood for centuries, one must not forget the differences in modern construction. Even a few decades ago, the use of large "window walls" was uncommon in all but the most extravagant structures, and most timber framed buildings had some type of infill throughout the structure that participated in the lateral load path. With modern construction of large open areas coupled with walls of mostly glass, designers of traditional timber frames must be cautious when relying on knee braces for lateral load resistance.

8.2. Qualified Recommendations

This section consists of eleven conclusions. Each conclusion is followed by a bulleted recommendation for the design of traditional timber frame structures. These recommendations are intended for use by those who design, engineer and build timber frames. These recommendations will also be of assistance to those who develop codes specific to the timber frame industry and to those who administer such codes.

1. Excessive displacements of the unsheathed 1S1B and 2S2B frames indicated unacceptable frame stiffness when subjected to reversible lateral loads.

- It is recommended that an independent lateral load system complement unsheathed timber frames for resistance to service level lateral load.
- Lateral loads should be transferred through diaphragms to sheathed frames or similar shear wall components.

2. The parametric study of Chapter 4 indicated that frame stiffness is primarily a function of knee brace length and joint stiffness. If an unsheathed traditional timber frame is incorporated in a structure such that it will assist in resisting lateral loads, the following recommendations must be followed to maximize frame performance.

- The knee brace distance (vertical distance from bottom of knee brace to bottom of beam) must be at least 36". A greater knee brace distance further improves lateral stiffness.
- Joint stiffness should be maximized by constructing the frame of a relatively stiff material such as white oak.
- All joints should be constructed with at least two one-inch pegs.
- End and edge distances should follow the recommendations of previous research (Schmidt and Daniels 1999), (Schmidt and Scholl 2000).

3. The stiffness of a wood-pegged timber frame is highly dependent on the stiffness of the individual pegged connections. If a frame is statically determinate, frame actions

are not dependent on connection properties. However, as redundancies increase, frame actions increasingly become a function of connection stiffness.

- In order to accurately model the displacement characteristics of a frame and the internal actions in the frame members and connections, the stiffness characteristics of all connections must be included in a structural analysis model.

4. Implementation of nonlinear springs to model tensile pegged joints was shown to improve overall accuracy of analysis models.

- If a traditional timber frame is designed to carry lateral load, the nonlinearity of the tensile joint springs should be considered in lateral stiffness models.

5. The addition of SIP sheathing significantly improved frame stiffness of 1S1B and 2S2B frames.

- Sufficient lateral stiffness of an enclosed traditional timber frame can be obtained through the use of structural insulated panels (SIPs), conventional shear walls or a structurally similar method of sheathing.

6. Experimental testing of sheathed frames demonstrated that full perimeter attachment of the SIPs resulted in maximum sheathed frame stiffness. This behavior was replicated in the analysis models.

- SIPs should be attached around their full perimeter.

7. Both experimental testing and model analysis demonstrated that sheathed frames with SIP joints occurring at locations other than along frame members had reduced frame stiffness.

- SIPs should be attached to a timber frame such that all SIP joints are aligned with frame columns or beams.

8. Analysis of single fastener SIP to timber connections revealed that the use of a shim between the SIP and timber significantly reduces connection stiffness and strength. The average initial stiffness of un-shimmed connections was nearly three times that of a shimmed connection.

- The use of shims between SIPs and timber frame members is discouraged.
- If a shim must be installed between SIPs and a timber frame, the shim must be mechanically fastened according to NDS provisions for such connections. The flexibility of the shim to timber connection must be considered in addition to the flexibility of a similar un-shimmed SIP to timber connection.

9. The average initial lateral stiffness of screwed Douglas fir and eastern white pine to SIP connections was 47% greater than the average initial lateral stiffness of similar nailed connections. The average yield load of the screwed connections was 7% greater than the average yield load of the nailed connections.

- SIPs should be fastened with screws rather than nails.

10. While the examination of the SIP to timber connection proceeded on the assumption that the outer skin of a sheathed frame is not likely to carry a significant load, the experimental results indicate the outer skin supports the fastener head and thereby improves overall connection capacity. Removal of the outer skin and use of a thicker SIP both resulted in decreased connection strength and stiffness. The average initial lateral stiffness of a Douglas fir to 4-inch (nominal) SIP connection was 33% greater than the average initial lateral stiffness of a Douglas fir to 6-inch (nominal) SIP connection. The yield load of the connection with the 4-inch SIP was 7% greater than the yield load of the 6-inch SIP.

- The thinnest possible SIP should be specified to maximize lateral stiffness of a sheathed timber frame.

11. Computer analysis models accurately predicted the behavior of sheathed frames by using a nonlinear link to represent the lateral behavior of the SIP to frame connection. The nonlinear link was based on experimental results correlated to the Foschi equation.

- A lateral stiffness model of a SIP-sheathed timber frame should utilize nonlinear springs to represent the SIP to timber connection.

8.3. Future Research

Even with large openings cut in the center of the panels, the sheathed frames had significantly greater stiffness than the unsheathed frames. While this project included a brief investigation into the effects of openings in sheathed timber frames, further study on this issue is recommended.

As exhibited by the difficulty to catastrophically fail a frame, the knee brace system provides exceptional strength characteristics. Although the pegged joints failed at relatively low loads, the compressive action of the mortise and tenon joint continued to carry load well beyond typical service level forces. Thus the overall strength of these frames was adequate to resist reversible lateral loads. These results indicate that traditional timber frames are able to withstand large deformations and may be able to absorb significant energy. Given these abilities it would be worthwhile to investigate the performance of timber frames subjected to seismic loading.

9. References

AFPA (2001). "National Design Specification for Wood Construction," American Forest and Paper Association (AFPA), Washington, D.C.

ASCE (2002) ASCE 7-02, Minimum Design Loads for Buildings and Other Structures, Reston, VA, American Society of Civil Engineers.

ASTM (1998) "Standard Test Methods for Mechanical Fasteners in Wood," ASTM D 1761-88, ASTM, West Conshohocken, PA.

ASTM (1998) "Standard Test Methods for Specific Gravity of Wood and Wood-Based Materials," ASTM D 2395-93, ASTM, West Conshohocken, PA.

ASTM (1998) "Standard Test Methods for Direct Moisture Content Measurement of Wood and Wood-Base Materials," ASTM D 4442-92, ASTM, West Conshohocken, PA.

ASTM (1998) "Standard Test Methods for Use and Calibration of Hand-Held Moisture Meters," ASTM D 4444-92, ASTM, West Conshohocken, PA.

Benson, T., Gruber, J. (1980). Building the Timber Frame House, The Revival of a Forgotten Craft, New York, Charles Scribner's Son's.

Benson, T. (1997). "The Timber Frame Home – Design, Construction, Finishing," Second Edition, Taunton Press, Inc.

Bulleit, W. M., Sandberg, L. B., Drewek, M. W., and O'Bryant, T. L., (1999). "Behavior and Modeling of Wood-Pegged Timber Frames," *Journal of Structural Engineering*, 125(1), 3-9.

Bulleit, W. M., Sandberg, L. B., O'Bryant, T. L., Weaver, D. A., and Pattison, W. E., (1996). "Analysis of Frames with Traditional Timber Connections," Proceedings, International Wood Engineering Conference, New Orleans, LA. 4, 232-239

Brungraber, R. L. (1992). "Assessing Capacities of Traditional Timber Connections," *Wood Design Focus*. 3(4), 17-21.

Brungraber, R. L. (1985). "Traditional Timber Joinery: A Modern Analysis," Ph.D. Dissertation, Stanford University, Palo Alto, California.

Carradine, D. M., Woeste, F. E., Dolan, J. D., and Loferski, J. R., (2000). "Demonstration of Wind Load Design for Timber Frame Structures Using Diaphragm Action," Transactions of ASAE 43(3), 729-734.

Church, J. R., and Tew, B. W., (1997). "Characterization of Bearing Strength Factors in Pegged Timber Connections," *Journal of Structural Engineering*, 123(3), 326-332.

Computers and Structures, Inc. (2003). SAP 2000 NonLinear Version 8.16, Berkeley, California.

Foschi, R. O. (1974). "Load Slip Characteristics of Nails," *Wood Science*, 7(1), 69-76.

Hunt, R. D., and Bryant, A. H. (1990). "Laterally Loaded Nail Joints in Wood," *Journal of Structural Engineering*, 116(1), 111-124.

Kessel, M. H., Speich, M. and Hinkes, F. J. (1988). "The Reconstruction of an Eight-Floor Timber Frame House at Hildesheim (FRG)," *Proceedings*, 1988 International Conference on Timber Engineering, Seattle, WA 415-421

Kessel, M. H., and Augustin, R., (1995). "Load Behavior of Connections With Oak Pegs," *Timber Framing*. 38, 6-9. *Translation of:* "Untersuchungen uber das Tragverhalten von Verbindungen mit Eichenholzageln," Bauen mit Holz, 246-250, April.

Kessel, M. H., and Augustin, R., (1996). "Load Behavior of Connections With Pegs II," *Timber Framing*. 39, 8-11. *Translation of:* "Untersuchungen der Tragfahigkeit von Holzverbindungen mit Holznageln fur Sanierung und Rekonstruktion alter Bausubstanz," Bauen mit Holz, 484-487, June.

Kuenzi, E. W., (1955). "Theoretical Design of a Nailed or Bolted Joint Under Lateral Load," *Report No*. D1951, U. S. Department of Agriculture, Forest Products Laboratory, Madison, WI.

Malhotra, S. K., and Thomas, B. (1982). "Behavior of Nailed Joints with Interface Characteristics," *Wood Science*, 15(2), 161-171.

Sandberg, L. B., Bulleit, W. M., O'Bryant, T. L., Postlewaite, J. J., and Schaffer, J. J. (1996). "Experimental Evaluation of Traditional Timber Connections," *Proceedings*, International Wood Engineering Conference, New Orleans, LA, 4, 225-231.

Sandberg, L. B., Bulleit, W. M., and Reid, E. H., (2000). "Strength and Stiffness of Oak Pegs in Traditional Timber-Frame Joints," *Journal of Structural Engineering*, 126(6), 717-723

Schmidt, R. J., and Daniels, C. E. (1999). "Design Considerations for Mortise and Tenon Connections," Research Report, Department of Civil and Architectural Engineering, University of Wyoming, Laramie, WY.

Schmidt, R. J., and MacKay, R. B (1997). "Timber Frame Tension Joinery," Research Report, Department of Civil and Architectural Engineering, University of Wyoming, Laramie, WY.

Schmidt, R. J., MacKay, R. B., and Leu, B. L. (1996). "Design of Joints in Traditional Timber Frame Buildings," *Proceedings*, International Wood Engineering Conference, New Orleans, L.A., 4, 240-247.

Schmidt, R. J., and Moody, R. C. (1989) "Modeling Laterally Loaded Light-Frame Buildings," *Journal of Structural Engineering*, 115(1), 201-217

Schmidt, R. J., and Scholl, G. F. (2000). "Load Duration and Seasoning Effects on Mortise and Tenon Joints," Research Report, Department of Civil and Architectural Engineering, University of Wyoming, Laramie, WY.

Sobon, J. and Schroeder, R. (1984). Timber Frame Construction, Pownal, VT, Garden Way Publishing.

Sobon, J. (1994). Build a Classic Timber-Framed House, Pownal, VT, Garden Way Publishing.

Vick, C. B., and Okkonen, E. A., (1998). "Strength and Durability of One-Part Polyurethane Adhesive Bonds to Wood," *Forest Products Journal*, 48(11/12), 71-76.

Wen, Y. K. (1976). "Method for Random Vibration of Hysteretic Systems," *Journal of the Engineering Mechanics Division*, 102(EM2).

Wilkinson, T. L. (1971). "Theoretical Lateral Resistance of Nailed Joints," *Journal of Structural Engineering*, 97(5), 1381-1398.

Wilkinson, T. L. (1972). "Analysis of Nailed Joints with Dissimilar Members," *Journal of Structural Engineering*, 98(9), 2005-2013.

"Wood Handbook" *Forest Products Laboratory General Technical Report FPL-GTR-113*, Madison, WI, Forest Products Society.

10. Appendices

Appendix A. 1S1B Moisture Content

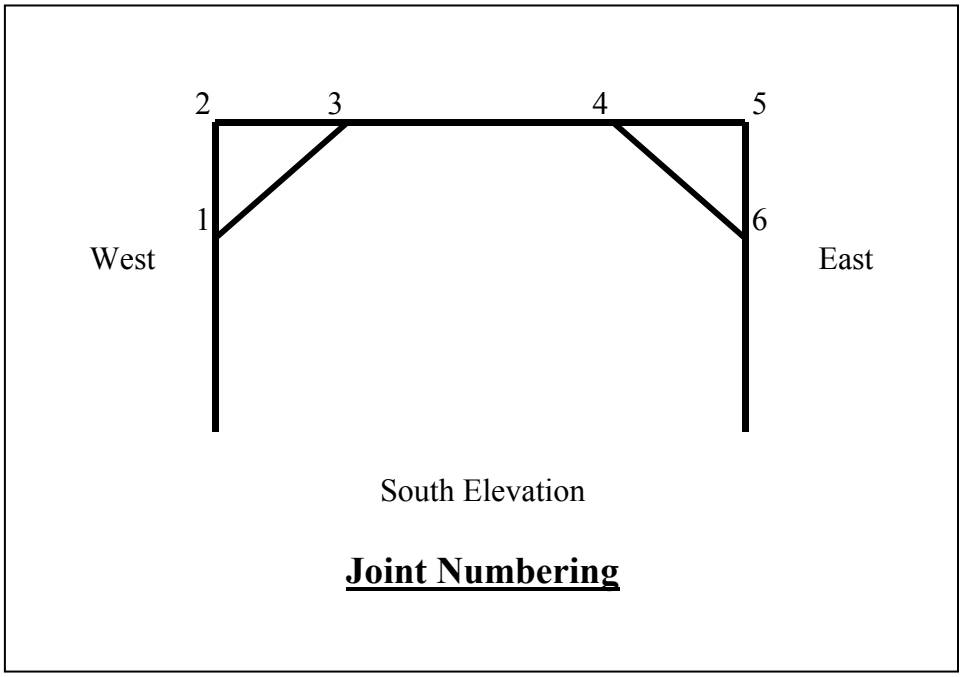

Figure A-1 Joint Identification

Table A-1 Douglas Fir

Frame ID:	Douglas Fir	
Date:	8/16/1999	
Element	Location	MC (%)
West Post	J1	17.8
	J2	16.7
East Post	J5	16.9
	J6	15.7
Beam	J2	15.6
	J3	15.4
	J4	14.5
	J5	15.2
West Knee Brace	J1	16.8
	J3	14.4
East Knee Brace	J4	14.4
	J6	16.8

Table A-2 Sheathed Douglas Fir

Frame ID:	Douglas Fir	
Date:	8/16/1999	
Element	Location	MC (%)
West Post	J1	15.9
	J2	15.9
East Post	J5	17.2
	J6	19.5
Beam	J2	16.8
	J3	16.7
	J4	17.3
	J5	17.8
West Knee Brace	J1	15.8
	J3	15.7
East Knee Brace	J4	16.0
	J6	15.6

Table A-3 Eastern White Pine

Frame ID:	Eastern White Pine	
Date:	6/8/1999	
Element	Location	MC (%)
West Post	J1	11.0
	J2	na
East Post	J5	19.0
	J6	17.1
Beam	J2	8.9
	J3	8.6
	J4	10.7
	J5	10.5
West Knee Brace	J1	7.7
	J3	8.9
East Knee Brace	J4	10.2
	J6	8.5

Table A-4 Port Orford Cedar

Frame ID:	Port Orford Cedar	
Date:	1/10/2000	
Element	Location	MC (%)
West Post	J1	9.6
	J2	9.3
East Post	J5	9.2
	J6	9.6
Beam	J2	10.1
	J3	9.1
	J4	10.4
	J5	9.5
West Knee Brace	J1	8.0
	J3	8.8
East Knee Brace	J4	10.0
	J6	8.9

Table A-5 White Oak

Frame ID:	White Oak	
Date:	7/22/1999	
Element	Location	MC (%)
West Post	J1	16.8
	J2	16.4
East Post	J5	20.0
	J6	21.3
Beam	J2	19.9
	J3	16.8
	J4	17.7
	J5	19.0
West Knee Brace	J1	17.6
	J3	16.2
East Knee Brace	J4	17.5
	J6	16.0

Appendix B. Summary of 1S1B Load Cycles

Table B-1 Douglas Fir

Cycle	Push Stroke		Pull Stroke		Average Stiffness (based on max disp and load) (lb/in)	Additional Gravity Load (lb)	Notes
	Maximum Load (lb)	Maximum Displacement (in)	Maximum Load (lb)	Maximum Displacement (in)			
1	1008	1.13	1009	1.14	888	0	
2	1002	1.07	1025	1.10	934	1800	
3	2646	3.22	2555	3.16	na	1800	

na: Stiffness values are not calculated for cycles where maximum load is significantly greater than expected service levels.

Table B-2 Sheathed Douglas Fir

Cycle	Push Stroke		Pull Stroke		Average Stiffness (based on max disp and load) (lb/in)	Additional Gravity Load (lb)	Notes
	Maximum Load (lb)	Maximum Displacement (in)	Maximum Load (lb)	Maximum Displacement (in)			
1	2986	1.01	2995	1.03	2928	0	6" SIPs with screws 12" o.c.
2	4368	3.04	0	0.00	na	0	6" SIPs with screws 12" o.c.
3	2975	0.79	2979	0.65	4136	0	6" SIPs with screws 8" o.c.
4	5812	3.01	7213	3.37	na	0	6" SIPs with screws 8" o.c.
5	346	0.92	0	0.00	377	0	No SIPs, damaged joints
6	1775	2.75	2606	3.63	686	0	No SIPs, damaged joints

na: Stiffness values are not calculated for cycles where maximum load is significantly greater than expected service levels.

Table B-3 Eastern White Pine

Cycle	Push Stroke		Pull Stroke		Average Stiffness (based on max disp and load) (lb/in)	Additional Gravity Load (lb)	Notes
	Maximum Load (lb)	Maximum Displacement (in)	Maximum Load (lb)	Maximum Displacement (in)			
1	1001	0.94	1000	1.10	979	0	
2	1009	0.68	1009	0.71	1457	1800	
3	996	0.81	1008	0.47	1566	1800	Steel knee brace pegs
4	609	0.78	612	0.40	1038	1800	No knee brace pegs
5	1002	0.92	999	0.55	1360	1800	Wood pegs replaced
6	2565	2.15	2855	2.01	1304	1800	
7	3134	2.56	3004	2.45	1225	1800	
8	1497	1.51	1505	1.32	1063	1800	
9	1516	1.54	1499	1.32	1055	1800	Spline pegs removed
10	483	2.02	591	2.05	264	1800	Spline pegs replaced, knee braces removed

Table B-4 Ponderosa Pine

Cycle	Push Stroke		Pull Stroke		Average Stiffness (based on max disp and load) (lb/in)	Additional Gravity Load (lb)	Notes
	Maximum Load (lb)	Maximum Displacement (in)	Maximum Load (lb)	Maximum Displacement (in)			
1	300	0.13	0	0.00	2254	0	
2	233	0.09	0	0.00	2690	0	
3	261	0.13	0	0.00	1958	0	
4	500	0.32	0	0.00	1559	0	
5	1003	0.71	0	0.00	1412	0	
6	266	0.15	0	0.00	1793	0	
7	805	0.49	0	0.00	1635	0	
8	0	0.00	400	0.63	635	0	
9	634	0.72	514	0.44	993	0	
10	1198	1.15	1199	1.18	1025	0	
11	1201	0.95	1198	0.95	1261	3000	
12	1206	1.08	1204	1.08	1116	1200	
13	714	0.47	730	0.98	1001	1200	
14	843	0.55	936	1.17	1035	1200	
15	936	0.85	0	0.00	1098	1200	
16	460	1.01	533	1.02	489	1200	Knee brace pegs removed
17	2297	2.05	0	0.00	1120	1200	Knee brace pegs replaced
18	2662	2.46	2190	2.25	1030	1200	Joints failed
19	1203	1.75	1206	1.55	728	1200	

Table B-5 Port Orford Cedar

Cycle	Push Stroke		Pull Stroke		Average Stiffness (based on max disp and load) (lb/in)	Additional Gravity Load (lb)	Notes
	Maximum Load (lb)	Maximum Displacement (in)	Maximum Load (lb)	Maximum Displacement (in)			
1	1023	0.90	1138	0.87	1220	0	
2	992	0.85	1005	0.83	1190	0	
3	1074	0.76	1033	1.02	1183	0	
4	994	0.72	1027	1.03	1158	0	
5 - 354	-	-	-	-	-	0	350 cycles, no data
355	874	1.03	1442	1.08	1100	0	
356 -365	-	-	-	-	-	0	10 cycles, no data
366	3456	3.22	2513	3.17	na	0	
367-376	-	-	-	-	-	0	10 cycles, no data
377	1011	0.63	1012	1.13	1151	0	Knee brace joints repaired
378	1036	0.80	987	1.02	1114	0	
379-909	-	-	-	-	-	0	531 cycles, no data
910	975	0.81	1429	1.58	1006	0	
911	1015	0.72	1024	1.08	1135	0	All pegs replaced
912	2512	3.23	2687	3.17	na	0	All pegs replaced

na: Stiffness values are not calculated for cycles where maximum load is significantly greater than expected service levels.

Table B-6 White Oak

Cycle	Push Stroke		Pull Stroke		Average Stiffness (based on max disp and load) (lb/in)	Additional Gravity Load (lb)	Notes
	Maximum Load (lb)	Maximum Displacement (in)	Maximum Load (lb)	Maximum Displacement (in)			
1	1516	0.50	1526	0.56	2870	0	
2	1504	0.35	1582	0.42	4040	1800	
3	-	-	-	-	-	1800	no data recorded
4	4924*	0.63	4982*	0.61	na	0	4" SIPs with screws 8" o.c.
5	1446*	0.38	660*	0.03	na	0	4" SIPs with screws 8" o.c.
6	2993*	0.24	3019*	0.21	na	0	4" SIPs with screws 8" o.c.
7	3009*	0.16	3022*	0.26	na	0	4" SIPs with screws 8" o.c.
8	12290*	1.21	10589*	0.94	na	1800	4" SIPs with screws 8" o.c.
9	3040	0.47	3081	0.42	6892	1800	4" SIPs with screws 16" o.c.
10	5039	0.88	5020	0.72	6283	1800	4" SIPs with screws 16" o.c.
11	2588	0.94	2600	0.85	2898	1800	
12	6295	3.71	-	-	na	1800	

* Data is not representative of SIP to frame load-slip behavior. Load was transferred directly from SIP to reaction.

na: Stiffness values are not calculated for cycles where maximum load is significantly greater than expected service levels.

Appendix C. 1S1B Service Level Loading Without Added Gravity Load

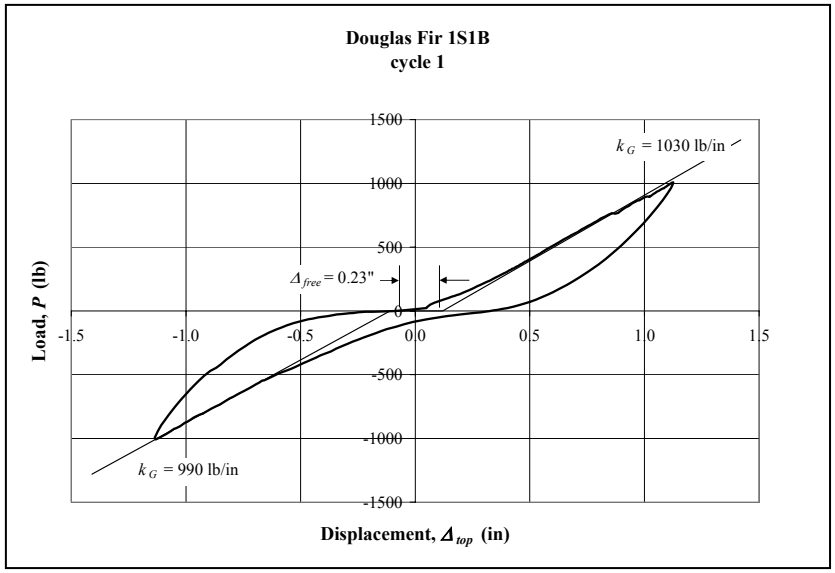

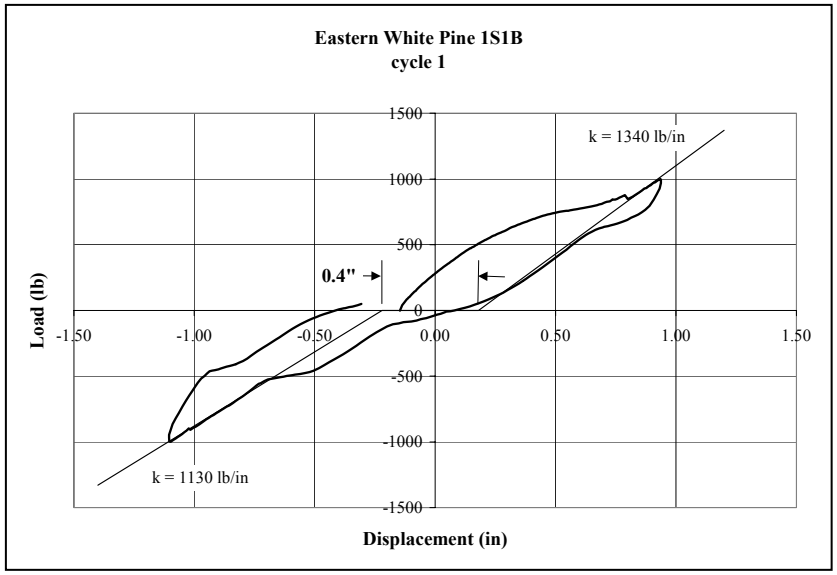

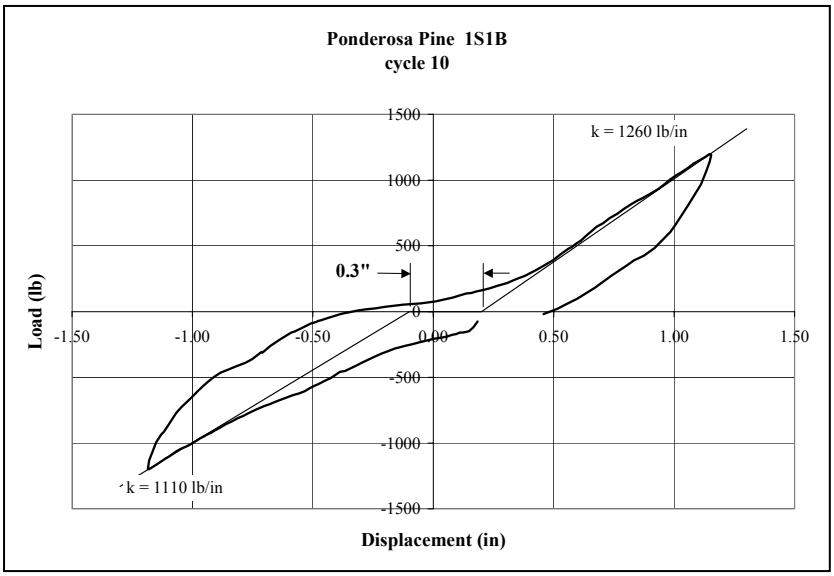
Ponderosa Pine 1S1B
cycle 10
k = 1260 lb/in
0.3"
k = 1110 lb/in
Load (lb)
Displacement (in)
1500
1000
500
0
-500
-1000
-1500
-1.50
-1.00
-0.50
0.00
0.50
1.00
1.50

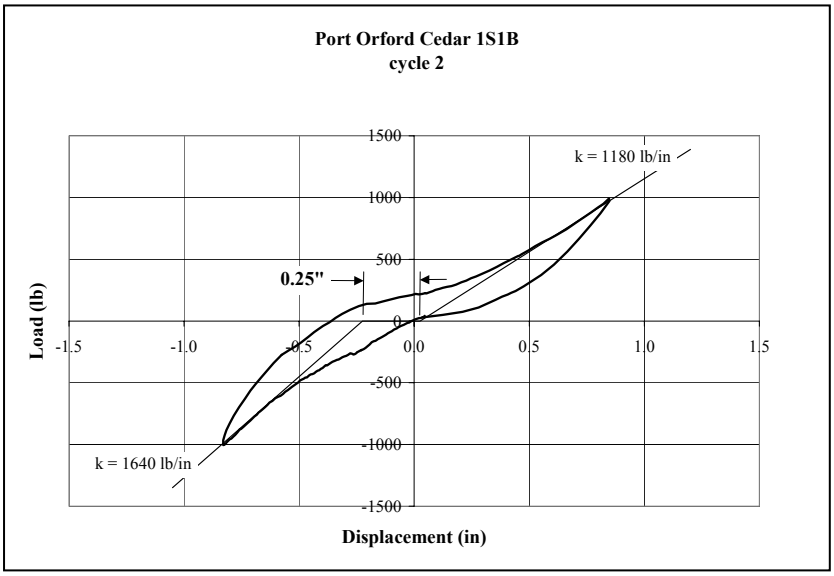
Port Orford Cedar 1S1B
cycle 2
k = 1180 lb/in
0.25"
k = 1640 lb/in
Load (lb)
Displacement (in)
1500
1000
500
0
-500
-1000
-1500
-1.5
-1.0
-0.5
0.0
0.5
1.0
1.5

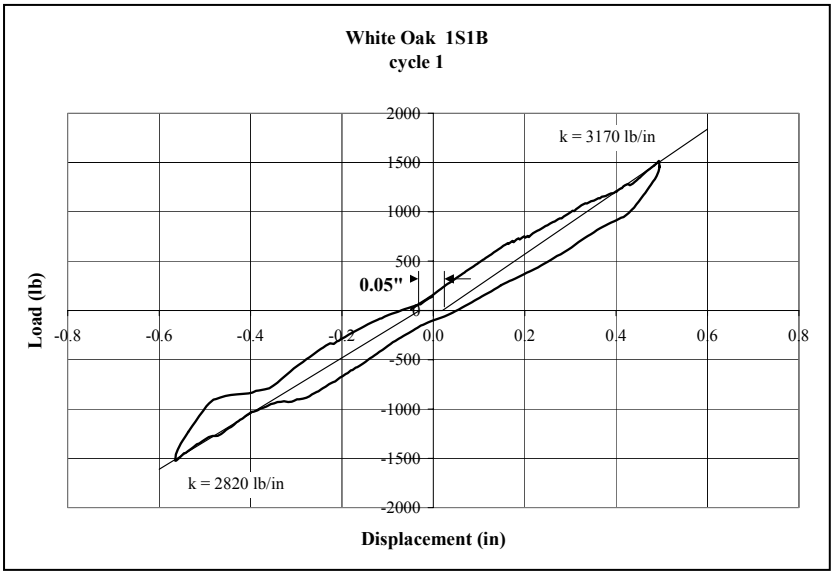
White Oak 1S1B
cycle 1
k = 3170 lb/in
0.05"
k = 2820 lb/in
Load (lb)
Displacement (in)
2000
1500
1000
500
0
-500
-1000
-1500
-2000
-0.8
-0.6
-0.4
-0.2
0.0
0.2
0.4
0.6
0.8

Appendix D. 1S1B Service Level Loading With Added Gravity Load

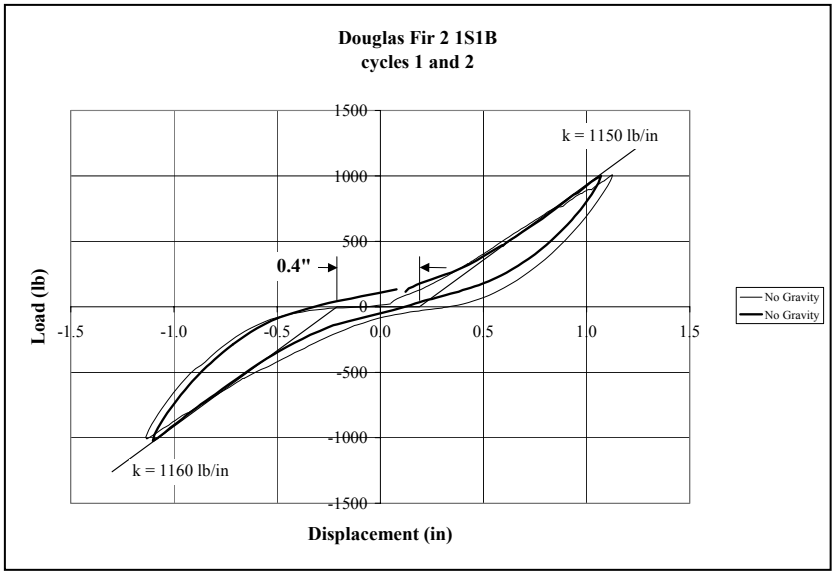

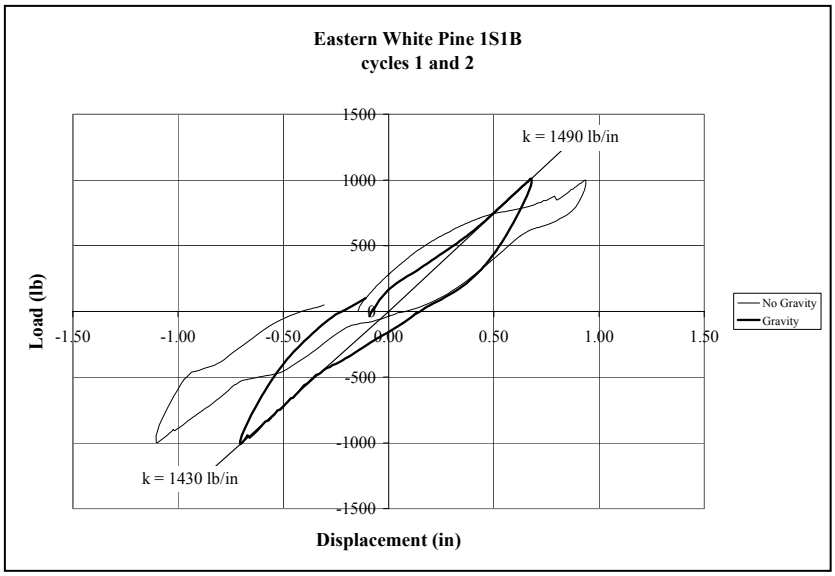

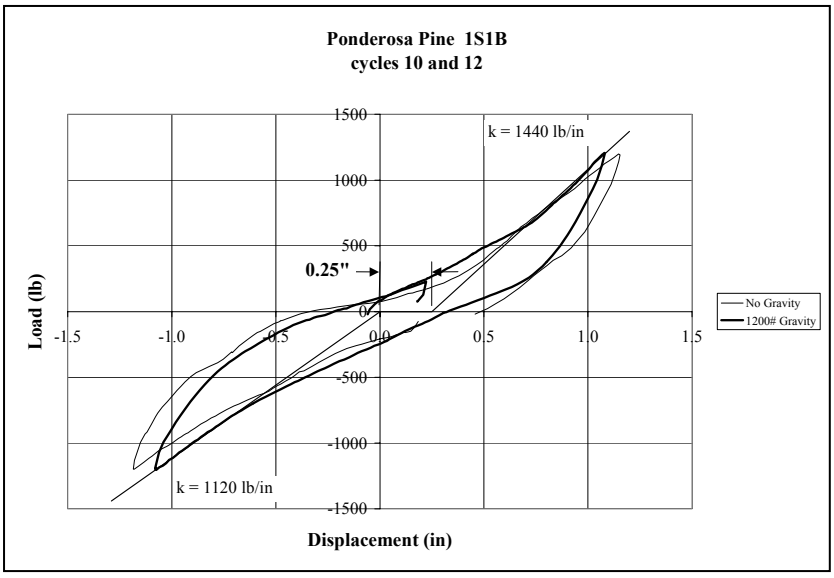
Ponderosa Pine 1S1B
cycles 10 and 12
k = 1440 lb/in
0.25"
k = 1120 lb/in
Load (lb)
Displacement (in)
No Gravity
1200# Gravity

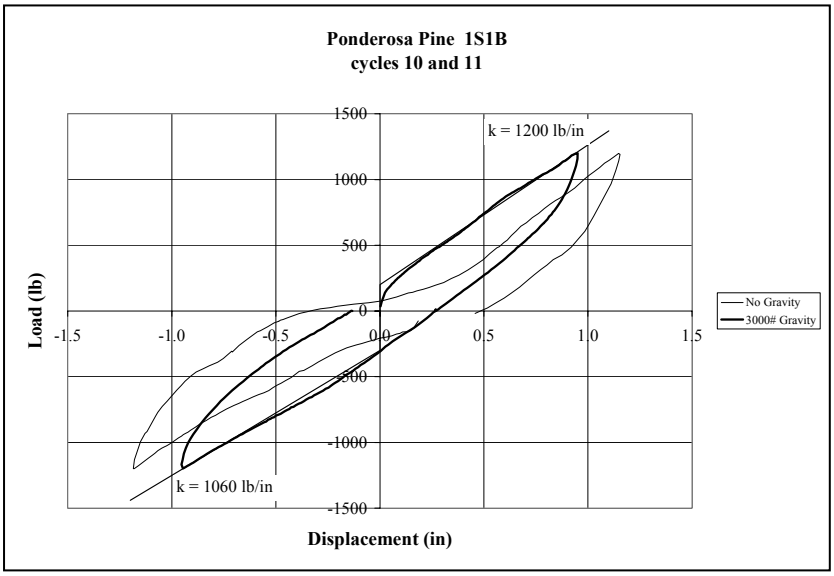
Ponderosa Pine 1S1B
cycles 10 and 11
k = 1200 lb/in
k = 1060 lb/in
Load (lb)
Displacement (in)
No Gravity
3000# Gravity

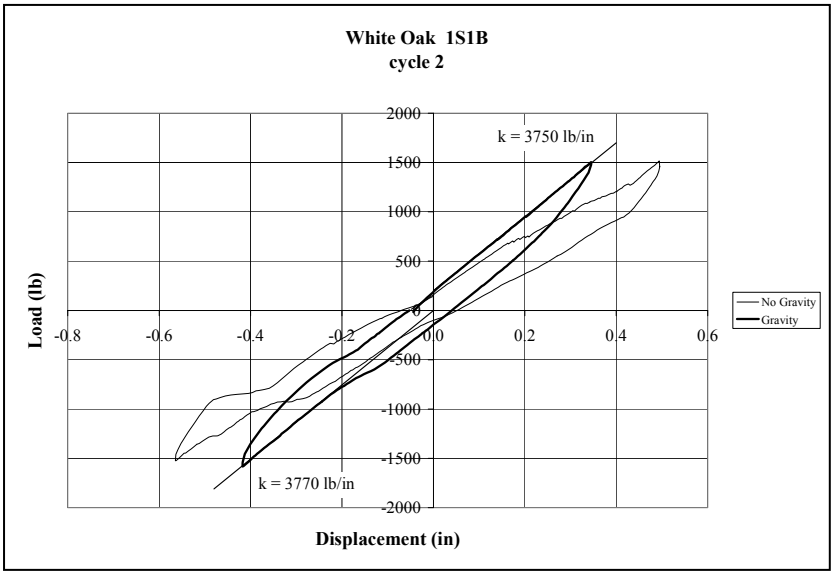
White Oak 1S1B
cycle 2
k = 3750 lb/in
k = 3770 lb/in
Load (lb)
Displacement (in)
No Gravity
Gravity

Appendix E. 1S1B Maximum Load

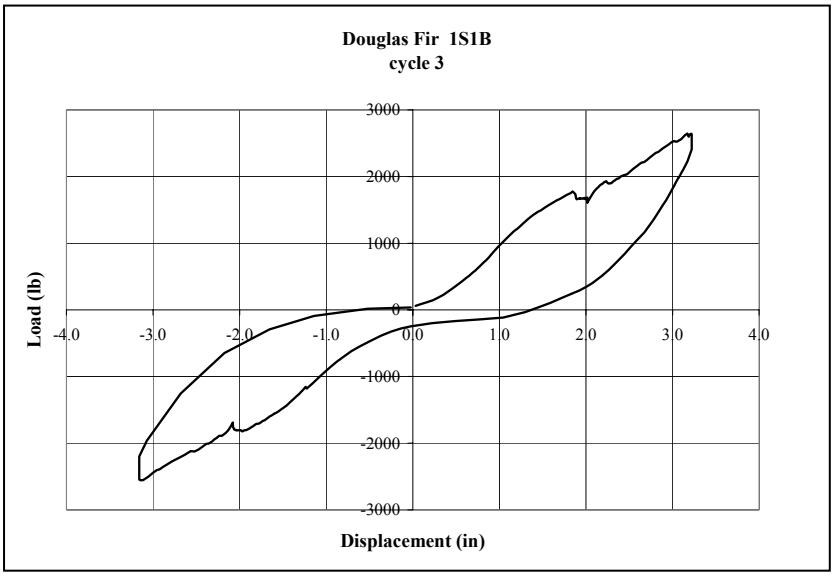

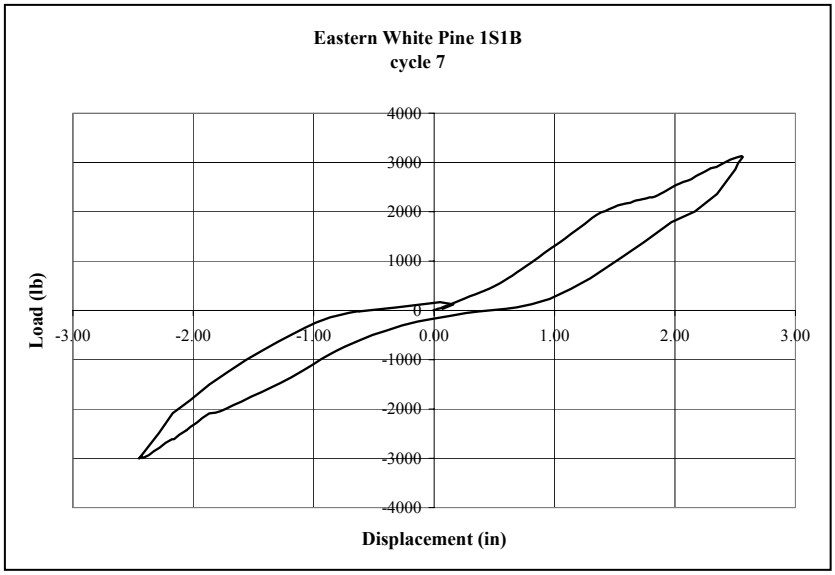

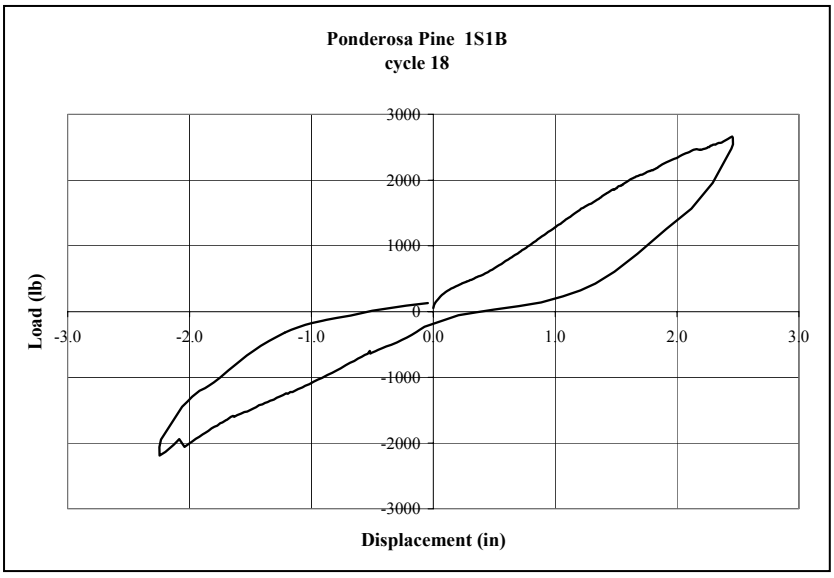
Ponderosa Pine 1S1B
cycle 18
Load (lb)
3000
2000
1000
0
-1000
-2000
-3000
-3.0
-2.0
-1.0
0.0
1.0
2.0
3.0
Displacement (in)

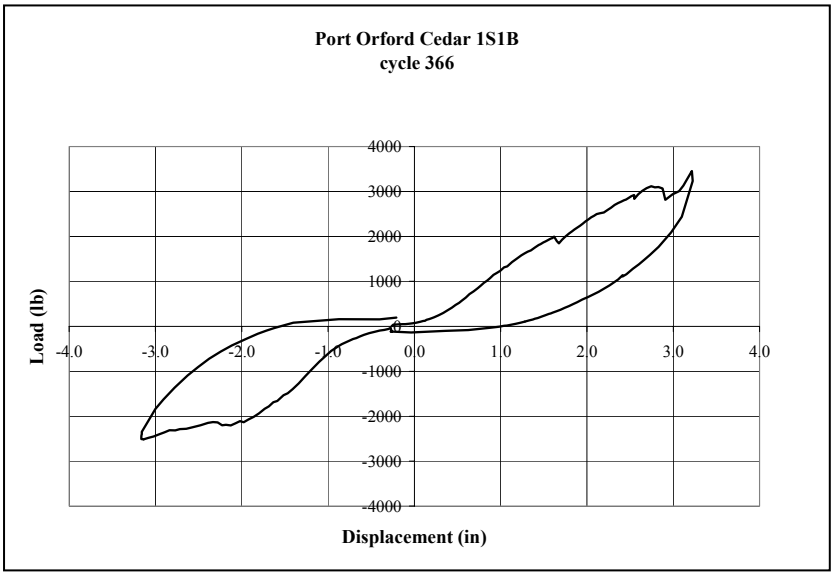
Port Orford Cedar 1S1B
cycle 366
Load (lb)
4000
3000
2000
1000
0
-1000
-2000
-3000
-4000
-4.0
-3.0
-2.0
-1.0
0.0
1.0
2.0
3.0
4.0
Displacement (in)

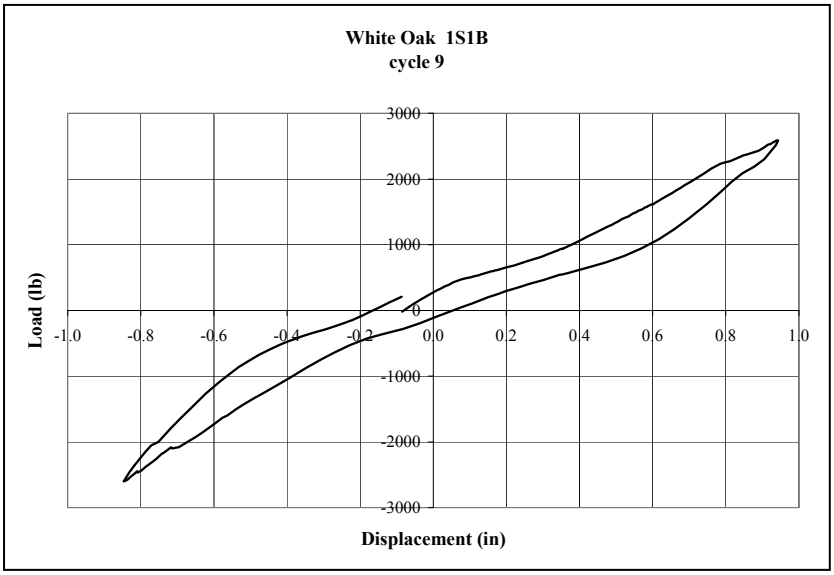
White Oak 1S1B
cycle 9
Load (lb)
3000
2000
1000
0
-1000
-2000
-3000
-1.0
-0.8
-0.6
-0.4
-0.2
0.0
0.2
0.4
0.6
0.8
1.0
Displacement (in)

Appendix F. 2S2B Moisture Content

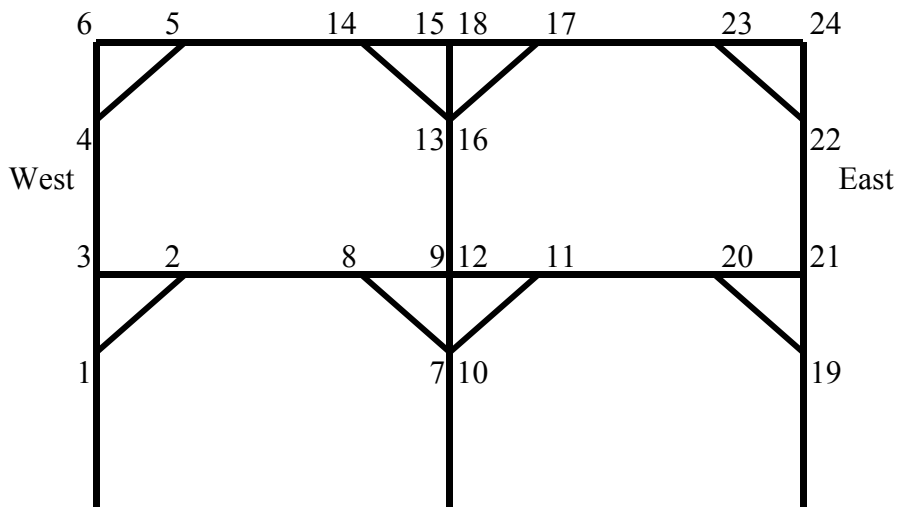

South Elevation

Joint Numbering

Species:	Douglas Fir					
Date:	7/18/2000					
Element	Location	MC (%)		Element	Location	MC (%)
West Post	Base	8.8		West Top Beam	J6	7.9
	J1	8.4			J5	8.3
	J3	8.3			J14	7.8
	J4	8.1			J15	7.8
	J6	7.3		East Top Beam	J18	8.0
Center Post	Base	11.2			J17	7.9
	J7/10	10.2			J23	7.9
	J9/12	10.4			J24	9.0
	J13/16	10.3		Knee Brace 1/2	J1	8.1
	J15/18	9.2			J2	7.8
East Post	Base	11.5		Knee Brace 4/5	J4	7.1
	J19	10.5			J5	7.9
	J21	9.9		Knee Brace 7/8	J7	7.9
	J22	9.8			J8	8.1
	J24	10.2		Knee Brace 10/11	J10	7.9
West Mid Beam	J3	10.0			J11	8.0
	J2	9.6		Knee Brace 13/14	J13	8.2
	J8	9.3			J14	8.0
	J9	7.7		Knee Brace 16/17	J16	8.1
East Mid Beam	J12	8.0			J17	8.0
	J11	8.3		Knee Brace 19/20	J19	8.3
	J20	8.0			J20	8.0
	J21	8.5		Knee Brace 22/23	J22	8.0
					J23	8.1
Maximum	**11.5 %**					
Minimum	**7.1 %**					
Average	**8.6 %**					

Species:	Eastern White Pine					
Date:	11/8/2000					
Element	Location	MC (%)		Element	Location	MC (%)
West Post	Base	7.1		Top Beam	J6	7.3
	J1	7.2			J5	7.2
	J3	6.2			J14	7.1
	J4	6.3			J15/18	6.3
	J6	6.3			J17	7.6
Center Post	Base	7.0			J23	5.7
	J7/10	6.1			J24	6.5
	J9/12	5.7		Knee Brace 1/2	J1	5.7
	J13/16	6.1			J2	6.0
	J15/18	7.1		Knee Brace 4/5	J4	6.3
East Post	Base	6.7			J5	6.1
	J19	7.1		Knee Brace 7/8	J7	6.2
	J21	5.9			J8	7.4
	J22	6.9		Knee Brace 10/11	J10	6.7
	J24	5.8			J11	6.5
West Mid Beam	J3	6.0		Knee Brace 13/14	J13	5.8
	J2	6.2			J14	6.2
	J8	5.7		Knee Brace 16/17	J16	5.7
	J9	6.1			J17	5.7
East Mid Beam	J12	6.1		Knee Brace 19/20	J19	6.1
	J11	7.1			J20	5.7
	J20	7.2		Knee Brace 22/23	J22	5.9
	J21	6.4			J23	7.0
Maximum	**7.6 %**					
Minimum	**5.7 %**					
Average	**6.4 %**					

Species:	Port Orford Cedar					
Date:	8/21/2000					
Element	Location	MC (%)		Element	Location	MC (%)
West Post	Base	8.0		Top Beam	J6	7.3
	J1	8.5			J5	7.5
	J3	8.8			J14	6.7
	J4	8.3			J15/18	7.0
	J6	7.6			J17	7.5
Center Post	Base	7.7			J23	6.5
	J7/10	8.1			J24	7.3
	J9/12	7.6		Knee Brace 1/2	J1	7.9
	J13/16	7.7			J2	7.6
	J15/18	7.1		Knee Brace 4/5	J4	7.6
East Post	Base	7.5			J5	7.8
	J19	7.0		Knee Brace 7/8	J7	7.8
	J21	7.7			J8	8.0
	J22	7.7		Knee Brace 10/11	J10	7.9
	J24	7.3			J11	7.9
West Mid Beam	J3	8.1		Knee Brace 13/14	J13	7.6
	J2	8.4			J14	7.5
	J8	8.4		Knee Brace 16/17	J16	7.9
	J9	8.2			J17	7.6
East Mid Beam	J12	7.7		Knee Brace 19/20	J19	7.5
	J11	8.2			J20	7.6
	J20	8.2		Knee Brace 22/23	J22	7.8
	J21	8.3			J23	7.9
Maximum	**8.8 %**					
Minimum	**6.5 %**					
Average	**7.7 %**					

Species:	White Oak					
Date:	3/10/2001					
Element	Location	MC (%)		Element	Location	MC (%)
West Post	Base	5.9		West Top Beam	J6	6.1
	J1	6.1			J5	7.2
	J3	5.9			J14	5.9
	J4	8.3			J15	6.7
	J6	5.9		East Top Beam	J18	7.6
Center Post	Base	8.2			J17	8.0
	J7/10	7.4			J23	7.3
	J9/12	7.6			J24	6.2
	J13/16	7.6		Knee Brace 1/2	J1	7.0
	J15/18	6.4			J2	6.6
East Post	Base	7.3		Knee Brace 4/5	J4	5.9
	J19	7.4			J5	6.5
	J21	7.2		Knee Brace 7/8	J7	6.2
	J22	7.2			J8	6.4
	J24	6.8		Knee Brace 10/11	J10	7.4
West Mid Beam	J3	6.7			J11	7.0
	J2	7.2		Knee Brace 13/14	J13	8.1
	J8	5.9			J14	7.9
	J9	7.3		Knee Brace 16/17	J16	6.0
East Mid Beam	J12	8.0			J17	7.3
	J11	8.1		Knee Brace 19/20	J19	7.4
	J20	7.6			J20	5.9
	J21	6.0		Knee Brace 22/23	J22	5.9
					J23	7.4
Maximum	**8.3 %**					
Minimum	**5.9 %**					
Average	**6.9 %**					

Appendix G. Summary of 2S2B Load Cycles

Table G-1 Douglas Fir

Cycle	Push Stroke		Pull Stroke		Average Stiffness (based on max disp and load) (lb/in)	notes
	Maximum Load (lb)	Maximum Displacement (in)	Maximum Load (lb)	Maximum Displacement (in)		
1	604	0.51	646	0.52	1,214	unsheathed
2	983	1.01	1,147	1.02	1,047	unsheathed
3	892	0.99	1,143	1.00	1,023	unsheathed
4	3,068	0.31	3,647	0.32	10,707	6" SIPs with screws 12" o.c.
5	6,024	0.76	6,023	0.67	na	6" SIPs with screws 12" o.c.
6	5,986	0.84	6,050	0.75	na	6" SIPs with screws 12" o.c.
7	6,073	0.87	6,016	0.79	na	6" SIPs with screws 12" o.c.
8-57						6" SIPs with screws 12" o.c.(no data recorded)
58	6,159	0.94	6,205	0.90	na	6" SIPs with screws 12" o.c.
59	9,020	1.95	8,942	1.90	na	6" SIPs with screws 12" o.c.
60	2,735	0.42	1,968	0.27	6,853	6" SIPs with screws 24" o.c.
61-110						6" SIPs with screws 24" o.c.(no data recorded)
111	2,869	0.68	1,984	0.10	6,200	6" SIPs with screws 24" o.c.
112	8,406	2.04	7,860	1.95	na	6" SIPs with screws 24" o.c.
113	518	0.62	544	0.63	848	unsheathed
114	912	1.03	760	1.02	815	unsheathed
115	3,608	4.23	3,176	2.88	954	unsheathed

Table G-2 Eastern White Pine

Cycle	Push Stroke		Pull Stroke		Average Stiffness (based on max disp and load) (lb/in)	notes
	Maximum Load (lb)	Maximum Displacement (in)	Maximum Load (lb)	Maximum Displacement (in)		
1	1,080	0.54	1,120	0.59	1,954	unsheathed
2	1,940	1.49	2,000	1.47	1,331	unsheathed
3	1,990	1.54	2,050	1.53	1,316	unsheathed
4	2,500	0.14	2,480	0.13	18,335	4" SIPs, no sill
5	4,000	0.22	3,990	0.26	16,542	4" SIPs, no sill
6	2,540	0.08	3,110	0.06	41,852	4" SIPs, with sill
7	3,980	0.12	4,020	0.10	37,559	4" SIPs, with sill
8	9,990	0.42	10,100	0.62	19,243	4" SIPs, with sill
9	4,110	0.15	4,080	0.28	19,002	4" SIPs, with sill
10	3,990	0.19	4,020	0.29	16,970	4" SIPs, with sill
11	3,410	0.26	3,840	0.25	14,160	4" SIPs, with sill & opening
12	2,140	0.25	3,340	0.26	10,661	4" SIPs, with sill & opening
13	1,840	0.26	2,680	0.25	8,933	4" SIPs, with sill & opening
14	6,090	1.01	6,990	0.92	6,788	4" SIPs, with sill & opening
15-114	-	-	-	-	-	no data recorded
115	6,020	1.01	6,950	0.91	6,745	4" SIPs, with sill & opening
116	10,000	2.16	3,760	0.37	5,432	4" SIPs, with sill & opening
117	1,040	0.93	1,090	1.16	1,015	unsheathed
118	6,150	8.08	0	0.00	760	unsheathed

Table G-3 Port Orford Cedar

Cycle	Push Stroke		Pull Stroke		Average Stiffness (based on max disp and load) (lb/in)	notes
	Maximum Load (lb)	Maximum Displacement (in)	Maximum Load (lb)	Maximum Displacement (in)		
1	444	0.20	561	0.30	2001	
2	947	0.65	1012	0.74	1410	
3	972	0.67	1023	0.75	1403	
4	1515	1.13	1524	1.20	1305	
5 -604	-	-	-	-	-	600 cycles, no data recorded
605	1571	1.22	1579	1.25	1277	
606	1814	1.42	1862	1.44	1284	
607	1023	0.95	1095	0.93	1127	
608	2050	1.68	2042	1.58	1254	
609	3881	3.48	4150	3.31	na	

Table G-4 White Oak

Cycle	Push Stroke		Pull Stroke		Average Stiffness (based on max disp and load) (lb/in)	notes
	Maximum Load (lb)	Maximum Displacement (in)	Maximum Load (lb)	Maximum Displacement (in)		
1	3050	1.02	3360	1.02	3142	
2	3063	1.04	0	0.00	2940	
3	2890	1.00	3340	1.03	3069	
4	0	0.00	3140	0.99	3188	
5	2190	1.01	2470	1.02	2296	one kb peg removed
6	698	1.00	623	0.99	663	both kb pegs removed
7	2940	1.00	3190	1.02	3036	
8	6520	2.03	5600	1.72	na	
9	15700	9.23	0	0.00	na	

Appendix H. 2S2B Service Level Loading

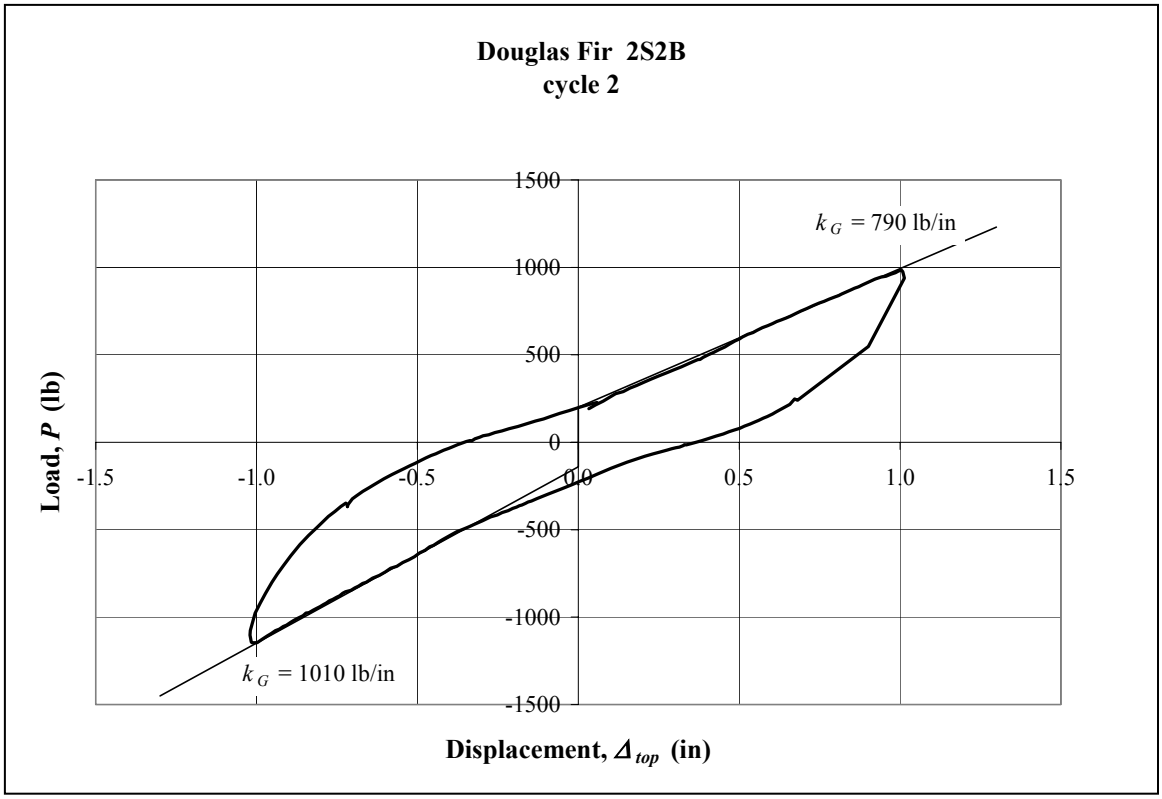

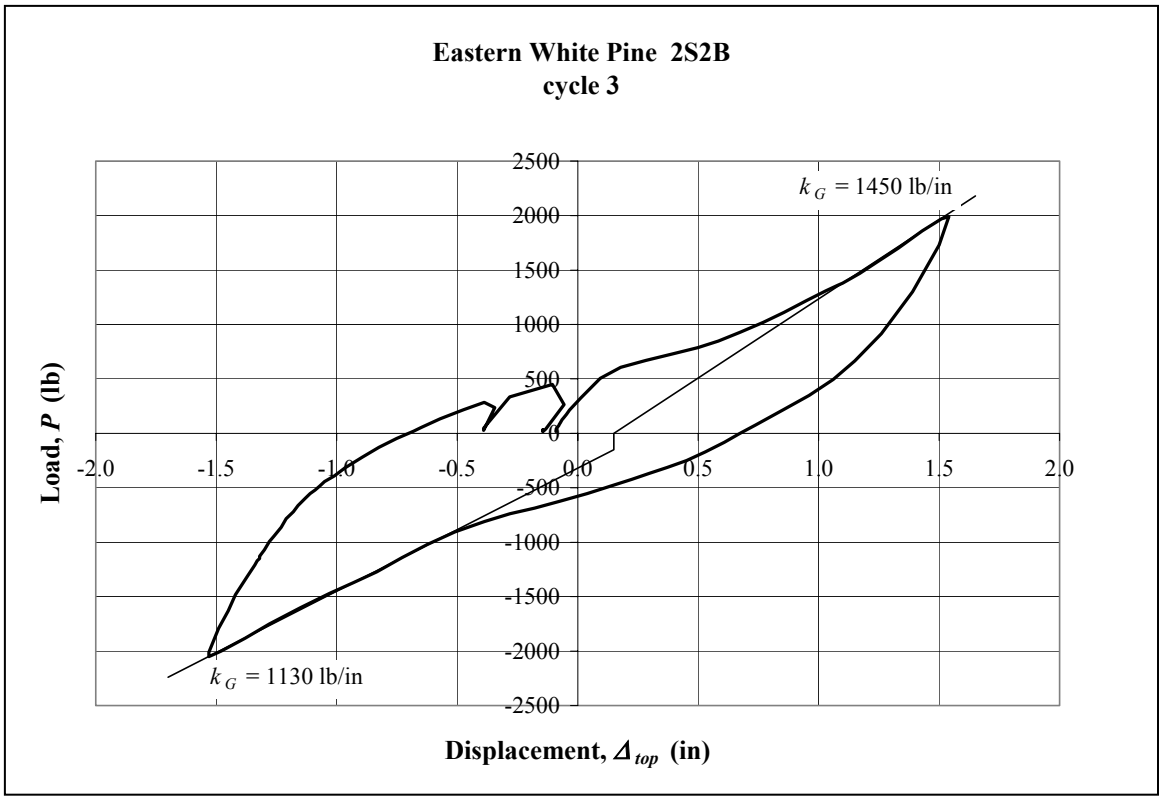

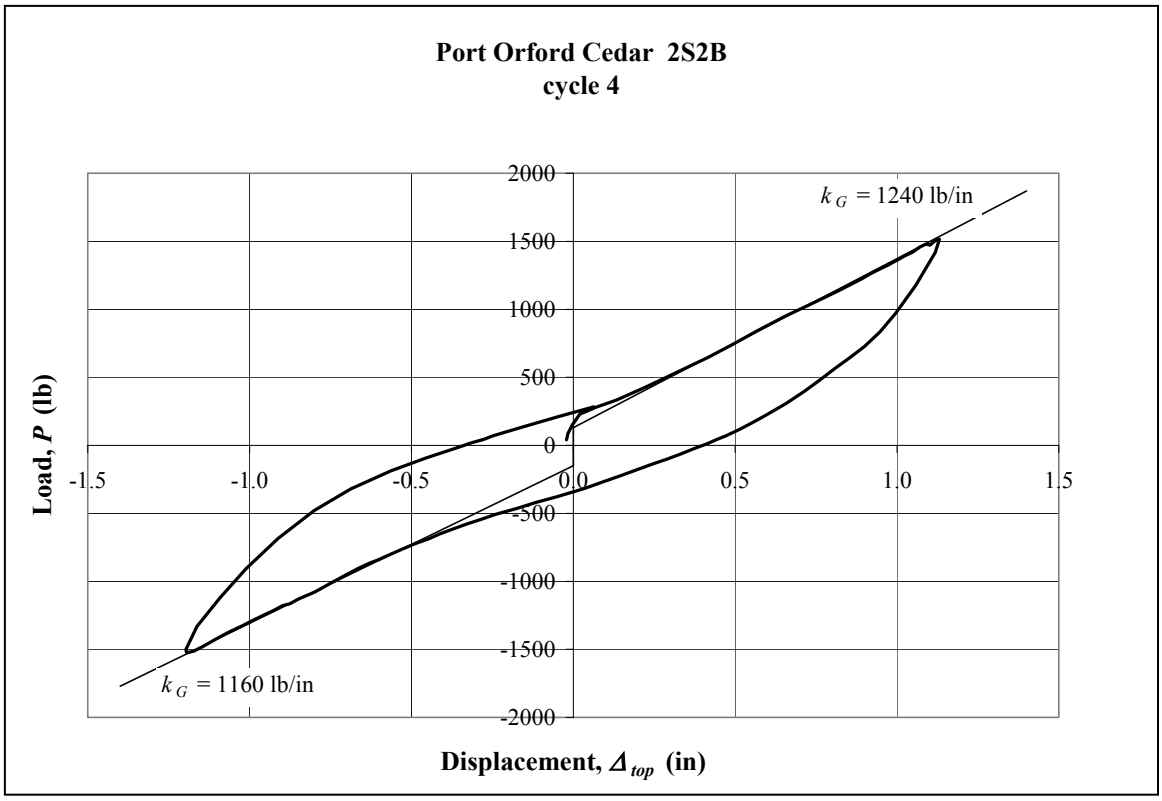
Port Orford Cedar 2S2B
cycle 4
Load, P (lb)
2000
1500
1000
500
0
-500
-1000
-1500
-2000
-1.5
-1.0
-0.5
0.0
0.5
1.0
1.5
k_G = 1240 lb/in
k_G = 1160 lb/in
Displacement, Δ_{top} (in)

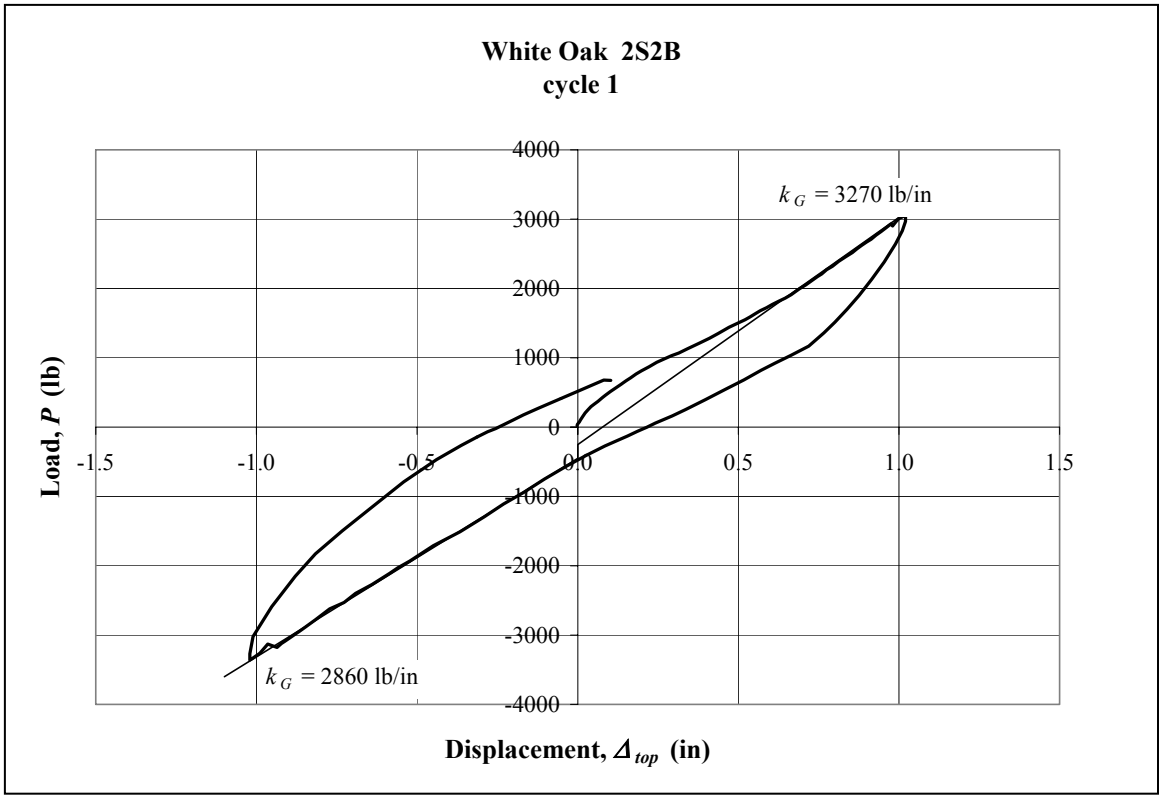
White Oak 2S2B
cycle 1
Load, P (lb)
4000
3000
2000
1000
0
-1000
-2000
-3000
-4000
-1.5
-1.0
-0.5
0.0
0.5
1.0
1.5
k_G = 3270 lb/in
k_G = 2860 lb/in
Displacement, Δ_{top} (in)

D

Appendix I. 2S2B Maximum Load

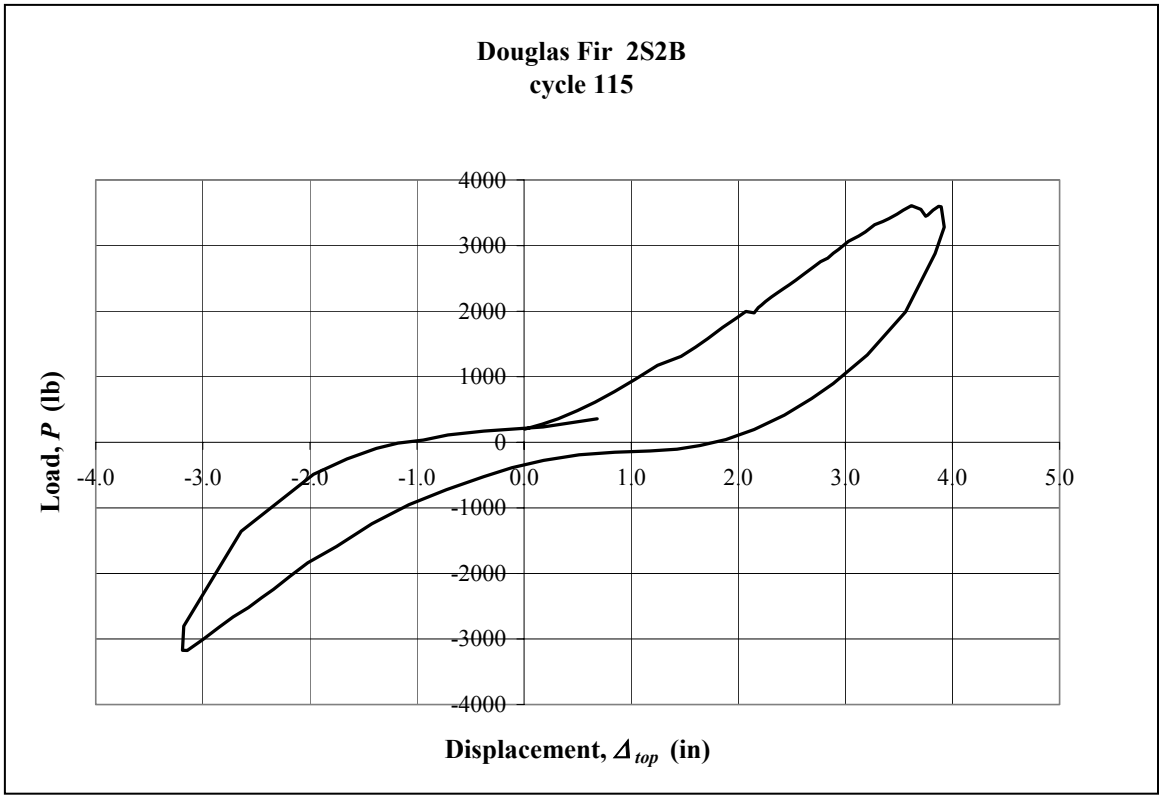

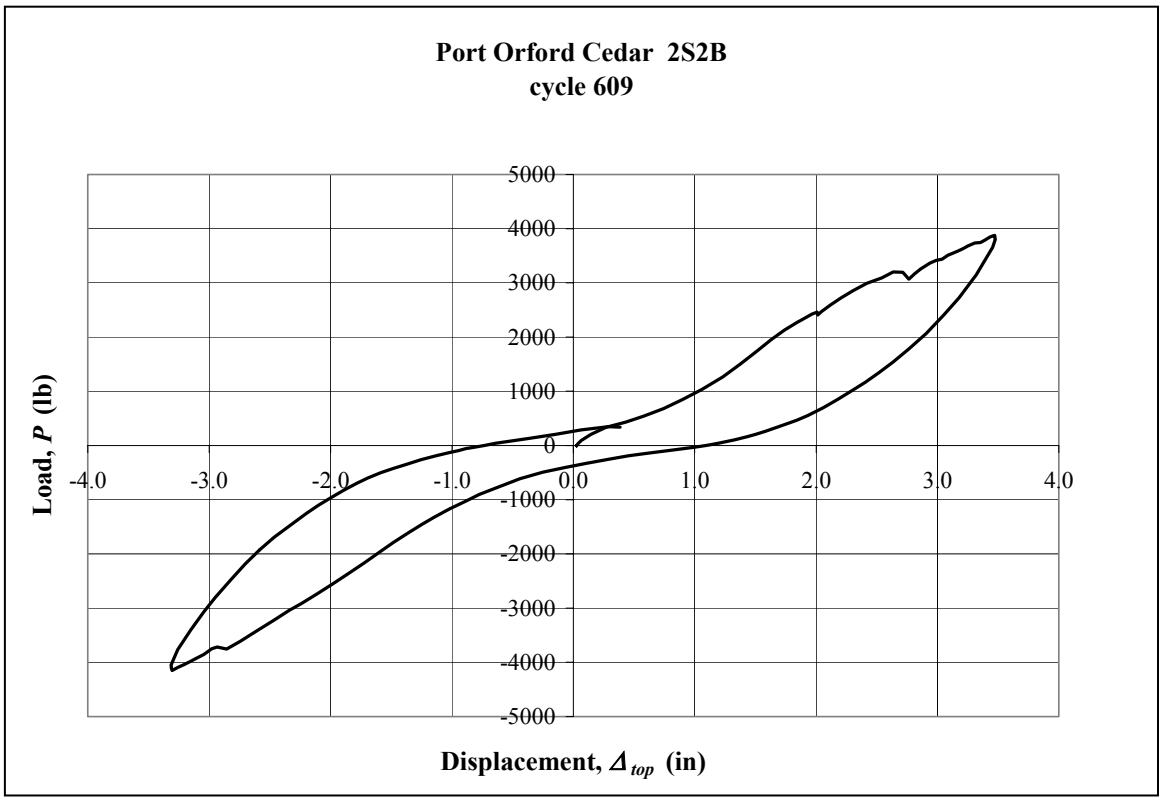
Port Orford Cedar 2S2B
cycle 609
Load, P (lb)
5000
4000
3000
2000
1000
0
-1000
-2000
-3000
-4000
-5000
-4.0
-3.0
-2.0
-1.0
0.0
1.0
2.0
3.0
4.0
Displacement, Δ top (in)

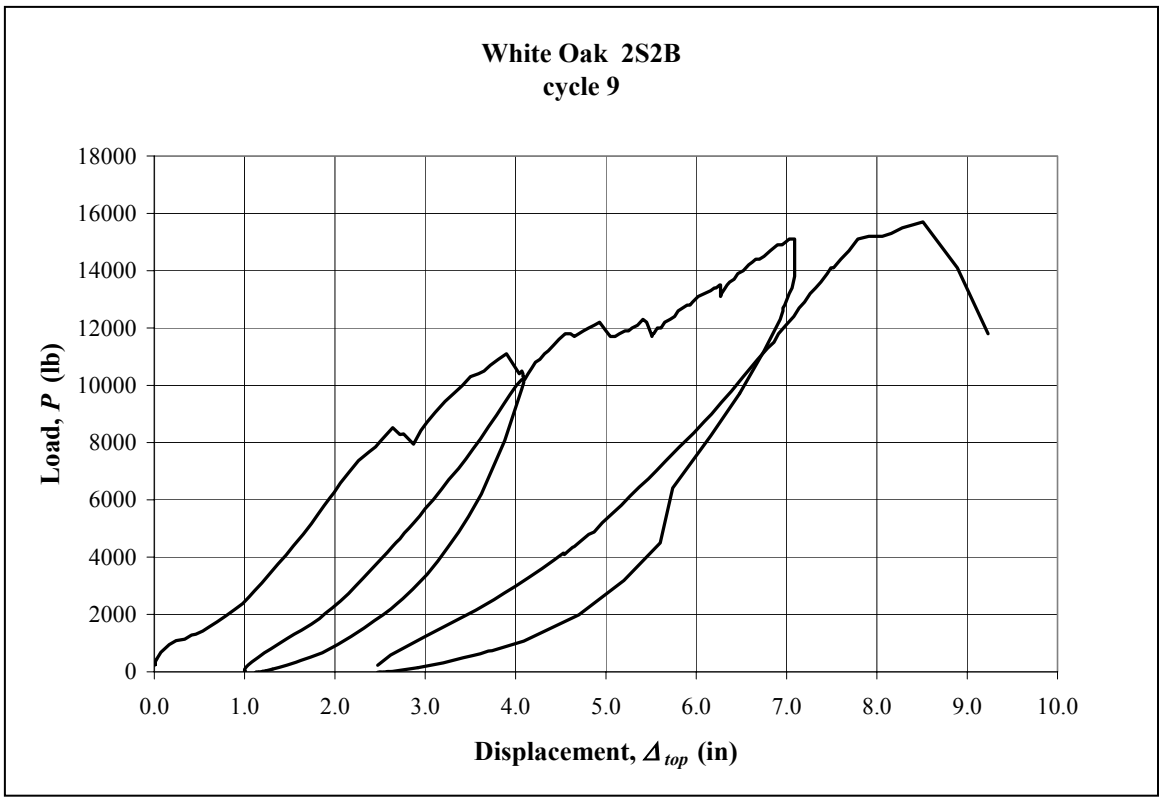
White Oak 2S2B
cycle 9
Load, P (lb)
18000
16000
14000
12000
10000
8000
6000
4000
2000
0
0.0
1.0
2.0
3.0
4.0
5.0
6.0
7.0
8.0
9.0
10.0
Displacement, Δ top (in)

Appendix J. Phase 1 SIP Connection Summaries of Curve Fits and Yield Load

Table J.1. 4-inch SIP Screwed to White Oak Timber

	$P=a\ln(\delta)+b$			$P=(A+B\delta)[1-\exp(-C\delta/A)]$			Yield Load*
Specimen	***a***	***b***	**R^2**	***A***	***B***	***C***	**(lb)**
screwwo04	150	952	0.99	552	790	23217	608
screwwo07	125	755	0.90	421	660	19387	477
screwwo10	172	1007	0.99	550	905	20028	602
screwwo16	155	898	0.97	487	814	17355	561
screwwo19	160	1014	0.99	587	845	21186	653
screwwo28	142	820	1.00	441	749	14323	475
screwwo31	171	1012	0.99	556	901	27279	637
screwwo34	121	784	0.97	463	635	15801	502
Std Deviation	19	107		62	101	4170	72
Mean	**150**	**905**	**0.98**	**507**	**787**	**19822**	**564**
- 5% Conf	134	816		456	703	16336	504
+5% Conf	166	995		559	872	23309	624

Table J.2. 4-inch SIP Screwed to White Oak Timber with Washer

	$P=a\ln(\delta)+b$			$P=(A+B\delta)[1-\exp(-C\delta/A)]$			Yield Load*
Specimen	***a***	***b***	**R^2**	***A***	***B***	***C***	**(lb)**
wash03	153	931	0.99	525	804	17535	563
wash06	120	774	0.99	454	632	22916	491
wash09	176	970	0.99	500	928	11650	552
wash15	191	1113	0.99	605	1004	20230	667
wash18	151	894	0.98	491	797	15570	569
wash21	190	1105	0.98	599	1000	19540	667
wash30	166	987	0.99	545	873	24385	609
wash33	132	772	0.98	422	694	11758	476
wash36	178	1056	0.99	583	937	18349	650
Std Deviation	25	127		64	131	4441	71
Mean	**162**	**956**	**0.99**	**525**	**852**	**17993**	**583**
- 5% Conf	143	858		476	751	14579	528
+5% Conf	181	1053		575	953	21407	638

* Yield load is defined as the resisting force occuring at a displacement of 0.095 inches

Table J.3. 4-inch SIP Screwed to White Oak Timber with Shim

Specimen	$P=a\ln(\delta)+b$			$P=(A+B\delta)[1-\exp(-C\delta/A)]$			Yield Load*
	a	*b*	R^2	*A*	*B*	*C*	(lb)
shim02	114	694	0.96	396	586	14651	425
shim05	163	661	0.99	236	835	3564	277
shim14	136	663	1.00	307	699	8178	341
shim17	153	685	1.00	286	784	5529	325
shim20	141	653	1.00	286	721	5510	321
shim29	163	665	0.99	239	838	3582	281
shim32	194	846	0.99	340	995	5827	389
shim35	177	782	1.00	320	908	6650	366
Std Deviation	25	70		53	128	3556	51
Mean	**155**	**706**	**0.99**	**301**	**796**	**6686**	**341**
- 5% Conf	134	647		257	689	3713	298
+5% Conf	176	765		345	903	9660	384

Table J.4. 4-inch SIP Screwed to White Oak Timber without Predrill

Specimen	$P=a\ln(\delta)+b$			$P=(A+B\delta)[1-\exp(-C\delta/A)]$			Yield Load*
	a	*b*	R^2	*A*	*B*	*C*	(lb)
nopredrill11	182	1031	0.99	545	960	18720	608
nopredrill12	114	648	0.99	345	598	10768	373
nopredrill13	134	757	0.99	401	705	13187	454
nopredrill24	172	972	0.99	515	904	15024	577
nopredrill25	100	653	0.99	387	526	18830	413
nopredrill26	155	939	1.00	526	818	19355	580
nopredrill37	114	719	0.97	416	600	16997	461
nopredrill38	95	615	0.95	362	499	15893	385
nopredrill39	85	556	0.99	330	448	17993	341
nopredrill40	171	937	0.99	481	901	11198	523
Std Deviation	36	172		80	188	3171	96
Mean	**132**	**783**	**0.99**	**431**	**696**	**15796**	**472**
- 5% Conf	107	660		374	561	13528	403
+5% Conf	158	905		488	830	18065	540

Appendix K. Phase 2 SIP Connection Summaries of Curve Fits and Yield Load

Table K.1. 4-inch SIP Screwed to Douglas Fir Timber

	$P=a\ln(\delta)+b$			$P=(A+B\,\delta)\,[1-\exp(-C\,\delta/A)]$			Yield Load*
Specimen	***a***	***b***	**R^2**	***A***	***B***	***C***	**(lb)**
screwdf01	164	894	0.98	458	863	14001	529
screwdf02	173	969	0.98	508	913	16636	599
screwdf03	177	932	0.99	462	931	12643	528
screwdf04	139	736	0.99	366	731	10215	399
screwdf05	129	681	0.96	339	678	9912	412
screwdf06	122	689	1.00	365	641	13301	402
screwdf07	170	948	0.98	496	894	16528	564
screwdf08	121	613	0.99	291	636	6390	342
screwdf09	185	967	0.99	474	975	11805	546
Std Deviation	26	143		78	134	3276	91
Mean	**153**	**825**	**0.98**	**418**	**807**	**12381**	**480**
- 5% Conf	134	715		358	704	9863	410
+5% Conf	173	936		477	910	14899	550

Table K.2. 4-inch SIP Nailed to Douglas Fir Timber

	$P=a\ln(\delta)+b$			$P=(A+B\,\delta)\,[1-\exp(-C\,\delta/A)]$			Yield Load*
Specimen	***a***	***b***	**R^2**	***A***	***B***	***C***	**(lb)**
naildf01	208	996	0.96	443	1094	9354	502
naildf02	187	870	0.97	373	982	8468	425
naildf04	201	877	0.98	343	1057	5669	409
naildf05	197	950	0.95	427	1035	10545	469
naildf06	201	944	0.96	409	1059	7383	494
naildf07	151	712	0.98	309	796	6060	366
naildf08	169	775	0.98	325	890	5992	379
naildf09	205	934	0.94	389	1078	7548	438
naildf10	165	779	0.97	339	870	7220	384
Std Deviation	20	97		47	107	1634	50
Mean	**187**	**871**	**0.97**	**373**	**984**	**7582**	**430**
- 5% Conf	171	797		337	902	6326	391
+5% Conf	203	945		409	1067	8839	468

* Yield load is defined as the resisting force occuring at a displacement of 0.095 inches

Table K.3. 4-inch SIP Screwed to Eastern White Pine Timber

	$P=a\ln(\delta)+b$			$P=(A+B\delta)[1-\exp(-C\delta/A)]$			Yield Load*
Specimen	***a***	***b***	**R^2**	***A***	***B***	***C***	**(lb)**
screwwp01	191	921	0.98	414	1005	10593	479
screwwp02	144	793	0.98	409	759	11994	475
screwwp03	162	835	0.99	404	854	10010	465
screwwp05	117	717	0.96	404	618	15845	528
screwwp06	144	836	0.99	453	757	16205	502
screwwp07	173	869	0.99	409	910	8707	464
screwwp08	127	673	0.97	336	666	11849	359
screwwp09	119	670	1.00	352	628	12101	394
screwwp10	134	731	0.99	373	707	12532	404
Std Deviation	25	90		36	132	2480	55
Mean	**146**	**783**	**0.98**	**395**	**767**	**12204**	**452**
- 5% Conf	126	714		368	665	10298	410
+5% Conf	165	852		422	869	14110	494

Table K.4. 4-inch SIP Nailed to Eastern White Pine Timber

	$P=a\ln(\delta)+b$			$P=(A+B\delta)[1-\exp(-C\delta/A)]$			Yield Load*
Specimen	***a***	***b***	**R^2**	***A***	***B***	***C***	**(lb)**
nailwp02	176	870	0.98	401	927	8423	457
nailwp03	148	859	0.98	465	779	17387	525
nailwp04	231	931	0.98	317	1216	4814	369
nailwp05	196	969	0.99	447	1031	9242	510
nailwp06	157	783	0.99	364	828	8243	421
nailwp07	204	961	0.98	418	1074	8359	475
nailwp08	141	737	0.97	362	742	11210	418
nailwp09	132	641	0.99	291	694	5795	331
nailwp10	169	845	0.99	394	891	8973	456
Std Deviation	33	109		57	171	3608	63
Mean	**173**	**844**	**0.98**	**384**	**909**	**9161**	**440**
- 5% Conf	148	761		340	778	6387	392
+5% Conf	198	927		428	1041	11934	489

Table K.5. 4-inch SIP Screwed to Douglas Fir Timber Loaded Perpendicular to Grain

Specimen	$P=a\ln(\delta)+b$			$P=(A+B\delta)[1-\exp(-C\delta/A)]$			Yield Load*
	a	*b*	R^2	*A*	*B*	*C*	(lb)
perpdf01	128	683	0.99	342	675	9200	381
perpdf02	133	711	1.00	356	702	9810	405
perpdf03	160	855	0.98	430	840	12558	475
perpdf04	115	632	0.99	326	604	8563	373
perpdf05	144	727	0.97	343	759	8631	367
perpdf06	159	862	0.99	439	836	12135	496
perpdf07	128	753	0.99	412	675	16155	457
perpdf08	121	634	0.99	312	638	7264	354
perpdf09	147	777	0.98	385	776	9045	459
Std Deviation	16	84		47	84	2756	53
Mean	**137**	**737**	**0.99**	**372**	**723**	**10373**	**419**
- 5% Conf	125	672		336	658	8255	378
+5% Conf	150	802		408	787	12492	460

Table K.6. Single Sheet OSB Screwed to Douglas Fir Timber

Specimen	$P=a\ln(\delta)+b$			$P=(A+B\delta)[1-\exp(-C\delta/A)]$			Yield Load*
	a	*b*	R^2	*A*	*B*	*C*	(lb)
osbdf01	119	628	0.99	312	625	8116	358
osbdf02	129	657	0.99	314	680	6861	361
osbdf03	108	562	0.99	275	567	6714	317
osbdf04	115	626	0.99	320	605	8786	360
osbdf05	106	549	1.00	266	559	5786	303
osbdf06	123	586	0.99	258	648	4860	303
osbdf07	117	602	0.99	291	615	6550	339
osbdf08	113	591	0.99	291	594	7303	333
osbdf09	129	644	0.98	302	677	6182	358
osbdf10	115	637	0.99	331	607	9241	378
Std Deviation	8	36		24	41	1357	26
Mean	**117**	**608**	**0.99**	**296**	**618**	**7040**	**341**
- 5% Conf	112	582		279	588	6069	322
+5% Conf	123	634		313	647	8010	360

Appendix L. Phase 3 SIP Connection Summaries of Curve Fits and Yield Load

Table L.1. 4-inch SIP Screwed to Douglas Fir Timber

	$P=a\ln(\delta)+b$			$P=(A+B\,\delta)\,[1-\exp(-C\,\delta/A)]$			Yield Load*
Specimen	***a***	***b***	**R^2**	***A***	***B***	***C***	**(lb)**
long01	204	1026	0.93	484	1072	20418	523
long02	163	931	0.99	497	860	16593	550
long03	92	589	0.98	344	485	16157	379
long04	114	596	0.98	293	599	6265	334
long05	133	780	0.99	427	700	13902	460
long06	202	1018	0.93	479	1065	15360	530
long07	147	806	1.00	415	773	12372	459
long08	143	787	0.93	406	753	19483	435
long09	141	883	0.99	508	741	29283	542
long10	147	826	0.99	435	773	13796	486
Std Deviation	35	151		69	183	6007	72
Mean	**149**	**824**	**0.97**	**429**	**782**	**16363**	**470**
- 5% Conf	124	717		379	651	12066	418
+5% Conf	174	932		478	913	20660	521

Table L.2. 4-inch SIP Countersunk Screwed to Douglas Fir Timber

	$P=a\ln(\delta)+b$			$P=(A+B\,\delta)\,[1-\exp(-C\,\delta/A)]$			Yield Load*
Specimen	***a***	***b***	**R^2**	***A***	***B***	***C***	**(lb)**
short01	135	817	0.99	457	713	19641	488
short02	177	938	0.91	468	929	21573	506
short03	158	864	0.96	445	830	18573	486
short04	157	911	0.94	493	826	28378	556
short05	141	724	0.96	349	743	11756	390
short06	170	963	0.94	510	895	26977	553
short07	203	1006	0.91	466	1069	23083	504
short08	155	889	0.97	476	816	22387	518
short09	185	885	0.92	394	972	8631	438
short10	188	1024	0.85	524	989	36391	567
Std Deviation	21	89		53	113	7988	55
Mean	**167**	**902**	**0.94**	**458**	**878**	**21739**	**501**
- 5% Conf	152	838		420	797	16025	461
+5% Conf	182	966		496	959	27453	540

* Yield load is defined as the resisting force occuring at a displacement of 0.095 inches

Table L.3. 4-inch SIP Screwed to Douglas Fir Timber with Waxed Paper

	$P=a\ln(\delta)+b$			$P=(A+B\,\delta)\,[1-\exp(-C\,\delta/A)]$			Yield Load*
Specimen	***a***	***b***	**R^2**	***A***	***B***	***C***	**(lb)**
wax01	141	752	0.99	377	741	10586	419
wax02	208	925	0.95	372	1093	8067	456
wax03	125	679	0.97	346	659	10578	369
wax04	218	910	0.97	332	1145	5092	396
wax05	128	750	0.99	410	673	13257	451
wax06	222	979	0.95	387	1171	8392	451
wax07	241	947	0.92	748	203	4959	367
wax08	245	920	0.95	867	112	3656	351
wax09	123	663	0.87	335	647	11535	349
wax10	147	772	0.91	380	776	13769	411
wax11	196	802	0.90	640	165	5135	320
wax12	161	836	0.91	407	849	15068	435
Std Deviation	47	107		180	368	3874	46
Mean	**180**	**828**	**0.94**	**467**	**686**	**9174**	**398**
- 5% Conf	146	751		338	423	6403	365
+5% Conf	213	905		596	949	11946	431

Table L.4. 6-inch SIP Screwed to Douglas Fir Timber

	$P=a\ln(\delta)+b$			$P=(A+B\,\delta)\,[1-\exp(-C\,\delta/A)]$			Yield Load*
Specimen	***a***	***b***	**R^2**	***A***	***B***	***C***	**(lb)**
thick02	151	786	0.99	385	794	11218	426
thick03	161	729	0.97	299	849	6154	340
thick04	99	551	0.97	287	523	9311	302
thick05	114	502	0.95	198	602	3903	241
thick06	205	753	0.93	207	1081	2991	254
thick07	170	924	1.00	472	892	12644	526
thick08	156	817	0.92	402	820	12055	431
thick09	145	665	0.91	278	765	7448	314
thick10	144	701	0.99	318	757	6875	365
thick11	185	705	0.91	214	972	3247	264
Std Deviation	31	123		91	163	3618	92
Mean	**153**	**713**	**0.95**	**306**	**806**	**7585**	**346**
- 5% Conf	131	625		241	689	4997	281
+5% Conf	175	801		371	922	10172	412

Appendix M. Phase 1 Load-Slip Curves

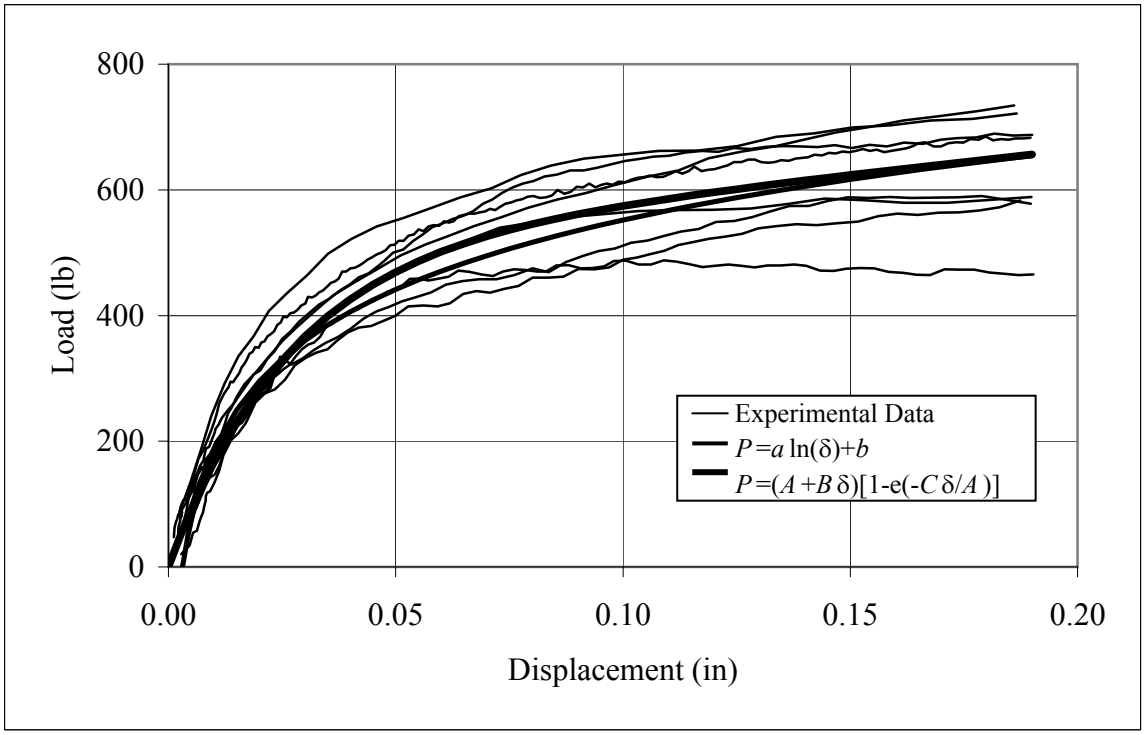

Figure M.1. 4-inch SIP Screwed to White Oak Timber

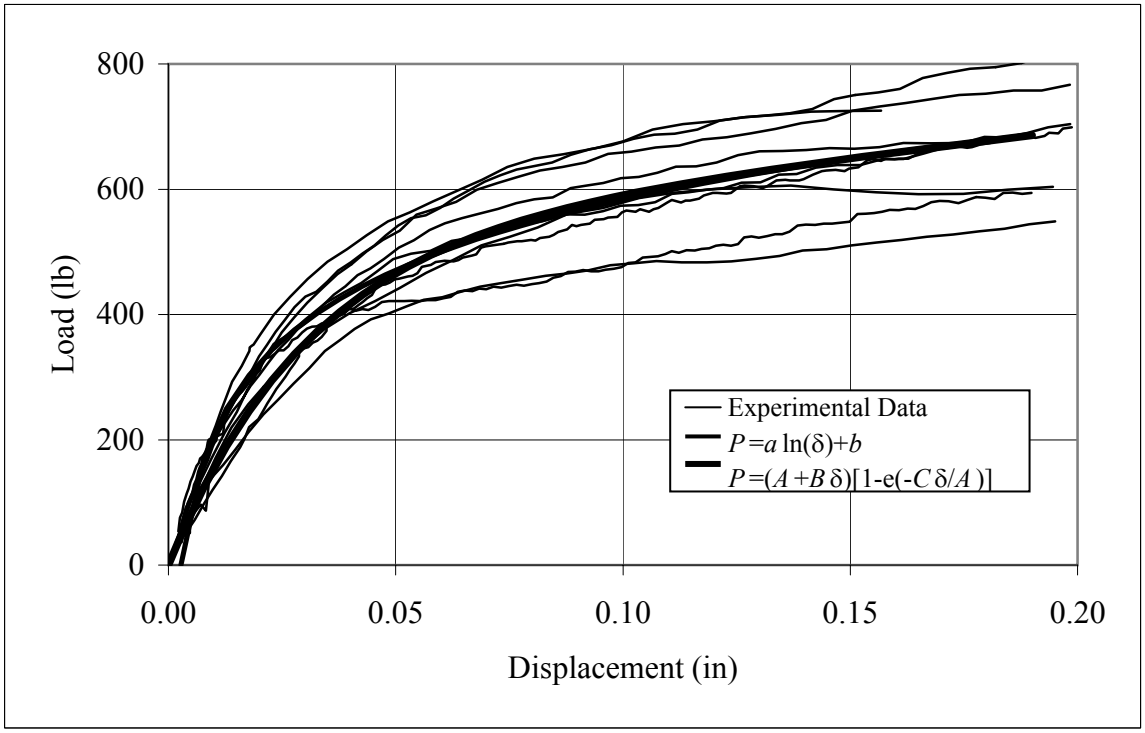

Figure M.2. 4-inch SIP Screwed to White Oak Timber with Washer

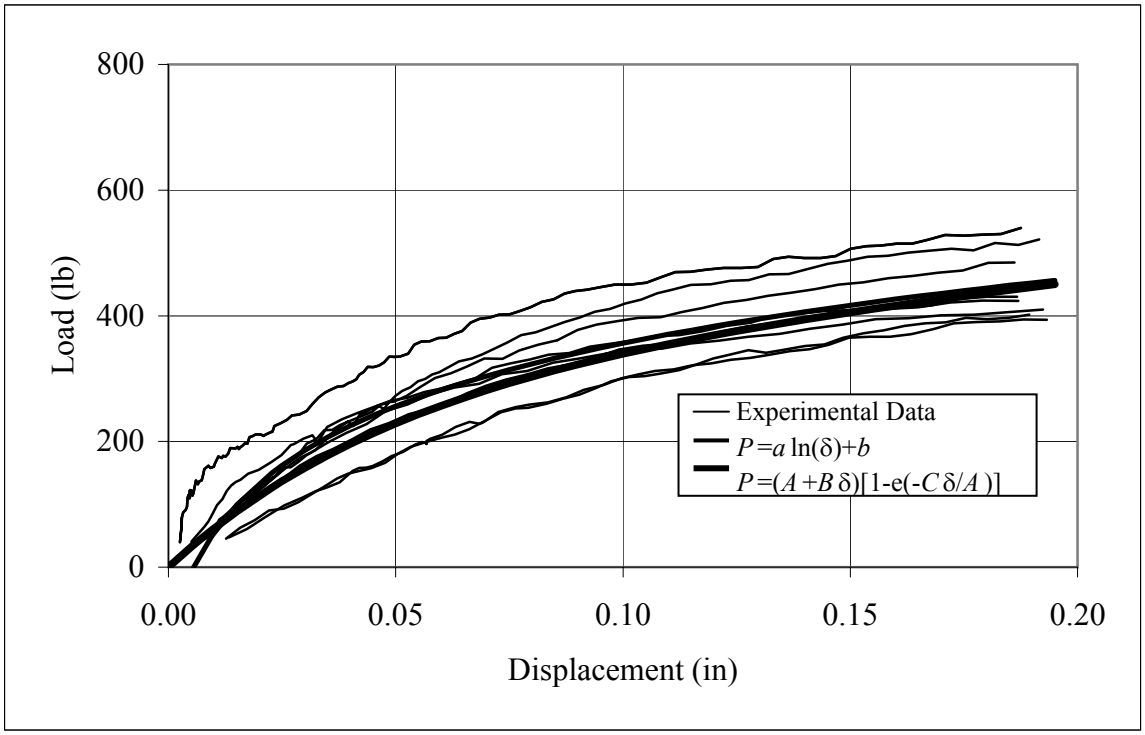

Figure M.3. 4-inch SIP Screwed to White Oak Timber with Shim

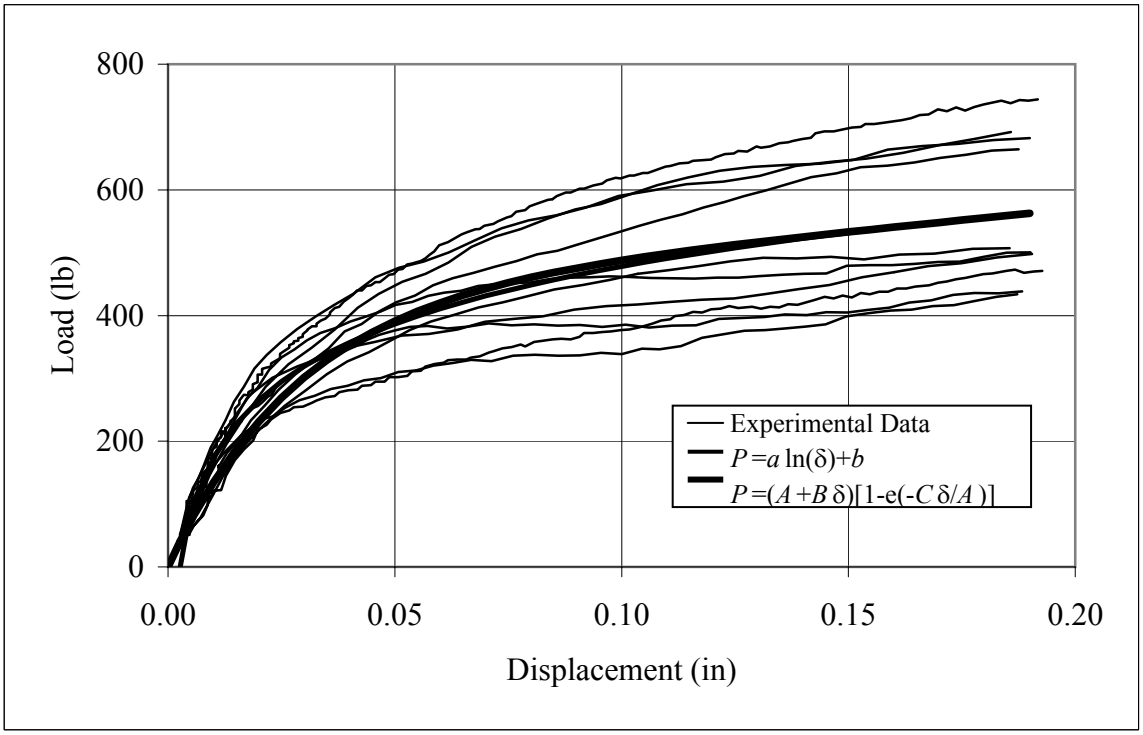

Figure M.4. 4-inch SIP Screwed to White Oak Timber without Predrill

Appendix N. Phase 2 Load-Slip Curves

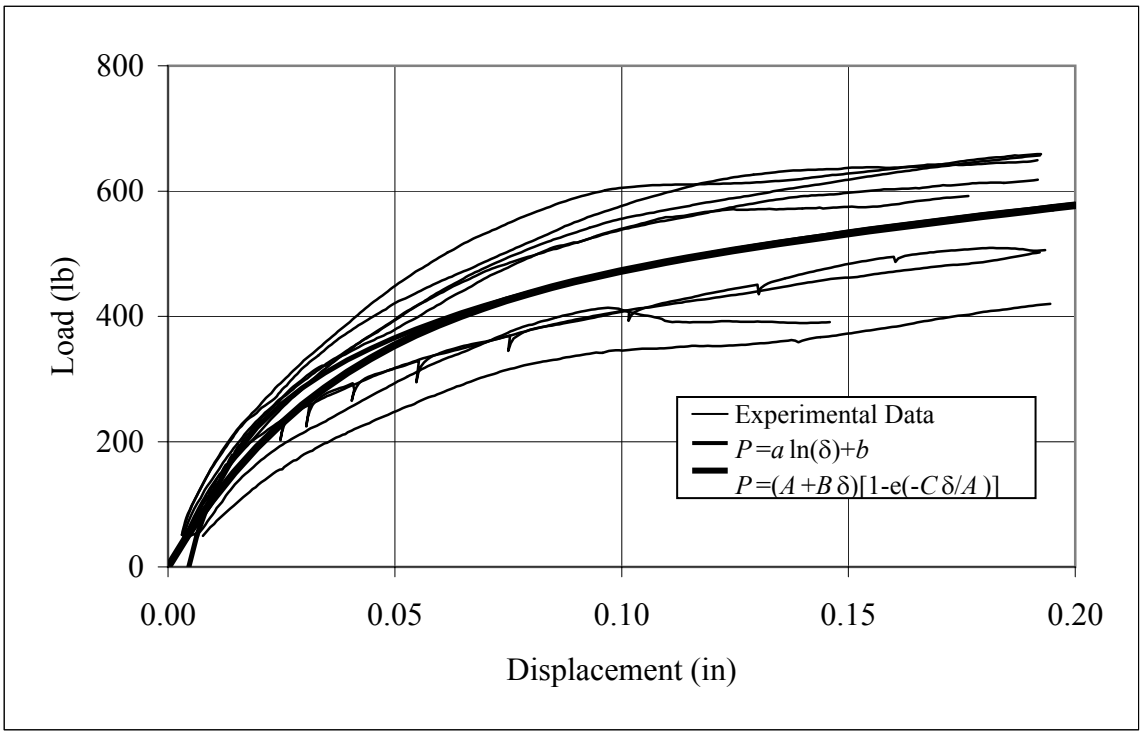

Figure N.1. 4-inch SIP Screwed to Douglas Fir Timber

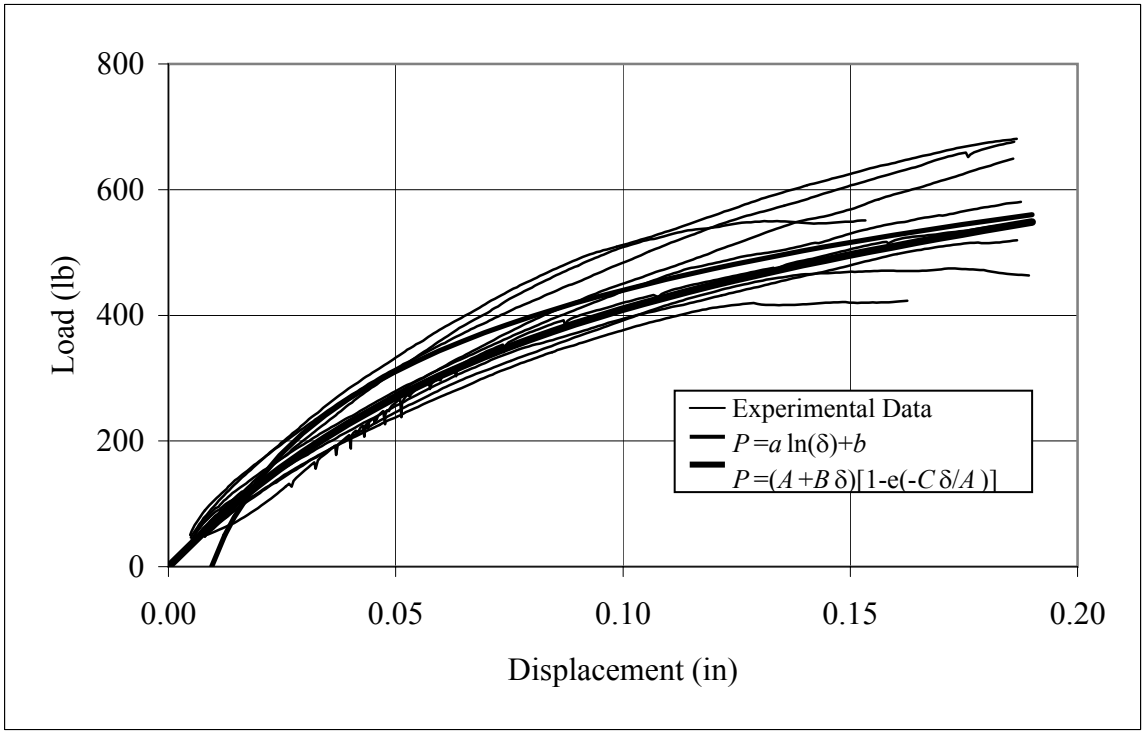

Figure N.2. 4-inch SIP Nailed to Douglas Fir Timber

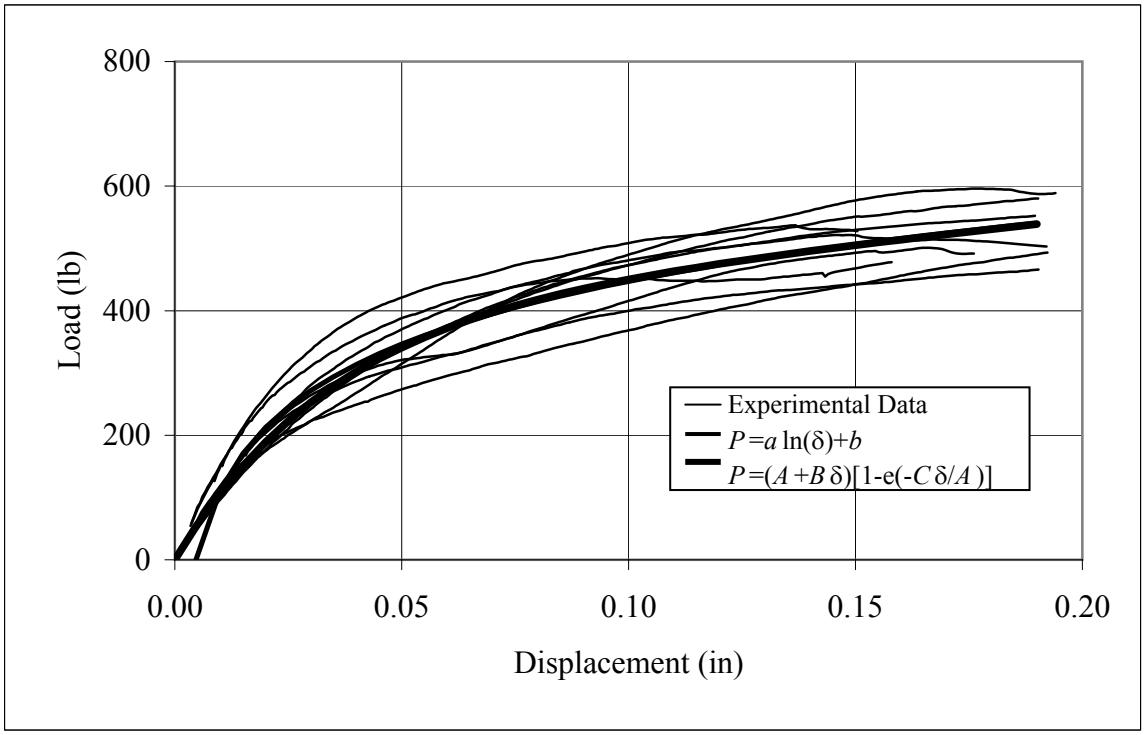

Figure N.3. 4-inch SIP Screwed to Eastern White Pine Timber

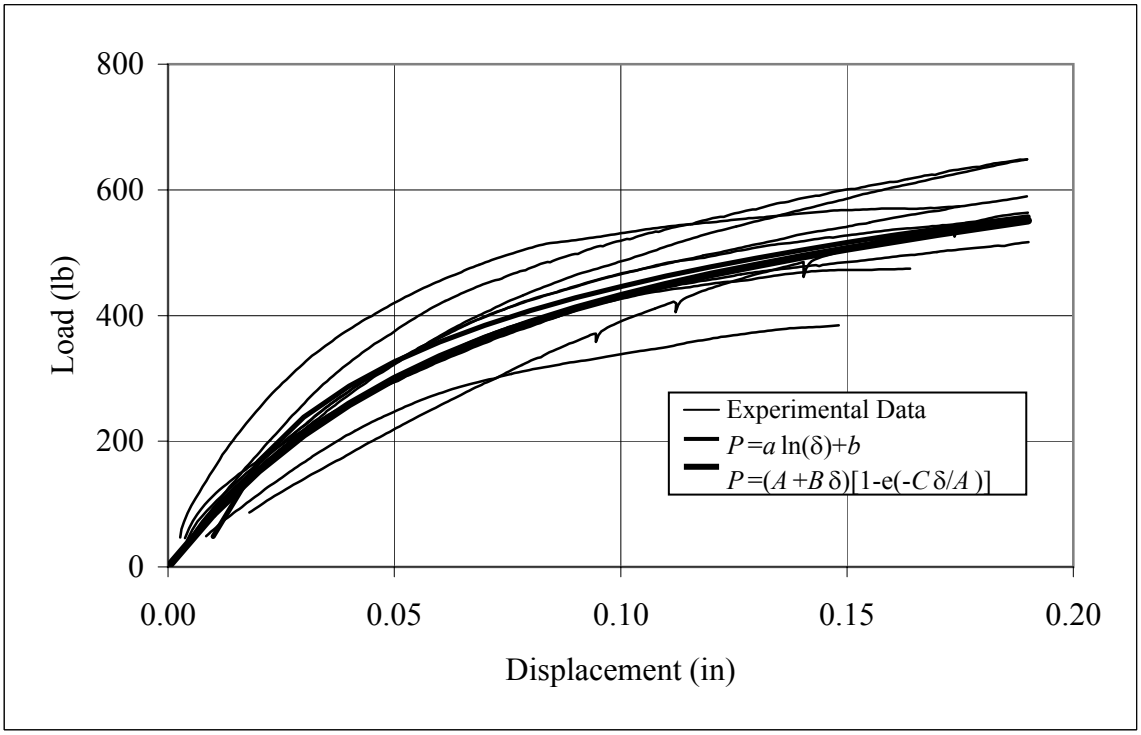

Figure N.4. 4-inch SIP Nailed to Eastern White Pine Timber

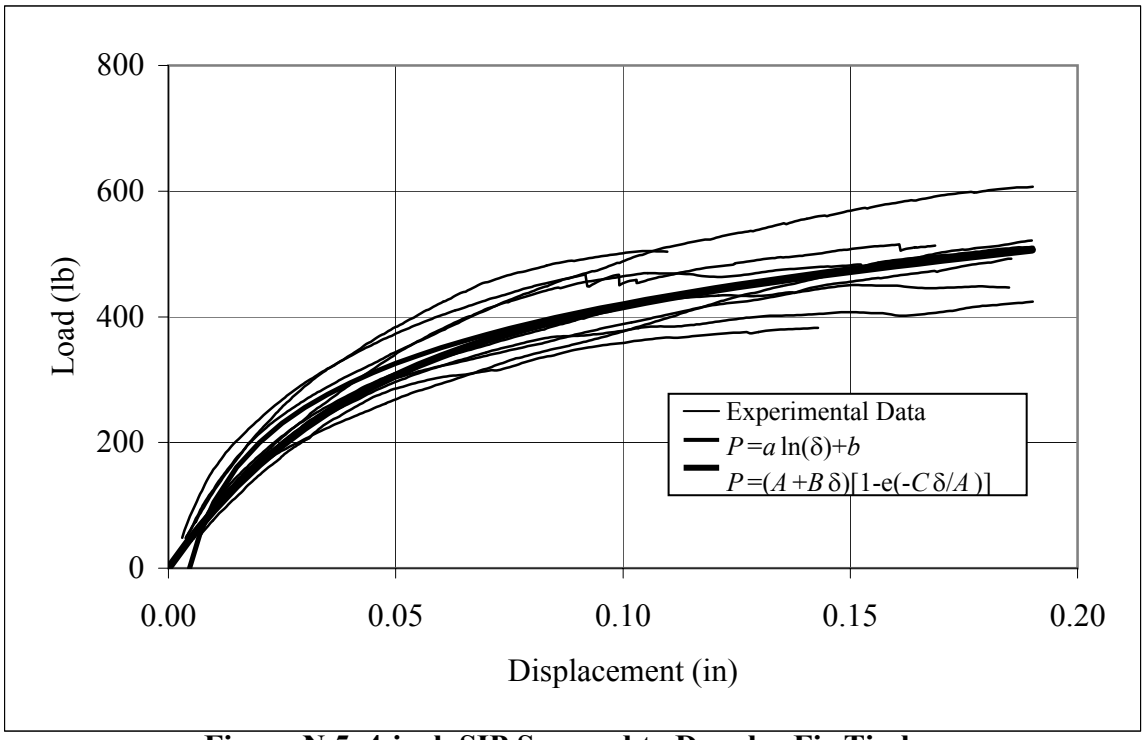

Figure N.5. 4-inch SIP Screwed to Douglas Fir Timber Loaded Perpendicular to Grain

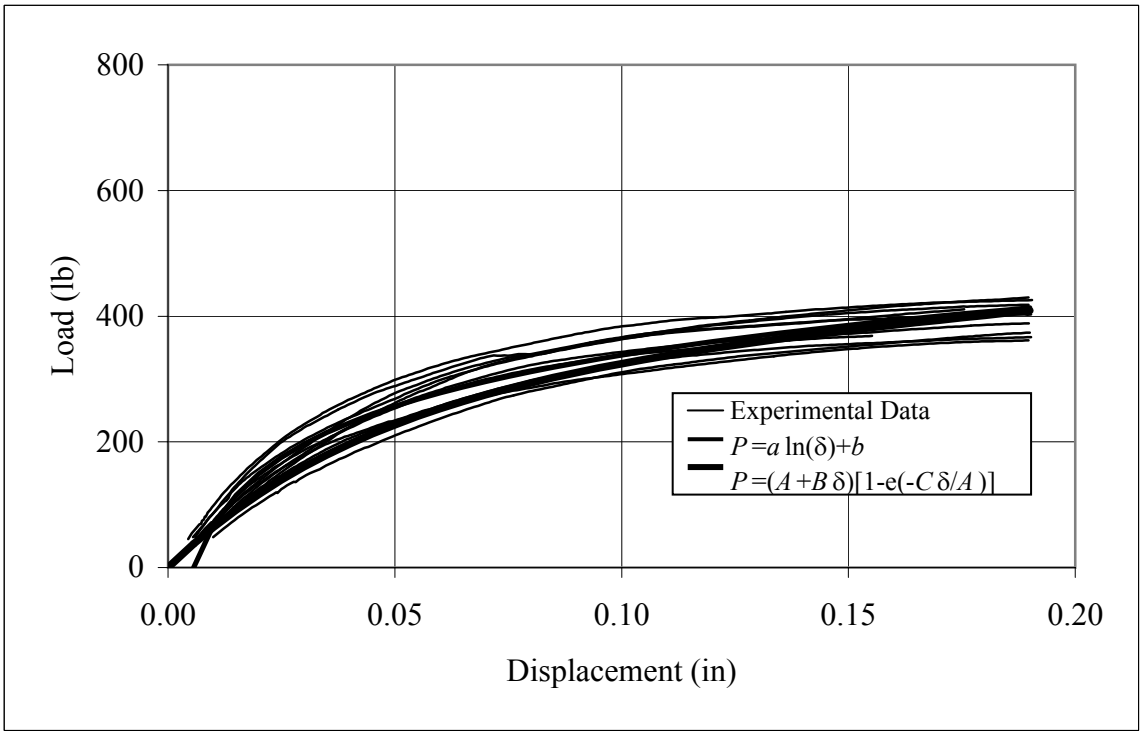

Figure N.6. Single Sheet OSB Screwed to Douglas Fir Timber

Appendix O. Phase 3 Load-Slip Curves

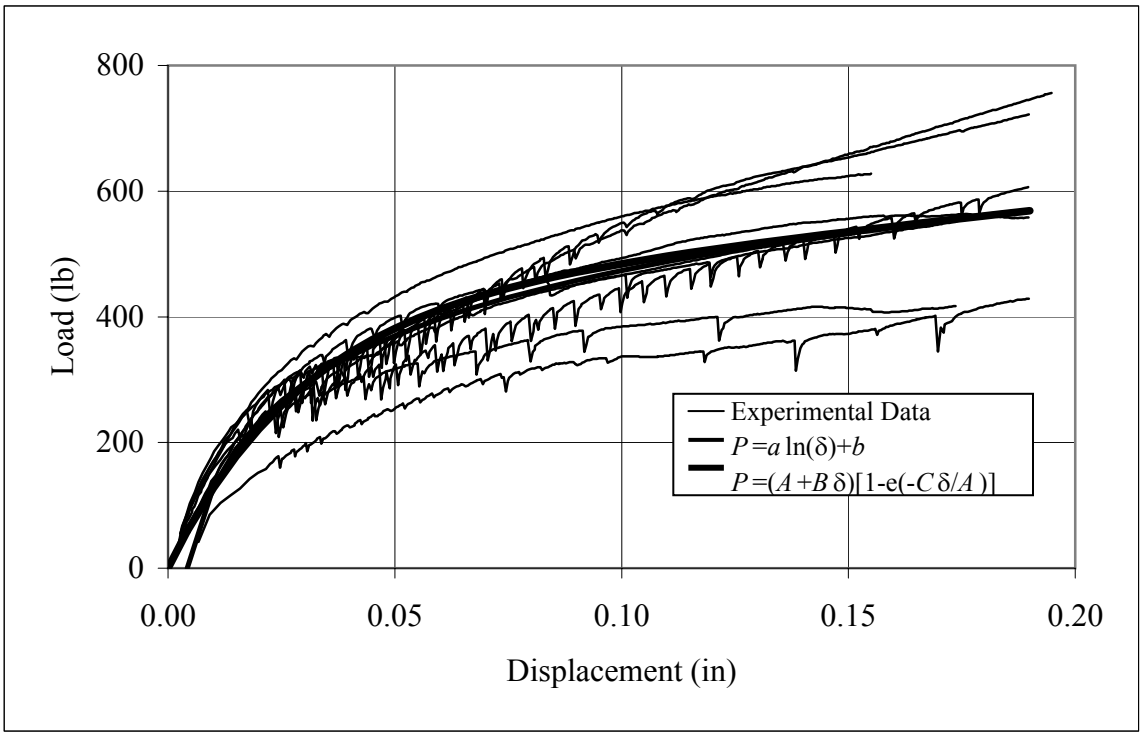

Figure O.1. 4-inch SIP Screwed to Douglas Fir Timber

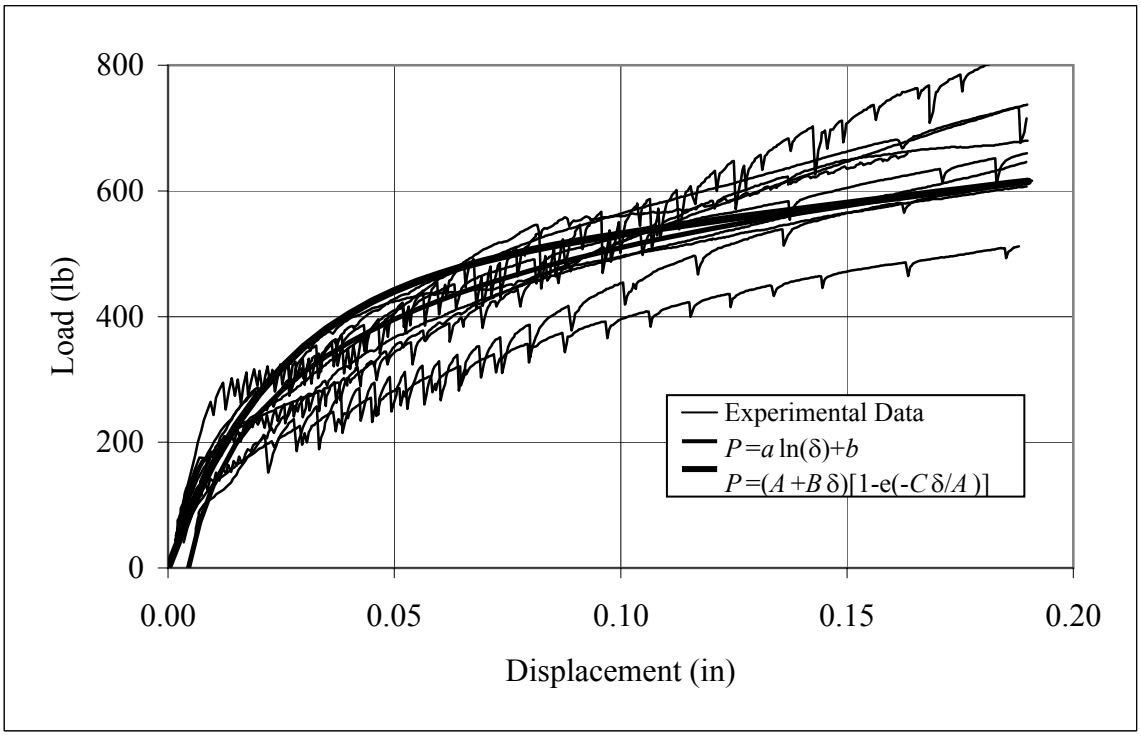

Figure O.2. 4-inch SIP Countersink Screwed to Douglas Fir Timber

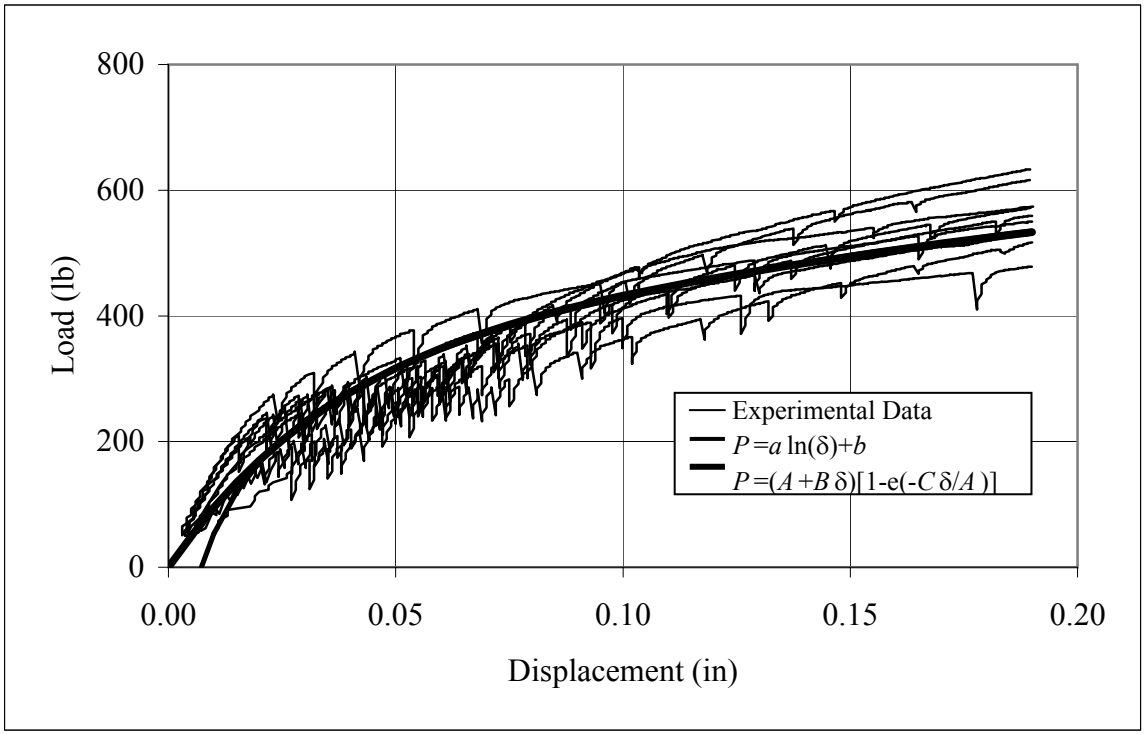

Figure O.3. 4-inch SIP Screwed to Douglas Fir Timber with Waxed Paper

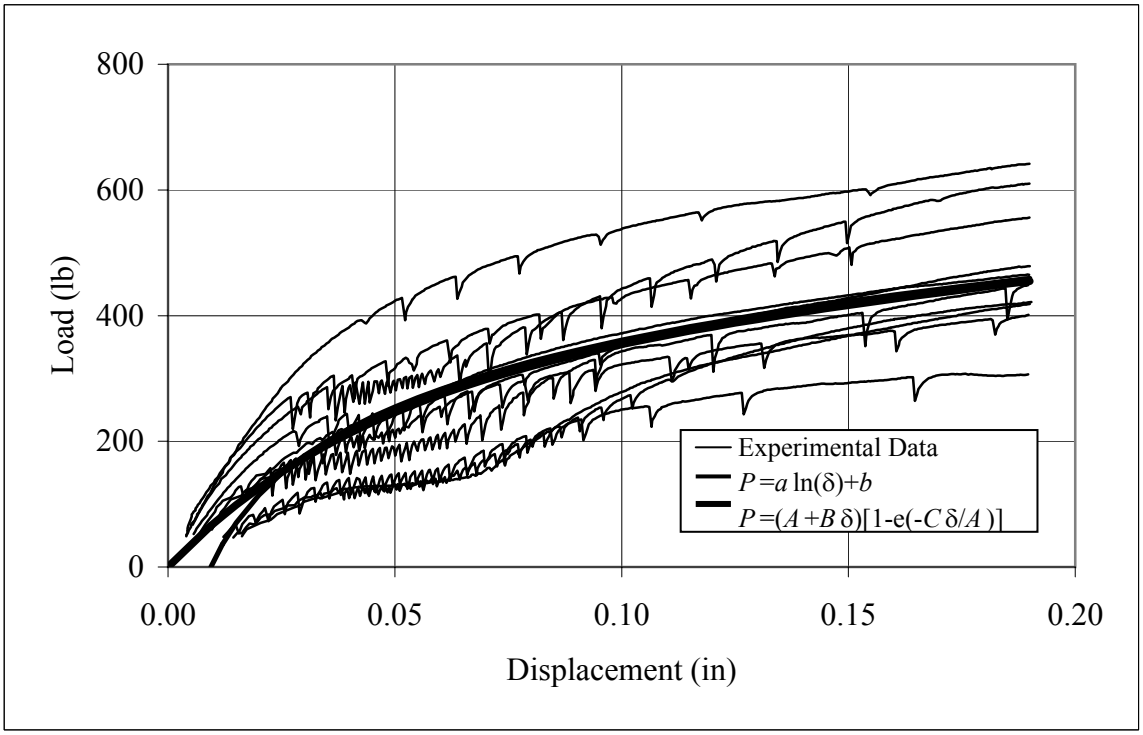

Figure O.4. 6-inch SIP Screwed to Douglas Fir Timber

Appendix P. Calculation of the Stiffness of a 1S1B Frame by Applying Work Energy Methods.

A point load P was applied to the frame as shown in Figure P1. Frame timbers were assumed to be rigid, and all frame displacement was assumed to be due to axial deformation in the pegged joints. All members were assumed to have pinned ends.

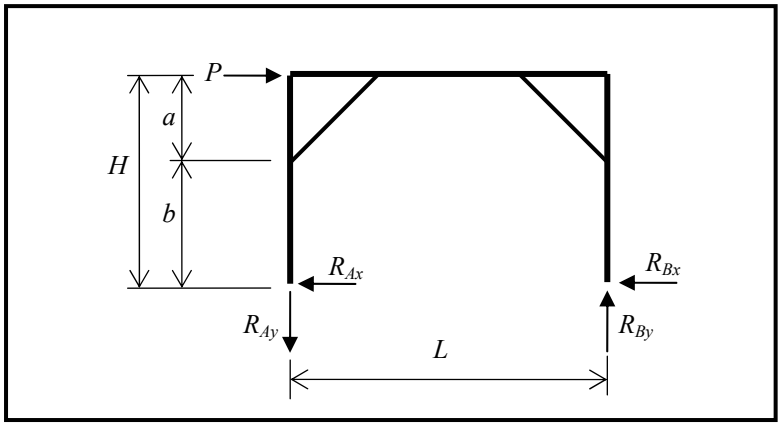

Figure P1. 1S1B Frame Free Body Diagram

Satisfaction of equilibrium (assume symmetry): $R_{Ax} = R_{Bx} = P/2$, $R_{Ay} = R_{By} = PH/L$

External Work: $W_e = P\Delta/2$

Δ : horizontal frame displacement at point of load application

Internal Work: $W_i = \Sigma F_j^2/2k_j$

F_j : internal axial force at joint

k_j : stiffness of joint

The forces acting on the left side column were determined by applying equilibrium equations to the free body diagram as shown in Figure P2.

$F_{KBL} = (0.707PH/a)$
$F_{BL} = (P/2)(H/a+1)$

F_{KBL} : internal axial force in left knee brace
F_{BL} : internal axial force in left end of the beam

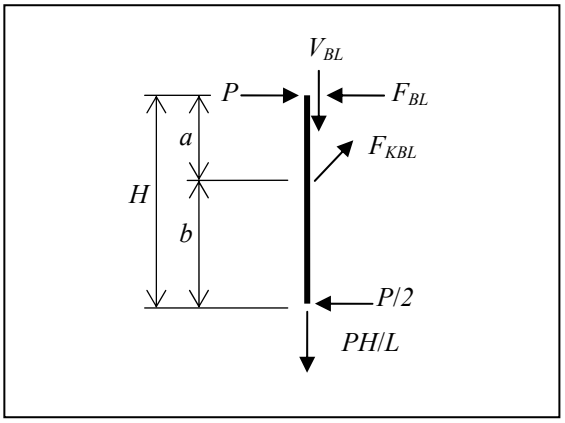

Figure P2. Left Side Column Free Body Diagram

The forces acting on the right side column were determined by applying equilibrium equations to the free body diagram as shown in Figure P3.

$F_{KBR} = (0.707PH/a)$
$F_{BR} = (P/2)(H/a-1)$

F_{KBR} : internal axial force in right knee brace
F_{BR} : internal axial force in right end of the beam

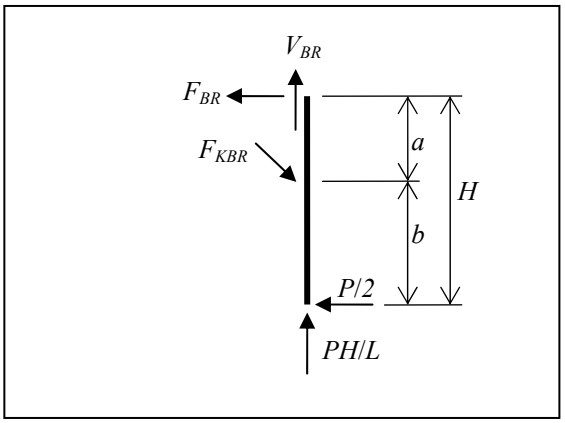

Figure P3. Right Side Column Free Body Diagram

Internal work was equated to external work. Knee brace forces were multiplied by 2 since there are two joints in each brace.

$$P\Delta/2 = F_{KBL}^2/k_{KB} + F_{BL}^2/2k_{BC} + F_{KBR}^2/k_{KB} + F_{BR}^2/2k_{BC}$$

k_{KB} : stiffness of the knee brace joint
k_{BC} : stiffness of the beam to column joint

Simplification to find frame stiffness k_f :

$$k_f = \frac{P}{\Delta} = \frac{1}{\frac{2}{k_{KB}}\left[\left(\frac{H}{a}\right)^2\right] + \frac{1}{2k_B}\left[\left(\frac{H}{a}\right)^2 + 1\right]}$$